The pleiotropic effects of vitamin D promoting bowel health

MR DANIEL J. LOCK BSC. MRSB.

Thesis submitted to the University of East Anglia in requirement for the degree of Doctor of Philosophy (Molecular cell biology with epigenetics)

School of Biological Sciences, University of East Anglia, Norwich, UK

And

Institute of Food Research, Norwich Research Park, Norwich, UK

September 2016

Declaration

This thesis is submitted to the University of East Anglia for the Degree of Doctor of Philosophy and has not been previously submitted at this, or any other university, for assessment, or for any other degree. Except where stated, and reference or acknowledgement is given, this work is original, and has been carried out by the author alone.

Thesis abstract

Vitamin D insufficiency is seasonally endemic in populations north of the 40th parallel, and epidemiological data show an association with colorectal cancer risk and prognosis. Molecular mechanisms that underpin the relationship are not well established. Vitamin D status is shown to be associated with age-related silencing of tumour suppressors in colonic stem cells via aberrant DNA methylation, suggesting that insufficiency contributes to transformation. In this text, vitamin D's ability to promote bowel health via modification of DNA methylation patterns has been investigated.

Chronic inflammation drives tumourigenesis, and vitamin D is recognised to promote proper immune function. Data presented here confirm that vitamin D differentiates monocytes to a tissue-resident macrophage phenotype. D-mediated differentiation is associated with hypomethylation of the TNFα promoter and response to LPS. Thus, we suggest that vitamin D attenuates aberrant DNA methylation in colonic stem cells by promoting resolution of systemic inflammation.

Mucosal inflammation mediated by PGE2 promotes aberrant DNA methylation. Pericryptal myofibroblasts interact with colonic stem cells via their secretomes, which are a source of PGE2. Supernatants from primary intestinal myofibroblasts were characterised by LC/MS mass spectroscopy in response to vitamin D. Vitamin D attenuated TNFα-induced transcription of COX2 and PGE2 secretion. PGE2 induced hypermethylation of SOX17 and DKK1 in colonic organoids, and myofibroblast supernatants regulated DNA methyltransferase activity in case-matched organoids. Furthermore, vitamin D ameliorated established aberrant DNA methylation in organoids propagated from inflamed mucosa. Thus, we suggest that vitamin D attenuates mucosal inflammation, and the effects of PGE2 driving aberrant DNA methylation in colonic stem cells.

Vitamin D status predicts colorectal cancer survival. The effects of vitamin D sufficiency on colorectal cancer cell lines was investigated. Vitamin D-treated cells exhibit a modified methylome, reduced transcription of MAP kinases, reduced phosphorylation of ERK1 and 2, and inhibition of proliferation. Thus we suggest that vitamin D sufficiency improves colorectal cancer prognosis via modification of established aberrant DNA methylation. Taken together, data support vitamin D sufficiency promoting bowel health via attenuation of aberrant age-related DNA methylation in colonic stem cells.

Acknowledgements

Without question, my sincere thanks are extended first and foremost to Dr Nigel Belshaw, not only for his unwavering support in the face of the challenging circumstances, but also for providing the insightful theoretical framework that forms the basis of this study. Thank you Nigel, for your commitment, lateral support, and championship.

Furthermore I appreciate greatly Professor Ian Johnson fighting my corner; your encouragement and objective criticism have enabled me to understand the scientific validity and impact of my work in a broader context. Thanks are also extended to Drs Giles Elliot, Wing Leung, and Ellen Maxwell for their companionship, and initial direction and assistance.

I'm indebted to Drs Paul Kroon, Nathalie Juge, and Carmen Pin for their pastoral care keeping me on track during tricky transitional periods. Thanks especially go to my friends Drs Barnabas Shaw, Aimee Parker, and Laura Vaux, for welcoming me to their group(s), and for the daily logistical support and encouragement; it's by no means an exaggeration to say that I couldn't have done it without you!

I must also sincerely thank UEA and The Institute for the *exceptional* opportunities afforded to me during the course of the project - practicing science on no fewer than three continents in as many years.

Finally I would like to extend warm thanks to my close friends and family, for their (apparent) interest in my research and rallying encouragement, which has proved indispensable - especially Jemma, whose inspiring words have given me the confidence to get the job done on countless occasions. I must also extend a debt of gratitude to my original champions, Professor Richard Ball, Drs Danni Peat, and Peter Cousens, for holding open the doors that have brought me to this juncture; I doubt they'll ever read this, but it's true none the less.

Cheers all - this text is in honour of, and in return for, your investment in me - I hope to continue doing it justice.

Contents

List of figures

List of common abbreviations

5AZA	5-Aza-2'-deoxycytidine
5hmC	Five Hydroxy Methyl Cytosine
5mC	Five Methyl Cytosine
7DHC	Seven De Hydro Cholesterol
APC	Antigen Presenting Cell/Adenomatous Polyposis Coli
aSMA	alpha Smooth Muscle Actin
BCAT	Beta Catenin
BMI	Body Mass Index
BMP	Bone Morphogenic Protein
CAC	Colitis-Associated Cancer
CAF	Cancer-Associated Fibroblast
CALP	Calprotectin
CD	Cluster of Differentiation
CG	Cytosine-phosphate-guanine (CpG dinucleotide)
CGI	CG Island
CGS	Cambridge Genomic Services
CHIP	Chromatin Immuno Precipitation
CIMP	CG Island Methylator Phenotype (a sub-type of CRC
COBRA	Combined Bisulphite Restriction Analysis
COMB	Combined/Combination
CRC	Colorectal cancer
CRP	C - reactive protein
CSC	Crypt/Colonic Stem Cell
CTRL	Control (vehicle)
CYC	Cyclin
Cyp24a1	Catabolic vitamin D enzyme
Cyp27a1	Anabolic vitamin D enzyme
DBP	D-binding protein
DKK	Dickkopf Protein
DNAm	DNA methylation
DNMT	DNA Methyltransferase (cytosine methylating enzyme)
ECM	Extra Cellular Matrix
FAP	Fibroblast Activation Protein
FBS	Foetal Calf Serum
GPCR	G-Coupled Protein Receptor
HDAC	Histone Deacetylase
IBD	Inflammatory Bowel Disease
IHC	Immunohistochemistry
INF	Intestinal Fibroblast
InMyoFib	Intestinal Myofibroblast

KB	Kilo-base
LC/MS-MS	Liquid chromatography/Mass Spectroscopy
LINE	Long Interspersed Nuclear Elements
LO	Lester's Oil
LPS	Lipopolysaccharide (Endotoxin)
Mac	Macrophage
MFB	Myofibroblast
MΦ	Monocyte
PB	Peripheral Blood
PBMC	Peripheral Blood Mononucleated Cell
PBS	Phosphate Buffered Saline
PGE2	Prostaglandin E2 Synthase
PMA	Phorbol 12-myristate 13-acetate
PS	Penicillin Streptomycin
PTH	Para Thyroid Hormone
QMSP	Quantitative Methylation Specific PCR
Q-rt-PCR	Quantitative Real Time Polymerase Chain Reaction
RSPO	r-spondin1
RXR	Retinoid X Receptor
SAM	S-Adenosyl-methionine (universal methyl donor)
SEM	Standard Error of the Mean
SFRP	Secreted Frizzled Related Protein
TBST	Tris Buffered Saline-Tween
TET	Ten-Eleven-Translocation (cytosine de-methylating enzyme)
TGFB1	Transforming Growth Factor Beta One
TLR	Toll-like Receptor
TNFα	Tumour Necrosis Factor Alpha
TRM	Tissue Resident Macrophage
TRNS	Transfected
TS	Tumour Suppressor
TSS	Transcription Start Site
TUSC	Tumour Suppressor Candidate
UC	Ulcerative Colitis
VDR	Vitamin D Receptor
VDRE	Vitamin D Response Element
VIM	Vimentin
VITD	Vitamin D
WA	Wnt Antagonist
WIF	Wnt Inhibitory Factor

Chapter 1

VITAMIN D STATUS AND COLORECTAL CANCER RISK; A ROLE FOR DNA METHYLATION?

Abstract

The secosteroid hormone Vitamin D is recognised to exert pleiotropic anti-proliferative and anti-inflammatory effects, and epidemiological data indicate vitamin D status is associated with a raft of age-related diseases, including auto-inflammatory and neoplastic pathologies of the distal bowel. This raises the possibility that chronic vitamin D insufficiency initiates and maintains colorectal pathogenesis. While incidence of severe deficiency is relatively rare, asymptomatic *insufficiency* is seasonally endemic in populations north of the 40th parallel, which may be addressed by proper supplementation. As such, this represents a significant opportunity for public health providers to favourably influence morbidity and mortality due to colorectal cancer (CRC).

Vitamin D's role as a causative factor in epithelial transformation remains speculative due to the paucity of corroborating evidence from clinical interventions. Recently however, prospective associations have been reported between vitamin D status and aberrant DNA methylation (DNAm) patterns in transformation-prone epithelia, suggesting an aetiological role for insufficiency in cancer initiation. In apparently healthy mature gut epithelia, aberrant methylation of promoter CG dinucleotides silences tumour suppressor antagonists of the Wnt pathway. This results in unchecked proliferation of colonic stem cells and tumour formation in the context of acquired mutations. Thus, aged epithelia may be thought of as 'epigenetically primed' for transformation. Vitamin D sufficiency is proposed to attenuate age-related increases in aberrant DNA methylation, preserving Wnt tumour suppressor function in later life.

In this review, the theoretical premise for the thesis is examined, exploring the consensus relationship between vitamin D and epithelial homeostasis in the distal bowel, as well as speculative epigenetic modes of action by which vitamin D might promote bowel health. Aspects of systemic physiology regarding chronic inflammation, chemokine signalling in the crypt niche, and autonomous regulation of Wnt with regard aberrant DNAm, are addressed. Taken together, the current framework suggests that vitamin D promotes bowel health by modulating DNAm in cancer-prone stem cells via management of local inflammation and/or 5-methyl-cytosine metabolism - overarching hypotheses upon which these experiments were based.

Vitamin D - an evolutionary perspective

In 1922, McCollum's observation - that a fat-soluble compound in cod liver oil could resolve childhood rickets - set the scene for the discovery of a novel hormone essential for proper skeletal development[1]. Shortly afterwards, Hess and colleagues in Vienna published their lateral observation that sunlight too conferred beneficial effects on bone health[2]. A few years later, Steenbok et al linked the two processes, concluding that irradiation of epidermal lipids by sunlight yields an active compound intrinsically involved in calcium metabolism[3]. Being the fourth essential nutrient to be discovered, the compound was given the unassuming title 'Vitamine D', and the hormone entered the collective consciousness.

Ten years later, Windaus and Bock identified the vitamin D precursor 7-dehydrocholesterol (7DHC), present as an impurity in epidermal cholesterol, and shortly afterwards described its structure, for which they were awarded the Nobel prize 1938[4]. They went on to establish that irradiation of 7DHC with UV light produces minute quantities of pre-vitamin D (cholecalciferol), and the complete photochemistry of the compound was published in 1955[5]. It was another 25 years however, until Hollick and his team published their seminal paper, detailing the physiology of vitamin D production from 7DHC, in the basal strata of the epidermis (figure 1a)[6].

A century on from its discovery, Vitamin D continues to engage researchers (figure 1b). In terms of tissue specificity, expression of the nutrient's cognate nuclear receptor - the Vitamin D Receptor (VDR) - is almost ubiquitous, directly regulating 1000+ genes exhibiting promoter binding sites, which in turn influence many more[7]. Since its discovery, publications addressing every facet of vitamin D metabolism and pathophysiology have increased exponentially and there is no indication that interest in the hormone is waning, particularly with contemporary insights into the 'silent' pandemic of vitamin D insufficiency (serum D <50nM/L) and associations with age-related disease [8].

In an evolutionary context, vitamin D metabolism is well conserved between clades, functioning even in phytoplankton, where it is thought to have conferred protection on photosensitive nucleic acids for over 500 million years[9]. Its role in mediating calcium absorption took centre stage during the Palaeozoic era where, in the absence of marine electrolytes, novel terrestrial organisms fortified newly evolved skeletons through consumption of flora, that in turn derived calcium from the soil, allowing them to support the increasingly heavy frames necessitated by advancing tissue complexity[10]. Specifically, bipedal locomotion has selected for individuals with an endoskeleton robust enough to endure passage through a constricted birth canal, and importantly the vitamin D system is thought to have been fundamental in determining skin pigmentation, allowing for sufficiency at higher latitudes (the exception being darker skinned Inuit populations and others who derive their vitamin D through the consumption of oily fish)[11]. The aetiology of deficiency itself is a relatively recent development in industrialised societies, precipitated by cultural practices that inhibit epidermal production of vitamin D, such as garment wearing, urbanisation, and ethnic migration – a phenomenon known as environmental mismatch[12].

Physiology and molecular biology of vitamin D

Endogenously produced, and containing an open steroid ring, vitamin D is technically a secosteroid pro-hormone, as opposed to an essential dietary vitamin, and the body is capable of synthesizing sufficient quantities of vitamin D for proper physiological function. Vitamin D may be derived either from sunlight or dietary factors, although proportionally dietary vitamin D (principally dairy, oily fish, mushrooms, and fortified cereals) accounts for only 15% of total[13].

Mechanistically, vitamin D is produced by the action of ultraviolet light (wavelength 280-230nM) in the basal strata of the epidermis, cleaving 7DHC to produce thermodynamically unstable pre-vitamin D. Further isomerisation forms the active precursor, cholecalciferol.

The metabolic activity of the pro-hormone is limited to its interaction with the D binding protein (DBP) in the blood, an alpha globulin that binds and transports vitamin D and all of its metabolites. Cholecalciferol is either taken up and stored in adipocytes, or activated enzymatically by hepatocytes, where it is hydroxylated to 25-hydroxy vitamin D (serum calcidiol). The reaction is catalysed by a host of feedback-regulated mitochondrial CYP450 enzymes, principally microsomal CYP2R1 and mitochondrial CYP27A1[14-16].

Clinically, plasma concentrations of calcidiol are considered the most relevant marker of vitamin D status due to its long half-life and high serum concentration relative to the activated form (~one month vs 24 hours)[17,18]. Concentrations are normally distributed within the range 20–150 nM/L, with insufficiency defined as <50-80 nM/L depending on source[19]. Impaired calcium absorption and risk of pathological bone metabolism manifests at levels <30nM/L[20,21]. Calcidiol production by hepatocytes is negatively regulated by feedback from increased CYP27A1 expression[22].

The D-binding protein transports calcidiol to the kidneys, whereupon it undergoes terminal hydroxylations in the renal tubules, yielding the biologically active form - 1α25(OH)D_3 (calcitriol), mediated via the action of CYP27B1[23,24].

Given the pivotal role of calcium in cellular signalling (nerve innervation/osteoid mineralisation/muscle contraction), stability of interstitial calcitriol is vital for robust control of ion gradients across cell-membranes; CYP27B1 activity, and thus calcitriol production, are tightly regulated according to the availability of calcidiol substrate, parathyroid hormone (PTH), and calcium ion concentration, as well as by negative feedback from calcitriol itself[25,26]. Consequently plasma concentrations remain relatively stable, ranging between 20-200 pM/L, with a half-life of between 4-36 hours depending on source[27,28]. Due to its unstable nature, a reference range has been difficult to determine, but a cut-off of around 40 pM/L has been for proposed for health (figure 1c)[29].

Anabolic CYP27B1 activity has also been observed at a variety of extra-renal sites not associated with classical vitamin D physiology such as the prostate, pancreatic islets, adrenal glands, lymph nodes, brain, lungs, thymus, placenta, epidermis, and intestinal epithelium[24]. The enzyme is also expressed in immune cells (macrophages, dendrocytes, & T cells)[30], in hyperproliferative inflammatory conditions such as psoriasis and sarcoidosis, and in various tumours and cancer cell lines[31], including colorectal carcinoma[32] where it is initially over-expressed in early tumourigenesis[33] but notably absent in higher grade cancers[34].

Finally, active D is degraded by CYP24A1, which converts vitamin D to water-soluble calcitroic acid that is subsequently excreted by the kidneys[35]. Aberrant transcription of CYP24A1 may be considered oncogenic, as over-expression in neoplastic tissues promotes pathological degradation of calcitriol, abrogating vitamin Ds homeostatic effects - as evidenced by over-expression of CYP24A1 in aggressive colorectal cancers[36,37].

Asymptomatic vitamin D insufficiency is seasonally endemic

Seasonal variation in serum vitamin D is reported in populations north of the 40th parallel (figure 1e)[38]. According to a definition for insufficiency of <75nM/L, it is estimated that more than one billion people globally suffer from asymptomatic seasonal hypovitaminosis D[21]. Furthermore, age-related impaired epidermal synthesis of vitamin D is exacerbated by chronic immobility in ageing populations[39]. Bioavailability also depreciates in obese subjects due to adipocyte

uptake or via reduced duodenal absorption from inflammatory bowel conditions[40,41]. Finally, chronic liver and kidney pathologies - key sites of vitamin D synthesis - result in decreased production[42]. These observations recently prompted the UK government to review vitamin D supplementation and issue official advice, suggesting that most individuals will benefit from 10ug per day seasonal supplementation, with at-risk groups indicated for year-round administration.[43]

Insufficiency is associated with higher all-cause mortality and implicated in the aetiology of several pathologies, increasing the risk of metabolic bone disorders[44], multiple sclerosis, diabetes[45], breast cancer[46] and prostate cancer[47], as well as neurocognitive dysfunction, infection and autoimmunity, and cardiovascular disease[48]. In 1980 Garland and Garland published their seminal paper observing the relationship between colorectal cancer rates and geographical location[49]. Subsequently many epidemiological studies have confirmed the inverse association between serum D and colorectal cancer risk (figure 1d)[50].

Molecular physiology

Interstitial vitamin D mediates a rapid genomic response in target cells via plasma membrane-associated VDR, enriched at caveolae, which effects prompt internalisation and signal transduction[51]. VDR is expressed ubiquitously throughout the body indicating the myriad of cellular activities administered by the vitamin D endocrine system. Given its near-universal expression it has been suggested that vitamin D directly or indirectly regulates up to 5% of the genome[52,]. Weight has been added to this assertion by array-targeted approaches that demonstrate genomic response elements numbering in excess of 2000, associated with more than1000 genes involved in 100+ independent pathways[53,54].

Once bound, VDR undergoes conformational change and translocates to the nucleus where it forms a heterodimer with retinoid X receptors (RXR)[55]. Typical of steroid hormones, the complex recruits coactivators/repressors, and zinc fingers bind DNA at Vitamin D Response Elements in the promoter regions of target genes (VDREs)[56]. VDREs consist of sequential hexameric binding sites with

a tri-nucleotide spacer, and target genes have been shown via CHIP-seq to contain several response motifs[57,58].

Coactivators induce chromatin accessibility via histone acetylation, and vitamin D receptor-interacting protein (DRIP) attracts RNA polymerase. Conversely, repression is mediated by VDR-interacting repressor (VDIR) and Williams's syndrome ATP-dependent chromatin remodelling complexes (WINACs) that associate with the VDR/RXR heterodimer, recruiting histone deacetylases and facilitating gene repression via chromatin remodelling[59]. Incidental to this project, vitamin D also stimulates a non-genomic response in calcium ion kinetics via GPCR binding with speedy RAS-MAPK transduction[60], fundamental for muscle innervation. Presenting symptoms of severe hypovitaminosis include sporadic muscle twitching (fasciculations)[61].

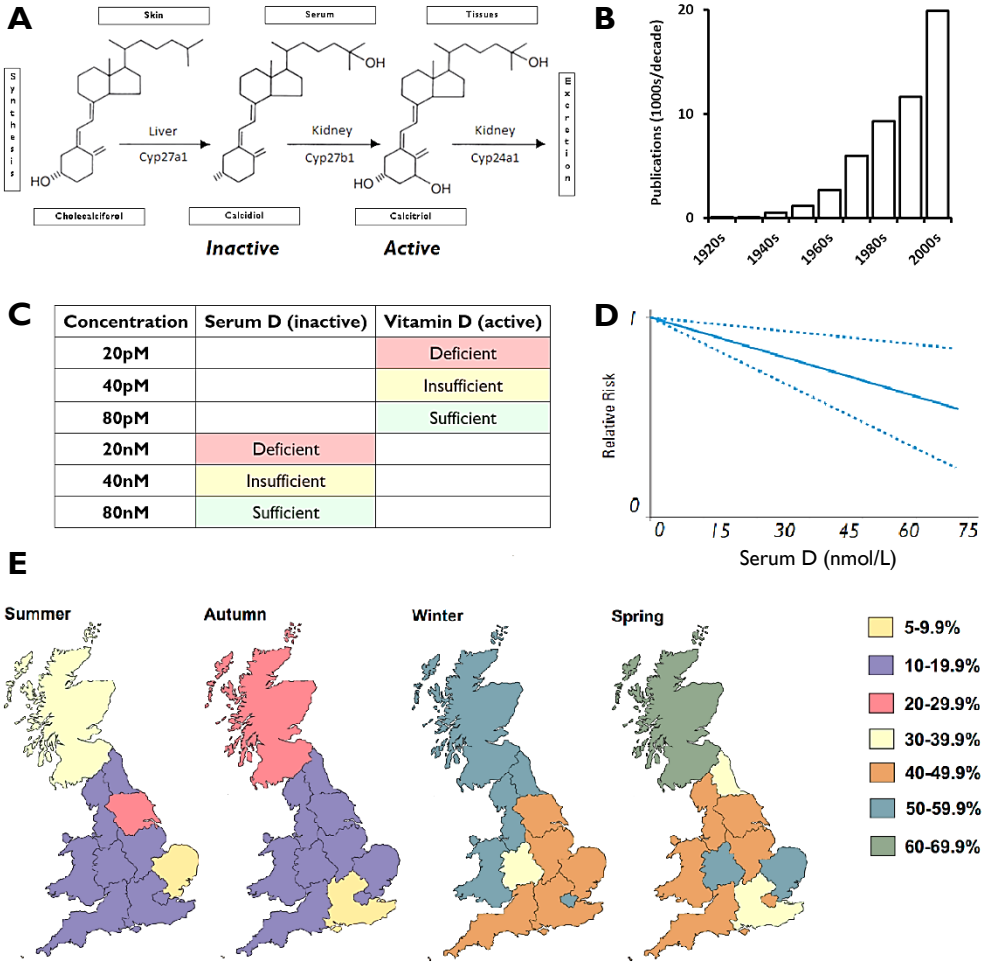

Figure 1 - Vitamin D physiology and epidemiology A) Photolytic degradation of epidermal 7DHC produces pro-hormone cholecalciferol. This is transported by the D-binding protein to the liver, and then the kidneys and other target tissues, where activating hydroxylations by Cyp27A and B1 catalyse the conversion of cholecalciferol to biologically active calcitriol via calcidiol. Finally, Cyp24a1 – a vitamin D regulated product – deactivates calcitriol, and water-soluble calcitroic acid is excreted. Cyp24a1 is oncogenic when overexpressed in neoplastic tissues, establishing vitamin D insensitivity, and promoting proliferation. B) A Pubmed search for articles containing the term 'vitamin D' in their title demonstrates an exponential (R^2 = 0.9376) increase in the number of publication pertaining to vitamin D since its inception in the early 20th century. C) Reference ranges for serum and activated vitamin D derived from various publications; there is no global consensus for vitamin D sufficiency, and these values represent the most commonly reported concentrations for the preservation of health[20,62,63]. Insufficiency is typically asymptomatic in the acute phase, however may act over the lifetime of an organism to precipitate associated health disparities. D) A meta-analysis of nine prospective studies investigating the relationship between serum vitamin D (x axis, nM/L) and colorectal cancer risk (y) suggests a dose-response association. Adjusted relative risks and 95% CIs (dashed lines) are reported (adapted from[64]). E) Shows proportion of the UK populace who's serum vitamin D levels seasonally fail to attain the 40nM/L definition for sufficiency, adapted from[65]. Even in summer months, as much as 30% of the English population and 40% of the Scottish population may be defined as having insufficient vitamin D, leaping to 60%+ at the end of winter. Vitamin D insufficiency as a public health concern was addressed recently by the UK government's advisory panel, suggesting supplementation for all citizens during winter months, although the necessity and value of this health initiative is contested[43,66]

Physiology/Pathophysiology

The classical role of vitamin D in target tissues is to control calcium and phosphate metabolism by regulating serum ion concentrations[67], promoting uptake of dietary calcium in the duodenal epithelium (via induction of calbindin) and reabsorption of plasma calcium in the renal tubules[68]. This is effected by low serum calcium induction of parathyroid hormone (PTH) synthesis in chief cells, that stimulates calcitriol production[69]. Ossification of osteoid collagen, and reabsorption of skeletal calcium by osteoclasts, is mediated in harmony with PTH and calcitonin via RANK/RANKL signalling, establishing proper mineralisation of skeletal bones[70,71].

As predicted by the ubiquity of VDR, vitamin D exerts a variety of non-calcaemic effects, particularly with regards to immune function, inflammatory mechanisms, and tissue homeostasis, inhibiting proliferation and inducing differentiation and apoptosis in a variety of models[72].

Vitamin D acts as an anti-inflammatory and is associated with chronic inflammatory pathologies of the distal bowel

Vitamin D status is associated with both adaptive and innate immune functions, evidenced by the increased risk of autoimmune disease and infection associated with vitamin D deficiency[73], and the presence of VDR and CYP27B1 in many immune cell types, including macrophages, B and T cells, antigen presenting cells, and dendricytes[74]. Systemically, serum vitamin D is inversely associated with serum TNFα in healthy athletes, obese participants, and patients with congestive heart failure alike, suggesting a common mechanism underpins the relationship between vitamin D and TNFα-mediated inflammatory processes (i.e. *not* associated exclusively with diseased states)[75,76]. However, the relationship is not fulfilled in Crohn's patients where TNFα levels are independent of vitamin D status, but positively associated with anti-inflammatory IL10[77], suggesting that vitamin D insufficiency in this context promotes resolution of inflammation rather than preventing its occurrence. A recent meta-review of vitamin D's effects in PBMCs supports a systemic anti-inflammatory effect both *in vivo* and *in*

vitro, with researchers routinely reporting inhibition of cytokine secretion, specifically those observed to be elevated systemically in Crohn's disease, TNFα, IL6, and IL1β[78].

The authors postulate mechanisms for the anti-inflammatory effect of vitamin D consequent to reduced Toll-like receptor expression in cell membranes (TLR2 and 4), and reduced cytosolic NFκB phosphorylation. Furthermore vitamin D is also reported to suppress NFκB activity via interaction between the VDR/RXR complex and IKKβ[79].

Due to its role as a systemic anti-inflammatory, and association with inflammatory bowel diseases Crohn's and ulcerative colitis, vitamin D insufficiency is suspected to play a role in the pathogenesis of inflammatory conditions in the distal bowel[80]. However, conversely vitamin D status is impacted by impaired absorption of the vitamin D derived from the diet, so the true relationship between vitamin D and IBD is not fully resolved[81]. Tissue resident macrophages, recruited from circulating monocyte populations that gravitate to beacons of cytokine activity, play a key role in mediating intestinal inflammation that is the hall mark of IBD, and numbers increase linearly with markers of mucosal inflammation[82]. The transition from circulating monocyte to mucosal macrophage is accompanied by phenotypic changes in the expression of cell surface receptors that define degree of differentiation, namely CD14, CD68, CD11b, F4/80 and CD16 (addressed in depth in chapter 3)[83], and these are reported to be regulated by vitamin D - a common bench technique for differentiating monocyte-derived macrophages[84]. Curiously, not all of these markers contain vitamin D response elements in their sequences, suggestive of non-canonical/non-genomic actions of vitamin D promoting differentiation[85].

The Cell Cycle and The Hall Marks of Cancer

Before considering any examples of vitamin D's anti-neoplastic effect, it is pertinent at this juncture to first define their context, by describing routine control of tissue growth and cellular proliferation at the molecular level, and the consequences for tissue homeostasis when these mechanisms fail.

At any given moment, the vast majority of somatic cells within an adult human are not dividing, and their growth is considered to be arrested (quiescence). In order to populate tissues during embryogenesis, or later on in life during wound healing or epithelial turnover, external/environmental molecular stimuli (typically growth factors) prompt a resting cell to trip back into the cycle of cellular division known as mitosis. Conversely, when the healing process nears completion, contact inhibition precipitates growth arrest by diametrically opposed signalling cascades[469].

Cycling cell goes through four active phases, as well as the semi-permanent quiescent/resting phase (detailed in table 1 and figure 1a)[470]. Well defined molecular activities take place during each phase, and at transitional check points between phases G1→S and G2→M. Active phases (DNA synthesis and cell division), are preceded by gap phases that allow for the synthesis of 1) proteins involved in mediating the anticipated S and M phases (transcription factors, phosphorylating kinases), and 2) the raw materials for building a new cell (membrane lipoproteins, cytoskeletal filaments). These check points are vital for homeostasis, as here regulatory checks on the integrity of the cell and its components are performed by maintenance proteins, determining the cell's viability.

State	Phase	Processes
Quiescent	G_0	Resting (performing normal tissue and metabolic functions)
Interphase	G_1 (1^{st} gap)	Preparing for DNA synthesis, associated protein production, increase in cell volume
	S (synthesis)	DNA synthesis/duplication
	G_2 (2^{nd} gap))	Preparing for mitosis, associated protein production, increase in cell volume
Dividing	M (mitosis)	Prophase, metaphase, anaphase, telophase, cytokenesis

Table 1 – Phases of the cell cycle. Four phases are observed during cell proliferation. In the absence of growth factor signalling, cell exit the cell cycle, differentiate and begin to perform normal metabolic function, sometimes for many years. Cells enter the cycle during the first gap phase and will not transition to DNA synthesis until regulatory checks are complete. After this restriction point and DNA duplication, a second gap phase occurs while proteins are synthesised necessary for mitosis.

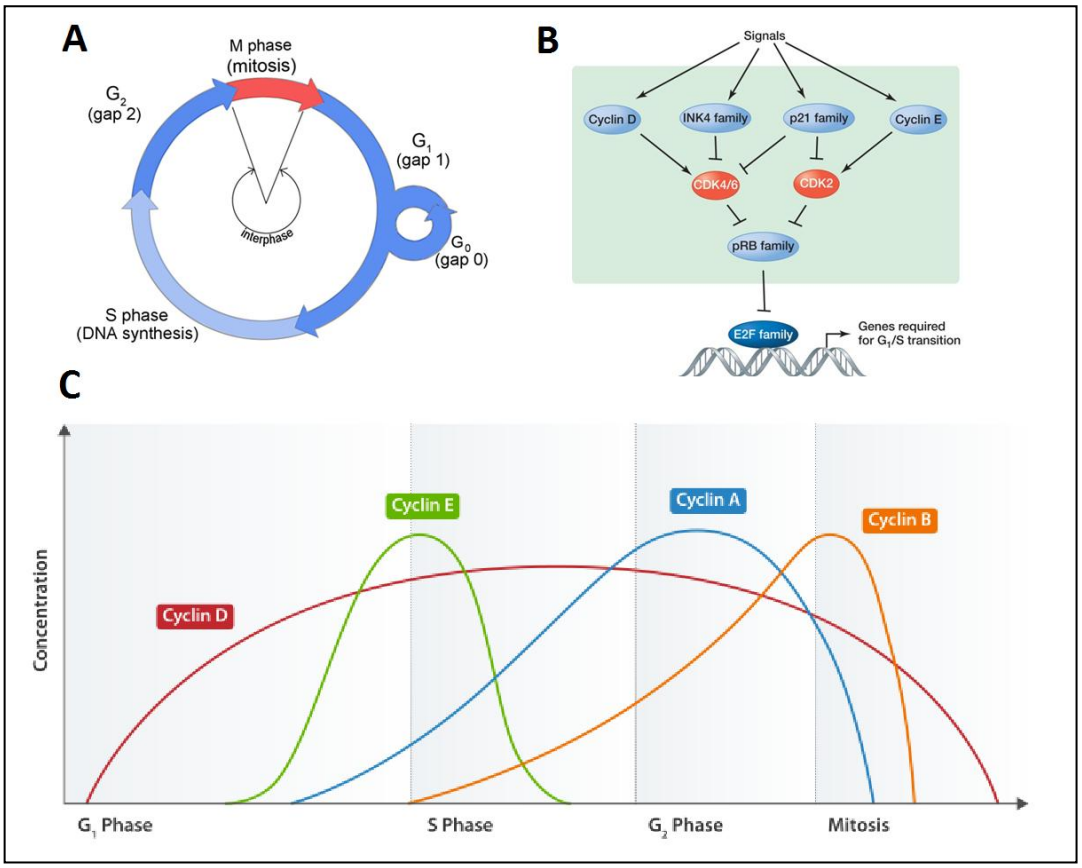

Figure 1 – Regulation of the cell cycle by cyclins, CDKs and Rb1. A) Interphase defines the period of preparation for M-phase (mitosis) when cells actively divide. Quiescent cells enter the cycle during G1. The two gap phases are necessary for protein synthesis and regulatory checks. Transition out of gap phases is tightly regulated by a host of cyclin/CDK complex phosphorylation events activating transcription factors. B) Mitogenic signals transcribe cyclins that associate with CDK enzymes, conferring phosphorylating potential to the complex. Phosphorylation of RB1 frees E2F transcription factors to transcribe genes that direct transition from GF-dependant G1 to GF-independent DNA synthesis phase (S-phase). C) Cyclin concentration is shown to cycle predictably throughout the cell cycle (as is Rb1 phosphorylation status). Cyclin E is a key mediator of G1-S phase transition, after which a cell is committed to dividing, regardless of external signals.

Integral to both DNA fidelity and cell cycle progression, is the G1-S phase transition check point that occurs towards the end of Gap 1 after preparatory growth and protein synthesis. Continuation through the cell cycle is still dependent on external growth factors at this point. This transitional period or restriction point is when the fate of the cell is determined (quiescence/differentiation, division, DNA repair, or death).

Progression of the cell cycle is positively regulated at each phase by cyclins and cyclin-dependant kinases, while negative regulation is performed by Rb1, p53 and p21. The interplay between cyclins/CDKs and RB1/p53 and their respective phosphorylation states determines whether cells are held at this restriction point or are allowed to pass. G1→S phase transition is instigated when external mitogenic signals promote synthesis of cyclins (figure 1b), that in turn bind and activate cyclin-dependant kinases with phosphorylating potential. Primarily, phosphorylation of the tumour suppressor Retinoblastoma1 (RB1) prevents it's association with E2F transcription factors that drive the transition to S-phase (figure 1b), thus Rb1 phosphorylation state correlates with stages of cell cycle progression – hypo-phosphorylated in gap phases, and hyper-phosphorylated during synthesis(figure 1c)[472].

During G1-S phase transition, DNA is screened (and repaired where necessary) prior to DNA duplication in S phase. This pause for regulatory checks on the integrity of the genome also allows the cell to commit programmed cell death if errors are deemed unmanageable. Like RB1, down-stream targets of the transcription factor p53 also block S-phase transition, while orchestrating DNA repair or suicide, earning p53 the moniker 'guardian of the genome'. This is evidenced by the observation that over 50% of all malignant cancers demonstrate mutated code or compromised p53 efficiency[473].

By transcribing p21, which binds and inhibits the complexes that drive transition to S-phase, p53 may stall the cell cycle while maintenance of the DNA is performed by repair proteins that are also under transcriptional control by p53[474] i.e. Muts-1 which mediates mismatch repair, or DNA glycosylases that perform base excisions. Furthermore, p53 may induce apoptosis in compromised

cells by activating caspases, via release of cytochrome C from mitochondria stimulated by the p53 targets, BID and BAX[475] (reviewed in[476]) Thus, a dysfunctional p53 sequence or protein is incapable of bringing about a pause in the cell cycle or directing apoptosis, and division proceeds unchecked.

Once transition to S phase is instigated, a cell is committed to division, regardless of variable external GF stimuli, due to a positive feedback loop established by E2F transcription factors, and may not quiesce until G1 comes around again after division.

Due to the ability of functional RB1 and p53 proteins to suppress tumour formation by negatively regulating the cell cycle, their gene sequences are referred to as tumour suppressors (TS). Ergo, mutational silencing or functional incompetence of the protein product is observed to result in uncontrolled cell proliferation. Conversely, genes that are typically *in*active in order to prevent cell cycle progression (i.e. switched following after embryogenesis), are termed proto-oncogenes. These genes have the potential to initiate tumour formation when mutated or over-expressed, which confers true oncogenic properties. Examples of proto-oncogene typically include those proteins whose expression promotes cell turnover, like Myc, Ras, Raf and CDKs. Classically, oncogenic aberrations are tumour-initiating with regards cell cycle, conversely, tumour suppressor dysfunction transforms the previously initiated (although as we shall explore later, epigenetic silencing of tumour suppressors may prime cells for transformation, and precede the initiating oncogenic event).

The hall marks of cancer

When control of the cell cycle is impaired in solid tissues through silencing of tumour suppressors, or activation or over expression of proto-oncogenes, a benign tumour mass begins to form. Further aberrations that compromise a cells ability to execute apoptotic pathways, maintain genome fidelity, or confer the ability to migrate from the primary site, mark the transformation of a benign lesion to a malignant phenotype (cancer). The diverse and temporally spontaneous nature of any particular cancer genome means that individual lesions are effectively unique in their molecular profile. However it has been asserted that *all* cancers demonstrate unifying traits with regards their overall biological phenotype. Hanahan and Weinberg's seminal paper – The Hall Marks of Cancer[477] – surmised six traits common to all cancers (table II), although it is important to note that several of these characteristics also apply to benign lesions too. Furthermore, while the authors cite multiple examples of specific tumours that demonstrate these properties, and detail evidence for the aberrant pathways responsible for conferring the cancer phenotype, by their own admission, the assertion that *all* cancers exhibit these features is, for the time being, an informed extrapolation of the established paradigm, until the missing data is complete. It is also now recognised that several of these traits are effected via paracrine regulation of the tumour microenvironment and the interstitium by transformed cells i.e. tumours harness the growth-promoting and mobilising potential of their non-transformed neighbours. Being effected by non-transformed cells, the phenotype of the cancer is thus not entirely autonomous but requires collusion and cooperation with healthy cells (myofibroblasts, immune mediators, vascular tissues etc). In 2011, Hanahan and Weinberg published an update, The Hallmarks of Cancer – The next Generation, which detailed four additional universal traits of neoplastic tissues that had become established in the literature during the intervening period (inflammatory infiltrate, evasion of immune detection, deregulated metabolism, and genomic instability)[478].

Vitamin D exerts pleiotropic effects on the genome via its cognate nuclear receptor and ubiquitous response elements. It seems likely that vitamin D might thus effect regulation of cell cycle via modulation of the aforementioned tumour suppressors, proto-oncogenes, and CDK phosphorylation events that orchestrate cell cycle progression.

Characteristic	Comment
Autonomous Growth Factor signalling	Paracrine GF signalling is typical of non-transformed proliferating tissues. In tumour cells these signals are constitutively activated via mutation to allow for autonomous stimulation of the growth response. Furthermore, over expression of surface receptors causes GF hypersensitivity. Finally, downstream mediators i.e. Ras/Raf, may also become locked on with identical consequences for prolioferation[479,480]
Resistance to programmed cell death	Uncontrolled proliferation does not create a pathological crisis were the autonomic mechanisms that initiate cell death remains functional. Deregulated caspase activation must also occur to negate apoptosis and increase tumour bulk[481].
Insensitivity to anti-mitotic factors	Most, if not all, exogenous anti-mitotic growth signalling is transduced via phosphorylation of Rb1 by cyclin/CDK complexes. Any disruption to Rb1 competence is postulated to confer insensitivity to paracrine efforts to negatively regulate cell turnover[482].
Transcendence of replicative limits	Telomere shortening due to telomerase insufficiency typically causes chromosomal instability during cell division, which, when detected, precipitates apoptosis of 'aged' cells. Reactivation of telomere catabolism allows a cancer cell to permanently avoid this homeostatic mechanism and become immortal[483]
Promotion angiogenesis	Angiogenesis is essential for supply of nutrients and metabolic respiration necessary to support continued growth. Up-regulation of neo-angiogenic factors (VEGF) combined suppression of negative angiogenic regulators is noted in roughly half of all cancers and is prognositically significant[484]
Metastatic potential	Tumours confined to a single organ or tissue may precipitate poor health but do not generally effect loss of homeostasis at the whole organism level. It is only when a tumour metastasises, first invading the surrounding tissues and sub-epithelium, then local lymph and blood networks, and finally to distant organs (brain, liver, bone), that whole systems begin to fail, endangering life. Mechanisms that promote cell-cell adhesion and cell motility are the key effectors of metastatic potential.

Table II – The Hallmarks of Cancer. Adapted from Hanahan and Weinbers seminal paper of 2011, which has been referenced over 25,000 times. Details common properties exhibited by cancer cells regardless of tissue of origin or complexity of underlying aberration. These six physiological quirks combined confer malignant growth on otherwise benign lesions (although some properties are also demonstrable in non-cancerous tumours), and arise when normal regulatory mechanisms are compromised.

Anti-neoplastic effects of vitamin D

Antiproliferative effects are implied by the vast body of epidemiological data that demonstrates serum vitamin D to be inversely associated with the relative risk for neoplasia, specifically breast, prostate and colorectal adenomas and carcinomas[86]. While a causal relationship between low vitamin D and epithelial tumourigenesis is supported by *in vitro* studies that demonstrate clear antiproliferative and pro-apoptotic effects of vitamin D[60], clinical interventions that seek to improve vitamin D status do not impact significantly on disease risk, implying correlation but not causality, although this could be attributable to compromised methodology and relatively short interventions not exceeding an average of 3 years[66]. High-dose Vitamin D as a chemotherapeutic is precluded by the risk of hypercalcaemia, that precipitates impaired calcium homeostasis (renal calculi, arrhythmias, polyuria/dehydration, and depression)[87].

At the molecular level, vitamin D regulates a variety of pathways in epithelial cells that dictate cell cycle progression and growth; the main drivers of vitamin D's antiproliferative effects are cyclins and cyclin-dependent kinases that block transition to DNA synthesis phase at G1[88]. A master regulator of the pleiotropic c-MYC network[89], vitamin D induces P21, P27, TCF4, DKK1, CCND3, CDK4 and CDK6, all of which act to down-regulate proliferation[90-92]. Simultaneously in glandular epithelia, vitamin D promotes differentiation (improved adhesion) via induction of epithelial cadherin (ECAD)[93]. Enticingly, vitamin D mediates *de novo* expression of ECAD in breast cancer cells via promoter demethylation[94]. Vitamin D also inhibits phosphorylation of the tumour-suppressor RB1, which in turn deactivates a host of cell-cycle transcription factors[95]. Finally, vitamin D may also promote p53-dependent (healthy) *and* independent (tumour) apoptosis, via induction of BAX and suppression of BCL2[96].

In vitro evidence is convincing, and growth inhibition and apoptosis have consistently been achieved in a variety of colon cancer cell lines and tumour explants following treatment with physiologically-relevant concentrations of vitamin D[97,98,99]. Furthermore, expression of VDR inversely correlates with the degree of differentiation, such that the antimitotic effects of vitamin D are annulled in poorly differentiated, aggressive tumours, due to vitamin D insensitivity[100]. This is consistent with observations that VDR itself binds cytosolic β-catenin, downregulating Wnt-mediated proliferation[95].

Colonic homeostasis and neoplasia

In order to better appreciate the dynamics of vitamin D promoting bowel health, it is first necessary to establish a framework for tissue homeostasis in healthy colonic mucosae.

The large bowel comprises the ascending, transverse, and descending colon, terminating distally in the sigmoid rectum. It serves two principal functions; storage, mechanical processing, and transit of digested food waste, and the recovery of water and other residual nutrients from chyme. Unlike the small intestine, the colon is not primarily an absorptive organ, and as such the surface is effectively smooth (although pleats exist to allow distension). The surface is punctuated by glandular pores known as the colonic crypts, whose primary purpose is to secrete goblet cell-derived mucins that lubricate faecal transit, and provide a viscous barrier between the luminal contents, permanent microbiota, and the epithelium (figure 2)[101].

The epithelial sheet is populated by multipotent crypt stem cells (CSC) that reside at the base of the colonic crypts[102]. These permanent cells are anchored to the basement lamina, and marked principally by their expression of LGR5, a protein that forms part of the membranous r-spondin receptor complex involved in Wnt signal transduction[103]. Asymmetric division of CSC produces fast cycling daughter progeny (termed progenitor or transit-amplifying cells, destined for differentiation as they traverse the wall of the crypt), and one replacement stem cell, thus maintaining a static population of four or five LGR5+ve cells in the niche[104]. As progenitors transit the crypt wall, their LGR5 positivity diminishes, and markers of terminal differentiation appear. Thus the crypt may be divided along its axis into three compartments (figure 3a); the stem cell niche (comprising slow cycling CSC and supporting mesenchyme), the proliferative or transit amplifying compartment (where rapid division of progenitors produces the bulk of cells required to populate the epithelia), and the differentiative compartment (where proliferative signals diffusing from the niche fade, precipitating terminal differentiation).

The epithelial sheet itself is composed of three dominant cell types, absorptive enterocytes, mucin-secreting goblet cells, and environment-sensing enteroendocrine cells[105].

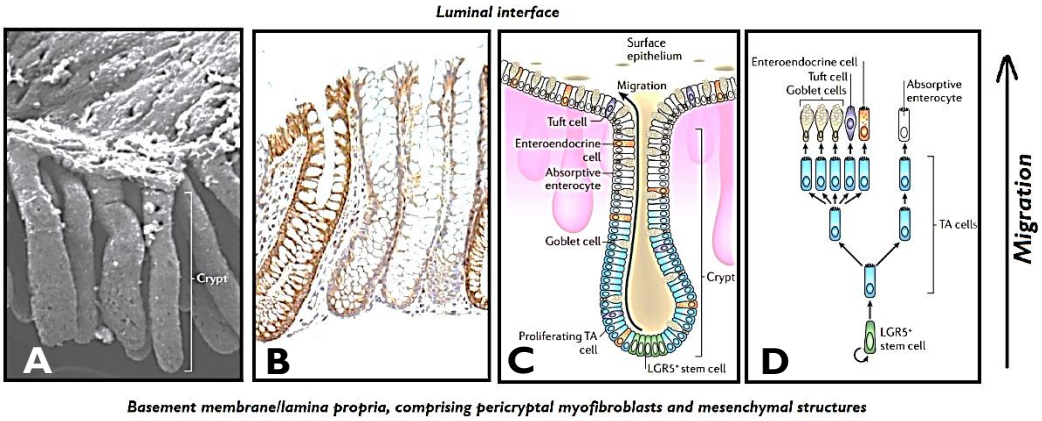

Figure 2 – microscopic topography of the colonic crypts a) 3D scanning electron micrograph of glandular invaginations comprising the epithelial sheet b) 2D histological cross section reveals numerous goblet cells (with prominent mucin filled vacuoles) c & d) cross-sectional schematic detailing the distribution of key cell phenotypes and asymmetric CSC division producing transit-amplifying (TA) progenitors that migrate along the crypt axis, differentiating to terminal colonocytes at the luminal interface. Adapted from[105] & [106].

Cryptogenesis is consequent to Wnt-mediated stem cell proliferation

To prevent dysplasia, it is essential that the rate cells are produced in the niche is balanced by apoptosis at the luminal surface. This is mediated by opposing gradients of soluble growth factors and inhibitors secreted along the length of the crypt that regulate proliferation, differentiation and apoptosis[107]. The principal signalling cascade that instigates stem cell division is the Wnt pathway (figure 3b), the end-point of which is the transcription of the TCF-LEF transcription factor targets c-MYC and Cyclin D1 that initiate cycle progression[108].

In quiescent cells, in the absence of Wnt stimulation, there is no interaction between surface components of the Wnt receptor (Frizzled and LRPs 5 & 6). Here, a destruction complex is present in the cytoplasm, formed from APC, GSK3β, and AXIN1, which tags cytosolic β-catenin (BCAT) with ubiquitin, marking it for degradation by the proteasome[109]. Typically BCAT, contributes to cell adhesion by linking epithelial cadherins to the actin cytoskeleton, thus cytosolic concentration of BCAT remains low in quiescent cells, and any free cytosolic BCAT is mopped up by the destruction complex. In the nucleus, TCF/LEF recruits corepressor Groucho, and histone deacetylases remodel the chromatin to inhibit RNA synthesis of target genes, halting proliferation.

To instigate cell division, ligation of Frizzled by secreted Wnt factors effects conformational association with membrane bound LRP5/6 coreceptor lipoproteins, potentiating signal transduction; the cytosolic tail of the receptor complex attracts Dishevelled, which in turn destabilises and inactivates the destruction complex. In the absence of ubiquitin-mediated clearance of BCAT, cytosolic concentrations increase to the point of saturation, followed by nuclear translocation of BCAT that displaces Groucho. Repression of TCF-LEF targets ceases, and transcription of c-MYC/Cyclin D1 initiates S-phase[110].

The epithelium itself is a source of paracrine Wnt ligands that drive cell division (r-spondins, Wnt3a)[111,112], but neighbouring peri-cryptal myofibroblasts have also

been shown to support cryptogenesis via secretion of Wnts[113]. When Wnt signalling from the epithelia is ablated by conditional knock-down of PORCN (a protein essential for endoplasmic processing of Wnts), there is no consequence for normal cryptogenesis *in vivo*, indicating redundant, extrinsic sources of Wnt, derived from sub-epithelial cell populations[114]. Wnt signalling is modulated by multiple internal and external mechanisms; BMP agonists, secreted by mature colonocytes, form an opposing gradient to Wnt diffusing down from the epithelium[107], and in the niche, secreted frizzled related proteins (SFRPs), Wnt inhibitory factor1 (WIF1), and Dickkopf-related proteins (DKKs), bind interstitial Wnt ligands and/or outcompete Wnt ligands at Frizzled receptors, reconstituting destruction complex activity (figure 3a). Wnt antagonists (WAs) are typically TCF-targets, so stem cells modulate proliferation via autocrine feedback mechanisms, but they are also expressed by other cell types in the niche, adding layers of extrinsic control[115,116].

Wnt-mediated stem cell turn-over is established during embryogenesis to propagate epithelial bulk in rapidly expanding tissues. Self-renewal is maintained throughout life in somatic tissues to compensate for cell loss due to the routine apoptosis of colonocytes (the entire epithelium may be entirely replaced every five days)[117]. Transient colonisation by invading pathogens or toxicity due to other pro-inflammatory/necrotic factors, necessitates rapid sloughing of compromised cells to limit penetration and protect the stem cell niche, concurrent to a loss of crypt architecture and epithelial hypotrophy[118]. Activation of Wnt is thus required to regenerate the epithelia, via symmetrical fission of crypts along their axis, and explains why inflammatory cytokines associated with chronic inflammation (INFγ, TNFα) exhibit Wnt-modulating properties, and themselves are managed by Wnt following resolution of transient stimuli[119,120, reviewed in 121]. Crypt fission is thought to be responsible for the propagation of genetic and epigenetic aberrations originating in individual stem cells (themselves the product inflammatory insults) throughout histologically normal epithelia - a concept known as the field cancerisation effect[122].

Deregulated Wnt signalling precedes hyperplasia

Effective inhibition of Wnt signalling is essential to maintain CSC/progenitor proliferation at a rate not exceeding that of cell loss at the lumen. Benign adenomatous tumours begin to form when Wnt-mediated proliferation goes unchecked, resulting in a net increase in cell number (hyperplasia). Four mechanisms by which this can occur are described; 1) loss of the destruction complex(DC), via mutation of APC, which is observed in the vast majority of sporadic colorectal tumours[123]. Less commonly, truncation of AXIN[124] or aberrant phosphorylation of GSK3b[125] impairs DC competence. 2) Gain of function due to BCAT mutations that prevent its association with the destruction complex[126]. 3) Over expression of Frizzled receptors (increasing stem cell sensitivity to Wnts)[127], and 4), loss of feedback mechanisms that interfere with receptor ligation, typically via inactivation of SFRPs, DKKs and WIFs due to aberrant promoter methylation that inhibits RNA synthesis[128-130].

Regardless, these effect the same response as Wnt-receptor ligation i.e. accumulation of cytoplasmic BCAT, nuclear translocation, and S-phase transition, only this time in the absence of sustained Wnt signalling. Constitution of Wnt drives the formation of microscopic hyperplastic lesions known as aberrant crypt foci - observable histologically by the accumulation of nuclear BCAT that precedes macroscopic tumourigenesis[131]. The dependency of homeostasis on proper regulation of Wnt is elegantly demonstrated by the conditional inactivation of APC in normal epithelia by RNA interference, which triggers polyp formation. Conversely, withdrawal of treatment reconstitutes degradation of BCAT, the rapid regression of established lesions, and a return to normal epithelial architeture[132].

Mutational incompetence of Wnt regulation differs temporally to loss of redundancy via antagonist inactivation; the former is a consequence of sporadic genomic events, while the latter is consequent to creeping deregulation of methylation metabolism over time, with no change to the underlying sequence or associated protein functionality. Epigenetic silencing of Wnt antagonists (Was) in this context is only tumourigenic when alternative options for regulating

proliferation have been exhausted. Aberrant DNA methylation, an early observation in colorectal tumourigenesis, forms a corner stone of our hypothesis and will be discussed in greater depth shortly.

Importantly, constitutive activation of Wnt signalling in CSC does not necessarily transform lesions to a carcinogenic phenotype, with risk of progression being age-dependent; around 25% in under 60s and 40% beyond[133]; APC mutations and deleterious DNA methylation are initiating factors in tumourigenesis, but typically lesions are well circumscribed, properly differentiated, slow growing, and confined to the epithelium[134]. This is due to an upregulation of compensatory anti-proliferative pathways by which CSC control tissue growth, such as the RAS/RAF or PI3K/AKT pathways. Due to impaired regulation of Wnt, CSC become necessarily dependent on these alternative pathways[135]. When further mutations are effected in compensatory streams, benign adenomas transition to a more aggressive phenotype, and proliferation goes into over-drive, resulting in large bulky tumours that may obstruct the bowel - a classic presenting symptom of an otherwise benign mass[136].

The final insult, conferring true malignancy, is the loss of DNA repair protein P53, leading to spontaneous genome instability and the *de novo* activation of a host of dormant activities optimised for tissue growth and motility in embryogenesis - encouraging angiogenesis, invasion through the bowel wall, and ultimately metastasis to distant organs[137]. This multistep paradigm of initiation, through progression, to transformation was initially proposed by Vogelstein in 1990, and check-points in the process have since been comprehensively characterised (figure 3c)[138]. The early appearance of epigenetic lesions, suggests that preventing initiation by modulating DNA methylation patterns, could compensate for activating mutations later, favourably modifying the risk of progression[139].

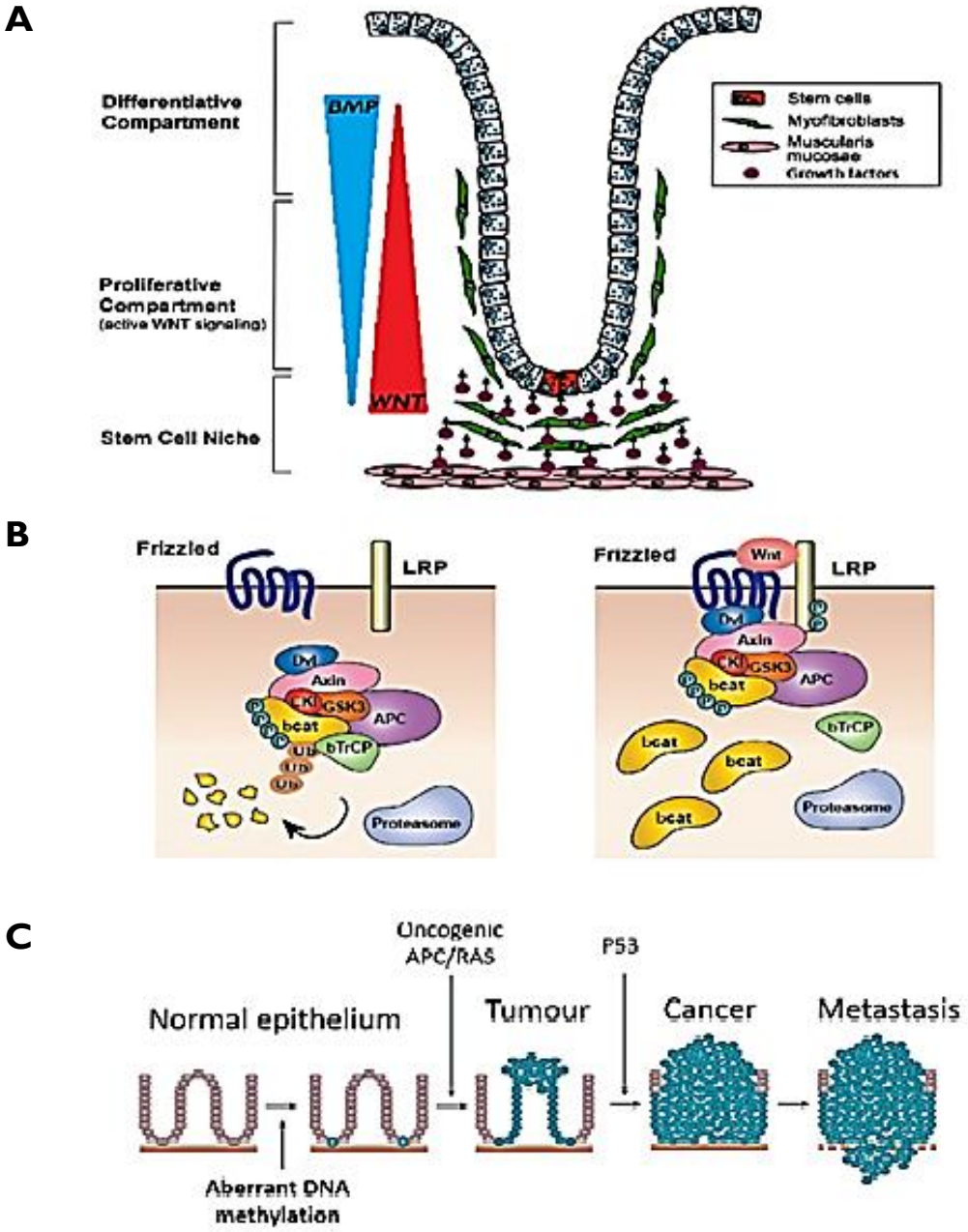

Figure 3 – Epithelial homeostasis in the distal bowel A) The colonic crypt is comprised of three compartments; a stem cell niche containing pericryptal myofibroblasts that provide a source of paracrine growth factors and structural proteins to support stem cell function (green cells); a transit amplifying compartment with committed progenitors supplying progeny for the epithelia; and a differentiated epithelial sheet that emanates Wnt antagonists and BMP agonists, promoting terminal differentiation and apoptosis at the luminal interface. Gradients of growth factors are regulated along the crypt axis that ensures maintenance of crypt topography. B) The canonical Wnt pathway cycles stem cells – in the absence of Wnt ligands the Axin/APC/GSK destruction complex tags cytosolic β-catenin for proteasomal degradation. Ligation of membrane LRP attracts frizzled receptors and subsequent dissolution of the destruction complex; cytosolic saturation with β-catenin precipitates nuclear translocation and transcription of TCF-targets that drive stem cell turnover. The pathway is aberrantly activated in CRC C) Adaption of Vogelstein's multi-hit model of cancer initiation, where aberrant epigenetic silencing of Wnt mediators via promoter *hypermethylation* is an early finding in macroscopically normal epithelia, priming cells for transformation in the context of subsequent oncogenic mutations

Aberrant DNA methylation in CSC primes the epithelia for transformation

In the early 21st century, colorectal cancer (CRC) remains a significant health burden in developed countries, with lifetime risk of adenoma 40% and malignant carcinoma a little over 5%[140,141]. Importantly, the increase in CRC is associated with the evolution of pro-inflammatory Western diets (high in fat and protein, and deficient in nutrients, phytochemicals, and fibre), compounded by a shift towards sedentary lifestyles, suggesting that risk is dynamic in response to environmental exposures[142-144]. The association of environment with risk is evidenced by the mean global rate of colon polyp at 40%; 85% in Westernised populations and >2% elsewhere. With over one million cases reported globally, CRC accounts for 10% of all new cancer diagnoses each year, two thirds of which occur in developed nations[145]. In Europe and North America incidence is approximately 50 per 100,000[145] and in the UK it is the 2nd and 3rd highest cause of cancer death in males and females, respectively[146].

Importantly, the single biggest risk factor for sporadic CRC is advanced age, with rates increasing rapidly in the 50+ demographic, and 90% of all new diagnoses occurring in this group[147]. Medical advances have increased life expectancy during recent years, driving an anticipated increase in CRC incidence that is compensated for by bowel cancer screening programmes, ultimately reducing overall mortality due to CRC[148]. Currently the Dukes (tumour/lymph nodes/metastasis) staging system is employed to describe the progression of CRC, observing the size and physiological extent of the tumour, and metastatic spread, which negatively correlates with prognosis. Five-year survival rates stand at 93% for Dukes A (non-invasive) down to just 6% for Dukes D (distant metastases), highlighting the need for early intervention[149,150].

Much work has been done to identify modifiable risk factors for CRC. These principally indicate cessation of smoking, increased physical activity, reduced consumption of red meat and alcohol[151-154]. Inflammatory co-morbidities – namely Crohn's and UC, but also obesity-driven inflammation and age-related decline in immune function (immunosenescence or inflammageing) - negatively impact on lifetime CRC risk[155-157]. In patients with chronic IBD, the risk of developing a

malignant lesion following diagnosis is 1 in 5 over 30 years, killing 50%+ due to complications arising from colitis-associated cancer (CAC)[158]. The risk of CAC is attenuated by effective clinical management of the underlying condition[159]. While a role for chronic inflammation in the aetiology of colorectal tumourigenesis is well recognised, molecular mechanisms are diverse and incompletely categorised, but primarily involve IBD initiation by INF□, followed by persistent elevation of mucosal cytokines TNFα, IL6 and IL1β[160,161].

Inflammation is involved in the propagation of CRC at every stage; initiating mutations are expedited by sustained DNA damage from reactive oxygen species released by inflammatory mediators and/or direct oxidation of mismatch repair proteins. Inhibition of the NFκB/COX2/PGE2 pathway is recognised to attenuate the molecular signatures of transformation[155,162], and vitamin D is shown to attenuate NFκB signalling in intestinal epithelium - posited as a mechanism by which sufficiency modifies mucosal inflammation and thus CRC risk[163]. Maintenance of sporadic tumours is passively promoted by inflammatory cytokines that encourage proliferation and angiogenesis as a means of resolving epithelial hypotrophy effected by inflammation. During metastatic progression, *de novo* secretion of chemokines by tumour cells amplifies the inflammatory milieu, promoting a brisk T-cell infiltrate and establishing a positive feedback loop[164].

Colorectal tumourigenesis typically follows a well-established progression from non-invasive adenoma to malignant carcinoma[165]. Evidence includes a spike in adenoma incidence five years prior to peak CRC rate[166], polyps excision reducing the incidence of CRC, and adenomas presenting with foci of poorly differentiated cells[167]. Equally, invasive tumours are frequently found to harbour central areas of adenoma[168]. While sporadic mutation of tumour suppressors, activation of quiescent oncogenes, and impaired mismatch repair/microsatellite instability, initiate tumour formation, epigenetic silencing of Wnt tumour suppressors is documented in macroscopically normal epithelium[169] – a process itself accelerated by inflammatory mediators[170].

Referring to the fact that the genome may be modified without alteration to the underlying nucleotide sequence, epigenetic phenomena allow for the differential expression of gene products in a myriad of cell types, with heterogeneous phenotypes derived from a common genome. Epigenetic modifications define tissue-specificity during embryogenesis, drive differentiation, and confer cellular plasticity in response to environmental cues[171]. Modifications direct transient (histone modification, RNA interference) or stable (DNA methylation) stereochemical remodelling of the chromatin, and epigenetic management of conformation achieves several goals. Practically it allows over two meters of DNA to fit within the nucleus, and locks down pernicious retrotransposon sequences - acquired over evolutionary time - that sporadically disrupt sequence integrity[172]. Heritable modifications inhibit transcription of sequences not contributing to phenotypic function, particularly in the case of imprinting that defines sex-linked inheritance during gametogenesis[173]. To facilitate a plastic response to environmental stimuli, acetyl and methyl groups are transiently applied to DNA histones by modifying enzymes, recruited by cognate transcription complexes - as described for vitamin D.

Perhaps due to its stability as an epigenetic mark, and binary dynamic, DNA methylation is the most studied epigenetic mark, recognised for its role in establishing and maintaining phenotype-specific methylomes between successive generations of cells[174]. Succinctly, it involves the enzymatic addition of a methyl group to the 5th carbon of cytosine's central ring (C $\rightarrow$ 5mC) - only thermodynamically permissible when the nucleotide occurs directly before a guanine i.e. cytosine methylation occurs exclusively in the context of CG dinucleotides (although exceptions to this rule are observed during embryogenesis and haemopoietic differentiation)[175].

CG cytosines account for less than one percent of all cytosines in the human genome, of which some 70% are methylated, typically present in long interspersed elements (LINEs), promoting heterochromatin conformation and genome stability. Conversely cytosines in coding sequences tend to be unmethylated, hinting at their role in transcriptional regulation[176].

CG frequency throughout the genome is lower than the anticipated 1/16 due to the phenomena of CG suppression, where-by methylated cytosines spontaneously de-aminate over evolutionary time, mutating to thymine residues. Unmethylated cytosines also deaminate, but to uracil residues, which are identified by DNA repair mechanisms, unlike 5mC-derived thymines[177]. Sequences where the frequency of CG dinucleotides is conserved, approaching the anticipated ratio, are known as CG islands (CGIs), defined as being between 200 and 500 bases in length, with a CG content exceeding 50%[178].

Half of all transcribed genes exhibit promoter sequences containing islands proximal to their transcription start site, which serve as attachment regions for transcriptional machinery and co-modulators[176]. The established paradigm is that, to permit interaction of TFs, promoters must be unmethylated. Methylated CGIs, attracts 5mC binding factors (MECP2) and associated corepressors that re-model the local chromatin environment through the recruitment of HDACs[179]. However, promoter hypomethylation confers only transcriptional competence, as opposed to guaranteeing expression[180]. The dogma that increases in promoter methylation status necessarily correlate with decreased transcription, has recently been called into question by novel reports of hypermethylated gene promoters being associated with active transcription in multiple tissues. Although it is not yet known if conditional demethylation of these *hyper-* sites functionally inhibits transcription, the authors identify distinct sequence motifs in hypermethylated sites of active transcription verses *hypo-* sites, suggesting two independent mechanisms are involved in the metabolism of 5mC and transcription factor binding of *hypo-* vs *hyper-* methylated CGIs[181]. The paradigm is further compromised by techniques for methylome analysis not biased towards defined CGIs; these reveal additional hypermethylated CG rich regions several KB proximal to TSS CGI (termed enhancers, or CG island shelves and shores), that are associated both with active transcription, and downstream CGI hypomethylation, raising the possibility that the process of CGI methylation itself is dependent on upstream motifs or chromatin status[182].

The idea that *de novo* methylation of promoter CGIs is dependent on upstream events is not a new one, having been speculated by our group and others[183]. Specifically, binding of the transcription factor SP1 in island shelves appears to confer protection from *de novo* methylation of the islands themselves, and it's loss precipitates CGI hypermethylation and inhibition of transcription[184].

With regards *de novo* promoter CGI methylation in CRC initiation, Belshaw et al suggest an all-or-nothing process, supported by others, that shows gene promoter regions are found to exhibit methylation values of either less than 10%, or more than 90%, of all island CGs (figure 4b)[185]. Un-characterised upstream motifs or binding factors are again implicated by the directional accumulation of methyl marks in Wnt antagonist promoters (5' → 3')[186].

Methyl groups required for *de novo* methylation are provided by s-adenosyl-methionine (SAM), synthesised from dietary folate[187]. Recent reports associate folate intake and circulating folic acid positively with the rate of aberrant DNA methylation in the colonic epithelia[188] – although these findings may be a cause for concern, they again bring to light the opportunity to modify methylation patterns throughout life via nutritional intervention.

5mC metabolism is mediated by two classes of enzymes (figure 4a); DNA methyltransferases (DNMTs) catalyse the addition of methyl groups to CGs[189], while ten-eleven translocation enzymes (TETs), demethylate 5mC via oxidation of 5-hydroxy-mC intermediates[190]. There are three DNMTs responsible for DNA methylation; DNMT1, 3a, and 3b. Primarily, during gametogenesis, 3a and 3b cooperate to establish genomic methylation patterns necessary for phenotypic specificity on globally *hypo*-methylated DNA (*de novo* methylation)[191]. Loss of either or both during embryogenesis maintains embryonic stem cells in a pluripotent state[192]. Once established, DNMT1, which exhibits a preference for hemi-methylated DNA strands during mitosis, takes responsibility for somatic replication of the pattern on the opposing strand (maintenance of DNAm patterns)[193], so loss of 5mC is also consequent to impaired replication fidelity, which sees successive reduction in global methylation between iterations of cells following deletion of DNMT1[194].

Conditional knock down of DNMT1 is fatal in embryogenesis, but not necessary for survival of CRC *in vitro*, where surprisingly 80% of methylation is conserved in progeny. Furthermore, knock down of either 1 or 3b demonstrates dynamic compensatory mechanisms, whereby the effects of deficiency of either appears to be annulled by the continued expression of the other, and it is only simultaneous knock down that perturbs methylation metabolism sufficiently to effect genomic instability via global hypomethylation[195,196], i.e. DNMT1 and 3b cooperate to effect and maintain DNAm patterns in CRC.

Metabolism of 5mC is invariably dysregulated in CRC. In fact Baylin et al observe that aberrant CGI methylation patterns have been documented for practically every known neoplastic disease[197]. Deregulation falls into three categories; gene-specific tumour suppressor hypermethylation (macroscopically healthy epithelium), global (non-CGI) hypomethylation (healthy mucosae and tumours), and a non-specific CGI hypermethylating phenotype in CRC, termed CIMP.

Global hypomethylation increases with age[198], leading to the unlocking of transposable elements, chromosomal instability, increased tumour frequency, and oncogene activation[199]. Global methylation status may be assessed by the analysis LINEs, which constitute as much as 20% of the genome. Their methylation status is therefore assumed to extrapolate to a global view of the DNAm landscape. Baba et al have defined a subset of CRCs which exhibit extreme LINE1 hypomethylation, and more recently LINE1 hypomethylation is shown to be associated with proximal colorectal lesions, much like CIMP[200-202].

DNMT3b in particular has an important role to play in CRC aetiology and is unique amongst the DNA methyltransferases in that it is represented by a number of alternatively spliced isoforms, expressed in a tissue-specific fashion[203]. Aberrant age-related DNAm of Wnt antagonists is well documented in un-involved mucosae[186,204], and is associated with deregulated DNMT3b activity: overexpression of 3b in APC mutants increases tumour incidence and size and is associated with hypermethylated gene silencing. In contrast overexpression of DNMT3a shows no increase in promoter methylation, and tumour burden is comparable to control mutants[205]. DNMT3b expression, effecting

hypermethylation of tumour suppressors, typically increases over time in multiple cancer-prone tissues[206-208]. Presumably the two forms of hypermethylation (age-related verses CIMP) are independent phenomena, as the former is not pathogenic in and of itself, while the latter is associated with rapid progression and poor prognosis.

A corner-stone of our informing hypothesis, Belshaw et al observed that a subset of Wnt tumour suppressors (APC, DKK, WIF1, SFRP1, 2, 5) were differentially methylated in individual colonic crypts in both an age-dependent fashion, and in relation to disease status[186]. These results are supported by the observations of Tapp et al, who correlate age with differential methylation in a cohort of 185 healthy individuals. Their principal component analysis shows an increase in CGI methylation related to age for the panel of genes characterised (figure 4c), and supports the theory of aberrant age-dependent gene silencing by hypermethylation contributing to epigenetic field effects, that prime the epithelia for transformation by removing options by which CSC may regulate constitutive Wnt activity[209].

Age-related aberrant DNA methylation of WAs is influenced by nutritional factors

Importantly Tapp et al also correlate a variety of nutritional factors with the rate of acquisition of age-related DNA methylation for genes analysed (figure 4d); the methyl donor folate, was found to increase methylation of APC, SFRPs1 and 2, SOX17, and N33 (aka tumour suppressor candidate 3, TUSC3) in a pattern similar to age-related effects. Interestingly folate has previously been linked to abnormal methylation of SFRP1 in adenomatous polyps[210], supporting the hypothesis that age-dependent methylation is a) modifiable by nutritional regimen and b) may dispose the colonic epithelia to neoplastic progression.

Consistent with the paradigm that serum vitamin D has a protective effect against colorectal cancer[211], and specifically relevant to this project, Tapp et al also found that vitamin D status positively influenced age-related DNAm effects for HPP1, APC, SFRPs1 and 2, WIF1, MYOD1 and N33, as well as contributing to genomic stability by maintaining *hypermethylation* of LINEs[212].

Vitamin D has also been shown to down–regulate BMP2 *in vitro* in bone marrow stromal cells via VDR binding in the gene's promoter, which induced complete methylation of the lone CGI in that region, strongly suggesting transcriptional repression by vitamin D-mediated DNA *hypermethylation*, demonstrating a role for vitamin D influencing DNAm patterns[213].

The negative association of vitamin D sufficiency with promoter methylation has been reproduced in other WAs by Rawson et al, who established an inverse linear relationship between vitamin D status and DKK1 methylation in a large cohort of CRC patients (n = 992). The same study also established that vitamin D favourably influenced the methylation status of WNT5a, an extrinsic Wnt antagonist secreted by mature colonocytes, concentrated in the differentiative compartment [214]. As well as the attenuation of age-related DNAm, intriguingly vitamin D has also been shown to ameliorate established hypermethylation of ECAD in epithelial breast cancer cells *in vitro*, reconstituting its expression and promoting cancer cell differentiation[94]. Vitamin D is also reported to effect spontaneous *hypomethylation* of MG63 (osteosarcoma), PTEN, RARB2, and PDLIM2 (breast cancer)[95]. Stefanska et al speculate that, as an anti-proliferative, vitamin D induces the master transcription factor AP-1, itself a negative regulator of DNMT1 - thus vitamin D might effect gradual loss of promoter 5mC via passive demethylation associated with impaired DNMT1 copying fidelity[215], as opposed to inhibiting *de novo* DNAm.

Specifically, although vitamin D is observed to be *associated* with dynamic DNA methylation in both healthy and transformed epithelia, there are no reports detailing mechanistic aspects by which vitamin D might mediate these effects. Elucidation of these is important given the epidemiology of vitamin D insufficiency, and potential to mitigate for neoplastic transformation in the context of acquired mutation later in life.

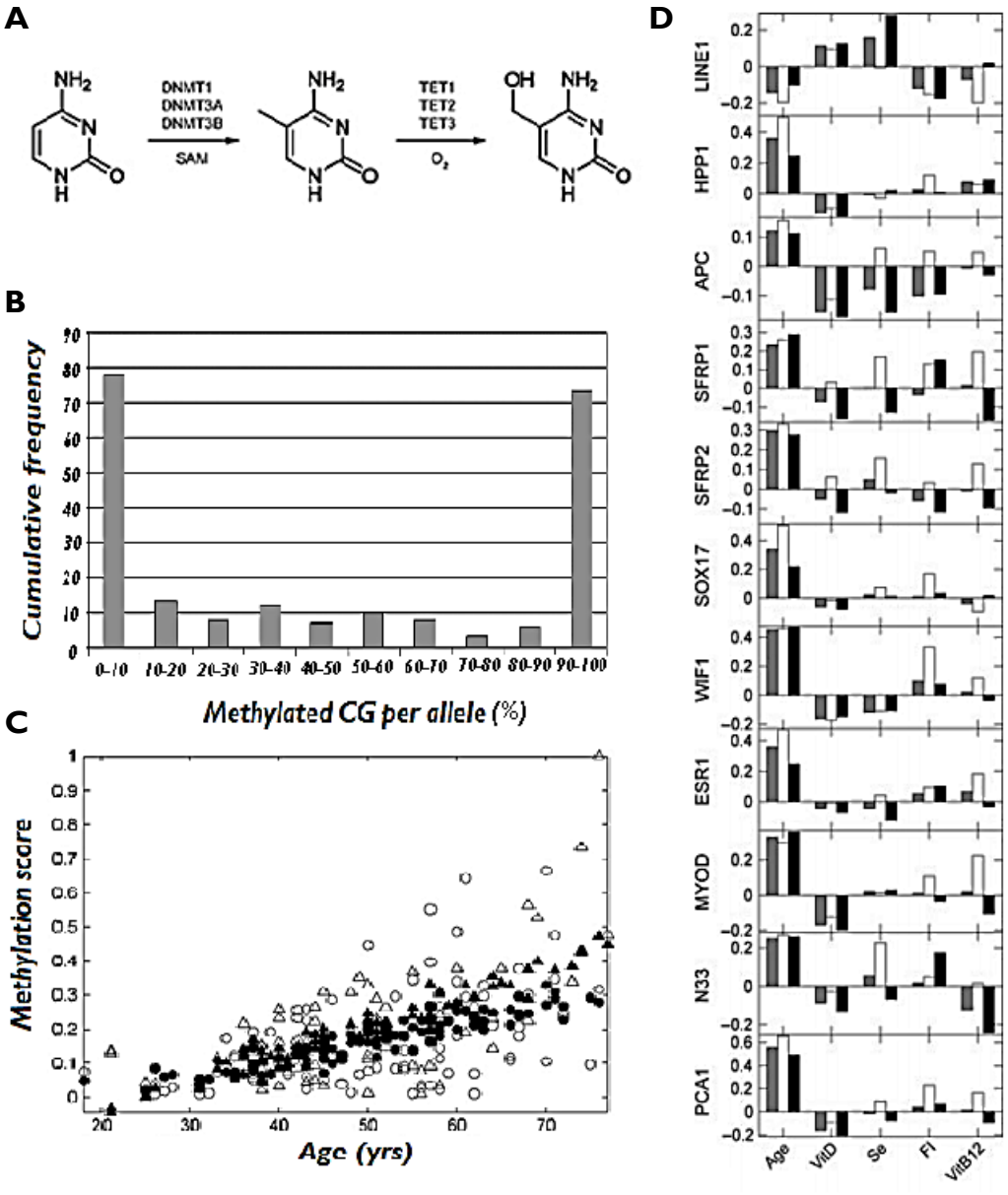

Figure 4 – Dynamics of DNA methylation a) Methyltransferase enzymes catalyse the conversion of cytosine to 5mC during embryogenesis and mitosis. S-adenosyl methionine (SAM) acts as the universal methyl donor. Recently 10/11 translocation enzymes (TETs) have been shown to orchestrate active demethylation of 5mC via 5hmC b) CG island methylation is demonstrated to be an all-or-nothing process, with methyl marks flooding in from the 5' direction, proximal to the gene body. This work by Belshaw et al shows that while average DNAm increases in promoters over time, for individual islands, hypermethylation is a spontaneous event, i.e. occurs rapidly and completely, suggestive of a threshold or trigger event. C) A principal component analysis by Tapp et al assigns a methylation score, based on the methylation status of a panel of surrogate genes in healthy colonic biopsies, which is shown to positively correlate with participant age d) Pearson correlation coefficients for the associations between the exposure variables (age, vitamin D status, selenium, and the methylation of the nine genes, LINE-1 and principal component analysis for all subjects (grey), males only (white) and females only (black). Age shows a strong correlation with DNAm in the promoters of all genes, while conversely, vitamin D is negatively associated with aberrant, most strongly for HPP1, APC, WIF1 and MYOD1. Sex-effects are noted for SFRPs. Adapted from[212]

In summary

Vitamin D acts as both a systemic and local anti-inflammatory, modulating immune function. Sufficiency is well established to be associated with reduced rates of inflammatory bowel disease and colorectal neoplasia, and furthermore, being prognostically favourable, predicts the course of both diseases. Vitamin D insufficiency is prevalent. Vitamin D status is negatively associated with the rate of aberrant age-related methylation silencing Wnt tumour suppressors in the distal colon, and is shown mechanistically to effect *hypomethylation* and reconstitution of tumour suppressors in transformed epithelia.

It is not established whether the association of vitamin D status with aberrant DNAm patterns in the bowel is consequent to an effect of the compound mediating DNAm metabolism or inflammation-associated aberrant DNAm in healthy epithelia over time, or conversely, if Vitamin D status is determined synchronously by esoteric processes that are coincidentally associated with tumourigenesis.

Research questions;

Firstly, is the association of vitamin D with DNAm in healthy epithelia recapitulated *in vitro,* i.e. is vitamin D insufficiency mechanistically responsible for the prospective difference observed in DNAm patterns?

If so, how does vitamin D act to reduce aberrant methylation? As a systemic or local anti-inflammatory? By promoting differentiation of immune cells, immune function, resolution of inflammation? At the molecular level, does vitamin D effect cytokine secretion, or NFκB signalling associated with increased DNAm in epithelial cells? Equally, could vitamin D affect toll-like receptor expression or signalling implicated in aberrant DNAm of WAs in CSC?

Does vitamin D act mechanistically to modulate 5mC metabolism, directly attenuating effects of inflammation or ageing at the nucleic acid level? Does vitamin D effect a gradual loss via impaired DNAm pattern fidelity, inhibit *de novo* DNAm, or promote active demethylation via TET activity?

Hypotheses

In order to determine whether vitamin D specifically exerts a protective effect against WA *hypermethylation* in healthy CSC, and furthermore, whether vitamin D might resolve aberrant DNAm patterns in CRC compromising homeostasis, the following hypotheses are proposed that require elucidation;

1) Vitamin D moderates systemic inflammatory mediators shown to drive aberrant DNAm in CSC.
2) Vitamin D mediates inflammatory signalling in the crypt niche responsible for aberrant DNAm in CSC.
3) Vitamin D modulates 5mC metabolism in CSC via regulation of DNA methyltransferase and/or TET activity
4) Vitamin D's antiproliferative effects in CRC lines *in vitro* are in part effected via amelioration of established pathological DNAm patterns

Aims and objectives

1) With regard systemic inflammatory mechanisms mediated by vitamin D; Vitamin D promotes differentiation of circulating monocytes and acts to reduce systemic inflammation via regulation of inflammatory cytokines. Differentiation and transcription are both regulated in part by permissible DNA methylation patterns, and Vitamin D may mediate its effects via modulation of DNA methylation;

Characterise the effect of vitamin D on monocytes *in vitro* to determine if

I. Vitamin D promotes their differentiation
II. Vitamin D regulates cytokine expression
III. Vitamin D effects differential methylation controlling cytokine transcription

2) With regards mitigation of local inflammation in the crypt niche by vitamin D; mucosal inflammation is in part mediated by pericryptal myofibroblasts. Mucosal inflammation accelerates aberrant DNA methylation in CSC. Vitamin D is associated with reduced mucosal cytokine expression;

Characterise the effect of vitamin D on pericryptal myofibroblasts to determine if

I. Vitamin D modifies their secretory profile
II. Their secretory profile affects DNAm patterns in CSC
III. Their secretory profile regulates 5mC metabolic enzymes in CSC

3) With regards vitamin D mediated attenuation of aberrant age-related DNAm in CSC; Vitamin D is associated with the rate of aberrant DNA methylation in CSC, although there are no specific reports that demonstrate vitamin D directly modulates 5mC metabolism;

Characterise the effect of vitamin D in CSC to determine if

I. Vitamin D regulates transcription of WAs
II. Vitamin D attenuates the acquisition of aberrant DNAm
III. Vitamin D modulates 5mC metabolism/DNMT activity

4) With regards vitamin D mediated amelioration of established aberrant DNAm in CRC; vitamin D acts as an antiproliferative *in vitro* for most CRC cells lines with a functional VDR, although its mechanisms are not completely elucidated. Vitamin D sufficiency is associated with reduced mortality and improved prognosis following a diagnosis of CRC;

Characterise the effect of vitamin D sufficiency in CRC cell lines to determine if;

I. Anti-proliferative effects are sustained beyond treatment
II. Vitamin D ameliorates WA *hypermethylation*
III. Vitamin D modulates 5mC metabolism/DNMT activity

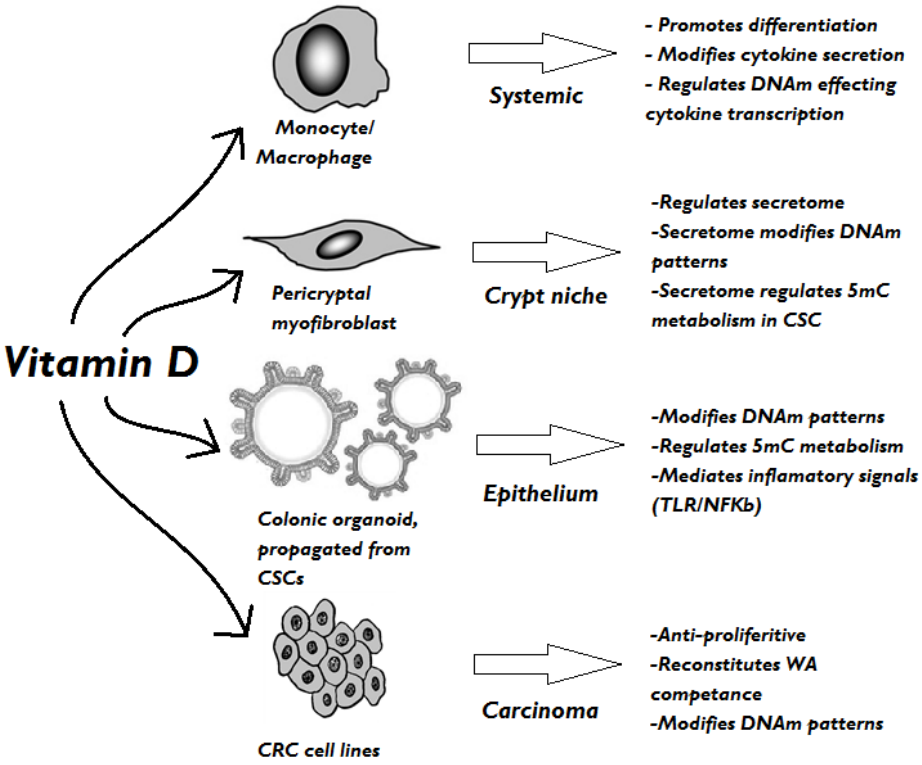

Graphical abstract

Figure 5 – Graphical abstract. Detailing cell lines employed to investigate vitamin D's effects promoting bowel health in systemic, mucosal, and epithelial environments.

Notes

A brief note on terminology – unless stated, hence fourth the term 'vitamin D' will be used to refer to the biologically active form of the compound (calcitriol), while it's inactive precursor, calcidiol, will be referred to as 'serum vitamin D'.

Regarding the methylation status of promoter CGIs analysed in this text, while promoter methylation is established by nucleotide-level sequencing as an all or nothing process, typically the average DNAm status of multiple alleles is reported, which may be hypo- or hyper-methylated in individual cells that constitute the sample i.e. a methylation value of 40% refers to the fact that 40% of *all* alleles in the sample were 100% *hyper*-methylated, and vice versa, and does not refer to a partially methylated promoter CGI.

Chapter 2

EXPERIMENTAL APPROACH AND GENERAL METHODS

Experimental approach

Given the ubiquitous distribution of the VDR, multi-level molecular effects of the compound, and the association of serum vitamin D with a panoply of health outcomes, a canonical approach to experimental objectives was developed that established vitamin D's effects promoting bowel health, in the broader context of whole-organism homeostasis.

In this respect, concurrent to investigating stem cell-intrinsic effects of vitamin D on DNAm, the experimental approach also encompassed systemic effects (whole-blood/immune function), and paracrine mediation of the stem cell niche by pericryptal myofibroblasts. Furthermore, this comprehensive approach included healthy and diseased models, incorporated a variety of tissues, and assessed both *in vivo* and *in vitro* aspects of vitamin D's function.

Systemic effects of vitamin D promoting bowel health

Chronic inflammatory diseases effecting the distal bowel are characterised in part by elevated serum cytokines, and patients are at greater risk from sporadic tumour formation[216-218]. In part this is due to systemic and mucosal inflammation accelerating the process of aberrant, age-related DNA hypermethylation in CSC. Vitamin D exerts potent anti-inflammatory effects and promotes immune cell differentiation, regulating cytokine production. It has been noted that DNAm patterns in peripheral blood mono-nucleated cells (PBMCs) regulate cytokine transcription and are associated with immune cell differentiation. Furthermore, leukocyte ratios in the peripheral blood are associated with aberrant DNAm in the colon. These observations led to speculation that vitamin D exerts it's protective effects in the colonic epithelium by acting as a systemic anti-inflammatory, modulating the leukocyte pool and influencing serum inflammatory markers[219]. In collaboration with The University of Auckland, NZ, the effects of vitamin D supplementation (delivered via a randomised cross-over intervention), on serum vitamin D, markers of chronic inflammation, and DNA methylation patterns in PBMCs, from a small cohort of healthy individuals was investigated. The results from these experiments were verified *in vitro* using the THP1 monocyte line.

Pericryptal myofibroblast regulation of the stem cell niche

Sub-epithelial pericryptal myofibroblasts (MFBs) interact with CSC via chemokine signalling in the niche. In tumour stroma, dysregulation of the fibroblast secretome permits carcinogenic transformation by encouraging invasion, migration and angiogenesis. Furthermore, vitamin D status is associated with a reduced risk for IBD, the hall mark of which is mucosal inflammation mediated in part by pericryptal myofibroblasts. It was speculated that MFBs in transformation-prone epithelia might promote aberrant age-related DNAm in CSC via a deregulated secretory profile, and that vitamin D indirectly influenced DNAm patterns in CSC by moderating inflammatory processes in pericryptal myofibroblasts. Culture conditions were optimised to procure three primary lines of sub-epithelial myofibroblasts from the uninvolved mucosa of colorectal cancer resection specimens, and characterised their secretomes in response to TNFα and vitamin D using LC-MS/MS proteomics and sandwich ELISAs. To elucidate the effect on DNAm in CSC, colonic organoids (propagated from the same biopsies i.e. case-matched), were cultured with MFB supernatants or inflammatory mediators for one month, and their DNAm patterns interrogated by Illumina methylation array.

Colonic organoids

Sato's revolutionary papers in 2009 and 2011 refined methods for the extraction of colonic crypts, and optimised *in vitro* culture in a three dimensional collagen matrix[220,221]. Here, crypts spontaneously form spherical cysts, later producing buds that proliferate and differentiate into functional crypts, with circumscribed compartments, a luminal interface, and importantly, static populations of $LGR5^{+ve}$ stem cells. Organoids have been comprehensively demonstrated to emulate the topography of the colonic epithelia, however this is in the absence of a supporting niche, meaning mechanisms of epithelial homeostasis can be investigated in isolation. This model was utilised for experiments investigating the effects of vitamin D and inflammatory mediator PGE2, on DNAm patterns in CSC. Organoid DNA was interrogated on the latest iteration of Illumina's EPIC DNA methylation array that characterises the methylation status of over 850,000

CG dinucleotides, reported as a beta-score that equates to percentage promoter methylation.

Colorectal cancer cell lines

Not only is vitamin D status associated with a reduced risk of developing CRC, following diagnosis, those with vitamin D sufficiency show better rates of remission and improved over-all five year survival. Having speculated that vitamin D might attenuate the process of aberrant DNAm, in light of its prognostic properties it was hypothesised vitamin D might also ameliorate DNA hypermethylation, thereby reconstituting epigenetically silenced tumour suppressors. There are a multitude of validated colorectal cancer cells lines available for *in vitro* studies; four were selected for their mutational diversity and discrete phenotypes (figure 6). CaCO2 and DLD1 are of particular interest as they exhibit the APC deficiency necessary for hyper-proliferation, but with intact BCAT function. CaCO2 cells also show intact alternative pathways which can modulate proliferation, so it was anticipated that these cells would be the most sensitive to inhibition of Wnt by *de novo* WA hypomethylation.

	CaCO2	**DLD1**	**HCT116**	**HT29**
APC	x	x	Wt	xx
β-CAT	Wt	Wt	x	x
B-RAF	Wt	Wt	Wt	x
K-RAS	Wt	x	x	Wt
TGβr2	Wt	x	x	Wt
p53	x	x	Wt	x

Figure 6 – Oncogene mutations reported by the manufacturers (ATCC) for the cell lines employed in investigations. X = heterozygous mutant allele XX = homozygous mutant allele. Wt = wild type.

Model overview

Model	***Source***	***1γ Readout***	***Insight***	***Validity***	***Limitations***
PBMCs	Peripheral blood, healthy individuals	Regulation of cytokines	Systemic, whole organism	*In vivo*, human, healthy cohort	Heterogeneous lineage, small cohort
THP1 monocytes	ATCC. Peripheral blood, AML	Regulation of cytokines	Systemic, whole organism	Verify PBMC results	Neoplastic, genomic instability
Pericryptal MFBs	Un-involved mucosa, proximal to tumour	Mucosal inflammation, GF signalling	Regulation of the stem cell niche	Primary, Patient-matched, $VIM^+/\alpha SMA^+$	Aged, disease-associated tissue
Intestinal MFBs	Lonza. Embryonic	Mucosal inflammation, GF signalling,	Regulation of the stem cell niche	Validation in healthy cells, positive control for primary MFBs	Embryonic, Replicative senescence
Colonic organoids	Un-involved mucosa, proximal to tumour	DNA methylation patterns	Cell intrinsic modes, protective effect	Primary, non-transformed, niche independent	Aged, disease-associated tissue
CRC cell lines	ATCC. Adeno-carcinoma	DNA methylation patterns	Cell intrinsic modes, restitution	Established Wnt antagonist hypermethylation	Not translatable to healthy tissue

Figure 7 – Comparison of models. Table detailing the suitability and limitations of model employed to investigate the effects of vitamin D promoting bowel health.

Readouts

In order to investigate the effects of vitamin D, a set of readouts were defined to give comprehensive insights into the mechanisms by which end-points were brought about. The informing hypothesis in most cases was that dynamic DNA methylation in the gene promoter would affect transcription, that in turn would influence protein expression, ultimately modulating the phenotype of the cell. Thus, it was sought to verify any differential DNAm by consolidating the results to RNA and protein readouts, and measurement of some phenotypic characteristic. If verification failed at any level, new testable hypotheses are indicated to identify the point in the chain that events were disrupted, having excluded the primary scenario (for example post translational modifications or RNA interference). Analysis was either performed in a gene-specific fashion where likely targets were identified, or using array-based approaches like LC/MS-MS proteomics and DNAm bead chips.

Assay	***Readout***	***Effect***
CoBRA	Promoter CGI methylation status	DNA methylation
QMSP	Promoter CGI methylation status	DNA methylation
Illumina Bead Chip	Global methylome	DNA methylation
Q-rt-PCR	Relative transcripts	RNA
Wnt reporter activity	TCF-LEF activity	RNA
WST1	Proliferation	Phenotype
Trypan blue staining	Cell viability	Phenotype
Western blot	Phospho- status, protein quantification	Phenotype
LC/MS-MS	Semi-quantitative secretome	Phenotype
Immunohistochemistry	Protein expression/localisation	Phenotype

Figure 8 – Assay repertoire. Assays employed to investigate effects of vitamin D promoting bowel health, detailing read-outs and the effect they measure.

Materials

A comprehensive list of kits, reagents, and compounds used is included in appendix 1, detailing supplier product codes and batch numbers where available. Henceforth in the text, only the item and the supplier will be referred to, which can be referenced to that sheet. A link to the manufacturer's instructions online is included where available, and detailed in brief here.

General methods

Specific treatment regimens are detailed in each chapter; to prevent unnecessary repetition later, here general methods employed throughout the project are outlined, with examples of optimisation and validation protocols where necessary. The methods detailed are routine wet bench techniques for cell culture and molecular cell biology techniques used to characterise cell phenotype and function - a training PhD project should furnish students with the analytical tools to practice independently, and as such this section may also be considered as an appropriate record of the training received.

Cell culture[222]

Transformed or immortalised cell lines were cultured in preparation for experiments in either 25cm^2 or 75cm^2 culture flasks (Thermo), passage number in most cases was under 20 for transformed lines and under 5 for primary lines. Culture was practiced aseptically in a class 2 extraction hood, and all materials were disinfected using 70% ethanol spray or 10% Bioguard. Cultures were routinely tested for mycoplasma as part of laboratory quality control procedures. Cells were incubated at 37°C at 5% CO_2. To passage, suspended cells were removed, spun at 300G for 5 minutes in a 15 mL falcon tube, and re-suspended in an appropriate volume of pre-warmed fresh medium. For adherent cells, media was removed, cells washed once with PBS (FBS in the media neutralises trypsin), and 2mL of Trypsin/EDTA (0.05%/0.53mM) (Life Technologies) added to the flask for 5 minutes at 37°C. Next, flasks were gently agitated to release adherent cells, media collected in 15mL falcon tubes, and spun at 300G. Cells were suspended in fresh media, and either seeded into new flasks to propagate lines, or seeded into cell culture plates (Corning) for experiments.

Cell line	Medium	Additives
DLD1, CaCO2, HCT116, HT29 CRC cell lines (ATCC)	DMEM F/12 + Glutamax (Life Tech)	10% Foetal Bovine Serum (FBS) 1% Penicillin/streptomycin (PS) (Life Tech)
Intestinal Myofibroblasts (InMyoFib) (Lonza)	Smooth Muscle Basal Medium (Lonza)	SmGM-2 SingleQuot Kit
THP1 monocytes (ATCC)	RPMI 1640 + Glutamax	10% FBS, 1% PS

Figure 9 – Media for cell culture**. Cell culture media preparations for transformed/immortal cell lines used to investigate the effects of vitamin D promoting bowel health.**

Participants

In line with the ethical approval for the project (FMH Ethics committee, University of East Anglia, REF 12/1385HT), participants with a diagnosis of recto-sigmoid adenocarcinoma were consented by authorised gastroenterology surgeons. A preference for males over females was specified due to the sex associations between $CIMP^{high}$ tumours in the proximal colon typical in females, versus $CIMP^{low}$ tumours in the distal colon typical in males[223]. Advanced age (>65 years old) was also specified where possible, to increase the likelihood of age-related DNAm processes having been previously initiated. Preliminary experiments optimising the protocol came from participants 1 through 10. Organoids and pericryptal myofibroblasts propagated for the arrays came from participants 11, 12, and 13.

Pathology

Case 11 - 45 year old male, ulcerating low rectal tumour – grade 2, Dukes B equivalent, adenocarcinoma arising on a background of adenoma. Non-invasive with no involvement of the nodes or vasculature. Negative for MLH1, MHS2, MSH6 with no evidence of microsatellite instability. No idiopathic inflammatory bowel disease. Case 12 - 65 year old male, low rectal tumour – grade 2, Dukes A equivalent, moderately differentiated adenocarcinoma invading the muscularis propria. No lympho-vascular invasion. Evidence of diverticulitis, but otherwise unremarkable. Case 13 - 61 year old male, mid rectal tumour – grade 2, Dukes B equivalent, moderate and poorly differentiated adenocarcinoma with apparent origin from a background adenoma. Invades the meso-rectum. Probable lymphatic invasion, no venous invasion. See appendix 3 for participant information.

Sampling and crypt recovery[224,225]

[In short, samples were washed with antibiotics, dissected and washed twice with antioxidant. 3x5 minute incubations with 2mM EDTA were performed, shaking to remove debris, before a final 35 minute incubation at room temp to dissociate crypts. 5 fractions were prepared in ice-cold PBS by 5 serial rounds of vigorous shaking. Crypts were spun (100G) and re-suspended in wash buffer ASAP to prevent crypt deterioration/necrosis]

Bowel resections were opened longitudinally and the faecal contents removed. The full thickness of the epithelia, mucosa and submucosa, were pinched together with forceps, and a ~5mm biopsy sample sliced off. This was immediately placed into transport buffer containing anti-biotic/mycotic preparations, on ice for at least 15 minutes. Samples were rinsed with ice-cold PBS, then dissected into 1mm^2 pieces. Pieces were placed in ice-cold DTT buffer for 5 minutes, twice. DTT buffer was removed and replaced with 5mL ice-cold 2mM EDTA for 5 minutes on ice, after which the falcon tube was vigorously agitated to release apoptotic debris, faecal matter, and mucous. This was repeated until no more single cells or debris were released. Samples were then incubated for 30minutes at 37°C for 30 minutes with 2mM EDTA. Vigorous shaking of the digested samples in PBS released 1000s of intact crypts, whose numbers were visually assessed. 200-300 crypts per well were removed, spun at 100G, and resuspended in wash buffer prior to seeding into matrigel.

Transport buffer

- 5mL PBS
- 50uL Fungizone
- 25uL Gentomycin
- 50uL Pen Strep
- 20uL Normycin

1mM DTT wash

- 10mL PBS
- 20uL of 0.5M DTT stock solution

2mM EDTA buffer

- 25mL PBS
- 100uL 0.5M EDTA stock solution

Re-sus/wash media/buffer

- 20mL Advanced DMEM
- 200uL Glutamax
- 200uL 1M HEPES (pH 7.4)
- 200uL Pen Strep
- 1mL FBS

Organoid culture[220,221]

Recovered crypts were seeded at 200-300 crypts per well. Crypts were re-suspended in 25uL of Matrigel (Corning) containing 1uL of Jagged1 (1μM) and 1uL Y27632 (10mM), and gently pipetted with a P1000 to evenly distribute crypts throughout the suspension. 30uL droplets were seeded into 24 well plates and cured for 15 minutes at 37°C, after which wells were flooded with 500uL organoid growth medium (see appendix 4) (to which treatments were added as detailed). Cysts typically form after 2-3 days and persist for up to 14 days, often bursting due to luminal turgidity and degradation of the matrigel. Cultures were passaged weekly, or as appropriate; media was removed, the well rinsed with PBS, the droplet detached and pipetted several times through a p1000 tip to breakup matrigel and release organoid fragments. Cultures were spun at 100G for 4 minutes at 4°C, which allowed apoptotic debris to be removed with the supernatant, leaving pellet of whole cysts and larger cyst fragments. These were digested using 200uL of TrypleE (Life Tech) for 5 minutes at 37°C, neutralised with 200uL wash buffer, and then disrupted by vigorous pipetting with a p1000 tip to dissociate single cells comprising the LGR5+ve population. These were re-suspended in matrigel and seeded into new plates as described.

Organoid media: 500uL of wash buffer with the addition of (see reagents list, appendix 1 and 4 for supplier) -

1x	B27	(from x50 stock)
1x	N2	(from x100 stock)
1mM	NAC	(from 100mM stock)
10uM	SB201090	(from 1mM stock)
1mM	Valporic acid	(from 100mM stock)
3uM	CHIR	(from 300uM stock)
140nM	PGE2	(from 14uM stock)
10mM	Nicotinamide	(from 1M stock)
50ng/mL	EGF	(from 50ug/mL stock)
375ng/mL	r-spo1	(from 100ng/mL stock)
100ng/mL	Wnt3a	(from 100ug/mL stock)
10nM	Gastrin	(from 1uM stock)
500nM	A-83-01	(from 500uM stock)
100ng/mL	Noggin	(from 100ug/mL stock)

Primary myofibroblasts culture[226,227]

The remaining pieces of mucosa that had been stripped of their epithelium were re-suspended in 5mL of wash buffer containing collagenase 1 (1 mg/ml), DNase I (0.3 mg/ml), Dispase (500uL), 5uL Ca2+ and 50uL Mg2+, for 30 minutes at 37 °C. The digestion buffer was then removed and cold PBS added. Fragments were shaken very vigorously for 20 seconds, which released the majority of remaining cells. The tissue fragments were removed, and the cells spun at 200G to form a pellet, which was re-suspended in Smooth Muscle growth medium and seeded into t25 flasks (formulated specifically to promote the growth of intestinal myofibroblasts). Media was replaced every 2-3 days to remove suspended leukocytes and non-viable cells. The dominant morphological phenotype after 2-3 weeks were stellate myofibroblasts – confirmed by IHC staining that showed homogenous expression of a-Smooth Muscle Actin and Vimentin (SMA, VIM).

Nucleic acid recovery

DNA was recovered from PBS-rinsed pellets using the Sigma mammalian GenElute DNA mini-prep kit according to the manufacturer's instructions. Alternatively phenol-chloroform extraction was performed. In brief, pellets were re-suspended in 100uL of Sigma r-suspension buffer and incubated for 2 minutes at room temperature with 20uL of RNase1 (Sigma). 20ul of Proteinase K was added to inhibit nucleases, and the cells lysed with NB lysis buffer ((0.2M Tris, 0.25M NaCL, 25mM EDTA, 0.5% SDS, adjusted to pH 8.5). 340uL of phenol:chloroform (equal volume) was added and samples shaken vigorously to dissolve nucleic acids, which was then spun at >1000G (4°C) for 5 minutes to separate the fractions. The aqueous phase was removed and the process repeated with chloroform:isoamyl alcohol (24:1), and finally with pure chloroform. DNA was precipitated by adding 1/10th 3M NaOAc pH 5.5, and 1uL glycogen, and spinning for 30 minutes at 4°C. The supernatant was removed, the DNA pellet rinsed with 70% ethanol, and left to dry at room temperature for 10 minutes.

RNA was extracted throughout the project using the Bioline ISOLATE II RNA mini kit according to the manufacturer's instructions, which includes an on-

column DNase step to eradicate contaminating genomic DNA. Pure RNA was re-suspended in 40uL of nuclease-free water and quantified on the Nanodrop.

Pellets were re-suspended in a final volume of nuclease-free water, and concentration quantified using the Nanodrop ND 1000 spectrophotometer, as detailed in the manufacturer's instructions. Samples with a 260:280 ratio approaching 1.8 for DNA and 2.0 for RNA were taken to be free from ethanol contamination.

Illumina array and analysis[228]

The Infinium Methylation EPIC BeadChip Kit (Illumina) interrogates >850,000 methylation sites quantitatively across the genome at single-nucleotide resolution. The previous iteration works according to similar principals but interrogates only 450,000 sites. Both arrays were utilised during the course of this project. DNA samples were prepared as outlined, and 500ng dispatched in nuclease-free water on dry-ice to Cambridge Genomic Services, where the array was executed according to the manufacturer's instructions. Data were analysed by CGS bioinformatics using the RnBeads plugin for 'R' studio. P-values were computed using hierarchical linear models from the limma package fitted using an empirical Bayes approach on derived methylation values. Differential methylation was computed based on a variety of metrics. The following quantities for each site or region are reported I) the difference in mean methylation levels of the two groups being compared, II) the quotient in mean methylation and III) a statistical test (t-test or limma depending on the settings) assessing whether the methylation values in the two groups originate from distinct distributions. Additionally each site was assigned a rank based on each of these three criteria. A combined rank is computed as the maximum (i.e. worst) rank among the three ranks.

Q-rt-PCR

Primers (appendix 6) were designed using the Roche Probe Library against the RefSeq messenger RNA NM number for the gene of interest (www.universalprobelibrary.com). Assay parameters stipulated a GC clamp, 18-27 BPs in length (optimum 20), with a TM of 60°C, and to be intron spanning to mitigate for residual contaminating genomic DNA. Where multiple transcript variants were identified, a common assay was selected. Reverse transcription was performed on 50-500ng of RNA (depending on yield) using Q-Script cDNA super mix (Quanta bioscience) according to the manufacturer's instructions, in 10uL reactions. These were diluted in 100-200uL of nuclease-free water. 10uL Q-rt-PCR reactions were prepared using 3uL of cDNA template, with 7uL of reaction buffer containing 5uL of Immomix (Bioline), 1uL of BSA (10mg/mL), 0.1uL $MgCL_2$ (50mM), 0.0625uL of 1:100 Sybr Green (Qiagen), 0.02uL of each primer at a final concentration of 100uM, 0.4uL ROX reference dye (Thermo), and 0.4uL of milliQ water. Samples were run on the Applied Bioscience 7300 RT-PCR system using the following protocol; 95°C dissociation for 10 minutes, followed by 40 cycles of [95°C dissociation 30 seconds, 60°C annealing, 30 seconds, 72°C extension and measurement, 30 seconds]. Primers were validated at 60°C using mixed cDNA of serial dilution (1, 1:10, 1:100, 1:1000 and water). The gradient of the linear equation was expected to be 3.5 CTs to demonstrate >95% efficiency, and a melt curve performed to demonstrate a single amplification product. Several house-keeping genes were validated including 18S, ACTB, and GAPDH. CT values were normalised to the reference gene to mitigate for loading discrepancies (ΔCT), and the relative transcripts determined by the equation ($2^{-\Delta CT}$) x100,000. Typically – unless otherwise stated - experiments (treatments) were performed in biological triplicate, and technical triplicates run on the machine. For each replicate, the mean of the three samples was determined +/- the standard error. A three-tailed students T test was used to infer the significance of the result of the treatment verses the vehicle control without assuming a normal distribution. Significance was assumed if $p < 0.05$ (represented by *) or $p < 0.01$ (represented by **).

Combine Bisulphite Restriction Analysis[229]

Genomic DNA (200-500ng) was first bisulphite modified using the EZ DNA methylation GOLD kit (Zymo) according to the manufacturer's instructions. The principal of the modification is that methylated cytosines undergo demethylation, yielding cytosine residues. Unmethylated cytosines on the other hand, are converted to uracil residues. This results in a methylation-specific sequence. The initial step is to amplify the CG island of interest in the promoter region, using primers that lie outside the island that do not incorporate any CGs, so the island is amplified regardless - typically a 200-500bp amplicon is generated. The assay assumes that all CG sites are methylated in the first instance, and non-CG cytosines are converted. Thus restriction enzymes that cleave specifically at a single CG in the amplicon can be utilised to cut the fragment in half. This will yield two half fragments if the CG site was original methylated in all alleles, one whole fragment if the site was 100% unmethylated. Or, if only a percentage of alleles were unmethylated, a ratio of cut fragments to uncut fragments can be determined, to give a figure for the percentage of methylated to unmethylated alleles (figure 10). Assays employed for genes of interest (mainly cytokines and Wnt antagonists) are detailed in appendix 5, showing the primers validated, and the restriction enzyme for the digestion. The initial amplification is similar to the protocol for cDNA, however, in respect of the fact that these amplicons are often up to 500BP, the extension time is increased to 1 minute. Commonly only 35 cycles were performed to mitigate for non-specific amplification of other sequences. As the reaction is not quantified, no Sybr Green or ROX reference are necessary, and Hot Star Taq (Qiagen) is used for reaction mixtures instead of Immomix. 10uL reactions containing 3uL of bisulphite modified DNA (bmDNA) template were prepared in technical triplicates from experiments performed in biological triplicate. Bisulphite modification was also performed on 20ng of 100% and 0% methylated genomic DNA (Zymo, human or mouse as appropriate) as controls to demonstrate complete cleavage of the fragment by the restriction enzymes. A third control of MilliQ water was also amplified to ensure absence of non-specific binding. Once amplified, the amplicon was precipitated as detailed using ethanol and Sodium Acetate, rinsed with 70% ethanol, and re-suspended in

10uL of the restriction enzyme buffer. Samples were digested at the designated temperature for three hours, spun, 2uL of loading dye added, mixed, and then loaded into the polyacrylamide gel[230]. DNA was separated by vertical electrophoresis at 200V (approximately three hours). Gels were developed for 2 hours in the dark using 1:10,000 Sybr Green in 1xTBE buffer (1L MilliQ water, 54g Trizma, 25,5 boric acid, 4.65g EDTA). The gels were imaged using the Pharos FX Molecular imager (BIORAD), and visualised using BIORAD Image Lab software (http://www.bio-rad.com/en-uk/product/image-lab-software). Band analysis was optimised to subtract the background from each lane, and fragment band intensity quantified to determine percent of methylated alleles (total cut fragment intensity/total all fragment intensity*100). Data are reported as the mean of replicates +/- the standard error.

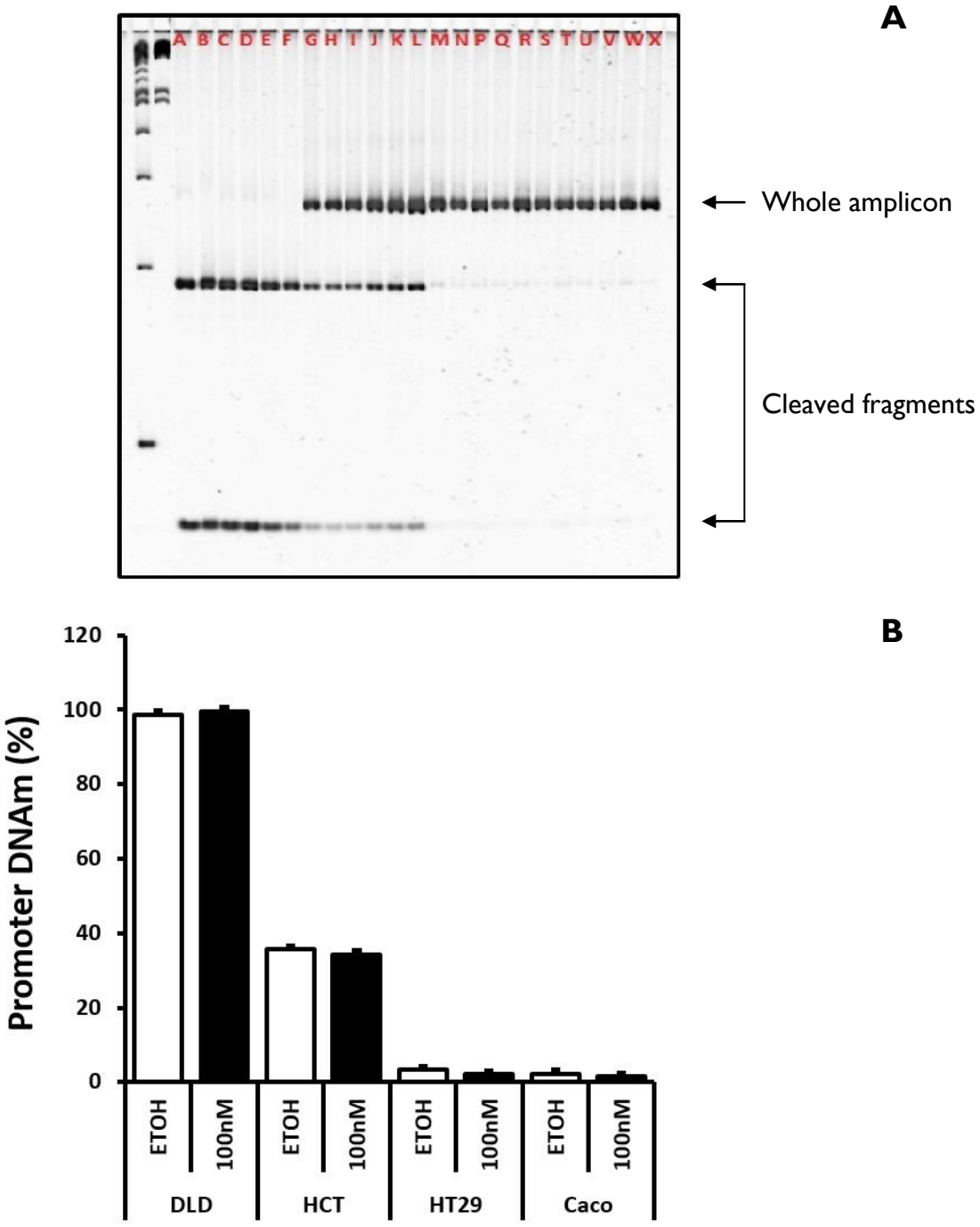

Figure 10 - Example of a CoBRA polyacrylamide MEGA gel. Figure A is the image of the gel, while figure B represents the ratio of the intensity of the cut fragment to the whole fragment as a percentage, derived from gel A (n=3 lanes, coloumn is mean +/- the SEM.This assay probed the P14ARF promoter region. The promoter amplicon is cleaved only where the CG interrogated was originally methylated. Lanes A-F show complete cleavage, which equates to 100% methylation at that site. Bands G-L show partial cleavage indicating that some alleles are methylated, while others are not, while lanes M-X are predominantly un-cleaved, indicating hypomethylation of the CG in these cell lines. This assay elegantly demonstrates the heterogeneity of promoter methylation in the cell lines selected for experiments. Although the assay only interrogates a single CG in the promoter island, promoter DNAm is reported to be an all-or-nothing process i.e. the assays assume that the methylation status of the CG interrogated represents the entire promoter. Here, there is no difference in P14ARF promoter methylation between ethanol controls and vitamin D treated cells.

Protein extraction (whole-cell and fractions).

Cells were released by trypsin-EDTA chelation, and protein extracted using either the Pierce M-PER (for whole-cell extracts) or NE-PER protein extraction reagents (for nuclear and cytoplasmic fractions) according to the manufacturer's instructions, which included the addition of HALT protease and phosphatase inhibitor cocktail (1:1000) to prevent proteolysis and any further phosphorylation events (all items from Thermo). Protein samples were stored at -80°C and defrosted on ice for analysis. Samples were quantified using the Pierce BCA Protein Assay Kit (Thermo), which includes albumin standards for plotting the standard curve. Absorbance was determined on a Bio-Rad Benchmark Plus colourimeter as indicated in the manufacturer's instructions.

Western blotting

Proteins were separated by gel electrophoresis in pre-cast graduated NuPAGE Bis-Tris polyacrylamide gels following the manufacturer's instructions (Invitrogen). Briefly, to samples containing up to 30ug of protein, 2uL of NuPAGE reducing agent and 5uL of LDS buffer were added. Samples were mixed and denatured at 70°C for 10 minutes. Pre-stained protein ladder IV (Bioline) and samples in triplicate were loaded into wells and run at 200V until appropriate separation was achieved. Proteins were transferred to PVDF stacks using the iBlot II transfer module (Life Tech). Membranes were rinsed with Tris-buffered saline, 0.1% Tween 20 (TBST). The membrane was blocked using 5% BSA in TBST for 2 hours at room temperature to prevent non-specific binding, after which the membrane was typically incubated with the primary antibody overnight at 4°C. Membranes were rinsed several times with TBST, and then developed using an appropriate secondary antibody for 2 hours at room temperature. Bands were imaged using the ChemiDoc MP imaging system (BioRad) after 5 minutes incubation with Clarity Western ECL substrate to generate a chemiluminescent signal. Bands were quantified using image J (box method), and the data reported as the mean +/- the standard error. The ratio of the phosphorylated band to the total band is reported for each sample. Membranes were stripped by incubation in Reblot Plus membrane stripping solution (Merck) and the process repeated for probing with an alternative primary antibody.

Proteomics[231-233]

Cell supernatants were collected as described and concentrated by centrifugation at 14,000G for 2 hours using protein filters with a MW cut-off of 3000Da (Merck). Samples were quantified by BCA assay and processed as per Western Blot protocols. Samples were run in triplicate on a 10% pre-cast polyacrylamide gel (Life tech) for 10 minutes. The lanes were dissected into 1mm squares using a razor blade and stored in 500µl water overnight. Gel plugs were washed with 1M Ammonium bicarbonate in acetonitrile for 15 minutes, twice, and then washed with 1ml acetonitrile to remove excess aqueous solutions. Samples were air dried for 10 minutes. Next, samples were incubated for 30 minutes in a water bath at 60°C with 1ml of 10mM DTT in 50mM Ammonium Bicarbonate, then rinsed with 100mM iodoacetamide in 50mM Ammonium bicarbonate at room temperature in the dark. Gel plugs were again washed twice with 1M Ammonium bicarbonate in acetonitrile for 15 minutes, rinsed with 1ml acetonitrile and air dried. Peptides were digested using 5µl (5µg) Trypsin Gold (Promega) in 20mM ammonium bicarbonate, incubated overnight in the water bath at 37°C. Next, an equivalent volume of 2% formic acid was added before freezing on dry ice for 30 minutes. Samples were thawed and the digest solution removed and dried down at the Low Drying setting (no heat) on a Speed Vac SC110 (Savant), fitted with a Refrigerated Condensation Trap and a Vac V-500 (Buchi). The samples were then frozen on dry ice and stored at -80°C for Orbitrap analysis. LC MS/MS analysis was executed by IFR's proteomics department. Data were analysed using Scaffold software (version IV). Tandem mass spectra were extracted and samples were analysed using Mascot (Matrix Science) to search the Uniprot human database. Scaffold was used to validate MS/MS based peptide and protein identifications. Peptide identifications were accepted if they could be established at greater than 95.0% probability by the Scaffold Local FDR algorithm and contained at least 2 identified peptides. Protein probabilities were assigned by the Protein Prophet algorithm. Proteins were annotated with GO terms from NCBI. For interventions, Scaffold was instructed to perform a two-way analysis of variance on normalised spectra (ANOVA) with Hochberg-Benjamini Correction, with significance reported at $p<0.05$.

Chapter 3

VITAMIN D PROMOTES A TISSUE-RESIDENT PHENOTYPE IN THP1 MONOCYTES ASSOCIATED WITH TNFA HYPOMETHYLATION

Preface to the work

Incidence of Inflammatory bowel disease (IBD) is increasing globally in Westernised populations, and particularly in New Zealand[234,235]. The diseases that comprise IBD (Crohn's and UC) are characterised by persistent inflammatory lesions in the intestinal mucosa, which frequently foreshadow epithelial transformation. While the aetiology of IBD remains incompletely catalogued, studies indicate a multifactorial pathogenesis, encompassing immune-regulatory defects, perturbation of the commensal microbiota, heritable predispositions (genetic and epigenetic), and structural deficiencies impairing barrier integrity.

The multifactorial nature necessitates a diverse spectrum of expertise, to gain sufficiently broad insights to advance community understanding – a diversity not always afforded to post-graduate researchers. In this respect, The REINFORCE consortium - established by a European grant administered by The University of Bologna - seeks to facilitate collaboration-by-exchange between gut health researchers around the globe, furnishing PGRs with additional tools and experiences beyond their field of expertise - ultimately allowing them to develop a broader understanding of the physiological context of their work.

In light of vitamin D's established anti-inflammatory and immune modulatory effects, taken together with the association between systemic inflammation and aberrant age-related DNA methylation, we pursued an opportunity for a REINFORCE collaboration with colleagues at The University of Auckland, NZ, investigating vitamin D supplementation as a means of inhibiting systemic inflammation.

Professor Lynette Fergusson and her team in the Faculty of Medical and Health Sciences had recently completed a clinical intervention, supplementing a small cohort of healthy individuals (n = 30) with Lester's Oil – a commercially available health supplement purported to promote systemic anti-inflammatory effects.

Their laboratory were commissioned by the manufacturers of Lester's Oil to perform an independent study investigating the bioavailability of the supplement and it's physiological effects - encompassing metabolomics, transcriptomics, and

the assay of biomarkers of systemic and local inflammation. It is important to note that this premise introduces a conflict of interest by its nature. The group in New Zealand designed and executed the study, collected biological specimens, and processed PMBCs to recover DNA, and serum to determine vitamin D status. The group also furnished us with cohort data for statistical tests.

The exchange took place in October and November of 2014. Peripheral Blood Mononucleated Cell (PBMC) DNA was assayed by CoBRA, to quantify the methylation status of genes involved in the pathogenesis of IBD. Preliminary experiments raised the possibility that vitamin D status might dynamically regulate TNFα promoter methylation and transcription, so we set about investigating the relationship between vitamin D and TNFα *in vitro.* Initially this thesis project's remit was exclusively focussed on epithelial homeostasis, but this short exchange has allowed for valuable insight into the nature of chronic inflammation, and its relationship with tumourigenesis and transformation.

Abstract

Chronic inflammation accelerates tumourigenesis in multiple tissues, suggesting that systemic mediators have a role to play in the aetiology of epithelial cancers. Inflammatory bowel pathologies are associated with increased peripheral blood monocyte count and elevated cytokines, which in turn are associated with age-dependent genetic and epigenetic defects that deregulate crypt stem cell homeostasis. Specifically, mucosal macrophages, derived from the peripheral monocyte pool, express TNFα that contributes to the initiation and maintenance of inflammatory lesions.

Vitamin D's role as an anti-inflammatory is well established *in vitro* and *in vivo,* and serum vitamin D is found to be low at presentation in IBD, and prospectively associated with CRC risk. Vitamin D promotes monocyte differentiation and inhibits TNFα. Furthermore, TNFα transcription is influenced by promoter methylation status.

The effect of vitamin D supplementation on inflammatory biomarkers in a cohort of heathy individuals (n=27) was investigated. Supplements improved serum vitamin D by 11.3nmol/L ($p < 0.001$), and inhibited C-reactive protein by 2.46mg/L ($p = 0.04$), but not faecal calprotectin, suggesting systemic but not tissue-specific effects. In a subset of participants (n = 8), TNFα promoter methylation status showed a significant trend towards hypomethylation with increasing serum vitamin D (RSQ = 0.37, $p = 0.0002$). In THP1 monocytes *in vitro,* vitamin D also promoted TNFα *hypomethylation*, associated with the induction of an adherent tissue-resident macrophage phenotype ($CD14^+$, $CD68^+$, $CD11b^+$). Conditional demethylation of TNFα by 5AZA was not associated with the adherent phenotype, but regression analysis suggests CD11b expression, and thus macrophage sub-type, is influenced by TNFα methylation.

Our data support vitamin D inhibiting systemic inflammation, promoting monocyte-to-macrophage differentiation, and modulating TNFα transcription independently of DNA methylation status. These effects are proposed to regulate mucosal immunity, indirectly affecting DNA methylation patterns in the colonic epithelia. Further testing in epithelial models is indicated.

Introduction

The inflammatory bowel diseases comprise Crohn's Disease (CD) and Ulcerative Colitis (UC). Both subtypes are prevalent in Westernised populations at approximately 200 per 100,000, representing a considerable public health burden. Studies in migrants to the West show a concomitant increase in the rate of both UC and CD over time, indicating the environmental component of the aetiology[236], however it is noted that incidence has plateaued across Europe in recent years[237], suggesting that rate of diagnosis contributes to the cultural discrepancy.

The aetiology of IBD is multifactorial, representing distinct pathogenic pathways that cumulatively effect chronic mucosal inflammation. The hallmark of CD is patchy, erythematous lesions throughout the GI tract, while UC presents distally, with inflammation involving the whole sheet[238]. Epithelial hypotrophy precipitates ulcerating lesions and granulomatous fibrosis. Both diseases have an autoimmune component, marked by leukocytic infiltrates of B and T cells, neutrophils, DCs, and tissue-resident macrophages[239]. Dysbiosis of the commensurate microbiota is established in the pathogenesis of IBD, which is compounded by impaired barrier integrity[240]. The conditions are chronic, in that periods of induced remission invariable falter. Due to genetic components comprising 100-200 risk loci that include infamous NOD2, CARD9, and IL10 SNPs (responsible for dysregulation of the host auto-immune response)[241,242], - there are presently no curative therapies. Thus, pharmaco-intervention focuses on management of inflammation and its end points. Specifically, Infliximab, an anti-TNFα monoclonal antibody, is indicated in severe refractory disease states, pinpointing TNFα as a key node in this complex aetiological network[243]. The current paradigm for initiation and progression is that genetic predisposition impairs the immune response against luminal symbionts, which precipitates chronic intestinal inflammation maintained by mucosal populations of immune reguators[239].

Regarding prognosis, IBD is associated with an increased risk of overall mortality (17 per 1000 verses 11 per 1000 – risk ratio of 1.54)[244]. Chronic inflammation

promotes tumourigenesis, demonstrated by a five-fold increased risk of colorectal carcinoma in those diagnosed with IBD relative to healthy controls[245].

Thus IBD models have proved valuable in elucidating the inflammatory mechanisms that bring about aberrations found in sporadic tumours of the distal bowel. Specifically relevant to this topic, age-related DNA hypermethylation of tumour suppressors in colonic stem cells is accelerated by both mucosal and systemic inflammation; in their seminal paper from 2001, Issa et al report sequential increases in MYOD1, ER, and CDKN2a promoter methylation for normal mucosa (non-UC), uninvolved mucosa (UC), and neoplastic lesions (UC), demonstrating the association of chronic inflammation in the pathogenesis of sporadic lesions[246]. Another gene frequently reported to be silenced via hypermethylation in UC lesions is ECAD, which in turn has implications for Wnt signalling, cell-adhesion, and barrier integrity[247,248].

Postulated mechanisms for the increase in DNAm associated with inflammatory processes, include over-expression of IL6 in both serum and mucosa of IBD patients, which is shown to promote aberrant DNAm via increased DNMT1 activity in epithelial models[249]. Aberrant TLR2 expression in the gut epithelia is also associated with gene silencing via DNA hypermethylation[250], as is increased PGE2 in the crypt niche (see chapter 5)[251], and anti-inflammatories like Aspirin, recognised to modify CRC risk via suppression of NFκB/COX2/PGE2[252], have recently been reported to favourably influence both age-related and tumour-associated DNAm patterns in the colonic epithelia[253]. Tapp et al also allude to increased numbers of circulating monocytes as positively associated with age-related DNAm, for six of the nine genes they interrogated in tumour-prone epithelia[212], suggesting that modulation of the monocyte pool could be beneficial for the epigenetic ageing of colonic stem cells. Notably, while TNFα is recognised to be elevated in both serum and mucosa of IBD patients, and mechanistically responsible for lesion maintenance and tumourigenesis (via persistent DNA damage[254]), there are presently no studies that correlate serum TNFα with aberrant age-related DNAm, although this is implied as TNFα signals via NFκB.

Elevated serum and mucosal TNFα is associated with IBD, the principal sources of which are circulating monocytes and tissue-resident macrophages respectively. Interestingly, Kobor et al observe differential methylation in Peripheral Blood Mononucleated Cells (PBMCs) according to the percentage of monocytes they contain, suggesting the DNAm has a role to play in the immune-regulatory functions of these cells. Indeed, the authors report that DNAm patterns predict the cytokine response of PBMCs to stimulation with recombinant TLR-ligands[255]. Global DNAm patterns also vary longitudinally in leukocytes[256], but to date, with regards cell-type, the majority of studies looking at DNAm in PBMCs have focussed on T-cells, not the lesser monocyte contribution[257], or are employed as systemic markers of epigenetic ageing as opposed to characterising inflammatory mechanisms[258,259].

With regards transcriptional control of TNFα, the primary epigenetic events are classically histone modifications that are dynamic in response to TLR/NFκB signalling. While the TNFα promoter does not contain a defined CG island, a single CG 150 BP proximal to the TSS is documented in transcriptional competence of the neutrophilic cell line HL60 in the hypomethylated state[219]. Gowers et al report an age-associated decrease in CG methylation in the TNFα promoter region, specifically in monocyte-derived macrophages from healthy participants, that is associated with increased expression, and thus may contribute to age-associated systemic and local inflammatory pathogenesis.

As well as a comprehensively described role as a systemic anti-inflammatory[260], deficiency associations with IBD, aberrant DNAm in CRC[212,261], and *in vitro* differentiation of monocyte-derived macrophages[84], vitamin D also regulates TNFα expression in monocytes[262,263]. Given access to PMBC DNA from a cohort of healthy vitamin D-supplemented participants, it was hypothesised that serum vitamin D would be associated with markers of systemic inflammation, the macrophage phenotype, and TNFα methylation – plausible mechanisms by which vitamin D sufficiency promotes bowel health. We employed THP1 monocytes to investigate observed cohort trends *in vitro*, and report here that the methylation status of the TNFα promoter is associated with, but not defined by, vitamin D status and macrophage phenotype and function, but not TNFα transcription. Hypomethylation was synchronous to regulation of DNMT1 and TET enzymes by vitamin D, posited as a mechanism for vitamin D's epigenetic effects.

Methods

Lester's Oil intervention

Thirty healthy individuals from the Auckland metropolitan area were recruited to the study. The intervention was of a randomised, double-blinded, placebo-controlled, cross-over design (figure 11). Blood and faecal samples were collected at base line, after intervention 1, after the primary wash-out period (before intervention 2), and after intervention 2. Anthropomorphic features were also determined at these time points (height, weight). Participants received two soft gel caps per day, for 28 consecutive days, containing either Lester's Oil, or encapsulated Canola oil, followed by 28 days of wash-out, and the programme was executed between March and June in 2014. Participants were screened to include male and females aged between 20 and 65 years, with no history of cancer in last 5 years, no history of IBD, not on medication, non-smokers, and not currently taking any vitamin D, fish oil/flax seed oil supplements, or eating more than 4 servings of oily fish per week. 8.5mL of peripheral blood was collected in BD Vacutainer Serum Separation Tubes, which was inverted five times, allowed 30 minutes clotting time, and centrifuged for 10 minutes at room temperature at 1000-1300G. A 40uL aliquot of serum was pipetted off and stored at -80°C for analysis by vitamin D X-press ELISA (ImmuniDiagnostiks). A further 4mL of PB was collected with EDTA on ice, PBMCs were separated by routine methods, and DNA and RNA extracted using the Qiagen ALL-prep kit, for transcriptomics or bisulphite modification using the EZ DNA methylation GOLD kit (Zymo). 4.5mL PB was collected with lithium heparin to determine C-reactive protein (LabPlus). Faecal samples for calprotectin were stored at -80°C.

TNFα promoter methylation

500ng of bisulphite modified DNA was amplified by PCR and digested by restriction enzyme as outlined in General Methods. Hypo- and hyper-methylated control DNA was also included (Zymo). For analysis in Auckland, digested fragments were run horizontally on 1% agarose gels as opposed to PAGE. In contrast, *in vitro* verification with THP1 monocyte DNA was performed by PAGE as outlined.

Cell culture and treatment

The THP1 cell line (ATCC) was maintained according to the manufacturer's instructions, in RPMI 1640 + 10% FBS + 1% penicillin/streptomycin, at 37°C. To induce differentiation, cells were seeded in 12 wells plates at a density of 50,000 cells per well, to give a final yield of ~400,000 after 6 days (assuming a 48 hour doubling-time). After 24 hours to restore homeostatic equilibrium, wells were treated in triplicate with either ethanol vehicle at the highest concentration, or increasing doses of active vitamin D in ethanol, giving final concentrations 1, 10, or 100nM (10x physiological to 1000x physiological relevance). On the final day, cells either were recovered for DNA extraction, or were primed with LPS at a final concentration of 5ng/mL for four hours prior to RNA extraction. Further tests investigating differentiation utilised PMA (200nM final concentration, 24 hour treatment), IL10, (25ng/mL final concentration, six day treatment), or demethylating agent 5-azacytidine (5AZA, 1uM final concentration, six day treatment). Treatment was re-applied at 24 hour intervals. On the third day, media was removed, the cells collected by centrifugation, and re-suspended in fresh media to mitigate for nutrient deficiency. Cell counts to determine the ratio of adherent to suspended populations was determined in chamber slides using the Cellometre Mini (Nexelom) according to the manufacturer's instructions.

Q-rt-PCR

Cell pellets were washed with PBS, and RNA recovered using the Isolate II RNA mini-kit (Bioline). 500ng was reverse transcribed using Q-Script (Roche) in 10uL reactions as per the manufacturer's instructions. Assuming a 75% conversion, 375ng was resuspended in 100uL of RNAse-free water, and Q-rt-PCR reaction prepared in technical triplicate (11.25ng cDNA per reaction). Q-rt-PCR was executed as detailed in General Methods, and the number of relative transcripts (against either 18S or ACTB as a housekeeper) determined by the delta CT method. A three-tailed students T-test was used to determine significant difference between treatment groups, and data are reported as the mean +/- the standard error. Primer pairs specific to this chapter are detailed in appendix 6)

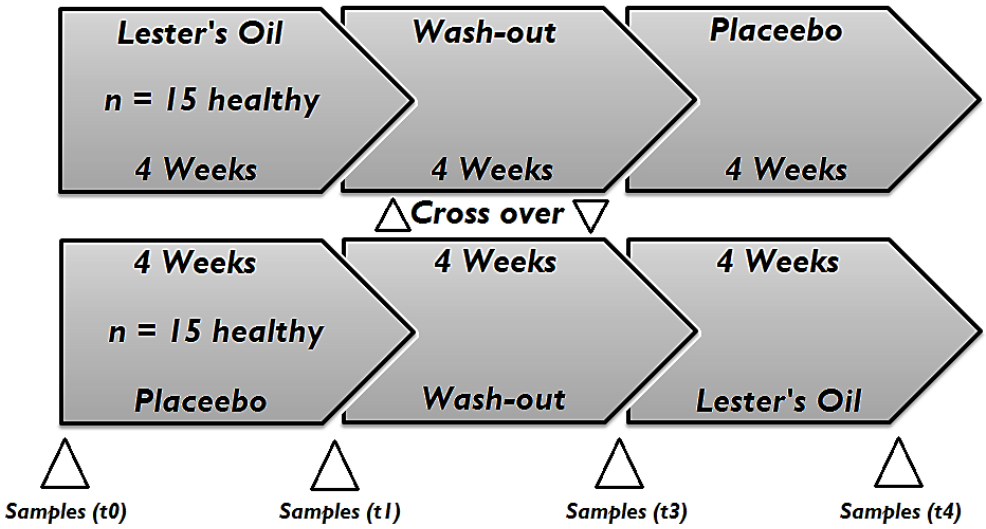

COMPONENT	MASS/UNITS
DHA (DOCOSAHEXAENOIC ACID)	255mg
EPA (EICOSAPENTAENOIC ACID)	170mg
TOTAL OMEGA-3 FATTY ACIDS	500mg
COENZYME Q10	50mg
ASTAXANTHIN	500ug
LUTEIN	3mg
VITAMIN D3	12.5ug
VITAMIN E	1mg

Figure 11 – Trial protocol. The cohorts were assigned randomly, and administration was double blinded. Participants received either 2 soft gel caps of Lester's Oil, or 2 gel caps of inert canola oil per day for 4 weeks. Components of the supplement are also detailed.

Results

Lester's Oil intervention

Cohort characteristics

Of the 30 healthy participants from the NZ cohort supplemented with Lester's Oil, two failed to complete the study and one data set was removed due to an ongoing infection during the trial period. Figure 12 details cohort statistics at base line. Data were incomplete for a further 3 participants. Our final cohort included 11 females and 13 males whose biomarkers exhibited skewed distributions, with no significant differences between male and female groups. Log transformation corrected significantly skewed variables (BMI and CRP) for further testing. Log transformation of the calprotectin data set did not correct for the skewed distribution, and so a three-tailed students T-test was applied to assume a non-normal distribution. Mean BMI for both males and females bordered on overweight (BMI >30) due to the presence of an outlying obese individual (BMI > 35) within each group. All other biomarkers measured (vitamin D, CRP, CALP) fell within clinical reference ranges. No individuals were deemed to be vitamin D deficient (serum D <40nmol/L) at the start of the trial.

	All		**Females**		**Male**		
	(n = 24)		***(n = 11)***		***(n = 13)***		***p* (F vs M)**
	Mean	SEM	Mean	SEM	Mean	SEM	
Age (years)	45.4	2.6	43.2	4.3	47.3	3.1	0.44
Height (cm)	171.7	2.2	163.2	2.4	178.9	1.8	N/A
Weight (kg)	74.9	4.1	63.1	4.6	84.8	4.9	N/A
BMI ($kg/m^{2)}$	25.0	1.0	23.6	1.5	26.3	1.2	0.17
VITD (nmol/L)	66.5	2.9	65.5	4.0	67.4	3.9	0.75
CRP (mg/L)	2.0	0.8	1.6	0.9	2.3	1.2	0.67
CALP (ug/g)	55.9	19.6	35.2	9.6	73.5	33.8	0.34

Figure 12 – Cohort variables. NZ Lester's Oil cohort variables at *t0* (mean +/- SEM). Two or three tailed student's T-tests were applied to normalised data sets as appropriate.

Lester's oil supplements improve serum vitamin D status

Supplementation with Lester's Oil significantly improved serum vitamin D status concomitant to reduced circulating CRP, suggesting a reduction in systemic inflammation. Other biomarkers measured were not significantly affected by supplementation. Specifically, the trend for calprotectin in males was positive, suggesting that mucosal inflammation in the distal colon was not impacted. Detailed in figure 13. Surprisingly, vitamin D was significantly reduced in the placebo group, but regression analysis of the relationship between reported sunlight hours in Auckland across the trial period, and serum vitamin D in the placebo groups, suggested that seasonal variation is responsible for falling serum vitamin D in the control participants.

All (n = 24)	Placebo		Lester's Oil		p
	Mean	SEM	Mean	SEM	
Δ BMI (kg/m^2)	-0.01	0.09	1.19	1.19	0.33
Δ VITD (nmol/L)	-9.06	1.97	5.97	2.07	**9E-07**
Δ CRP (mg/L)	1.07	0.89	-1.39	0.19	**0.04**
Δ CALP (ug/g)	-4.02	19.6	3.43	27.45	0.63

Males (n = 13)	Placebo		Lester's Oil		p
	Mean	SEM	Mean	SEM	
Δ BMI (kg/m^2)	0.03	0.11	-0.09	0.11	0.46
Δ VITD (nmol/L)	-9.46	2.15	4.46	2.60	**1E-03**
Δ CRP (mg/L)	1.81	1.61	-2.46	1.35	**0.05**
Δ CALP (ug/g)	-1.54	7.30	28.60	11.28	**0.04**

Females (n = 11)	Placebo		Lester's Oil		p
	Mean	SEM	Mean	SEM	
Δ BMI (kg/m^2)	-0.01	0.08	0.12	0.06	0.99
Δ VITD (nmol/L)	-8.09	2.31	7.36	3.36	**1E-03**
Δ CRP (mg/L)	0.00	0.15	-0.27	0.19	0.28
Δ CALP (ug/g)	-8.57	8.99	18.82	18.98	0.21

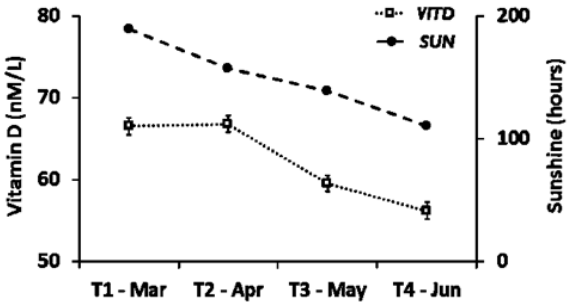

Figure 13 – <u>The effect of Lester's Oil on various Biomarkers.</u> Detailing cohort response to either placebo or Lester's Oil supplements. BMI does not vary according to treatment, precluding a role for BMI in serum vitamin D bioavailability. Circulating vitamin D is significantly increased in the supplemented cohort, an increase of 7.4nmol/L in females and 4.6nmol/L in males. There was a modest trend towards reduced CRP in this sub-set of participants, which was confirmed by a larger study performed by the group in NZ (data not shown). Calprotectin levels trend towards an increase in the Lester's Oil cohort, suggesting that vitamin D's anti-inflammatory effects were systemic, not mucosal. Vitamin D levels in the placebo group fell across the intervention period, our collaborators proposed sequestration of serum vitamin D by components of the placebo pill, however, seasonal variation in sunlight hours is suggested as an alternative explanation for falling vitamin D levels. NB – this study was performed in the southern hemisphere, where seasons are reversed i.e. T1-T4 represent autumn approaching winter.

Vitamin D status is inversely associated with dynamic TNFα promoter methylation

To investigate any effect of serum vitamin D on TNFα promoter methylation status, DNA was extracted from recovered PBMCs at each time point (before and after placebo, and before and after intervention*)* for the first eight participants as proof of concept. The TNFα promoter was assayed by CoBRA as described. Regression analysis suggested an inverse relationship between TNFα promoter DNAm and vitamin D status (figure 14a RSQ=0.367, p = 0.0002). When data are stratified according to sample group a non-significant trend is observed for the effect of intervention verses placebo on TNFα promoter DNA methylation. The intervention in these eight participants significantly increased circulating vitamin D. No other trends were observed between TNFα promoter status and other biological biomarkers measured. Specifically, age and BMI (both associated with DNAm in the distal colonic epithelia) had no effect of TNFα methylation in PBMCs in this group. Equally, while intervention and improved vitamin D status both decreased CRP levels, CRP itself was not associated with any change in TNFα methylation (figure 14b-d).

Interestingly, TNFα promoter DNAm appeared dynamic within individuals at each time point, regardless of intervention i.e. dynamic with regards serum vitamin D independent of stratification. This suggested to us that promoter methylation status in the context of PBMCs might have a role to play in regulating TNFα transcription, as reported elsewhere. Transcriptomics did not report any change in TNFα transcripts in PBMC at any time point, regardless of vitamin D status, consistent with the contemporary hypothesis that promoter hypomethylation need not necessarily drive transcription.

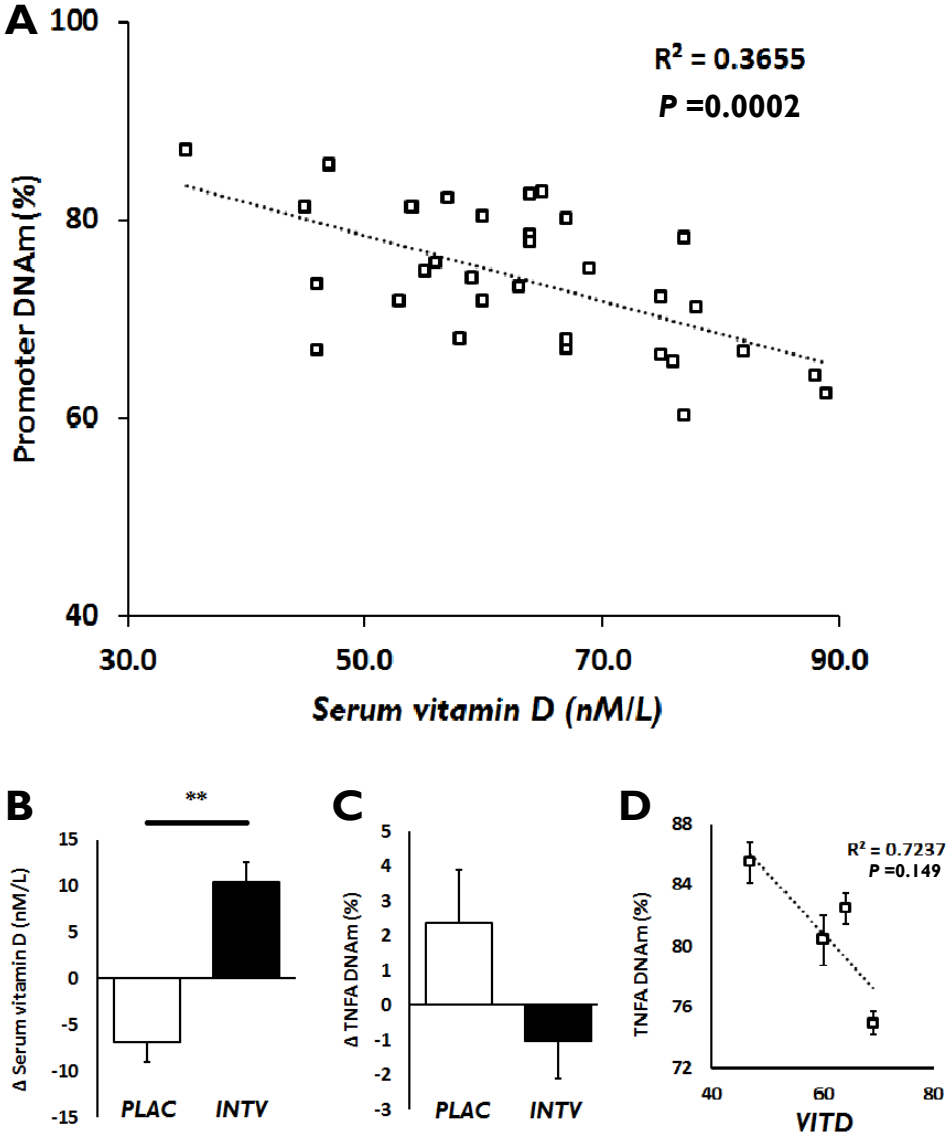

Figure 14 – <u>The relationship between serum vitamin D and TNFα promoter methylation in PBMCs.</u> A) TNFα methylation status trends towards hypomethylation as vitamin D status improves in this sub-set (*n = 8*). Validation is indicated in a larger cohort. B) When samples are stratified by intervention, serum vitamin D is significantly improved in those participants receiving the Lester's Oil tablet (25ug vitamin D, equivalent to 1000IU – the current recommended daily dose is 300IU for comparison) versus the placebo. This was associated with reduced CRP, but not CALP, suggesting inhibition of systemic, but not mucosal inflammation. C) TNFα methylation in patients receiving LO trends toward a reduction that was not significant, in keeping with our regression analysis. D) TNFα methylation status was dynamic within individuals according to their vitamin D status (participant number 8 shown), raising the possibility that vitamin D directly modulated TNFα methylation in PBMCs.

In vitro verification with THP1 leukemic monocytes

In humans, PBMCs comprise; lymphocytes (~80%), monocytes (~20%), and dendricytes (>1%). It was speculated that the weak relationship between vitamin D and TNFα methylation in PBMCs, represented a more pronounced relationship in one subset of the total cell population. Furthermore, Lester's Oil supplements contain other bioavailable factors which influence systemic inflammation (fatty acids[264], CoQ10[265], carotenoids). To determine if vitamin D was mechanistically responsible for the observed trends, *in vitro* verification was proposed. In light of reports that TNFα transcription in monocytes is influenced by promoter methylation[266], and given their relative abundance in PBMC populations, monocytes presented themselves as primary candidates. The THP1 monocyte cell line was selected as a well differentiated monocyte model[267]. Encouragingly, the methylation status of the TNFα promoter in un-primed THP1 monocytes *in vitro* is similar to that documented in the NZ cohort, supporting the use of these cells (70.3% +/- 2.6 verses 72.0% +/-1.2). It was further speculated that demethylating effects might be passive in nature, given that sampling was performed several weeks apart. Thus, cells were treated for six days with increasing concentrations of vitamin D, applied every 24 hours, to establish dose effects.

Initially, monocytes were distributed evenly throughout the suspension as single cells. By day three, cells began to coalesce into aggregates, and by day six approximately 10% of cells were adherent in vehicle-treated wells. In contrast, D-treated cells formed larger aggregates sooner, and percent adherence increased in a linear fashion with dose. It was hypothesised that the adherent and suspended populations represented distinct phenotypes, and so TNFα methylation was interrogated in both, by gently removing suspended cells, rinsing, and recovering the remaining adherent population. In vehicle controls, there was no difference in TNFα methylation between suspended cells and adherent cells. Neither did vitamin D affect the promoter status of TNFα in any of the suspended populations. However, vitamin D significantly reduced TNFα methylation by an average of 8.6% +/-0.4 in all three D-treated adherent populations. Unlike the adherent phenotype, the effect was not dose-dependent,

suggesting either a spontaneous threshold response, or temporal effect of vitamin D (figure 15a).

Pre-treatment with vitamin D modulates TNFα transcription in response to LPS in a phenotype-specific fashion

A reduction in promoter methylation status from 70% to 60%, conversely equates to the number of *hypo*-methylated alleles increasing from 30% to 40%, or put succinctly, a 33% increase in the number of *hypo*-methylated alleles. It was hypothesised that if transcription were to be regulated by promoter methylation status, adherent vitamin D treated cells would produce more TNFα transcripts in response to an inflammatory stimulus than untreated hyper-methylated adherent and suspended cells. We repeated the vitamin D protocol at the concentration showing the greatest effect (10nM for six days), and then stimulated cell populations for four hours with LPS at 5ng/mL, before recovering RNA.

Synchronous to promoter demethylation, vitamin D in isolation inhibited TNFα transcription in adherent cells (figure 15b). Naïve adherent cells primed with LPS mobilise significantly more TNFα transcripts, which vitamin D attenuates, countering our prediction that the demethylating effect of vitamin D would enhance the TNFα response to LPS in adherent cells. Furthermore, in suspended cells, that experienced no change in their promoter methylation status, the pattern is repeated, although it is apparent that TNFα transcription in these cells is significantly reduced regardless of environment, in comparison to the adherent phenotype. However, it is true that vitamin D-treated adherent cells produce more transcripts in response to LPS than vitamin D-induced cells in suspension stimulated with LPS, supporting the case for vitamin D promoting an adherent phenotype that mobilises more TNFα transcripts due to hypomethylation of the TNFα promoter. This suggests that multiple regulatory events prescribe the response of TNFα to LPS in a phenotype-dependent fashion. Certainly, vitamin D promotes anti-inflammatory effects in THP1 monocytes with regards TNFα

transcription, and the compound also appears to encourage an adhesive phenotype in these cells.

Vitamin D induces transcription of biomarkers that define a tissue-resident macrophage phenotype

Tissue resident macrophages (TRMs) have an important role to play in the resolution of mucosal inflammation in the distal bowel. Populations are recruited from circulating monocytes (MOs), and differentiate *in situ* according to well documented schedules, which are both diverse and plastic. Specifically, high expression of CD14, CD68, CD16a, F480, and CD11b are documented to characterise the tissue-resident phenotype. A significant induction of all of these genes in both adherent naive cells and suspended vitamin D-treated cells is observed (figure 15c-f). The effect is cumulative in vitamin D-treated adherent cells, particularly for CD14 and CD16a which, in keeping with the literature, was not detected after 40 cycles in naive suspended cells. Given that both plastic-adhesion and vitamin D treatment are well-documented bench techniques for propagating monocyte-derived macrophages, and in respect of their adhesive phenotype and transcriptional profiles, henceforth suspended cells will be referred to as MOs and adherent cells as TRMs.

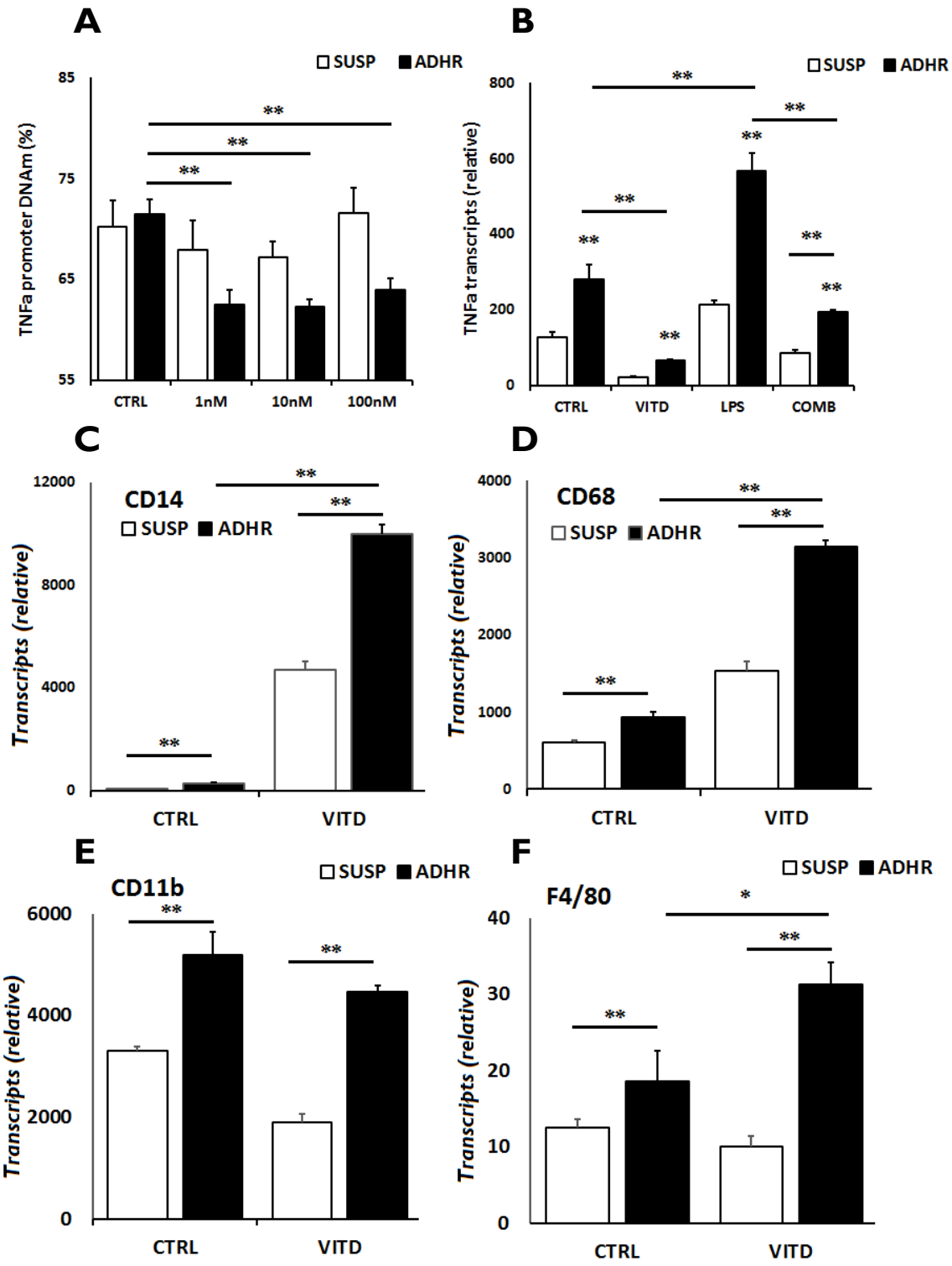

Figure 15 – Vitamin D induces TNFα hypomethylation but inhibits transcription in THP1 monocytes over 6 days. * p<0.05, ** p<0.01. 3 biological replicates, 3 technical replicates. Data represtent the mean +/- the SEM. A) The TNFα is hypo-methylated in adherent cells, but not cells remaining in suspension. The effect (DNAm ↓8.6% +/-0.4) was not dose-dependent. B) Adherent cells exhibit increased TNFα transcription relative to suspended counterparts. Vitamin D acts to inhibit TNFα, and LPS acts to induce, TNFα in both phenotypes. Treatment with vitamin D does not promote TNFα transcription when cells are primed with LPS, contrary to the founding hypothesis, in fact vitamin D attenuates LPS-induction of TNF, supporting vitamin D's role as an anti-inflammatory, but not effected via modulation of the TNFα promoter. C-F) In both suspended and adherent cells, vitamin D induces markers associated with a tissue-resident macrophage phenotype, consistent with the literature. CD14, CD68, and F4/80 are induced in adherent controls and by vitamin D, suggesting a cumulative effect of both plastic adherence and vitamin D treatment in the promotion of the TRM phenotype

Next we sought to establish if the methylation status of TNFα correlated with the degree of differentiation. Two end points were deemed necessary 1) optimise techniques to derive TRMs of varying degrees of differentiation, and 2) optimise a technique to demethylate the TNFα promoter, to see if hypomethylation precipitates differentiation toward a TRM transcriptional profile. Several techniques are reported to promote the differentiation of MOs to various TRM phenotypes (including vitamin D) - treatment with phorbol-myristate-acetate (PMA, 200nM), and treatment with interleukin 10 (IL10, 25ng/mL) were also selected from the literature[465]. We also incorporated treatment with the demethylating agent 5-azacytidine (5AZA, 1uM). Cells were treated for six days, with treatments re-applied every 24 hours with the exception of PMA (PMA-treated cells became adherent within 24 hours of the initial treatment, and remained adherent for the duration of the protocol). Cells were harvested on the sixth day and the ratio of MOs:TRMs determined by Cellometre (in triplicate), which show varying degrees of adhesion according to treatment regimen (figure 16a).

The panel of TRM markers was interrogated by Q-rt-PCR to determine the phenotype of adherent vitamin D-, PMA-, IL10-, and 5AZA-treated cells. The methylation status of the TNFα promoter was also interrogated by CoBRA, to investigate its relationship with increased adherence. PMA and 5AZA almost completely demethylate the TNFα promoter, but interestingly, while markers of the TRM phenotype are induced in these cells, the levels of transcription remained relatively low compared with D- and IL10-treated cells (figure 16b and c). Specifically, while PMA and 5AZA promoted demethylation, 5AZA did not induce adherence during the course of the treatment, suggesting that the change in TNFα methylation is not what precipitates the adherent phenotype, thus, in this instance the null hypothesis should be accepted - TNFα promoter demethylation is associated with an adherent phenotype in previous experiments, but not exclusively and does not induce it. Vitamin D induced a trend towards demethylation, as previously observed, but this time the effect did not achieve significance. Given the modest reduction (<10%), and inclusion of only one sample with five technical replicates for comparison, it is strongly advised to

repeat this experiment to certify vitamin D's TNFα demethylating effect in adherent THP1 monocytes.

Although significantly induced relative to controls, F4/80 was expressed at negligible levels in treated cells. In retrospect, after further literature searches, this marker is not deemed suitable for classification of human macrophage populations, typically employed for murine modelling.

The phenotype of the cells did appear to be defined by treatment regimen, as would be anticipated given the TRMs dynamic environment-specific phenotype in vivo; all cells show discrete degrees of TNFα methylation and adherence ratios. D-treated cells represent a $CD14^{+}/CD68^{+}/CD11b^{+}$ phenotype. PMA treated cells are defined as TRM-$marker^{low}$, while IL10 induces a $CD14^{+}/CD68^{++}/CD11b^{low}$ (figure 16b). The TRM^{low} designation applies to both PMA and 5AZA adherent cells, which both experience severe TNFα hypomethylation – it may be pertinent to explore the effect of these treatments across the THP1 methylome, to be correlated with RNA-seq profiles. Validation of the proposed phenotypes by IHC, and investigation of associated properties regarding mucosal immunity may also bring forth insight into TRM physiology.

Finally, it was noted that the CD11b transcriptional profile closely matched the TNFα methylation status, regardless of treatment; regression analysis raises the possibility that the two are inter-dependent, but the trend did not achieve statistical significance (figure 16d).

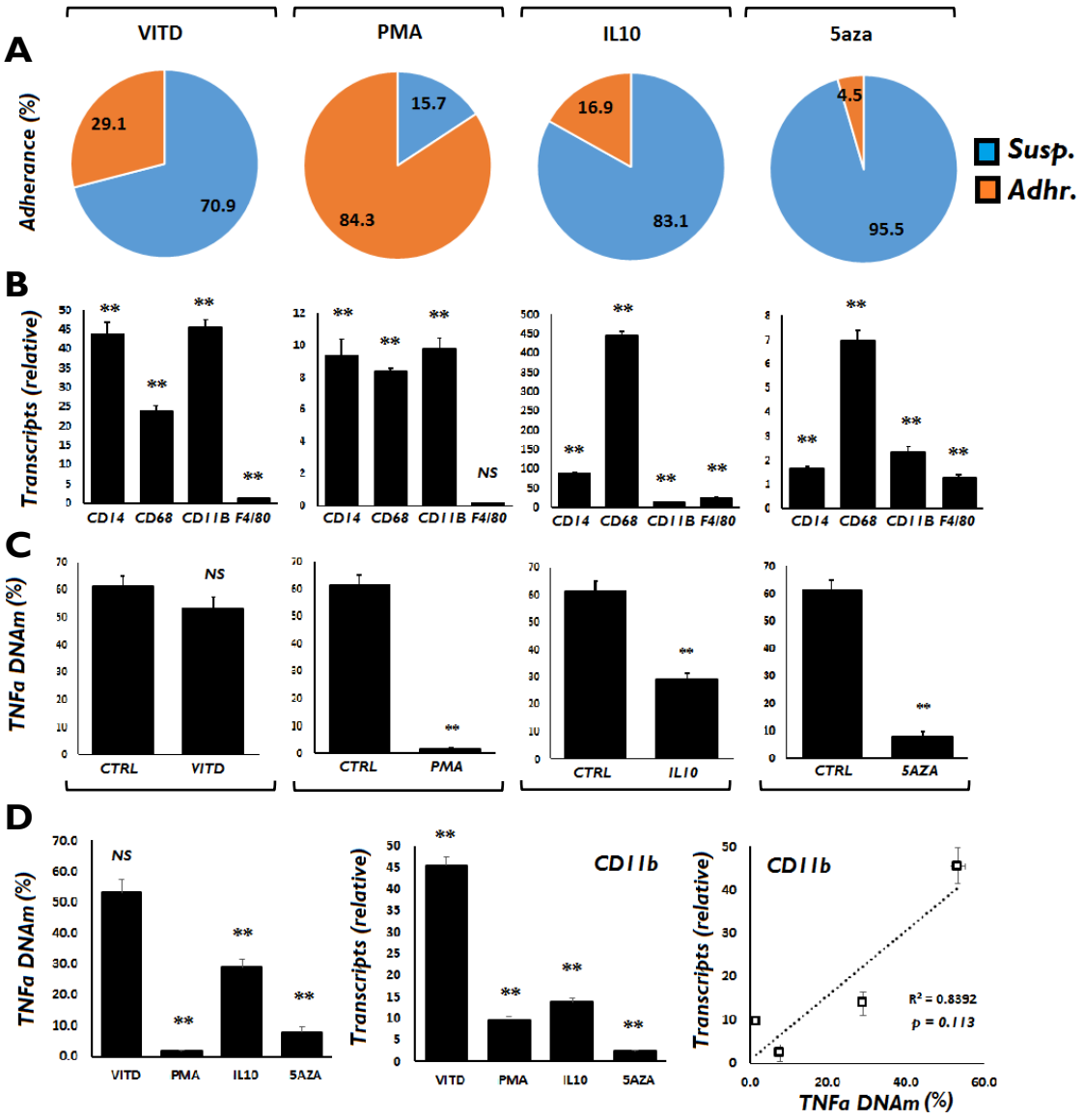

Figure 16 – <u>Induction of differentiation by vitamin D, PMA, IL10 and 5AZA.</u> . * p<0.05, ** p<0.01. 3 biological replicates, 3 technical replicates. Data represtent the mean +/- the SEM. A) Treatments increase adherence (% of viable cells) to varying degrees. PMA promoted rapid and permanent adhesion, whilst vitamin D and IL10 induce only partial adhesion of the total population. 5AZA did not promote the adhesive phenotype B) Treatments were associated with the induction of TRM-specific markers, relative to controls where expression was negligible (<1). Adherent vitamin D-treated cells demonstrate modest increases in transcription of CD14, CD68, and CD11b. Similarly, PMA induces these genes, suggestive of a shift towards a TRM phenotype, however relative expression is low in comparison to D- and IL10 treated cells. IL10 exhibits induction of CD14 and specifically CD68. Although TRM markers are induced by 5AZA, relative levels remain low – taken together with the null effect regarding adhesion, this suggests that 5AZA does not promote differentiation, despite hypomethylation of the TNFα promoter C) All treatments show trends towards hypomethylation of the TNFα promoter, but the degree does not correlate to adherence ratios, suggesting that TNFα promoter methylation status does not regulate the adherent phenotype. However, all treatments induce both hypomethylation and markers of TRMs, but the true relationship between adherence, biomarker phenotype and TNFα methylation is not resolved here. Methylation and transcriptomic arrays are indicated to comprehensively document interdependency. D) CD11b transcription appears weakly associated with TNFα methylation status. Although the trend was not significant, this finding warrants further elucidation. Immunhistochemical assays should also be performed to correlate transcription with variable expression and confirm phenotype.

Finally, to investigate potential mechanisms by which vitamin D might modulate TNFα methylation, we analysed gene transcripts for 5mC metabolic enzymes classically associated with DNA hypomethylation (DNMT1, and TETs 1, 2, and 3). DNMT1 is responsible for maintenance of DNAm during S-phase, and deregulation of activity precipitates global hypomethylation. Conversely, TET enzymes actively demethylate 5mC via 5hmC intermediates. Encouragingly, vitamin D promotes induction of all three TETs (figure 17), raising the possibility that activity is deregulated (induction may be driven by vitamin D, or conversely, a response to other changes in DNAm metabolism not characterised i.e. a feedback response, therefore it is not possible to speculate about the direction of activity). Synchronously, DNMT1 is induced – this could be an induced homeostatic mechanism, to counter active demethylation by TETs, although this hypothesis is speculative. Certainly, transcriptional data strongly implies deregulation of normal 5mC metabolism in THP1 monocytes by vitamin D. Activity assays (ELISA) are indicated to resolve these effects.

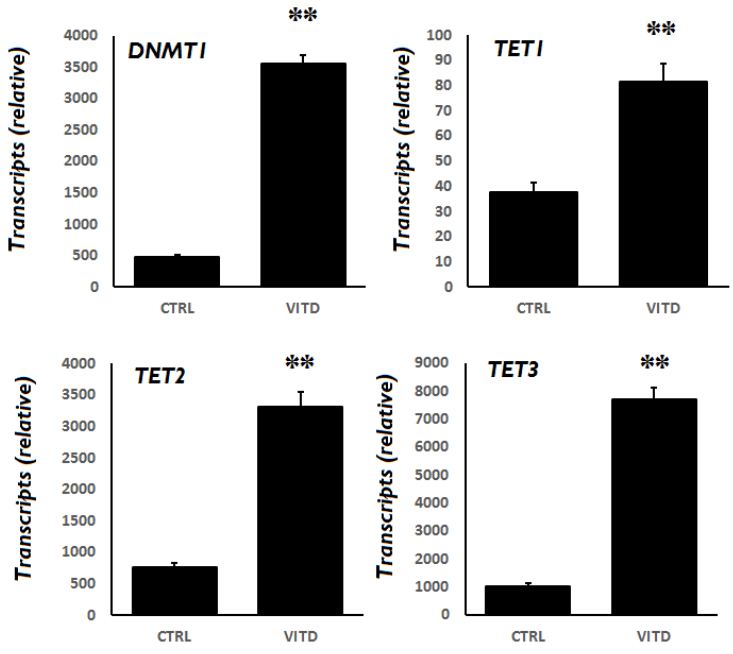

Figure 17 - <u>5mC metabolic enzyme transcription in adherent D-treated THP1 monocytes.</u> Vitamin D significantly induces DNMT1, TET1, TET2, and TET3. TET1 transcription is relatively low compared to the other genes, raising the possibility that responsibility for DNAm metabolism in these cells falls to the other TETs analysed. Activity assays are indicated to determine the relationship between transcription and enzyme activity to determine any mechanistic effects of vitamin D in regulating 5mC methylation and DNAm patterns in THP1 monocytes. Conditional interference will help to resolve the relationship between DNAm patterns and differentiation of the TRM phonotype hinted at here by our experiments.

Discussion

Vitamin D deficiency, indicated by serum calcidiol (pre-vitamin D) concentration <50nmol/L[19], is associated with an increased risk of Inflammatory Bowel Disease[268]. Both chronic inflammation and vitamin D deficiency are associated with CRC risk, and further associated with aberrant DNA methylation affecting Wnt tumour suppressors in the colonic epithelia. To resolve these associations mechanistically, it was speculated that vitamin D sufficiency attenuates systemic inflammation, thus indirectly attenuating age-related DNA methylation defects promoted by inflammatory mechanisms in the colonic epithelia. First, markers of systemic and local inflammation were characterised in a small cohort of healthy individuals from Auckland, NZ (n = 27), supplemented with Lester's Oil, which contains 1000 IU (25ug) of vitamin D – 3x the recommended daily intake.

Versus the placebo, supplementation with Lester's Oil promoted a significant increase in serum vitamin D of 15nmol/L. Given the exponential decrease in CRC odds ratio with increasing serum vitamin D[269], small improvements in circulating vitamin D in deficient patients have a greater impact on health outcomes than small improvements where sufficiency is established. As no individuals in our cohort were vitamin D deficient at any point during the intervention, it may be pertinent to investigate the effects of these supplements in a deficient cohort, where the impact on biomarkers should be more pronounced. Regardless, the increase in vitamin D in this cohort was associated with a significant reduction in serum C-reactive protein (↓2..46mg/L, p = 0.0423). Although CRP itself is not mechanistically responsible for effecting tumourigenesis, it's clinical usefulness as a marker of systemic inflammation is well established, as are its associations with cancer risk[270]. In fact, Erlinger et al report an odds ratio for developing CRC at 1.35-1.38 associated with a 1.02 mg/L increase in CRP[271], so in this respect, correcting for vitamin D deficiency via supplementation, where a 2.5mg/L improvement was noted, is proposed to favourably impact on CRC risk.

Conversely, IBD may be diagnosed non-invasively by measuring faecal calprotectin (FC)[272], which is elevated during inflammation and infection due to

neutrophilic infiltration of the mucosa. Contrary to our hypothesis, our cohort saw a non-significant trend towards elevated FC following supplementation, and when stratified by sex, the increase in males was significant. However, the large standard errors associated with these results suggests that caution should be exercised in asserting the null hypothesis, particularly in light of recent reports that FC is inversely associated with serum vitamin D in IBD, and the relationship is strengthened where the disease is in remission, suggesting that for disease-free individuals, the association may be even stronger[273]. In contrast to our findings in D-sufficient healthy individuals, Garg et al report serum vitamin D to be inversely associated with FC (but not CRP or other markers of systemic inflammation), in a cohort of 70 IBD patients, raising the possibility the vitamin D's mechanisms of action are either different in healthy versus disease tissues, or the same but impaired in IBD. Inclusive intervention studies that incorporate healthy, D-deficient, and IBD relapsing/remitting participants may be necessary to resolve the associations of serum vitamin D with biomarkers of systemic and mucosal inflammation. Certainly our data support larger studies investigating the effects of Lester's Oil on inflammation and disease risk in the distal bowel.

Tumour necrosis factor-alpha plays a key role in mediating acute phase inflammation, and both serum and mucosal concentrations are elevated in IBD[274,275]. Furthermore serum TNFα is positively associated with CRP status[276], and monocytes from TNFα-high IBD patients produce more TNFα relative to TNFα-low patients when primed with LPS[218], suggesting that serum TNFα is associated with aberrant TNFα transcription in IBD monocytes. We investigated the methylation status of a single CG in the TNFα promoter region in a subset of the Lester's Oil participants (n= 8) who's vitamin D status varied across the trial period. Vitamin D was inversely associated with TNFα methylation ($P<0.001$), but not when participants were stratified by treatment regimen, indicating analysis in the full cohort should be pursued. The NZ group report no change in TNFα transcription for the whole cohort, and transcriptional data was not available for our sub-set, which suggests that either our data are insufficient to extrapolate to the larger cohort, or that methylation status is independent of

TNFα transcription. Equally, TNFα transcription may have varied in our subset, but is masked in the full cohort. Determining TNFα transcription in vitamin D-supplemented participants whose promoter DNAm is dynamic, is essential to resolve the epigenetic regulation of TNFα in PBMCs. Methylation of TNFα is reported to decrease in PBMCs from obese participants given a calorie-restricted diet, but in this study of obese men, not only was TNFα methylation lower at base line than in our healthy participants, but serum TNFα at baseline was positively associated with TNFα methylation status, suggesting that hypomethylation does in fact promote TNFα transcription[277]. Silencing of TNFα by promoter hypermethylation is reported elsewhere[278]. Finally, to confirm the dynamic nature of TNFα, one would anticipate D-deficient monocytes to exhibit increased promoter methylation. Investigating promoter methylation longitudinally in vehicle-treated cells would contribute to our understanding of the nature of DNAm in TNFα.

We sought to a) identify the component of PBMCs contributing variable DNAm and b) demonstrate a mechanistic effect of vitamin D specifically versus Lester's Oil, which contains other anti-inflammatory compounds. Monocytes were selected for their relative frequency, and role in monocyte-derived TNFα in IBD. Treatment with vitamin D reduced TNFα methylation in adherent populations of THP1 monocytes, but not those remaining in suspension, which suggested to us that methylation status might be associated with an (adherent) tissue-resident macrophage phenotype. This appears conclusive in light of our data showing a concomitant increase in macrophage markers in adherent cell populations[83], although expression changes of end-point proteins (CD14 and CD68) should ideally be quantified by IHC or Western Blot. However, although conditional hypomethylation by 5AZA also showed induction of these markers, relative transcripts were low, and adhesion was not the prominent phenotype – this could be attributable to transdifferentiating effects of 5AZA, which are reported to impair macrophage adhesion[279]. Perhaps better insights are afforded by the PMA-treated cells, which showed severe hypomethylation, increased adhesion, and induction of phenotype markers. In support of our findings, TET demethylase

transcription is enhanced in D-treated cells, implying modulation of 5mC metabolism by vitamin D in THP1 monocytes; activity assays are indicated to confirm a functional pathway for vitamin D-mediated hypomethylation of TNFα, particularly as we also saw a dose-dependent *increase* in Interleukin 8 promoter methylation in the suspended fraction of D-treated cells (2.7% vs 7.7% p = 0.047, data not shown). Our conclusions are strongly supported by a very recent study, that fully characterised the methylomes of monocytes and monocyte-derived macrophages; the authors conclude that a panoply of genes associated with the macrophage phenotype are repressed by hypermethylation in monocytes, and that are actively hypomethylated by TETs 2 and 3 during differentiation. When TET activity is inhibited, hypermethylation is restored in induced-macrophages[280]. We also noted that TET1 transcription was relatively low compared to 2 and 3, and independently predicted their role in hypomethylation in this instance.

Specifically, Takei et al previously performed very similar experiments to us, treating THP1 monocytes with vitamin D and PMA, and determining TNFα methylation and transcription in response to LPS. With regards methylation and phenotype, the authors' results recapitulate our findings here, however they suggest that hypomethylation by vitamin D increased TNFα transcription both in isolation, and in combination with LPS[281], as we hypothesised. However we observe TNFα to be repressed after having its promoter hypo-methylated, and pre-treatment with vitamin D attenuated the response to LPS, rather than enhancing it as we predicted. Here the authors use 10ug/mL LPS, not 5ug/mL, but they also fail to note the length of stimulation. This contradiction should be fully resolved to determine the true role of TNFα promoter methylation status in regulating transcription. It is encouraging in a broader context that vitamin D appears to inhibit TNFα transcription in THP1 monocytes, supporting vitamin D's role as a systemic anti-inflammatory.

Several limitations should be considered when interpreting the data presented here, firstly the sub-group (n=8) may not represent the cohort, which in turn may not represent the broader population, nor D-deficient candidates. Secondly, caution is advised against extrapolating data here to the physiology of

monocytes/macrophages in IBD, which are established to be dysregulated. Thirdly, the contribution of circulating lymphocytes was not addressed; showing variable DNAm in monocytes does not preclude a synchronous effect of vitamin D on the methylome of T-cells. After all, TNFα methylation status is reported to be tissue specific[219], although it is posited to define myeloid lineage (when hyper-), and lymphoid lineage (when hypo-)[282], implying our data are representative. Further supplementation studies in D-deficient and IBD patients are indicated, as is verification in primary models, as opposed to transformed leukemic cells (THP1).

Finally, an important note on the Lester's Oil trial independent to the results from *in vitro* work; while vitamin D status was observed to correlate with markers of systemic inflammation and DNA methylation status in the cohort, causation is by no menas demonstrated – The composition of the Lester's Oil supplement also includes other compounds reported to modulate inflammatory pathways, for example vitamin E (transrectal lavage) is shown to inhibit TNFα, IL1β and IL6 in the colonic epithelium in a model of induced-colitis[466], while oral vitamin E reduced circulating CRP across 12 trials selected for meta-review by >0.5mg/mL[468], suggesting that here, that the mechanism of Lester's Oil suppressing CRP are indeed mulitfactorial. Similarly, oral astaxanthin inhibits colitis and modifies CRC risk via down-regulation of inflammatory mediators in the colonic mucosa[467].

In summary

Improving vitamin D status is associated with reduced CRP, taken as a marker of systemic inflammation, and may contribute to the attenuation of age-related hypermethylation in the distal colon. In support of other studies, our data suggests that vitamin D promotes differentiation of monocytes associated with TNFα-hypomethylation, and that both the monocyte-derived macrophage sub-phenotype, and TNFα methylation status, vary according to the differentiating stimulus. In vivo studies specifically addressing aspects of systemic inflammation and their impact on DNA methylation in the colonic epithelia are warranted to elucidate the contribution of vitamin D as an anti-inflammatory in the attenuation of age-related DNA hypermethylation.

Chapter 4

VITAMIN D ATTENUATES TGFB1 MODIFICATION OF THE INTESTINAL MYOFIBROBLAST METHYLOME

Preface to the work

A fundamental paradox remains regarding vitamin D and its relationship with poor health – an epidemiological association between serum vitamin D and a raft of diseases, affecting most tissue types, is well documented; were the relationship *causal*, one would expect clinical interventions correcting for insufficiency to impact favourably on disease risk. To date, the evidence for this is scant[66], implying that the observed association of low serum D, is synchronous to, but not necessarily a consequence of, poor health.

Speculative reasons for the dichotomy include the quality and paucity of clinical trials data, together with follow-up to interventions not typically exceeding three years[283]. Furthermore, serum D (calcidiol) as a marker of cytosolic bioavailability is not well established; activating hydroxylations are managed by enzymes that are polymorphic, heterogeneously efficient, and prone to single nucleotide point mutation, not to mention transport proteins, other cofactors, and vitamin D's cognate receptor, VDR, all of which have a role to play in active D cytosolic bioavailability[284,285]. Thus low serum D does not necessarily equate to impaired cytosolic active vitamin D.

Alternatively, gastrointestinal absorption of nutrients is typically dysregulated in IBD[286]; this could explain lower serum D found in CRC patients at presentation without implying causality. Equally, as a fat soluble compound, obesity might precipitate poor health (via chronic adipo-inflammation) *and* low serum D simultaneously[40]. Finally, the two scenarios are not mutually exclusive; vitamin D regulates thousands of genes, and status is associated with diseases of almost every tissue and system. Insufficient vitamin D driving pathology in one system (e.g. IBD), may be the consequence of impaired function that limits vitamin D bioavailability in another (obesity).

Promisingly, a role for vitamin D sufficiency effecting positive pressure on the methylome has not yet been extinguished – if nothing more, vitamin D appears at least mechanistically *capable* of modifying 5mC patterns (granted, in one gene, in

one cell type, in a context-specific fashion, *in vitro* – see chapter 3), possibly via transcriptional control of enzymes regulating methylome fidelity (DNMT1, TETs). In this respect, we asked if vitamin D's ability to impact 5mC patterns might be extended to other genes in other cell types.

Having investigated a role for vitamin D in the differentiation and competence of circulating monocytes, as a contributing factor to vitamin D's hypothesised effects promoting bowel health, it is now appropriate to turn our attention to the microenvironment of the crypt niche, and gain better insight into the paracrine relationship between crypt stem cells and their nearest neighbours, the pericryptal myofibroblasts.

It has been suggested that Intestinal Myofibroblasts (InMyoFib) contribute growth factors, cytokines, and other signalling molecules to the crypt niche[107], indeed, these cells promote *in vitro* culture of colonic organoids[113]. Reagents for organoid culture were a burgeoning cost for the project, so utilisation of primary mucosal myofibroblasts as a source of growth factors for experimental procedures was a logical extension warranting further investigation. Initial forays into the propagation of primary pericryptal myofibroblast (MFBs) – recovered from the uninvolved mucosa of CRC resection specimens – proved prohibitive under routine cell culture conditions; primary monolayers took 4-8 weeks to become established, frequently senesced prior to analysis, and invariably presented mixed populations, primarily comprised of alpha smooth muscle actin negative fibroblasts (aSMA positivity being the primary defining feature of an activated InMyoFib[287]).

To negate these logistical barriers, the addition of soluble growth factors to accelerate proliferation was contemplated, but considered uncertain with regards clandestine modifying effects on cell phenotype. Searching the literature for documented effects of potential growth factors, brought to light a good many papers focused on TGFβ1 and its actions converting stromal fibroblasts to myofibroblasts associated with the *de novo* induction of aSMA[288].

Thus, treatment of mixed primary fibroblast cultures with TGFβ1 was postulated as a potential method to rapidly establish ubiquitous aSMA expression and phenotype homogeneity. In particular, De Boeck et al allude to the irreversible establishment of a MFB phenotype in mesenchymal stem cells treated with TGFβ1, that commits naive cells to a MFB phenotype, preventing subsequent transdifferentiation[289]. To us, this suggested that heritable epigenetic modifications (DNAm), manifest by TGFβ1, might underpin transcription and expression of aSMA and/or other myofibroblast-intrinsic properties.

Previously, a validated line of primary intestinal myofibroblasts (InMyoFib) had been purchased from Lonza, for use as healthy controls when stimulating CRC-derived MFBs with recombinant cytokines (see chapter 5); it was therefore decided, to first characterise the effects of TGFβ1 on the phenotype, transcriptional profile, and DNAm status of this cell line and, in keeping with project objectives, investigate any role for vitamin D in mediating the effects.

[Credit for data included in this chapter must be attributed in part to my colleague and student, Federico Bernizio, who assisted in the preparation of samples and processing of some of the data, as part of a short project funded by The Big C cancer charity in the summer of 2015].

Abstract

Transforming-growth factor beta one signalling is frequently deregulated in colorectal tumours, inducing stable *de novo* expression of aSMA in stromal fibroblasts that in turn promote tumour invasion and metastasis via a modified secretome. These cells do not transdifferentiate, suggesting TGFβ1induces heritable epigenetic modifications during differentiation. Pericryptal *myo*fibroblasts represent healthy mucosal cells expressing aSMA that contribute growth factors and ECM components to the crypt niche, and are reported to maintain crypt stem cells in vitro. Further to the well-documented association between serum vitamin D and incidence of colorectal cancer, vitamin D's cognate receptor, VDR, negatively regulates TGFβ1 signalling in myofibroblasts. In this context, it was hypothesised that TGFβ1 remodels the methylome of intestinal myofibroblasts to effect cell phenotype and their influence on epithelial homeostasis. Once characterised, the ability of vitamin D to mediate the process was investigated.

TGFβ1 inhibited proliferation of MFBs and transcription of a panel Wnt-associated genes, that persisted post-induction. Although induced by TGFβ1, the methylation status of aSMA was not affected, precluding a role for dynamic DNAm in transcriptional regulation of the gene in this context. Methylation array (Illumina 450K) identified candidate genes who's DNA methylation status was associated with the novel TGFβ1-intitiated phenotype, synchronous to modulation of TET enzyme activity. Although vitamin D partially attenuated TGFβ1-induced DNA methylation, and the consequent transcription of affected genes, synergy was observed with other TGFβ1-regulated genes not differentially methylated, including TETs 1 and 3, indicating that vitamin D's effects mediating TGFβ1-induction are diverse and highly context specific. TGFβ1 also induced VDR, which may account for transcriptional synergy between these agents. The methylation status of a single CG in the Fibroblast Activation Protein (FAP) promoter significantly correlated with its transcription - an effect attenuated in combination with vitamin D – of note because elevated FAP promoted tumourigenesis.

This work raises the possibility of a role for TGFβ1 signalling in directing the intestinal myofibroblast phenotype via a modified methylome and regulation of TET enzymes. Vitamin D did not exhaustively attenuate TGFβ1's effects. Candidate genes regulated by DNAm involved in myofibroblast plasticity have been identified and their role in gut epithelial homeostasis discussed.

Introduction

In the colonic mucosa, multiple mechanisms are in place locally that allow for epithelial plasticity, manifest as regenerative potential that mitigates for hypotrophy in the wake of transient inflammation, and redundancy, such that control of stem cell turn-over is shared between converging autocrine and paracrine signalling cascades.

The crypt stem cell (CSC) niche is partially comprised of pericryptal, α-smooth muscle actin (aSMA) positive myofibroblasts, recognised for their contribution to paracrine Wnt signalling that ensures a tight balance between CSC proliferation at the base of the crypt, and apoptosis at the luminal interface[reviewed in 290]. Apportioning a degree of control to neighbouring non-epithelial cells adds a further layer of redundancy governing the vital process of epithelial homeostasis.

Pericryptal myofibroblasts are key contributors to the paracrine signals managing Wnt-mediated CSC turnover; antagonism of BMP signalling at the base of the crypt is observed *in vivo* via MFB secreted GREM1 and 2, that inhibits differentiation, thus maintaining Wnt-mediated stem cell turnover[107]. Primary MFB cultures have also been shown to support colonoid formation *in vitro*, and express relatively high levels of r-spondins (LGR5 ligands that transduce the Wnt-cascade)[226]. An example of the aforementioned redundancy is demonstrable in the small intestine, where conditional deletion of paneth cells, a paracrine source of Wnt3a, does not impede stem-cell turnover, suggesting a non-epithelial source of growth factors[291]. However, conditionally blocking Wnt-ligand secretion by ablation of PORCN in *both* the epithelia and submucosa, also fails to disrupt cryptogenesis, hinting at further esoteric sources of LGR5 ligands[292]. Finally, inhibition of Wnt may also be effected by other MFB-secreted factors, such as DKK1 and SFRP1, who out-compete Wnt agonists by preferentially binding LGR5 receptors[293,294].

A phenotypically similar population of aSMA+ve mesenchymal cells are also present in colorectal tumour stroma, increasingly recognised as mixed populations of trans-differentiated mucosal fibroblasts and bone marrow-derived mesenchymal stem cells (MSCs)[295]. In healthy tissue, the recruitment of elastic

myofibroblasts expressing aSMA is a key stage of the wound healing and tissue repair process[296], and benign transient trans-differentiation of fibroblasts to aSMA+ve myofibroblasts is driven principally by controlled TGFβ1 signalling[297]. In a cancer setting this control appears to be deregulated, with the *de novo* expression of aSMA in the stromal compartment documented to be induced by both aberrant autocrine and paracrine TGFβ signalling[298]. Cancer-associated fibroblasts (CAFs) promote tumour invasion by a pathologically altered secretome that encourages angiogenesis and remodelling of the extra-cellular matrix(ECM)[299], and there has been a great deal of research looking at myofibroblast regulation of ECM components and stromal architecture permissive to metastasis. Colorectal CAFs and MSCs (induced to express aSMA by TGFβ1 treatment) demonstrate partial overlap of their secretomes (200+ proteins), that include components of the ECM, proteases (MMP2 and 3), and growth factors (HGF, EGF). In that study, treatment with TGFβ1 fixed the phenotype of both MSCs and CAFs, prohibiting trans-differentiation or reversal of the established phenotype[289]. These observations led us to hypothesise that stable epigenetic modifications, precipitated by TGFβ1, induce aSMA transcription and changes to the myofibroblast phenotype. Encouragingly, inhibition of DNAm was observed to induce aSMA promoter *hypomethylation* associated with *de novo* aSMA expression in naive lung fibroblasts[300].

It is apparent that pericryptal myofibroblasts and CAFs are distinguishable only by virtue of locus and temporal context; pericryptal vs stromal, healthy vs disease-associated. Like CAFs, MFBs are mesenchymal in origin, organise their local environment via secreted ECM and growth factors, and importantly express aSMA. An increasing body of evidence documents the relationship between TGFβ1-initiated CAFs, stromal architecture, and the transformed cells they interact with. However, there is a paucity of information pertaining to the effects of TGFβ1 on healthy pericryptal myofibroblasts and their secretory profiles, particularly with regards regulation of Wnt signalling; aberrant activation of Wnt is after-all a hall mark of transformation. Furthermore, remodelling of the ECM typically precedes a microenvironment permissive to invasion[301], and increased

levels of TGFβ1 in the lamina propria are noted in chronic inflammatory diseases that expedite tumourigenesis[302].

In this context we have investigated the effect of recombinant TGFβ1 on growth factor transcription and the epigenome of an aSMA-expressing line of Intestinal Myofibroblasts (InMyoFib), and the consequences for epithelial homeostasis. In keeping with the over-arching hypothesis that vitamin D promotes bowel health, and in light of the observation that vitamin D regulates TGFβ1 signalling in activated fibroblasts[303], the ability of vitamin D to mediate any effects of TGFβ1 on the transcriptional profile and methylome of InMyoFib, has also been characterised. Primarily we sought to establish if TGFβ1's effect were indeed stable, if they could be attributed to dynamic promoter methylation status in the aSMA gene, and if TGFβ1 regulates transcription of enzymes involved in DNA methylation metabolism.

Methods

Cell culture

Intestinal Myofibroblasts (InMyoFib) were purchased from Lonza and cultured by routine cell culture protocols according to the manufacturer's instructions with prescribed SmGM-2 Smooth Muscle Growth Medium-2 (cat. no CC-3182). Cells were routinely passaged and used between passage numbers 2-6. Induction with recombinant (r)TGFβ1 in PBS was achieved at a final concentration of 0.1-10ng/mL in culture medium. Cells were treated for 48 hours, with refreshed at 24 hours.

To assess stability of the induced changes in gene expression, after the initial 48 hour induction protocol, media was removed, cells washed twice with PBS, and fresh media applied. Cells were subsequently cultured for a further 48 hours, with an additional wash after 24 hours, to mitigate for residual effects of rTGFβ1. Monolayers were then harvested by trypsin-EDTA chelation and cell pellets rinsed with PBS prior to nucleic acid extraction.

For media conditioning experiments, InMyoFib were initiated with TGFβ1 (10ng/mL) for 48 hours, washed twice over the subsequent 48 hours, and then fresh media applied at approximately 80% monolayer confluence, for conditioning over the subsequent 24 hours. Supernatants were collected, spun at 300G to remove cell debris, and passed through a 20μm filter, before being flash-frozen on dry ice and stored at -80°C. Conditioned supernatants were mixed 50:50 with fresh DMEM/f12 to mitigate for nutrient depletion

To condition media from HCT116 cells, cells were cultured to 80% confluence in 75cm^2 flasks, and fresh DMEM/f12 conditioned for 24 hours. Collected supernatants were spun as before and mixed 50:50 with InMyoFib culture media.

Biological triplicates were processed for each experiment and technical triplicates (Q-rt-PCR) or duplicates (Illumina 450K array) reported as the mean +/- the standard error.

Nucleic acid extraction and processing

As detailed in General Methods, RNA was extracted using the Isolate II RNA mini-kit from Bioline according to the manufacturer's instructions, which includes an on-column DNase step to digest contaminating genomic DNA. RNA was quantified by UV spectroscopy (Nanodrop, Thermo), and 500ng reverse transcribed using Q-script from Bioline according to the manufacturer's instructions. Assuming a 75% rate of efficiency for the reverse transcription, 375ng of cDNA was diluted in 180μL of MilliQ water to give a final concentration of 2ng/μL.

DNA was harvested by phenol-chloroform extraction as outlined in General Methods. Samples were precipitated, washed with 70% ethanol, and resuspended in water to yield a final concentration of 50ng/uL. Biological triplicates of 500ng were interrogated in duplicate by Cambridge Genomic Services on the Infinium HumanMethylation450 Bead Chip Kit according to the manufacturer's instructions.

WST1 and trypan blue assay

To determine the effect of treatment with TGFβ1 on proliferation of cells, InMyoFib were seeded in 96 well plates at a density of 5000 cells per well. After observing a 24 hour period to allow cells to adhere and enter log growth phase, media, with either PBS vehicle at the highest concentration or rTGFβ1 at the specified final concentration, was applied for 48 hours (refreshed after 24). The mean absorbance of 10 technical replicates was determined by tetrazolium salt assay after 2 hours incubation with 10% WST1 reagent (Roche) according to manufacturer's instructions (absorbance at 450nM). Data were normalised to the control and the data displayed as the mean +/- the SEM. A three-tailed T-test, assuming non-normal distribution of the data, was performed to determine statistical significance. For trypan blue staining, treated cells were harvested by EDTA chelation and 20uL of dissociated cells in suspension mixed with 20uL of trypan blue. Samples were loaded into cell counting chambers and counted (Nexcellom) to determine cell viability.

Q-rt-PCR

Q-rt-PCR were performed in triplicate with 6ng of cDNA per reaction. Cycle-threshold (Ct) after 40 cycles was normalised against that for the 18S 'house-keeping' reference gene. The number of relative transcripts, or the fold change normalised to PBS vehicle, was determined by the ΔCt or ΔΔCt method, respectively[304]. Intron-spanning primers were designed by using the human Universal Probe Library software (Roche) against the NCBI NM RNA reference sequences (appendix 6). All Q-rt-PCRs were validated at 60°C.

RnBeads pipeline for Infinium HumanMethylation450 data

Data were processed by CGS using the RnBeads plugin for 'R' console[228]. The mean methylation (β values between 0 and 1, representing percentage of methylated alleles at the site) +/- the SEM of three biological replicates was used for comparisons between sample groups. Whilst the array also generates β values for non-coding CpG islands (pseudogenes, micro RNA, repetitive elements), for the purposes of the analysis, regions of interest were defined as single CpG sites associated with functional genes (477,311), gene regulatory elements (30,840 promoters), or whole-gene sequences (30,681), limiting read-outs to regions of methylation effecting transcriptional control, and thus verifiable by gene–specific Q-rt-PCR.

Quality control

Control sample data were separately processed by CGS using Illumina's Genome Studio. All variables measures returned values within defined quality parameters and accurately predicted sex (male).

Regional variability

The variability of a sample group is the span between 5th and 95th percentile of β values, averaged over all valid sites and regions. This amounts to a number between 0 and 1 and corresponds to the relative area of deviation in the plots presented.

Distribution of β scores

Methylation score distributions were assessed based on sample group at the assigned levels (sites, promoters, genes), to identify shifts in the densities of β values associated with treatments.

Low-dimensional representation and sample group clustering

Dimension reduction (multidimensional scaling - MDS) was used to visually inspect the dataset for a strong signal in the methylation values related to sample grouping.

Results

Effect of TGFβ1 on the phenotype of Intestinal Myofibroblasts

TGFβ1 reduced proliferation and improved Intestinal Myofibroblast viability

To determine an appropriate treatment regimen, proliferation of Intestinal Myofibroblasts (InMyoFib) was first determined by WST1 tetrazolium salt assay. Cells were seeded in 96 well plates at a density of 5000 cell per well, and treated for 48 hours during the log-growth phase. TGFβ1 effects a dose-dependent response on InMyoFib over 48 hours, reducing proliferation by 35% at 10ng/mL relative to PBS vehicle, with no macroscopic effects on cell morphology. The antiproliferative effect was not associated with decreased cell viability - rather, viability was moderately improved by treatment with TGFβ1, as determined by trypan blue staining (figure 18a and b).

TGFβ1 induces a transcriptional profile suggested to antagonise Wnt

Next, to establish if TGFβ1 might influence the secretory profile of InMyoFib as posited, a panel of genes regulating paracrine stem-cell turnover in the niche were interrogated by Q-rt-PCR. As a marker of the aberrant phenotype documented in cancer-associated fibroblasts, the expression of αSMA was also quantified. In keeping with the observation that TGFβ1 reduces proliferation, there was a trend toward decreased expression of Ki67 that did not achieve statistical significance (p = 0.07). αSMA was induced 3-fold, and a gene profile suggested to antagonise Wnt and promote epithelial differentiation was established, showing induction of DKK1 and BMP1 transcripts synchronous to the suppression of secreted growth factor transcription (RSPO1, EGF, HGF and JAG1) (figure 18c).

The transcriptional profile induced by TGFβ1 is maintained in the absence of TGFβ1 stimulation

Induction of stromal fibroblasts with TGFβ1 is reported to stably alter their secretory profile and associated with *de novo* expression of αSMA, that persists in the absence of continued stimulation[305]. This raises the possibility that enduring epigenetic modifications, such as DNA methylation, inform the MFB phenotype. To first determine the persistence of the induced transcriptional profile, InMyoFib were activated with TGFβ1 (10ng/mL) as previously described, followed by a 48 hour wash-out period to mitigate for direct transcriptional effects of rTGFβ1 (media was removed, cells washed twice with PBS, and fresh media applied every 24 hours). As before, the transcriptional profile exhibits sustained induction of aSMA, DKK1, and BMP1, concomitant with continued suppression of other growth factors. Although the effect appears weakly diminished for DKK1 and EGF, while HGF and JAG1 transcription are enhanced relative to cells actively undergoing rTGFB1 stimulation (figure 18d), suggesting that the sustained transcriptional profile is not simply a tapering effect.

Cancer-cell supernatants did not recapitulate the effect of TGFβ1

Given that TGFβ1 expression is elevated in high-grade colorectal tumours[306], it was speculated that the induction of the TGFβ1-associated transcription might also be initiated by treatment with aggressive CRC supernatants. The HCT116 cell line represents a poorly differentiated cancer phenotype with invasive properties, secreting TGFβ1[307]. HCT116 cells were cultured to >80% confluence in 75cm^2 flasks and used to condition InMyoFib culture media for 24 hours. Conditioned media was mixed 50:50 with fresh media to mitigate for nutrient depletion. As per rTGFβ1 initiation protocol, InMyoFib were cultured for 48 hours with HCT-conditioned media, followed by a 48 hour wash-out period. Transcription of aSMA, RSPO1 and DKK1 was determined during initiation (*t*=48) and after wash-out (*t*=96). No significant changes in their transcription was observed relative to vehicle (data not shown), possibly implicating a flawed methodology pertaining to secreted TGFβ1s latent stability/concentration, as will be discussed.

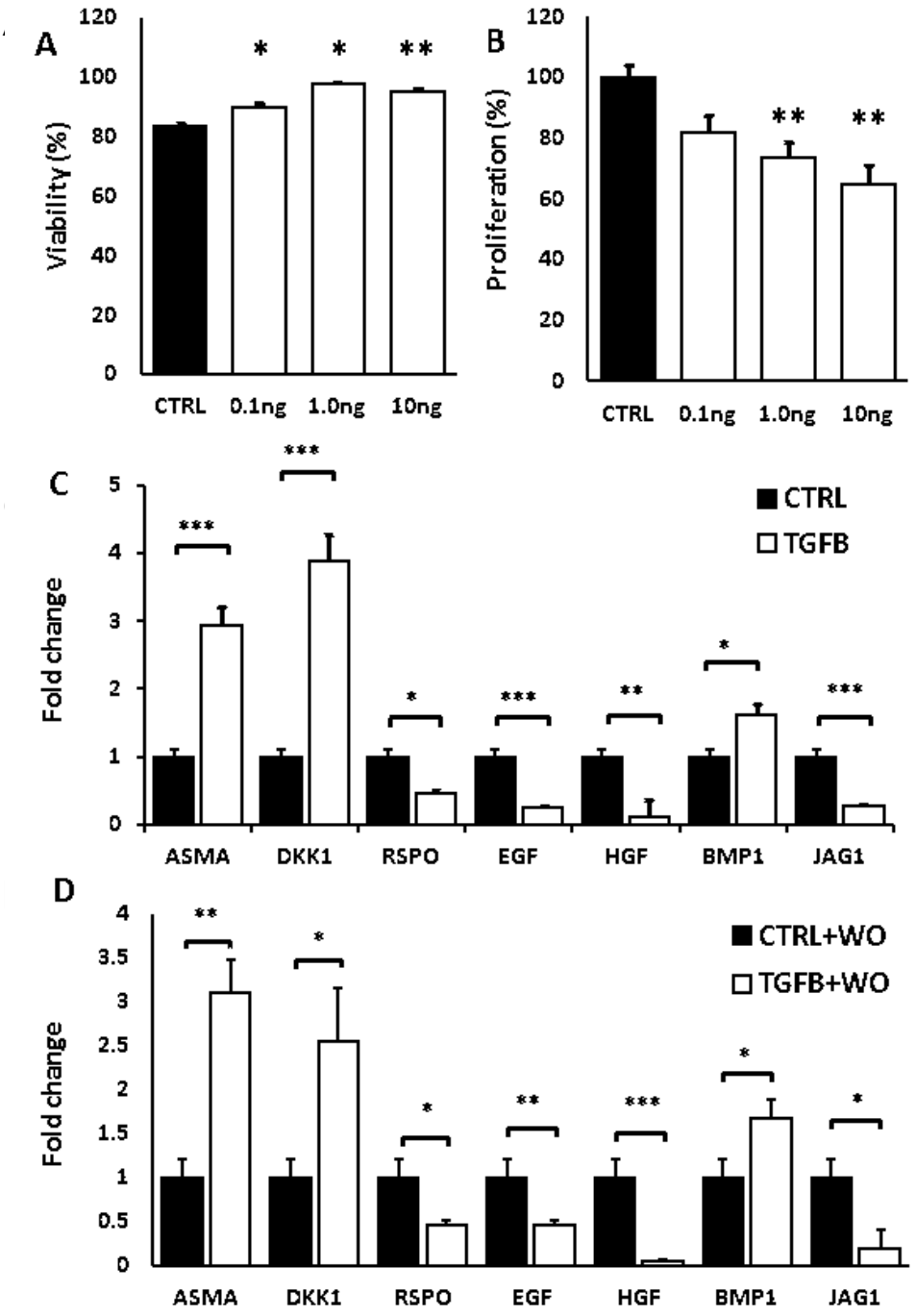

Figure 18 – TGFβ1 effects on the phenotype and gene transcription in InMyoFib. . * p<0.05, ** p<0.01, *** p<0.001. 3 biological replicates, 3 technical replicates. Data represtent the mean fold change relative the the control (normalised relative expression) +/- SEM A) Trypan blue staining suggests modest improvements in cell viability at 48 hours. B) After 48 hours proliferation, as measured by Wst assay, is concomitantly inhibited by recombinant TGFβ1 verses PBS vehicle, in a dose-dependent fashion. C) A transcriptional profile of a panel of epithelial growth factors and the lineage marker aSMA was determined at 48 hours, demonstrating induction of aSMA, DKK1 and BMP1 synchronous to the suppression of growth factors RSPO1, EGF, HGF and JAG1. This pattern was hypothesised to negatively regulate epithelial proliferation D) The modified transcription profile persists for at least 48 hours post-initiation; samples were treated for 48 hours with 10ng/mL TGFβ1, washed twice with PBS, and fresh media applied over the subsequent 48 hours to mitigate for residual rTGFβ1. The transcriptional profile recapitulated effects established prior to the wash-out period, with further suppression of HGF and JAG1 transcription, suggesting that the profile is entrenched and not a diminishing residual effect.

Supernatants fromTGFβ1-initiated cells reduced CRC cell line proliferation in vitro.

In order to investigate if the novel transcriptional profile modified the secretory phenotype of InMyoFib, colorectal cancer cell lines CaCO2 and HCT116 were treated for six days with TGFβ-initiated InMyoFib-conditioned media. After the 48hr/48hr initiation/washout period, fresh culture media was conditioned for 24 hours. The supernatant was collected and mixed 50:50 with fresh media to mitigate for nutrient depletion. CaCO2 and HCT116 cell lines, selected respectively for their well- and poorly-differentiated cancer phenotypes, were cultured for six days with either PBS-induced or TGFβ1-induced conditioned media, which was replaced every 24 hours. Proliferation was determined by Wst assay, and confirmed an antiproliferative effect of supernatants in both cell lines relative to PBS-treated control media. The more aggressive HCT116 line experienced greater antiproliferative effects (25%) than the better differentiated CaCO2 cells (10%) – figure 19a. CaCO2 and HCT116, are reported to be resistant to the antiproliferative effects of TGFβ-receptor ligation due to mutated signalling pathways[307,308], suggesting that the effect observed is a consequence of the altered InMyoFib secretory profile, and not residual recombinant or secreted TGFβ1.

TGFβ1-initiated InMyoFib supernatants regulate gene transcription in HCT116 cells

To investigate potential mechanisms for the antiproliferative effect of conditioned media, a panel of genes demarking cell-cycle, invasiveness, and differentiation, was interrogated in the more sensitive HCT116 cells. This time conditioned media was applied for four hours, assuming differential transcription precedes the antiproliferative response. Relative to vehicle control, TGFβ1-initiated InMyoFib media weakly induced a variety of homeostatic markers that, taken together, do not provide unifying insight into the antiproliferative effect of the supernatants. MUC2 was the only marker to exceed a fold change of two that might dominate other changes.

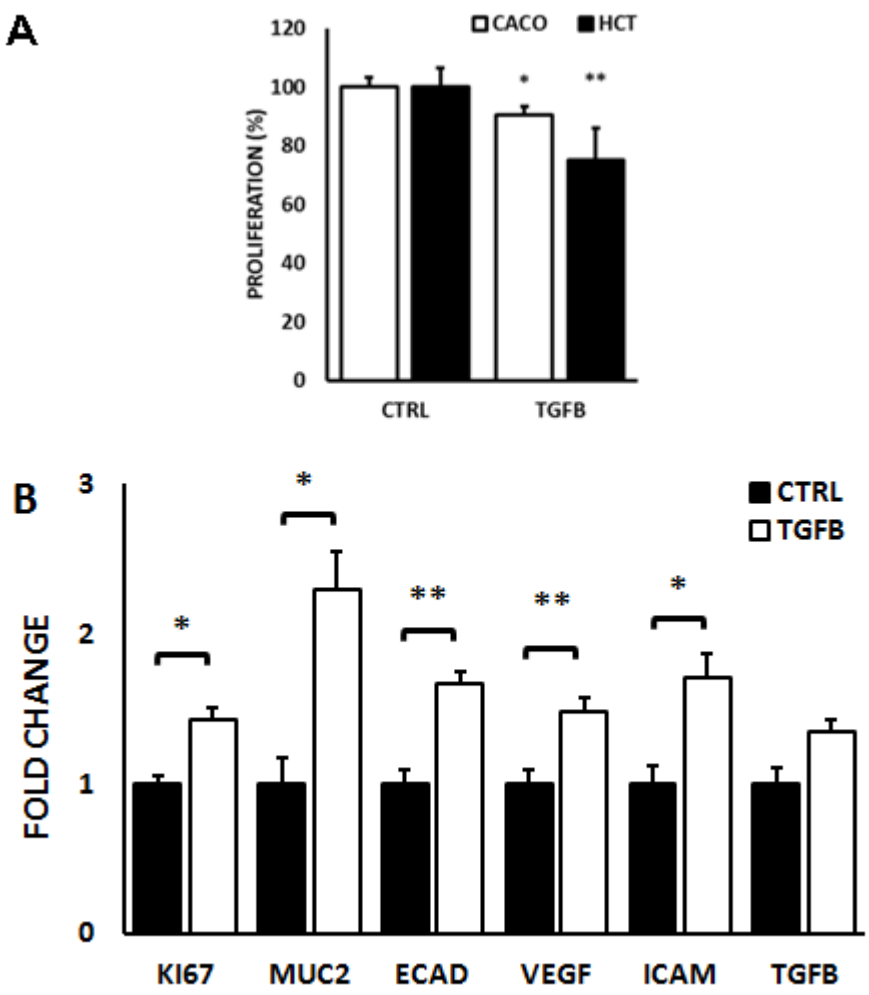

Figure 19 – TGFb1-treated InMyoFib media affects CRC cell phenotype *in vitro* . * p<0.05, ** p<0.01. 3 biological replicates, 3 technical replicates. Data represtent the mean +/- SEM A) Over six days, supernatants from TGFβ1-initiated InMyoFib reduced proliferation of CaCO2 and HCT116 cells 10 and 25% respectively, which is in keeping with the transcriptional profile established by TGFβ1-intiation B) HCT116 cells show a two-fold induction of MUC2, raising the possibility that conditioned media also promotes differentiation in the line. Other markers of proliferation and invasiveness were paradoxically raised in response to the conditioned media, but fold-changes did not exceed a factor of two, so do not specifically preclude an overall antiproliferative effect of the media. Modest promotion of TGFβ1 transcription was also observed in media-treated HCT116 cultures - this supports the hypothesis that tumour cells harness stromal fibroblasts to promote invasion by establishing a positive feedback loop that amplifies aberrant TGFB1 signalling.

Effect of TGFβ1 on the methylome of InMyoFib

The novel phenotype was not associated with changes in aSMA DNAm

Persistent induction of aSMA transcripts was hypothesised to be a consequence of changes in the methylation status of the gene. Bisulphite modified DNA from TGFβ1-induced InMyoFib was interrogated by Combined Bisulphite/restriction analysis (CoBRA), to determine any change in promoter methylation status. The αSMA promoter region was hypomethylated at base line (<2.1%), *and* in washed-out cells after treatment (data not shown). Further analysis of samples on the Infinium 450K bead chip array confirmed no significant changes in the methylation status of any CpG dinucleotides within the αSMA promoter or gene body. These findings preclude a role for dynamic DNAm in the gene sequence affecting the InMyoFib phenotype or α-smooth muscle actin transcription in Intestinal Myofibroblasts expressing aSMA at base line.

TGFβ1 induced methylome variability, and samples cluster according to treatment

Having established that, contrary to the informing hypothesis, TGFβ1 establishes an InMyoFib phenotype *independent* of aSMA methylation status, bmDNA was interrogated by Methylation 450 Bead Chip Array (Infinium)[309] to identify esoteric sites differentially methylated elsewhere in the methylome associated with the induced phenotype. Relative to vehicle controls, TGFβ1-initiated InMyoFib show sustained epigenome-wide β-score variability 48 hours post-induction (figure 20a-c). Plotting the top 1000 ranking differentially methylated regions, it is apparent that *hypomethylation* occurred more frequently than *hypermethylation* (at all regional levels), but a strong correlation between β-scores for sample groups suggests that TGFβ1 does not remodel the bulk of DNAm to produce two discrete methylomes (figure 20e-g). Dimensional representation indicates modest clustering of samples by treatment regimen that do not overlap (figure 20d), but clustering of samples could not be distinguished on β-scores heat maps (data not shown). Taken together, the array data suggest that the observed phenotypic response may be informed by a smaller subset of dynamic region-specific DNAm changes.

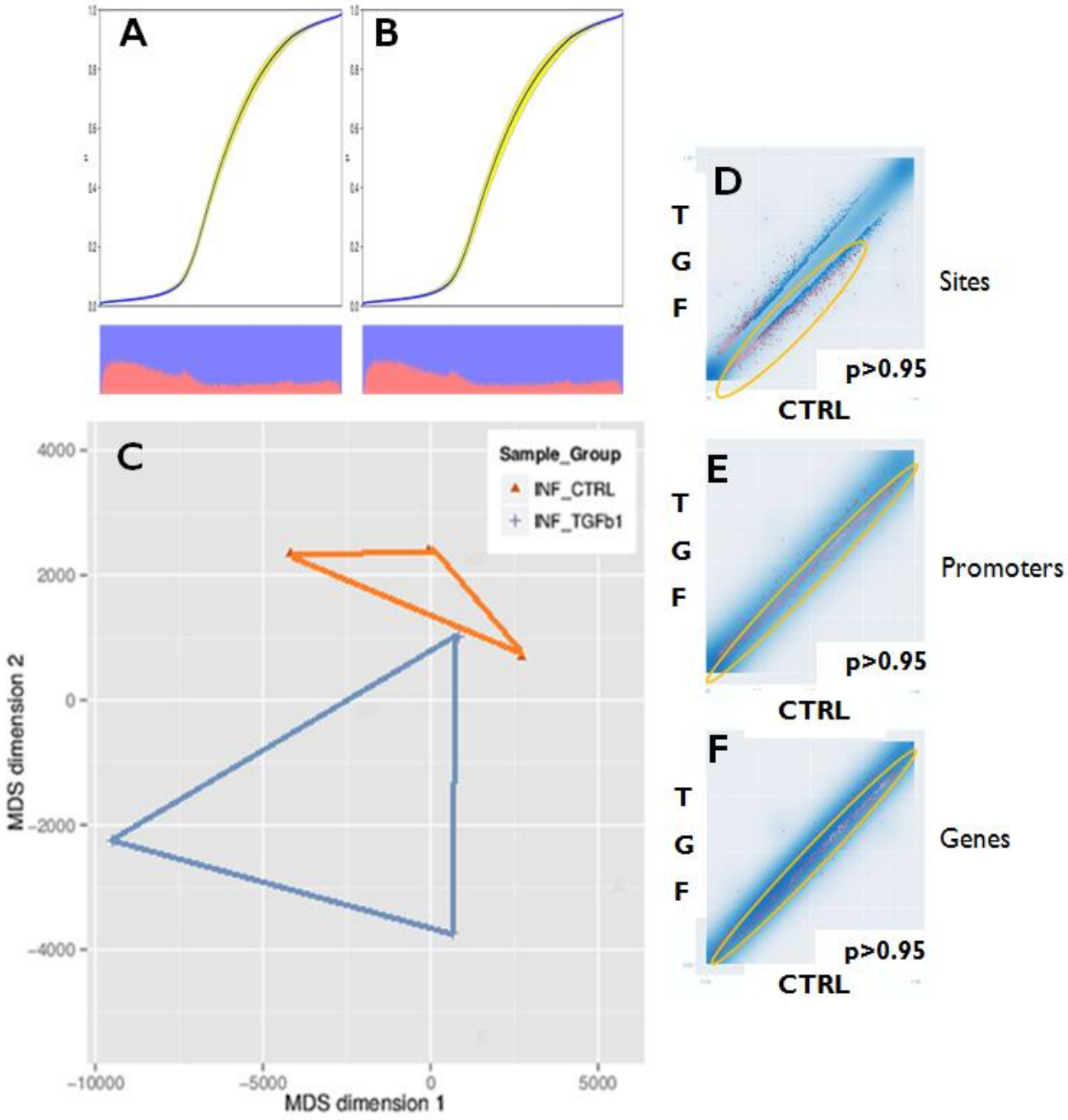

Figure 20 – Sample variability and clustering . Three biological replicates were pooled and extracted DNA probed in technical duplicates A & B) Deviation plots of sample groups. Probes are sorted in increasing order of their median methylation and are binned in groups of up to 120. The horizontal axis in the plot iterates over probe groups, and the vertical axis measures methylation degree. Median β values are depicted by a blue curve, and variability (yellow area) is greater in TGFβ1-initiated InMyoFib. C) Dimension reduction was used to visually inspect the dataset for a strong signal in the methylation values that is related to sample group. The scatter plot visualizes the samples transformed into a two-dimensional space using MDS; biological triplicates loosely cluster according to treatment regimen, with no overlap. Increased TGFβ1 variability here is represented by increased area coverage D,E,F) Scatter plots of β scores for each treatment do not suggest that treatment with TGFβ1 gives rise to a distinct methylome at either the site, promoter, or whole gene level; correlation values approach 1.0, a clear indication that methylation β scores in control samples are largely recapitulated in TGFβ1 samples. Pink markers indicate the top 1000 differentially methylated ranking sites for each level. At every level, *hypomethylation* is over-represented relative to hypermethylation in TGFβ1 samples, suggesting that demethylation is the dominant effect of TGFβ1 on the methylome of intestinal myofibroblasts under experimental conditions.

Indeed, treatment with TGFB1 was observed to modify DNAm status at a plethora of single CpG sites, gene promoters, and whole genes, across the methylome. Data were filtered to exclude; any region not attaining statistically significance (p = 0.05), exceeding the acceptable false-discovery rate, not achieving a change in β score above the 5% threshold, and, where necessary to limit the scope of validation experiments, not ranking in the top 1000 sites. Finally Ensembl annotations were mapped to functional genes, thus excluding un-assigned CpG islands, or those pertaining to miRNAs or pseudogenes. Figure 21.1 identifies 63 candidate genes differentially methylated at either the site (n=23), promoter (n=15) or whole gene (n=25) level, that were associated with the TGFβ1-initaited transcriptional profile. Notably, none of the GF genes previously characterised in transcriptional profiles experienced differential DNAm, precluding a role for dynamic DNAm in their transcription in this context.

Induced-network analyses of the 63 differential methylated candidate genes identified other nodes with biological significance, regarding colonic epithelial homeostasis and fibroblast differentiation, that might be impacted by an altered methylome (figure 21d); amongst others, fibroblast activation protein (FAP), interferon gamma (INFγ), amyloid precursor protein (APP), fibronectin1(FN1), the TGFβ-ligand SCUBE3, and Vimentin (VIM).

Ontology of networks in which these 63 genes occur in, suggested disease processes including ‘cancer’, ‘cell cycle’, and ‘focal adhesion’, as well as the ‘Wnt pathway’, ‘TGFβ1 signalling’ and ‘colorectal cancer’ (p < 0.05). Biological processes include ‘down-regulation of proliferation’, ‘cell-cycle’, and ‘mitosis’ (figure 21a-c).

Gene Name	Delta DNAm	p.value
ACR	5.77	0.03
AKR1B1	11.44	0.00
ANKRD20A1	5.70	0.03
AREG	10.41	0.00
ARHGAP15	12.24	0.00
ATP10D	-26.04	0.00
BPIFA3	6.41	0.04
C1orf195	7.83	0.03
C3AR1	5.60	0.04
CCND3	-26.70	0.00
CDH19	7.60	0.02
CFHR4	13.22	0.01
CYP4B1	8.20	0.02
DCBLD1	12.80	0.00
DEFB115	-5.30	0.01
DEFB134	7.15	0.01
FAM129A	-20.68	0.00
FAP	-10.57	0.00
FRMD4A	-10.39	0.00
GRIA2	8.36	0.01
HULC	-5.02	0.04
IFI44	6.84	0.03
ITGAE	-22.38	0.00
ITGB1BP2	5.29	0.05
LINGO2	5.02	0.04
LRBA	-19.92	0.00
LRIT3	5.38	0.03
NAALADL2	8.22	0.01
NALCN	-32.59	0.00
NAV3	-12.88	0.00
NBPF20	12.70	0.01
NPHP1	-11.96	0.00
OMD	6.89	0.02
OR10G9	6.49	0.04
OR4C12	11.89	0.03
OR4D10	7.32	0.01
OR5K2	5.40	0.02
OR6A2	-7.33	0.01
OR6B1	7.66	0.01
OR6B2	8.36	0.00
OSMR	-14.30	0.00
PABPC3	5.01	0.04
PHLDB2	-11.85	0.00
PIK3AP1	-10.44	0.00
PMCH	6.18	0.04
PRIM2	7.78	0.04
PROL1	6.65	0.04
PTHLH	-7.08	0.03
PTPRG	-12.34	0.00
RBM19	12.96	0.00
RDH12	7.28	0.02
REP15	5.06	0.03
RNF148	6.45	0.01
SERPINA11	-6.67	0.03
SGIP1	17.69	0.00
SNTN	-5.16	0.03
SULT1C3	6.29	0.01
TMPRSS11D	5.34	0.04
TUSC3	29.63	0.00
UGT2A2	9.36	0.04

Figure 21.1 – Table of candidate genes identified to be differentially methylated by TGFβ1 in Intestinal Myofibroblasts. Biological triplicates (n=3) were probed in technical duplicate.

Transcription of enzymes involved in DNAm metabolism is perturbed in InMyoFib following TGFβ1-initiation

Finally, to investigate potential mechanisms for the modification of gene-specific DNAm patterns by TGFβ1, InMyoFib were initiated according to the 48/48 hour treatment/wash protocol. A panel of markers involved 5mC metabolism (DNA methyltransferases and TET enzymes) was interrogated by Q-rt-PCR, to ascertain if transcription of methylation machinery might be impacted by TGFβ1-initiation. In retrospect, these changes most probably occur well in advance of changes in 5mC metabolic rate, and proper time course investigation of the response of DNAm enzyme transcription and activity is warranted to asses mechanistic aspects of the phenotypic observations.

Regardless, METTL7b, and TET1 were subjected to significant and sustained suppression following initiation by TGFB1, while TET3 was moderately induced (figure 21e), perhaps suggestive of a compensatory mechanism established to inhibit the demethylating potential of TGFβ1. Methyltransferase-like 7b has an emerging uncharacterised role in 5mC metabolism, of interest here as TGFβ1-induced METTL7b promoter hypermethylation was noted on the array data, associated with transcriptional suppression detailed.

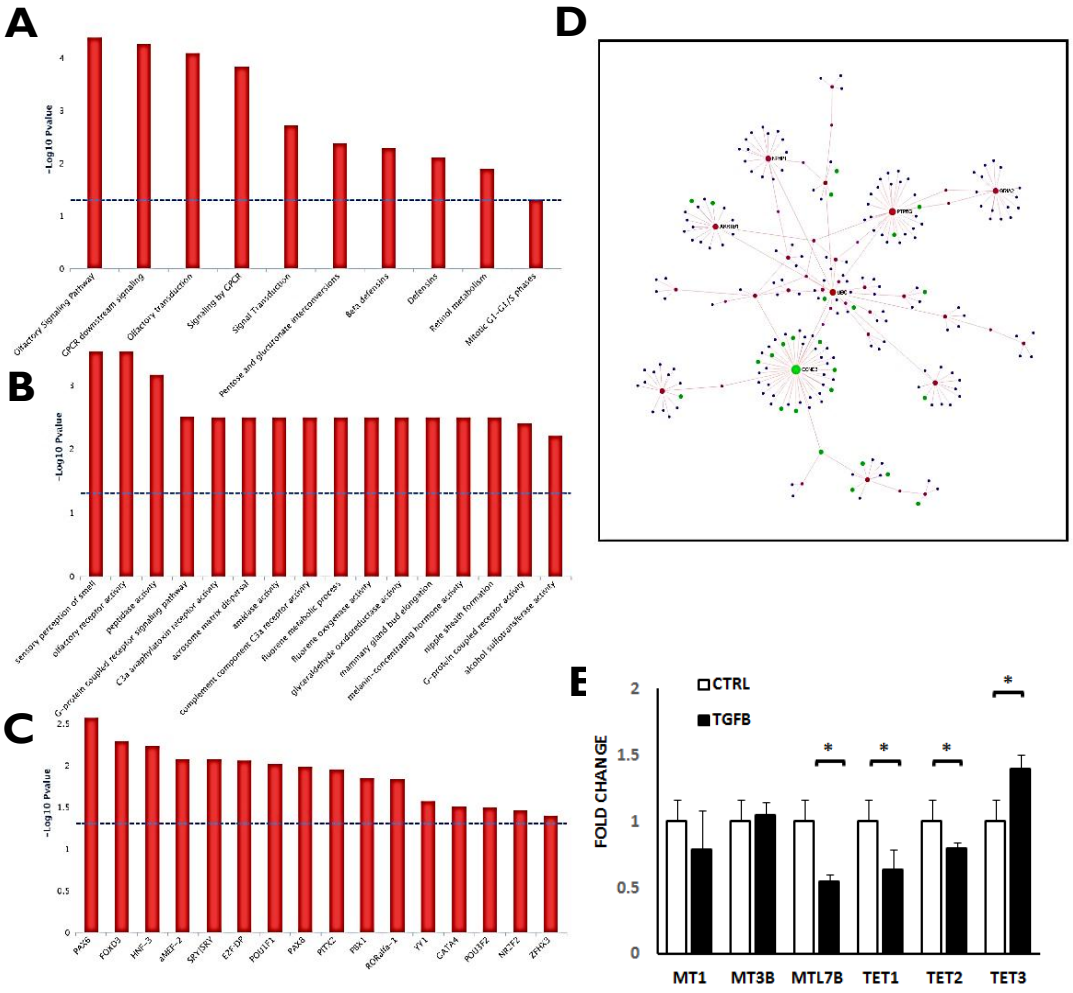

F

Pathway	Expected	Hits	P.Value	FDR
Pathways in cancer	8.54	31	1.16E-10	2.52E-08
Colorectal cancer	1.35	8	4.67E-05	0.000845
TGF-beta signaling pathway	2.32	8	0.00201	0.0133
Wnt signaling pathway	3.97	8	0.0442	0.177

Figure 21 – Pathway analysis of differentially methylated genes following TGFB1-initiation A) Over-represented pathways include GPCR signal transduction and olfactory sensing, an anomalous finding in the gut epithelia, however evolutionarily defunct olfactory receptor expression is reported B) Gene ontology supports activation of sensory pathways and GPCR activity. C) Transcription factor associations suggests TFs regulating differentially methylated genes, amongst others PAX6, FOXD3 and HNF-3. D) Network analysis exhibits seed nodes (marked in red) and associated nodes representing colorectal cancer, TGFβ1 signalling and Wnt signalling (marked in green). E) Transcription of a panel of genes involved 5mC metabolism. Initiation with TGFβ1 suppressed transcription of METTL7b, TET1 and also moderately suppressed TET2 at t=48 post stimulation. n = 3. Data represtent the mean of the fold change (see appendix x for the relative expression values with associated standard errors).TET3 appeared to be induced, but fold-induction did not achieve the 2x threshold for an assumed functional effect. METTL7b's function has yet to be characterised with regards DNAm, but roles for TET-demethylases in mediating active *hypomethylation* suggest that the transcriptional effect observed at this time point might be the product of TGFβ1-initiated hypomethylation, as opposed to driving it i.e. downregulating enzymes responsible for demethylation as a practical response to negate aberrant demethylation. . * p<0.05, ** p<0.01. 3 biological replicates, 3 technical replicates. Data represtent the mean +/- the SEM. F) KEGG pathway analysis of nodes associated with differentially methylated genes predicts deregulated pathways. Highlights include cancer, TGFβ and Wnt signalling in keeping with

Effect of TGFβ1 in combination with Vitamin D

Vitamin D sensitivity is impaired in fibroblasts which effect systemic sclerosis via deregulated TGFβ signalling[303]. Furthermore, there are documented reports of vitamin D attenuating TGFβ-induced *de novo* aSMA expression in interstitial myofibroblasts associated with renal pathology[310]. To investigate the ability of vitamin D to affect the TGFβ1-influenced methylome of InMyoFib, cells were pre-treated with vitamin D for 24h hours prior to 48hr/48hr initiation. Treatment with vitamin D was sustained at 24 hour intervals for the duration of the initiation period prior to wash-out. DNA methylation profiles (Infinium 450K array) were obtained and Beta scores for the combined treatments (COMB) were compared against individual TGFB and vitamin D scores. Criteria for functional effects were adhered to during the analysis i.e. any change in DNAm instigated by TGFβ1 should be attenuated by >5% to assume functional reversal of effects.

Pre-treatment with vitamin D attenuated a proportion of the DNAm changes induced by TGFβ1

Pre-treatment with vitamin D modified DNAm at 821 of the 7503 regions differentially methylated by TGFβ1 (10.9%). Of the single CG sites *hypo*-methylated by TGFβ1 (702), vitamin D prevented demethylation at 700 of these (99.7%), promoting demethylation at only two sites. Conversely, 119 CGs were *hyper*-methylated by TGFβ1, of which vitamin D prevented *de novo* methylation of 115 (96.6%), promoting the effect of TGFβ1 at only four sites. Similarly pre-treatment with vitamin D attenuated hypomethylation at 15 of the 147 TGFβ1-affected promoters (10.2%). Only one of these mapped to a functional gene, amphiregulin (AREG); AREG is an EGF-receptor ligand, which when expressed in colorectal tumours is prognostically significant[311]. Vitamin D attenuated AREG hypomethylation by TGFβ1. While AREG transcripts were relatively low in controls and individual treatments, none were detected in combination. Scatter plots suggest that TGFβ1's DNAm modifying effects were partially attenuated by pre-treatment with vitamin D, and β score variability across the methylome diminished to levels similar to those observed at base line (figure 22a-c). Taken together, these findings raise the possibility that vitamin D exerts a weak (~10%) protective effect against TGFβ1 remodelling of the methylome.

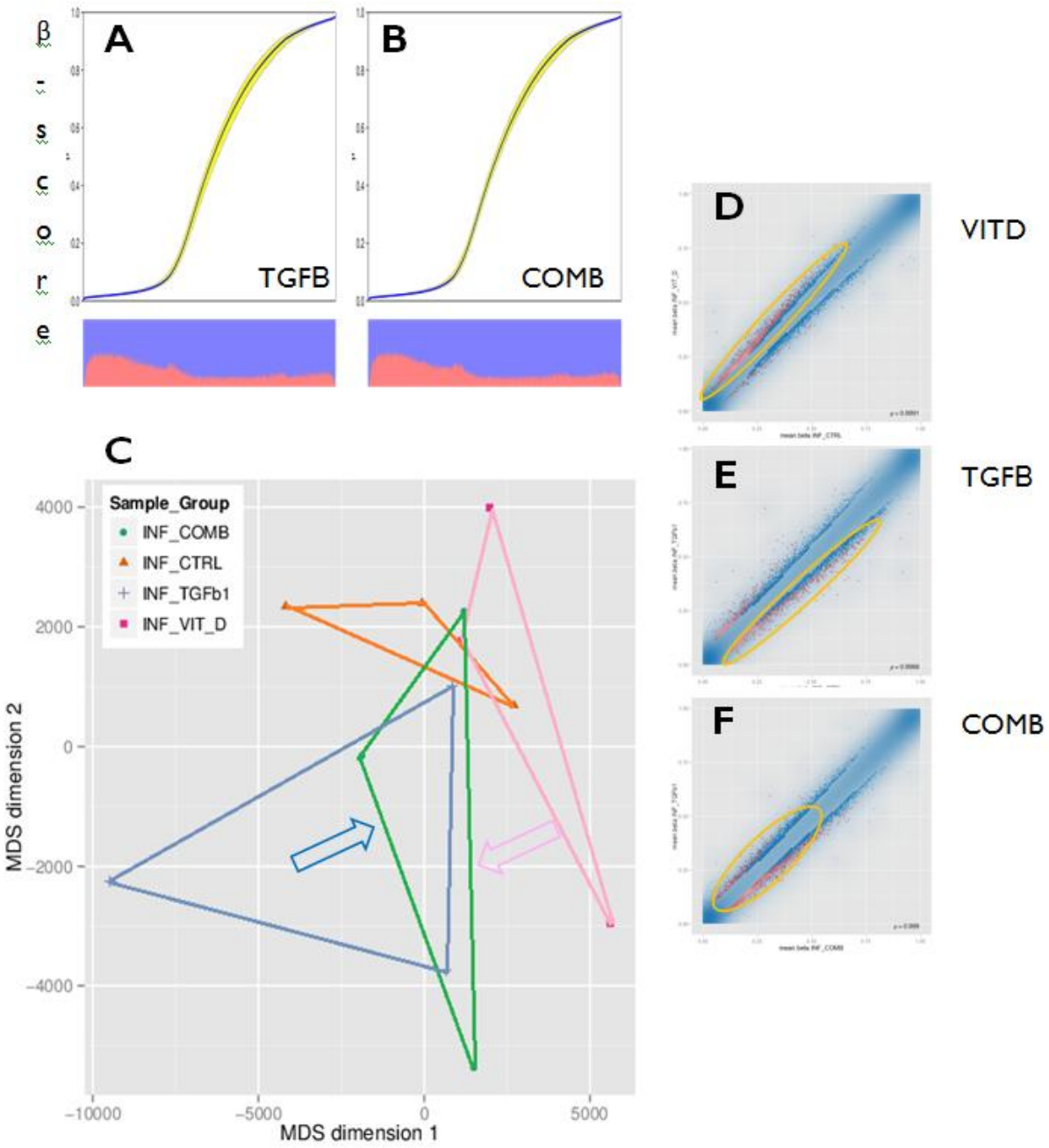

Figure 22 – Pre-treatment with vitamin D attenuates region-specific differential DNAm initiated by TGFβ1. Biological triplicates (n=3) were probed in technical duplicate. a) CpG DNAm in TGFβ1-initiated InMyoFib experience greater variability than that observed when cells are pre-treated with vitamin D prior to initiation b) variability in in the combined treatment is reduced to levels similar to that experienced by PBS-initiated controls c) sample groups cluster according to treatment regimen; grouping of the combined treatment (green), is intermediate to TGFβ1 (purple) and Vitamin D (pink) clusters, suggesting a protective effect of vitamin D pre-treatment that attenuates establishment of the full TGFβ1-initiated methylome d,e,f) Plotting the top 1000 differentially methylated sites for Vitamin D, TGFβ1, and combined treatments suggests *hypermethylation* dominance for vitamin D, *hypomethylation* dominance for TGFβ1, and attenuation of both effects in combination.

Vitamin D and TGFβ1 synergistically induce aSMA and BMP1 transcription.

Transcriptional profiles for the panel of genes previously interrogated were established for the combined treatments. aSMA exhibits an eight-fold induction in combination with vitamin D, suggestive of synergy between the two compounds regulating aSMA (figure 23a). Synergy was also observed for BMP1. It is of note that in isolation Vitamin D suppressed DKK1 while the growth factors were unaffected, hypothesised to promote epithelial proliferation if transcriptional repression were to translate to a reduction in secreted DKK1. In combination, vitamin D attenuated the suppression of RSPO1 by TGFβ1, enough to preclude statistical significance versus control. Other growth factors were unaffected in combination, remaining significantly suppressed, indicating that, while vitamin D may partially attenuate changes in DNAm, the compounds effects do not exclusively mitigate for aberrant TGFβ signalling, and in some instances may even promote it (figure 23b).

FAP transcription is associated with the methylation status of a single CpG (cg08826839)

Candidate genes differentially methylated by TGFβ1 were screened by Q-rt-PCR to establish any role for methylation status regulating transcription. Fibroblast activation protein (FAP) is induced by TGFβ1 in cancer-associated fibroblasts, and responsible for their pathological secretory profile[312]. FAP was observed to contain a single CpG site hypomethylated by TGFβ1-initiation (11% decrease). Concomitantly, FAP transcription increased three-fold - an induction attenuated in combination with vitamin D, which also restored methylation at the site. CpG methylation status and relative transcription of FAP correlated tightly, suggesting that this single site is fundamental in regulating transcription of FAP (figure 23c).

Pre-treatment with vitamin D enhances TGFβ1 transcription of TETs 1 & 3

TGFβ1 was previously observed to inhibit TET1 and METTL7b transcription, and weakly induce TET3. In combination with vitamin D, these effects were enhanced for TET1 and TET3, where expression was synergistically repressed and promoted, respectively. There was concomitant weak suppression of DNMT3b not previously observed with TGFβ1 treatment alone (figure 23d).

Pre-treatment with vitamin D modulates VDR and TGFβ-Receptor1 transcription

Methylation of The VDR promoter increased in the presence of vitamin D, an effect not previously reported in the literature, but this did not affect VDR transcription in response to vitamin D in isolation (figure 24a and b). Curiously, TGFβ1 *did* mobilise VDR transcripts; although this change was not associated with a change in VDR promoter methylation. Increased transcription of VDR by TGFβ1 may enhance InMyoFib sensitivity to vitamin D and is thus posited as an explanation for the observed synergy in the effects on the expression of some genes.

Having observed synergy between the compounds, taken together with reports of convergence of VDR and TGFβ1 on SMAD signalling in a variety of tissues[313], transcription of TGFβ1 and the TGFβ receptor1 also warranted assessment. Treatments in isolation did not impact on the transcription of either ligand or receptor, but in combination, a 2.4-fold induction of TGFβ1 occurred. Conversely, in combination significant suppression of TGFβR1 was documented. TGFβ1 and TGFβR1 promoter DNAm was not affected by either treatment (figure 24 c and d).

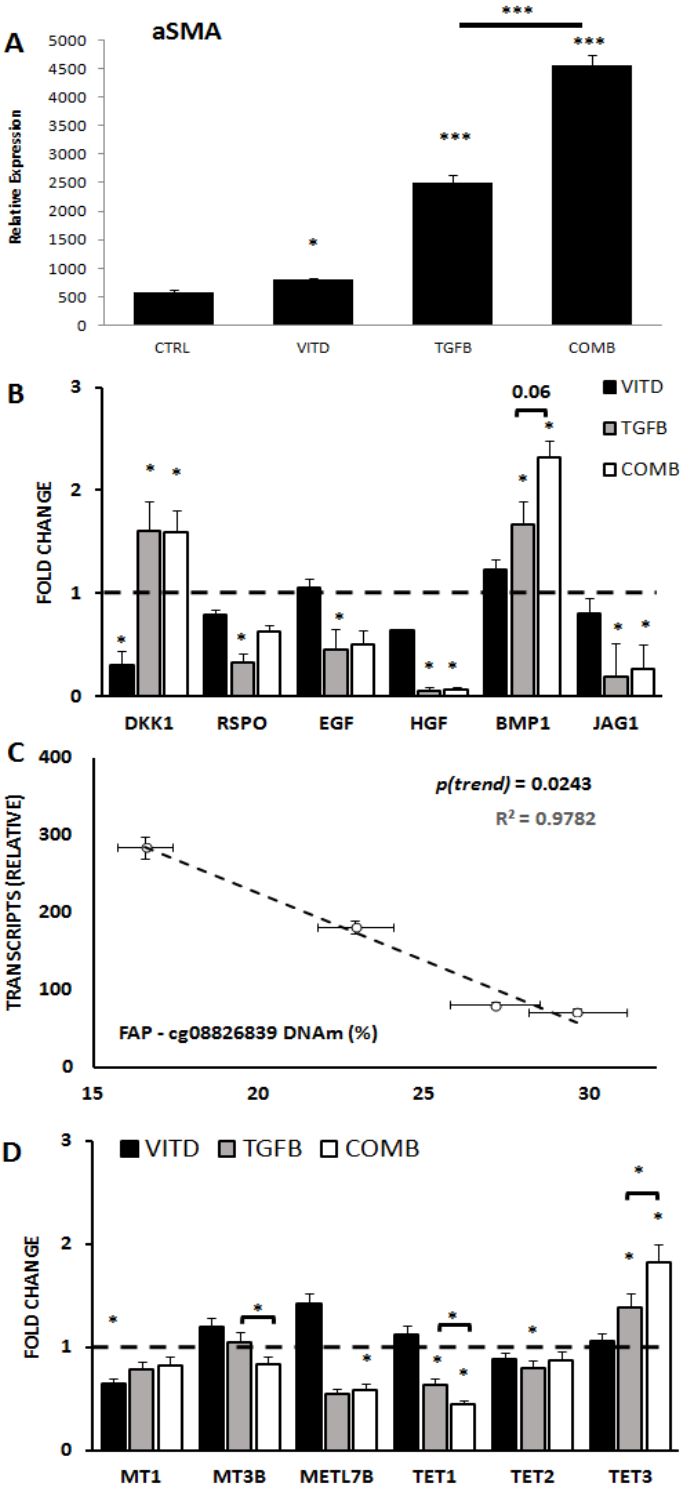

Figure 23 – Transcriptional profiles established in the combined treatment n=3, * p<0.05, ** p< 0.01, data represent mean fold change +/-SEM a) vitamin D and TGFβ1 effect synergy in their induction of aSMA transcription b) unlike differential DNAm, growth factor transcription profiles initiated by TGFβ1 were not largely attenuated in combination with vitamin D, in fact vitamin D promoted the induction of BMP1 in combination c) the methylation status (shown as % on x axis) of a single CpG in the FAP promoter region was reduced by TGFβ1 treatment; in combination vitamin D prevented hypomethylation at this site, and the transcription of FAP correlates with methylation status, suggesting that transcription of FAP depends upon DNAm at this site. Each point represents the control, vitamin D or TGFb treatments, or in combination d) TGFβ1-initiated differential transcription of TET1 and TET3 was promoted synergistically by combined treatment with vitamin D, associated with the attenuation of the TGFβ1-initiated phenotype.

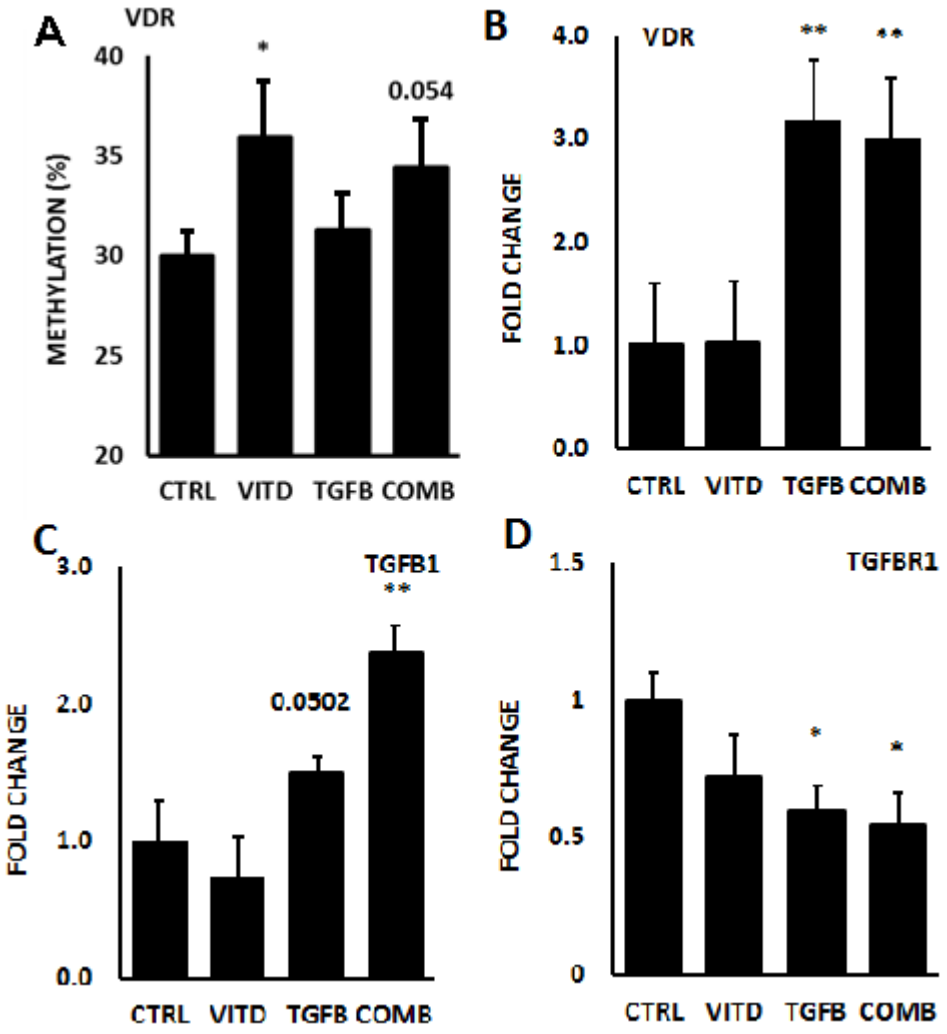

Figure 24 – Vitamin D effects changes in DNAm and transcription of VDR and TGFbR1 in InMyoFib. n=3, * p<0.05, ** p< 0.01, data represent mean % methlation or fold change +/- SEM a) Vitamin D induced significant hypermethylation of the VDR promoter, which was maintained in combination b) this was not reflected by a change in VDR transcripts in isolation, however, TGFB1 initiation induced a three-fold increase in VDR transcripts that was not attenuated by combined treatment, raising the possibility that TGFβ1 potentiates the effects of vitamin D as an explanation for the observed synergy c) TGFβ1 transcripts are upregulated following initiation of InMyoFib when pre-treated with vitamin D. There are implications of this late finding regarding autocrine TGFβ1 signalling in InMyoFib which will be discussed further d) The TGFβ receptor1 was suppressed following initiation with TGFβ1, an effect that persisted in combined treatment samples.

Discussion

In healthy gut mucosae, transforming growth factor-beta 1 exerts antiproliferative effects via rSMAD/coSMAD transduction, and downstream targets include a host of CDK-inhibitors that precipitate G1-phase arrest[314-316]. However, these properties are highly context-specific, and in particular, dysregulated in colorectal tumourigenesis and progression[317]. Over-expression of TGFβ1 in the tumour stroma is documented to induce *de novo* expression of aSMA in stromal fibroblasts[287], which is associated with stable phenotypic changes and an altered secretome permissive to angiogenesis and invasion[289]. Healthy pericryptal myofibroblasts are similar to CAFs in that they too express aSMA, are mesenchymal in origin, and inform their niche environment, organising ECM architecture as well as contributing growth factors that modulate Wnt signalling in neighbouring crypt stem cells[107,113,226]. We investigated the effect of TGFβ1 on primary intestinal myofibroblasts with regards a limited transcriptional profile, genome-wide DNA methylation patterns, and the consequence for epithelial proliferation, to ascertain if their CSC-supporting function might also be impaired by TGFβ1 activation.

TGFβ1's established antiproliferative effects were confirmed in these healthy InMyoFib, concurrent with inhibited transcription of several growth factors[318]. Reports detailing exogenous TGFβ1 stimulation of healthy gut myofibroblasts, with a focus on proliferation, are limited; our findings raise the possibility that the antiproliferative effects of TGFβ1 in this context are mediated via inhibition of autocrine GFs. Increased numbers of activated myofibroblasts persist in inflamed mucosae, driving fibrosis - a process that is accelerated in TGFβ1-transfected murine colons. Thus, for TGFβ1-activated myofibroblasts, suppressed proliferation following stimulus mitigates for the increased risk of fibrosis[319,320,321].

In light of the metastatic effects of TGFβ1-induced CAF supernatants, it was anticipated that rTGFβ1 might also promote a secretory profile in InMyoFib that accelerated epithelial cell turn-over in a paracrine fashion; surprisingly the

converse was apparent; GF transcription was suppressed, while secreted Wnt antagonists DKK1 and BMP1 were induced, suggestive of an *anti*proliferative secretory profile. This hypothesis was supported by reduced activation of the TCF-LEF reporter construct by supernatants, and two epithelial CRC cell lines treated with conditioned media experiencing antiproliferative effects and increased expression of MUC2 and e-cadherin. In direct contrast to these results, TGFβ1 is documented to effect increased transcription of Wnt agonists in skin fibroblasts during aSMA induction, promoting epithelial proliferation[322]. Furthermore, suppression of Wnt antagonist transcription is documented in a variety of fibrotic tissues, where transgenic reconstitution of TGFβ-silenced DKK1 ameliorates fibrosis[323]. Importantly, reports in the literature refer to pathological events, in contrast to the healthy InMyoFib we have characterised, consistent with the context specific-effects of TGFβ1 on fibroblast/myofibroblast phenotype. Although we did not characterise the entire transcriptome, nor quantify secreted proteins, the paracrine antiproliferative effect of the supernatants suggests that our limited panel of markers may be representative of the overall secretory effect on paracrine regulation of Wnt. However, because we did not quantify GF protein secretion, it cannot be resolved if the suppressive effect of the supernatants on CRC cell lines was mediated specifically by the factors shown to be transcriptionally regulated. Equally, it is possible only to infer effects of supernatants on non-transformed cells; the smaller effect on proliferation in the more epithelial CaCO2 relative to HCT116 lends itself to the notion that the effect might be further diminished in non-transformed CSC, but establishing if these antiproliferative effects are recapitulated in non-transformed models, and the influence of vitamin D on the outcome, requires robust elucidation using *in vitro* organoid models - a key recommendation for further work.

One hypothesis was resolved however; data suggest that initiation of the novel phenotype in these aSMA-expressing cells by TGFβ1 was not associated with changes in any of the CpGs documented to play a role in *de novo* expression of aSMA in naive fibroblasts. Although aSMA was induced significantly following treatment, we can assume that in this context, as cells are expressing aSMA at

base line, the stereo-chemical accessibility of the aSMA promoter is previously established as permissible to transcription. Thus, we infer that induction of aSMA by TGFβ1 here is associated directly with transcriptional regulation and not dynamic gene promoter methylation status. This is supported by the observation that TGFβ1 increases aSMA expression and differentiation of lung fibroblasts specifically via SMAD3[324]. DNAm is reported to have a role in aSMA activation by TGFβ1 in renal fibroblasts, via hypermethylation of Rasal1 promoter247 – in our study Rasal1 DNAm was unaffected by TGFβ1, but as noted, the InMyoFib cells studied here already express aSMA.

Regarding the stability of the TGFβI-initiated profile, we observed sustained differential transcription of growth factors at 48 hours post-induction, suggesting that initiation by TGFβ1 alone is sufficient to establish the modified methylome and phenotype, supporting our informing hypothesis. However we did not investigate whether trans-differentiation, or reversal once the phenotype is established, might be possible. PDGF and PGE2 are both documented to reverse the transient conversion of fibroblasts to myofibroblasts during TGFβ1-mediated wound healing[325] - this simple experiment is proposed as a suitable addition to the data required to conclude terminal differentiation.

TGFβ1 was observed to mediate differential DNAm in InMyoFib in a gene-specific context that did not produce two discrete methylomes, rather DNAm deviated modestly at specific locations. This was anticipated; DNAm patterns that commit pluripotent stem cells to tissue-specific lineages are largely established during embryogenesis[326], and a major re-organisation across the entire epigenome would likely result in radical dedifferentiation, *de novo* transcription of lethal proteins, and repression of essential ubiquitous house-keepers, proving ultimately fatal.

While there are still questions to resolve regarding the secretory phenotype of TGFβ1-initiated InMyoFib, the effects on gene-specific DNA methylation were clearer; differentially methylated genes tended to be *hypo*-methylated in response to TGFβ1, which is in keeping with observations that TGFβ1 drives SMAD-mediated promoter *hypomethylation* in both breast and skin cancer cell lines[327]. In

our study, differentially methylated genes were largely identified by gene ontology and network analysis to be involved in the pathogenesis of bowel disease, consistent with our informing hypothesis. However similar effects seen in ovarian cancers are specifically *not* associated with the TGFβ1-induced changes in TET enzyme transcription that we observed, where expression remains static *despite* deregulated TGFβ1 signalling[328]. A putative mechanism for TGFβ1's effects on DNA methylation is suggested by the observed promotion of TET3, which is a novel finding; the dominance of *hypomethylation* in the wake of TGFβ1 stimulation might suggest increased TET activity as opposed to a loss of fidelity effected by DNMT1 deregulation, which was unaffected. Vitamin D's synergy in this respect is paradoxical in light of its attenuating effects on TGFβ1-induced hypomethylation, however our experiments only looked at transcription of DNAm enzymes 96 hours after the initial stimulation of InMyoFib by TGFβ1; as noted it is possible that the profile we captured represents the cellular response to DNAm modification, not the instigator of it. Whether deregulation of TETs drives TGFβ1-initiated *hypomethylation* in this context, or conversely, is a plastic response to it, can only be ascertained by proper time/dose studies, and conditional interference with TET activity; suggested to clarify if regulation of TETs by TGFβ1 instigates promoter *hypomethylation* in InMyoFib.

Vitamin D's effects on the TGFβ1-initiated methylome were almost exclusively inhibitory, but only attenuated about 10% of the differential methylation effected by TGFβ1. Furthermore, vitamin D attenuated TGFβ1 hypomethylation and induction of FAP. In contrast vitamin D synergistically promoted aSMA, BMP1, TET 1 and 3, and TGFβ1 transcription in InMyoFib, creating an apparent paradox regarding vitamin D's role in mediating TGFβ1's effects. Certainly its effects were not exclusively reparative, in the same way that TGFβ1's effects were not exclusively pernicious. Ultimately, phenotype should be the mark of the over-all relationship between TGFβ1 and vitamin D, and as we did not investigate vitamin D's effects in combination with regards the secretory profile, or effect on epithelial cell line, data is insufficient to resolve this apparent paradox.

Fibronectin1

Pathway analysis of differentially methylated genes identified Fibronectin 1 (FN1) as a key intermediary node. TGFβ1-initiation saw a sustained eight-fold induction of FN1 ($p < 0.0001$), which is also observed to be upregulated in metastatic CRC[329] and detectable in serum and urine, where concentration is prognostically significant[330]. Furthermore FN1 is TGFβ1-inducible independent of SMAD4[331]; enticingly our data raise the possibility that TGFβ1-induction of FN1 may be mediated by an altered DNA methylation profile of genes modulating FN1 transcription. Vitamin D attenuated FN1 induction by 13% but this was not statistically significant.

Fibroblast activation protein

FAP is over-expressed in the CRC stromal compartment and more common in CGI methylator phenotype (CIMP)-high tumours[332]. We observed a significant 3.5-fold induction in FAP expression by TGFβ1 that was associated with hypomethylation (27.1% → 16.6%) of a single CpG (cg08826839). Vitamin D pre-treatment significantly attenuated both induction and hypomethylation at the site, and furthermore, regression analysis suggests that FAP transcription is negatively associated with DNAm at this site, not previously reported. Here is our first piece of evidence that DNAm patterns may be maintained by vitamin D to promote bowel health.

VDR

Sustained three-fold induction of VDR by TGFβ1 initiation was unprecedented and would not have been investigated had vitamin D treatment in isolation not significantly increased VDR promoter methylation. Positive regulation of VDR by TGFβ1 is a novel finding; VDR is documented to mediate TGFβ1 signalling in sclerosing fibroblasts by complexing with pSMAD3, thus negatively regulating transduction, but in these cells, VDR expression is inhibited by TGFβ1[303]. In contrast, in our experiments, combined treatments either saw no change in transcription, or synergy between TGFβ1 and Vitamin D, which might be explained by the induction of VDR by TGFβ1, increasing sensitivity of the cells to vitamin D.

An important limitation our work must be observed; the InMyoFib cell line employed to interrogate the effects of TGFβ1 is itself embryonic in origin; TGFβ superfamily signalling is well documented to play a role in differentiation during embryogenesis[reviewed in 333], and this limits what can be inferred from our data about effects of TGFβ1 in mature colonic pericryptal myofibroblasts. TGFβ1 signalling in InMyoFib during embryogenesis may however be recapitulated in healthy adult tissues during tissue repair, processes which have similar end goals. In order to determine the relevance of our results, effects would have to be recapitulated in a mature MFB cell line.

In summary

As hypothesised, recombinant TGFβ1 exerted modest pressure on the methylome of InMyoFib in a gene-specific fashion, associated with a modified secretory phenotype, and increased aSMA transcription that was not related to its methylation status. Deregulated transcription of factors involved in DNAm metabolism is posited as a mechanism by which TGFβ1 might alter the methylome in InMyoFib and requires further validation. The permanence of these changes was not fully established. Vitamin D partially attenuated TGFβ1's effects on the methylome, but displayed synergy elsewhere regarding gene transcription, and so vitamin D's role in mediating TGFβ1's effects, and the consequences of either treatment for secretory profiles and epithelial homeostasis, requires further elucidation.

Treatment of InMyoFib with TGFβI induced phenotypic changes including reduced cell proliferation and modifications to the secretome that affected epithelial cell proliferation. These phenotypic changes were associated with significant changes to the expression of a number of genes established to play a role in epithelial homeostasis. The altered phenotype was sustained following withdrawal of TGFβI stimulation suggesting that these changes may be permanent. The TGFβI-induced phenotypic changes were associated with significant gene-specific changes to the DNA methylome raising the possibility

that at least some of the differential gene-specific DNA methylation, is responsible for the altered phenotype. Further experiments are required to establish this. TGFβI affected the expression of several genes involved in DNA methylation highlighting a potential mechanism explaining the observed effects on the methylome.

Pre-treatment of InMyoFib with vitamin D attenuated some of the effects of TGFβI on the DNA methylome including the complete inhibition of the TGFβI-induced demethylation of FAP, which may prove significant in the context of bowel health. However, while attenuating some of the effects of TGFβI, vitamin D also synergistically enhance other effects including on the expression of a number of genes, and so vitamin D's role in mediating TGFβ1's effects, and the consequences of either treatment for secretory profiles and epithelial homeostasis, requires further elucidation.

Chapter 5

VITAMIN D MEDIATES THE SECRETOME OF PERICRYPTAL MYOFIBROBLASTS, AND DNA METHYLATION PATTERNS IN COLONIC ORGANOIDS

Preface to the work

Two over-arching hypotheses are proposed to explain why serum vitamin D might affect the rate of aberrant age-related DNA hypermethylation in the uninvolved mucosae of colorectal cancer patients; 1) vitamin D attenuates age-related deregulation of DNAm metabolism directly, via modulation of enzyme activity or other cell-intrinsic factors mediating the process 2) Inflammatory mediators drive aberrant DNAm via NFκB networks which, as a systemic and local anti-inflammatory, vitamin D attenuates, indirectly maintaining DNAm patterns within crypt stem cells. As well as characterising the effects of vitamin D on DNAm in CSC, it was also deemed pertinent to investigate if vitamin D's anti-inflammatory effects might modulate inflammatory networks in the crypt microenvironment.

With regards project objectives, organoid culture from colonic crypts was complex, with cultures regularly failing to yield sufficient DNA for methylation analysis. Furthermore, these healthy primary cultures are particularly sensitive to recombinant protein/hormone concentrations routinely used to stimulate cancer cell lines, which by their nature resist apoptotic stimuli. As aberrant DNAm is a processes of aging, it was recognised that in order to try and accelerate the process (with inflammatory cytokines), or ameliorate/attenuate the process (with vitamin D), cultures would need to be stimulated with physiologically relevant concentrations and maintained for extended periods, as opposed to protocols typically used with transformed cell lines (high dose, short intervention). Although Sato et al report that under appropriate culture conditions, there appears to be no threshold population doubling for crypt stem cells, we routinely observed a decrease in viable organoids at each passage, suggestive that passage technique is a key factor in organoid longevity.

To mitigate for these logistical hurdles during the early stages of the project and, as discussed, to investigate the secretory potential of pericryptal myofibroblasts in informing the niche and mediating paracrine stem cell turn over, we focused our attention on validating primary lines of mucosal myofibroblasts from the

same bowel resection specimens for use in alternative experiments while organoid culture efficiency was optimised.

Specifically pericryptal myofibroblasts represent an actively secreting phenotype intermediate to structural fibroblasts (aSMA^{-ve}) and elastic myocytes (Vimentin^{-ve}) that disseminate the instructions of inflammatory mediators to effect niche architecture and epithelial regeneration in response to stress[334]. After propagating three human lines of morphologically homogenous stellate primary mucosal cells, we performed IHC with antibodies directed against both aSMA and VIM to demonstrate that all three primary cultures were homogenously expressing both structural filaments, defining a pure population of aSMA/VIM^{+ve} myofibroblasts (figure 25)[17].

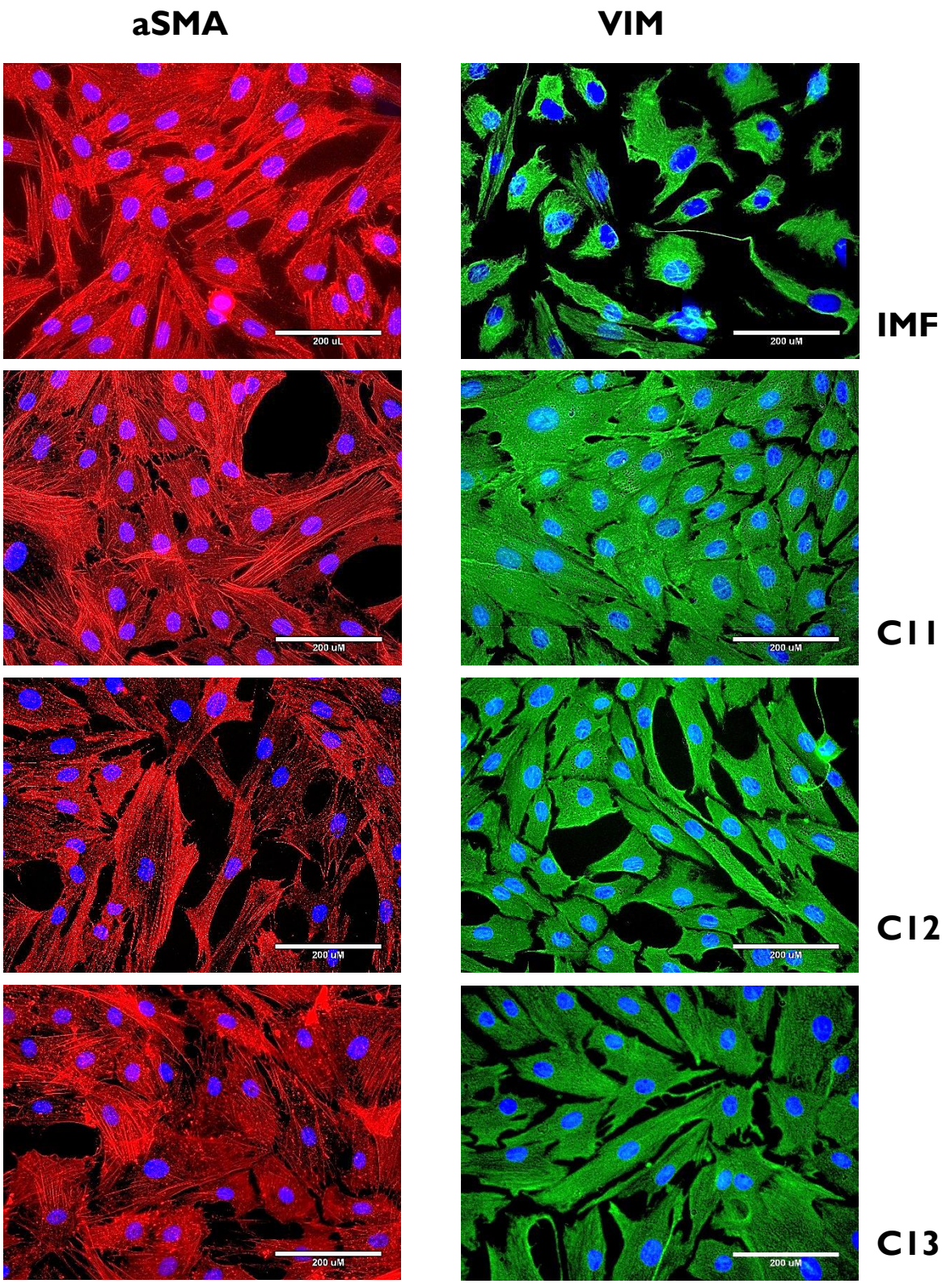

Figure 25 – Colonic myofibroblast validation. Cell monolayers at passage 2-4 seeded on chamber slides were stained with primary polyclonal antibodies against aSMA (Texas Red) or Vimentin (Alexa 448 green). aSMA+VE InMyoFib guaranteed by Lonza were used as a positive control. Smooth muscle actin and vimentin filaments are homogenously present in all cells, demonstrating pure cultures of colonic myofibroblasts propagated from mucosal biopsies. Cell were used for media conditioning experiments to investigate potential mechanism by which pericryptal myofibroblasts might mediate inflammation in the stem cell crypt niche.

Abstract

Chronic inflammation in the distal bowel maintained by TNFα, predisposes the epithelia to transformation, and is associated with deregulated 5mC metabolism, genomic instability, and silencing of Wnt-tumour suppressors, via age-related effects on DNAm patterns in crypt stem cells. We hypothesised that primary pericryptal myofibroblasts supporting CSC might contribute inflammatory mediators to the crypt niche in response to cytokine stimulation, and that these factors in turn effect differential DNAm patterns in case-matched colonic organoids.

To this end, we validated three lines of $aSMA^{+ve}/VIM^{+ve}$ primary colonic myofibroblasts, propagated from uninvolved mucosa proximal to rectal tumours in mature bowel resections. LC/MS-MS proteomics was employed to identify commonly secreted factors at baseline (124), following stimulation with vitamin D (one, Laminin2), and following stimulation with TNFα (0). Vitamin D did not universally attenuate COX2 transcription, but did inhibit secreted PGE2, suggestive of interference via an uncharacterised mechanism. Two MFB lines exhibited high levels of COX2 transcripts relative to healthy controls, prompting speculation of a COX2/PGE2-high phenotype that was associated with aspects of the secretory profile at base line. Supernatants modulated DNMT3a and 3b transcription, and were noted to also induce Cyp24a1 transcription, in case-matched organoids. Interrogation of organoid methylomes by Illumina EPIC array was inconclusive, but non-significant trends in Wnt-antagonist promoter methylation status do not specifically confirm a null hypothesis and indicate experiments with increased power are warranted.

We show that pericryptal myofibroblasts from diseased colons contribute pernicious niche factors that can modulate DNMT transcription in epithelial organoids in a context-specific fashion regarding their inflammatory status.

Introduction

It is increasingly recognised that chronic inflammation in the distal bowel precedes and predisposes the epithelium to transformation in later years, and initiation is invariably associated with microenvironmental changes that promote accumulation of activating mutations in intestinal epithelial cells[335]. Primarily, mechanisms have been inferred from models of the inflammatory bowel pathologies, Crohn's and ulcerative colitis (UC), where pathogenesis is foremost a complex interplay between the gut micro-flora, mucosal immunity, and predisposing genetic factors[336]. However, over extended periods, persistent, asymptomatic, low-level chronic mucosal inflammation, associated with environmental (diet) and metabolic (obesity) factors, recapitulates the pathological effect of IBDs in non-diseased bowels[337-339].

Regardless of aetiology, chronic inflammation perturbs homeostasis via similar mechanisms at the molecular level, instigated in part by networks of inflammatory mediators that form the cross-talk between luminal, epithelial, and submucosal compartments, to preserve barrier integrity, epithelial function, and immune regulation in times of homeostasis [reviewed in 340]. Tumour necrosis factor alpha (TNFα), a pleiotropic cytokine secreted by gut lymphocytes, antigen presenting cells, and tissue resident macrophages (as detailed in chapter 3), is a primary provocateur, stimulating a cascade of other pro-inflammatory cytokines, including IL6, in a paracrine fashion. TNFα mediates its immune-modulatory effects via it's cognate cell surface receptor, in a similar way to pathogen-stimulated toll-like receptor signalling, that is, via activating serine phosphorylations that degrade cytosolic IKK complexes, and rapidly precipitate nuclear translocation of the transcription factor NFκB.

One downstream target of NFκB, consistently over-expressed in both inflammatory and neoplastic bowel wall lesions, is Prostaglandin-endoperoxide synthase 2 (COX2)[341]. In uninflamed tissues COX2 over-sees the catabolism of prostaglandins - specifically prostaglandin E2 (PGE2) - from arachidonic acid, to establish a negative feedback loop that resolves transient inflammation. In

chronically inflamed tissues, this process is deregulated, and increased levels of PGE2 secretion contribute to the amplification of pro-inflammatory signalling[342].

Not only is COX2/PGE2 dysregulation directly tumouri- and carcino-genic in the epithelium[343], PGE2 is also shown to modulate DNMT activity *in vitro* and in murine $APC^{min/+}$ colons, effecting hypermethylation of MGMT associated with tumour promotion[344]. Selective inhibition of COX2 conversion of arachidonic acid to PGE2 by non-steroidal anti-inflammatory drugs is widely recognised to favourably influence risk of mortality from CRC[345], and vitamin D has also been shown to negatively regulate COX2 activity in macrophages,[346,347] leading us to speculate that PGE2 modulation in the niche might affect DNAm patterns in the epithelia.

Sentinels of the crypt microenvironment, pericryptal myofibroblasts contribute niche factors that interact with the epithelium[348]. PGE2 secretion, stimulated by TNFα has been previously reported in gingival fibroblasts, tracheal smooth muscle, and synovial fibroblasts[349-351], and this led us to speculate that TNFα regulation of COX2 in pericryptal myofibroblasts promotes prostaglandin synthesis and secretion in the crypt niche. Furthermore, we hypothesised that the secretory profile of a TNFα-stimulated myofibroblast might also affect aberrant DNA hypermethylation in an organoid model of the colonic epithelia.

We set out to characterise the secretory profiles of primary MFB from transformed colons in respect of TNFα-stimulated COX2 regulation and PGE2 output. We also investigated the ability of TNFα-inflamed supernatants to affect aberrant DNA methylation in case-matched colonoids, and the ability of vitamin D to mediate any observed effects, with the informing hypothesis that vitamin D might inhibit COX2 transcription, PGE2 secretion, and aberrant effects of supernatants on DNAm patterns in epithelial cells.

Methods

Cell recovery and culture

Mucosal samples were taken from three fresh bowel resection specimens, 20cm proximal to rectal adenocarcinomatous tumours, and transported in wash buffer on ice. Five minute serial digestions on ice with 2mM EDTA in PBS first released apoptotic cell debris and faecal matter and then epithelial crypts (for organoid culture). The stripped mucosal remains were further digested in EDTA-dispase solution at 37°C and agitated to release a mixed population of mucosal fibroblasts, myofibroblasts and other non-adherent tissue resident cell types. Pellets were rinsed with PBS and seeded into 75cm^2 flasks containing 10mL of InMyoFib culture medium (Lonza). Primary cells were propagated to confluence, with frequent media changes to remove non-adherent cells, during which time adherent cells exhibiting a macroscopic stellate morphology became the dominant phenotype (Figure 25).

Validation of MFB cultures by IHC

Primary cell cultures were released by trypsin-EDTA chelation, rinsed, and seeded on chamber slides. At 80% confluence, adherent cells were fixed with 4% para-formaldehyde, permeabilised with Triton X (1:100), blocked with 5% BSA in PBST, and incubated over-night at 4°C with primary antibodies anti-aSMA and anti-Vimentin (1:300 in PBST, ABCAM ab7817 and ab92547 respectively). Secondary fluorescent antibodies (anti-rabbit Alexa 488 green and Texas Red, 1:500) applied after several washes for 2 hours at room temperature. Finally DAPI was applied for 10 minutes to stain nucleic acids blue, before visualisation by fluorescent light microscopy.

TNFα stimulation

The three validated human lines of MFBs and the commercial InMyoFib line were seeded into 12 well plates at 30,000 cells per well. After allowing 24 hours to establish, cells were treated with either ethanol vehicle or 1nM vitamin D (Tocris, 2551) final concentration for 72 hours. For the final 24 hours, TNFα (Sigma, SRP3177) was applied at 1ng/mL to either vehicle or vitamin D pre-treated wells. Media was collected, spun at 300G, passed through a 20μm filter,

before diluting 1:2 in ELISA buffer. Cell pellets were harvested for RNA extraction/Q-rt-PCR as previously described in general methods

Q-rt-PCR

Typically yields were low from MFBs due to a high cytoplasmic to nuclear ratio (even confluent wells only yield about half the RNA of epithelial lines), so here 100ng was reverse transcribed for Q-rt-PCR, which was carried out as previously described. Lists of primers are included in appendix 6.

PGE2 Elisa

A 96 well plate monoclonal PGE2 Elisa kit was purchased from Cambridge Bioscience Ltd (CAY514010), and executed as per manufacturer instructions. Conditioned media samples were diluted by 50% in Elisa buffer to ensure PGE2 concentration fell within the reliable working range of the standard curve. Biological triplicates from each line and each treatment were interrogated in technical duplicate, and the data represent the mean of biological triplicates +/- the SEM.

LC/MS-MS Proteomics

Was performed as detailed in General Methods. Samples for analysis were prepared as follows. The three human MFB cases were cultured in 25cm^2 flasks to 80% confluence. Cells were treated as described with 1nM vitamin D +/- 1ng/mL rTNFα. To mitigate for albumin interference, FBS was removed during TNFα stimulation, and it is noted that this introduces a necessary discrepancy relative to the PCR data. Media was harvested and processed to remove debris, and inhibitor cocktail added. Conditioned media was spun for 2 hours at 14,000g through a 3K AmiconUltra4 protein filter (Merck,). Protein concentration was determined by BCA assay as described, and 15µg triplicates separated for 10 minutes by PAGE electrophoresis at 200V (Novex). Lanes were visualised by Coomassie blue and dissected into 1mm pieces. Peptides were digested with 20mM Ammonium Bicarbonate added to 5µl (5µg) Trypsin Gold (Promega) in 50mM Acetic Acid. The gel pieces were washed with 50% acetonitrile (Fisher) to recover digested peptides from the gel. The extracted samples were then dried

at room temperature on a Speed Vac SC110 (Savant) and frozen on dry ice to be stored at -80°C.

Organoid culture

Pure crypts from case 11, 12 and 13 mucosal biopsies were seeded in 25uL drops of Matrigel (Corning 354230) containing 1:1000 JAG1 (1uM) and 1:1000 Y27632 (10mM) in 24 well plates with 500uL of routine organoid culture medium. Stimulated myofibroblast culture medium was prepared as previously described without inhibitor cocktail and concentrated through 3K protein filters. Triplicate wells of organoids for each case were treated for 30 days with either vehicle- vitamin D- TNFα- or combined treatment-matched myofibroblast supernatants (500ng). Media were replaced every 2-3 days for the duration of the protocol. Organoids were passaged at days 10, 20, and 30, and following the final passage, all treatments were removed and fresh routine media added for a 48 hour washout period. Treatment replicates were pooled for DNA extraction as described and 500ng of genomic DNA dispatched for EPIC array analysis.

InnateDB analysis

Ensembl codes for proteins identified by secretomics and genes identified by EPIC array were uploaded to InnateDB to determine statistically over-represented biological pathways and molecular interaction networks between seed genes. InnateDB interrogates public curated databases of biological interactions including KEGG, Reactome, NetPath, INOH, BioCarta and PID. For analysis and visualisation, the recommended hypergeometric algorithm with Benjamini Hochberg correction was selected.

Results

Effects of vitamin D in primary myofibroblasts

Vitamin D inhibits TNFα induction of COX2 and IL1β transcripts in a dose-dependent fashion

To establish a suitable protocol to inflame pericryptal myofibroblasts, un-validated homogenous cultures propagated from case 1 were incubated at 80% confluence for four hours with 10ng/mL of rTNFα as a test case. For combined treatments, MFB were pre-treated with 10nM (COMB1) or 100nM (COMB2) of vitamin D, for 48 hours prior to stimulation with TNFα. COX2, and IL1β transcripts were quantified by Q-rt-PCR to demonstrate the pro-inflammatory effect of TNFα in these cells. In keeping with the hypothesis that MFBs contribute Wnt ligands to the niche environment, the transcription of RSPO1 and WNT3a (essential components of organoid culture medium) were also interrogated.

Vitamin D inhibited COX2 transcription, but not IL1β. TNFα significantly induced COX2 (two-fold) and IL1β (50-fold) transcripts. Combined treatment with vitamin D attenuated the effect in a dose-dependent fashion for both COX2 and IL1β, with statistical significance being achieved at the higher concentration (figure 26a and b). Regarding Wnt agonist transcription, base line Wnt3a transcripts were relatively low (CT values approaching the 40 cycle threshold limit and thus not detectable in all replicates), precluding statistical analysis – included here because the trend reflects the pattern observed for RSPO1; in isolation and in combination, both TNFα and vitamin D significantly induce RSPO1 transcription (figure 26c and d). This suggests that were these changes to translate to increased RSPO1 secretion by MFBs, increased epithelial turnover may be induced in response to both vitamin D treatment and TNFα-mediated inflammation in the crypt niche.

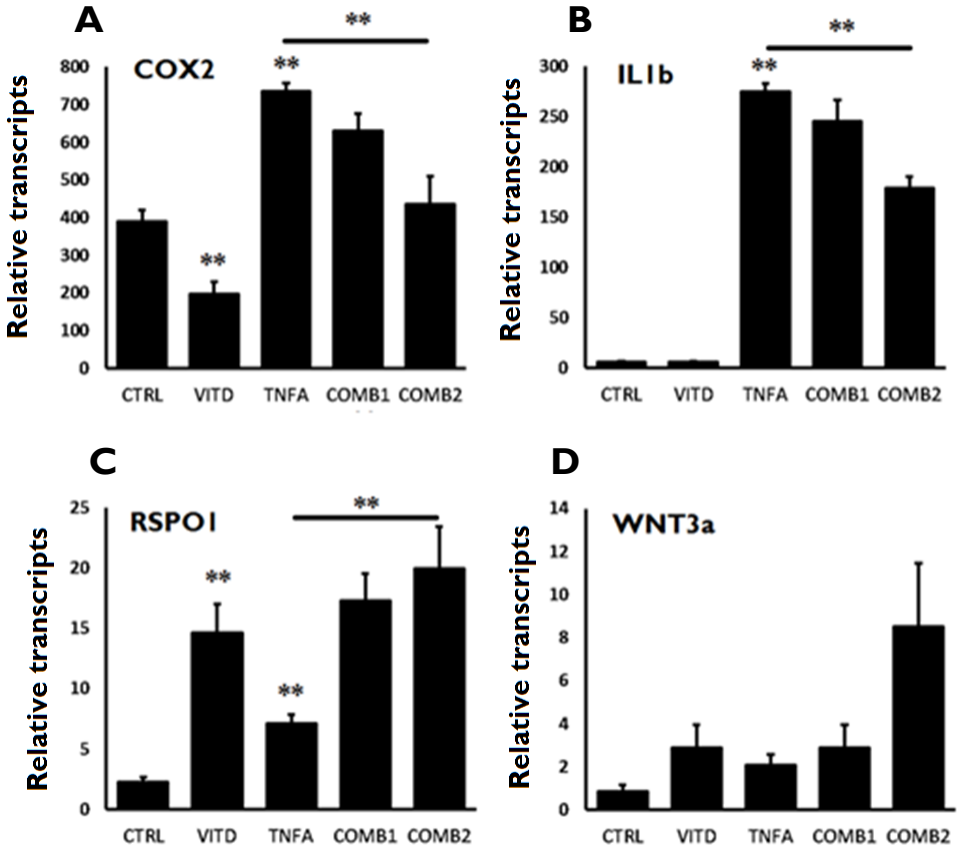

Figure 26 – Vitamin D and TNFα modify gene transcription in primary myofibroblasts. I MFBs Heterogeneous intestinal myofibroblast cultures (case 1) in the log growth phase were treated with either ethanol vehicle, vitamin D (100nM, 48 hours), rTNFα (10ng/mL, 4 hours), or in combination (COMB1; 10nM vitamin D + 10ng/mL rTNFα. COMB2; 100nM vitamin D + 10ng/mL rTNFα). RNA was reverse transcribed and interrogated by Q-rt-PCR to determine gene transcription. Data show relative transcripts determined by the ΔCT method +/- SEM. n=3, * p<0.05, ** p< 0.01. A) Inflammatory mediator COX2 transcription is repressed by vitamin D, induced by TNFα, and attenuated in a dose-dependent fashion in combination B) To confirm the pro-inflammatory effect of TNFα on MFB, IL1β transcription was also assessed, again showing a dose-dependent attenuation in combination with vitamin D. C & D) Secreted Wnt ligand RSPO1 is significantly induced by both vitamin D and TNFα, a trend recapitulated for Wnt3a transcription, another recombinant ligand utilised in organoid culture, raising the possibility that both vitamin D and TNFα promote stem cell turn-over via increased paracrine signalling in the crypt niche.

COX2 transcription correlates with, and vitamin D inhibits, myofibroblast-secreted PGE2

Secreted prostaglandin E2 is an end point of COX2 regulation and is shown to promote tumourigenesis via aberrant DNAm in colonic epithelia. In light of COX2 regulation by TNFα, it was hypothesised that stimulation might also increase secreted PGE2 from myofibroblasts, and that vitamin D might attenuate this.

To ensure sufficient conditioning of the media by inflamed MFBs following COX2 induction observed at four hours, the treatment protocol was extended; in respect of the dose-dependency of the combined treatments, and to better reproduce the situation in vivo, three validated MFBs lines (case 11, 12 and 13) were pre-treated for 48 hours with a lower concentration of vitamin D (1nM – 10x physiological sufficiency). Preliminary experiments with InMyoFib – employed as a healthy control against the MFBs recovered from CRC resections – indicated that 10ng/mL of TNFα was comprehensively fatal at 24 hours, so it was decided to also reduce the TNFα stimulus to 1ng/mL for the extended conditioning period. Supernatants were collected and processed as previously described to remove cellular debris, diluted as appropriate, and the concentration of PGE2 determined by ELISA according to the manufacturer's instructions.

Vitamin D in isolation (1nM for 72 hours) significantly reduced PGE2 in the conditioned media in three of the four MFB cell lines, and the trend was evident in the fourth. Data were pooled and normalised to the control (to allow for comparisons between cell lines), and suggest that vitamin D for 72 hours at 1nM significantly reduces PGE2 secreted by intestinal myofibroblasts by approximately 25% (figure 25a). Similarly, stimulation with TNFα significantly increases PGE2 concentrations 3.5-fold in intestinal myofibroblasts, as anticipated. However, in combination, a 48 hour pre-treatment with vitamin D was not able to significantly attenuate the increase, as was suggested by vitamin D's ability to down-regulate COX2 transcripts.

In this respect, it is of note that, at base line, cases 11 and 12 MFBs exhibit a four-fold increase in secreted PGE2 relative to healthy InMyoFib and case 13, raising the possibility that *in vivo*, these cells had previously acquired an inflamed phenotype (figure 28b).

Due to the apparent discrepancy between results from the preliminary experiments, regarding vitamin D's attenuation of TNFα-induced COX2 *not* reflected by diminished PGE2 secretion, RNA was harvested from all four lines after media conditioning to re-establish the relationship between COX2 transcription and secreted PGE2. Supporting the developing hypothesis that case 11 and 12 represent an inflamed phenotype distinct to case 13 at base line, COX2 transcripts are significantly raised in these two cases relative to case 13 MFBs and InMyoFib at base line (figure 28a). While TNFα still significantly induced COX2 under the new protocol, vitamin D was not able to attenuate it's induction in any line, consistent with results for secreted PGE2. In fact, vitamin D in isolation *induces* COX2 in the two basally inflamed lines, supporting a modified 'inflamed' phenotype relative to the two other lines. Finally, regression analysis of data from each line shows a strong correlation between relative COX2 transcripts and secreted PGE2 in response to TNFα stimulation (figure 28a).

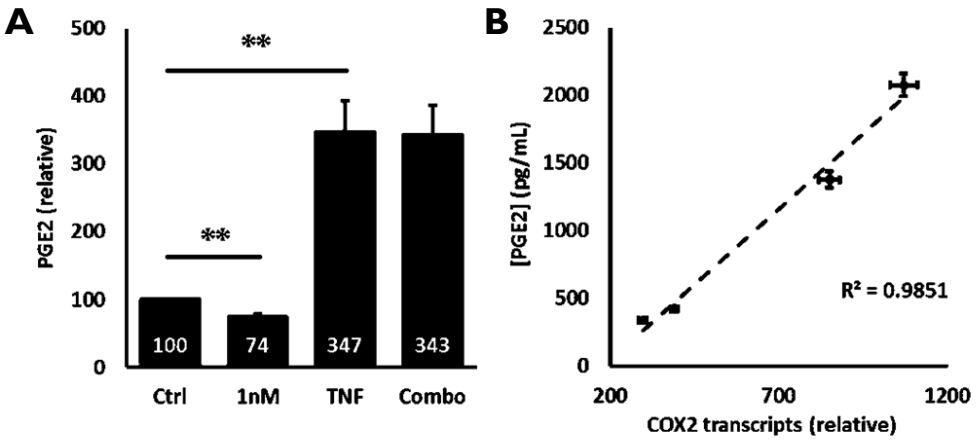

Figure 27 – PGE2 production by inflamed myofibroblasts. Secreted PGE2 was determined by ELISA for InMyoFib and case 11, 12 and 13 MFBs. Biological triplicates were treated with either ethanol vehicle, 1nM vitamin D (72 hours), 1ng/mL TNFα (24 hours), or in combination. A) When data are pooled from the four lines interrogated (normalised to the control), VITAMIN D treatment significantly suppresses PGE2 secretion by ~25%. Similarly rTNFα induces a 3.5-fold increase in secreted PGE2. In combination, pre-treatment with vitamin D did not attenuate TNFα-induced PGE2 secretion. B) Regression analysis shows a significant correlation between COX2 transcription and secreted PGE2 following stimulation with TNFα (RSQ = 0.99, p = 0.0075, suggesting that TNFα-stimulated PGE2 secretion is consequent to COX2 induction. n=3, * p<0.05, ** p< 0.01, data represent mean +/- SEM.

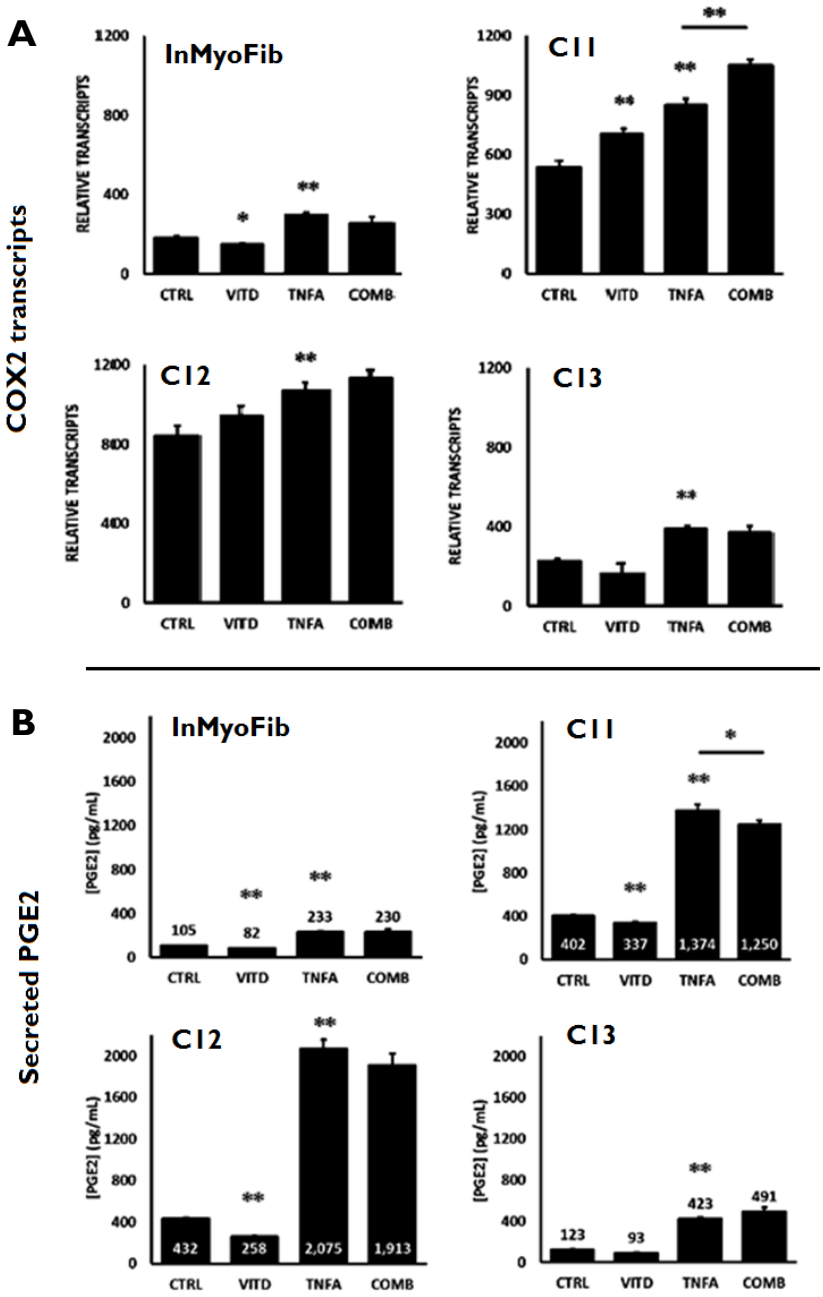

Figure 28 - <u>COX2 transcription verses secreted PGE2 in intestinal myofibroblasts.</u> Cells were treated with either 1nM vitamin D for 72 hours, rTNFα at 1ng/mL for 24 hours, or in combination A) COX2 transcription is observed to be increased case in 11 and case 12 MFBs at base line relative to InMyoFib and case 13 MFBs at this time point. In the two basally inflamed cases, VITAMIN D does not ameliorate COX2 transcription, and only partially ameliorates it in the other two. TNFα significantly induces COX2 in all four lines, however, combined treatment does not attenuate TNFα induction of COX2 in any line. B) PGE2 concentration in conditioned supernatants is elevated in the two COX2-high MFB lines relative to the two COX2-low lines. Vitamin D treatment ameliorates secreted PGE2 in all four lines, and rTNFα significantly induces PGE2 secretion. However, in combination, vitamin D in not able to attenuate TNFα-induced PGE2 secretion. Data suggest that case 11 and 12 represent a COX2/PGE2-high basal phenotype. n=3, * $p<0.05$, ** $p< 0.01$, data represent mean +/- SEM

The myofibroblast secretome

To further qualitatively investigate any differences in secretory protein profiles mediated by vitamin D or TNFα treatment, LC/MS-MS proteomics analysis of the conditioned media from cases 11, 12 and 13 was performed. The protocol was repeated as detailed, with the exception that for the final 24 hours of conditioning foetal calf serum was removed from the media, to mitigate for albumin interference. In brief, supernatants were spun to remove cell debris, and passed through a 20um filter. Next protease/phosphatase inhibitor cocktail was added, and 5mL of conditioned media spun through a 3K protein filter to concentrate the supernatants. Technical triplicates of 15ug for each treatment were separated by PAGE electrophoresis and each lane dissected and digested with trypsin, washed, and precipitated to yield desiccated peptides for mass-spec analysis. Peptides were compared against the Uniprot human database using Scaffold proteome software to identify secreted proteins. Scaffold applies a student's T-test to sample groups with Hochberg-Benjamini correction of normalised total spectra to determine statistically significant differences between treatments.

In respect of the fact that, under the modified protocol, pre-treatment with vitamin D failed to attenuate TNFα-induced COX2 transcription or PGE2 secretion, the analysis focused exclusively on the secretome in response to Vitamin D (1nM, 72hours), or TNFα (1ng/mL, 24 hours) in isolation relative to vehicle control, for each of the three validated human lines of MFBs. As vitamin D inhibition is suggested to be dose-dependent, extrapolation of the combined effect may be inferred.

The basal MFB secretome supports niche architecture and chemokine signalling.

Secretomics for case 11 procured the most diverse secretory profile of the three cases; 491 unique proteins in MFB supernatants were identified at base line (76.6% demarked as extra-cellular), reported to be involved in immune system processes (n = 105), establishment of localisation (n = 94), biological adhesion (n = 60), locomotion (n = 53), growth (n = 11), and cell killing (n = 6).

In case 12, there were 318 unique proteins identified at base line (65.5% demarked as extra-cellular), involved in localisation (n = 75), immune system processes (n = 35), biological adhesion (n = 34), locomotion (n = 21), growth (n = 4), and cell killing (n = 3).

In case 13, there were 209 unique proteins identified at base line (70.1% demarked as extra-cellular), involved in localisation (n = 59), immune system processes (n = 32), biological adhesion (n = 22), locomotion (n = 20), growth (n = 3), and cell killing (n = 2).

Consistent with the developing concept of heterogeneous secretory profiles represented at base line, case 11 and 12 exhibit an expanded panel of secreted proteins relative to case 13, with considerable over-lap between the two panels (81 common to the COX2-high phenotype) – more than were shared by case 13 with either line (19 and 28 respectively).

Regardless, 124 proteins were identified as common to all three validated MFB lines (figure 29a). Not surprisingly the most prevalent in terms of total spectra comprised extra-cellular structural components such as keratins, collagens, fibrilin1, ECM1, and, again fibronectin1, as well as matrix metalloproteases and MMP inhibitors (TIMP1 and 2). Curiously, all three MFB lines were found to secrete the Vitamin D-binding protein at relatively low levels in the un-primed state, which raises possible implications for vitamin D bioavailability in the crypt niche. In respect of the fact that these uninvolved myofibroblasts were recovered from diseased colons, network analysis was employed to identify biological processes associated with the common secretory profile at base line. The 124 common seed nodes were associated with 34 'colorectal cancer' nodes ($p = 1.19e-10$), 48 'TLR-signalling' nodes ($p = 2.61e-7$), and 53 nodes involved in 'Wnt signalling' ($p = 0.00157$, figure 29b-d). Network analysis of the 81 proteins common to COX2/PGE2-high MFBs did not reveal notably different profiles in terms of gene ontology or pathway over-representation (data not shown) but did reveal that these MFBs were secreting IL6 at base line, recognised for its role in IBD, but the COX2-low case 13 was not, providing support for a more inflamed phenotype for these two MFB lines.

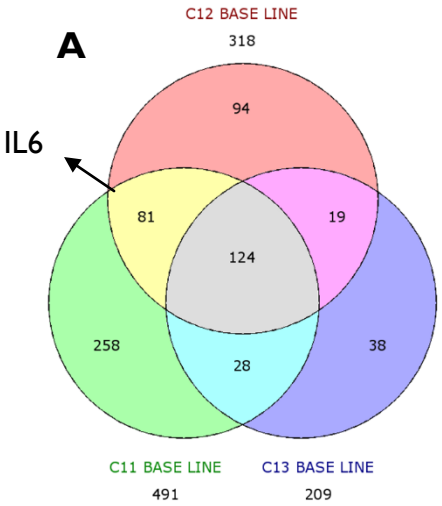

B

Pathway	Expected	Hits	P.Value
Pathways in cancer	79.2	167	2.27E-28
MAPK signalling	67.7	123	3E-14
Focal adhesion	51.1	110	1.08E-19
Chemokine signalling	48.3	74	1.85E-05
Actin cytoskeleton	46.5	87	3.3E-11
Wnt signalling	36.8	53	0.00157
Insulin signalling	35	68	6.72E-10
Cell cycle	31.7	60	2.38E-08
TLR signalling	24.8	48	2.61E-07
CRC	12.5	34	1.19E-10
ECM-receptor int.	21.4	39	2.39E-05

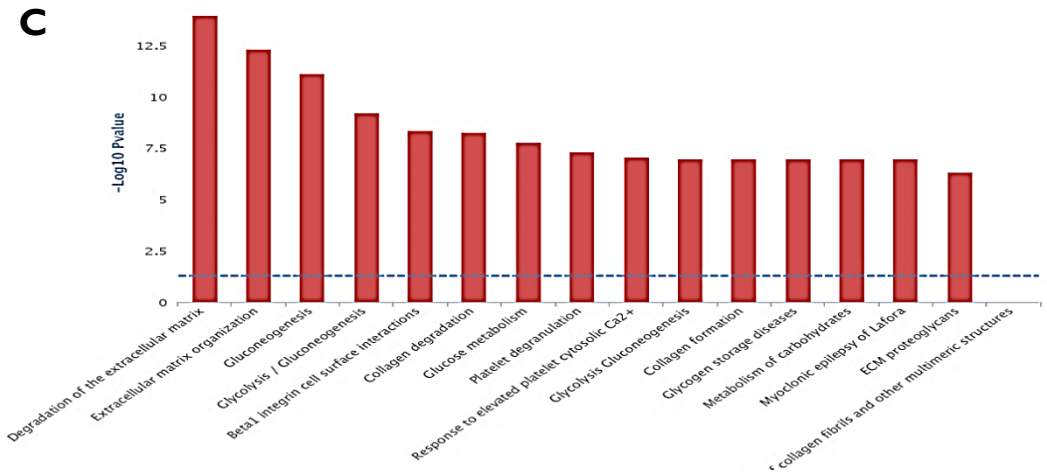

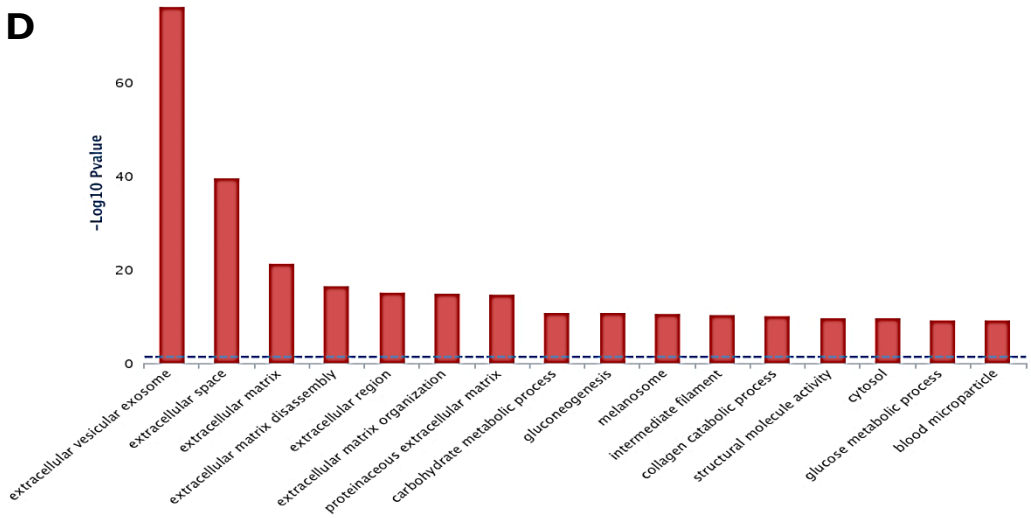

Figure 29 – <u>The basal myofibroblast secretome.</u> A) 491, 318 and 209 unique proteins were identified respectively in case 11, 12 and 13 MFB supernatants. Secretomes exhibit individual diversity at base line, however considerable over-lap of commonly secreted proteins is noted (124, indicated in grey area). B) KEGG pathway analysis returns top hits for anticipated biological function of pericryptal myofibroblasts; colorectal cancer, chemokine, Wnt, and TLR signalling, cell cycle, ECM, and actin cytoskeleton. C) Pathway over-representation analysis (Innate DB) of secreted proteins posits roles for MFBs in ECM degradation and organisation, and D) GO term over-representation analysis (Innate DB) returns the top seven gene ontology terms as pertaining to extracellular functions.

Vitamin D and TNFα independently modify the myofibroblast secretome

Effect of vitamin D

Of 504 identified proteins from case 11, 124 (24.6%) produced differential counts of total spectra following treatment with vitamin D. Vitamin D treatment completely eliminated seven proteins and induced *de novo* secretion of a further seven proteins (appended in 8). Of the 295 unique proteins identified from case 12, 86 (28.9%) show differential counts of total spectra following treatment with vitamin D. Twenty four secreted proteins were not present following vitamin D treatment, but no *de novo* proteins were identified (appended in 9). Lastly, only 12 of the 209 proteins secreted by case 13 exhibit differential counts of total spectra following treatment with vitamin D (5.7%). Three proteins were eliminated by vitamin D, and none were induced (appended in 10).

Of the *de novo* proteins effected by vitamin D, none were common to all three MFB lines, and so validation focussed on proteins reported as either 'high' or 'low' relative to vehicle in vitamin D treated samples. Proteins identified to be differentially secreted following vitamin D treatment show limited commonality between lines. Specifically Laminin subunit alpha two (LAMA2) was the only protein detected in all three supernatants that was consistently suppressed by vitamin D treatment (figure 31a and b). LAMA2 is a basement membrane laminin that mediates stromal communication with the epithelium, and is found to be over-expressed in inflamed UC mucosae[352]. The effect of vitamin D (repressed or induced) was also consistent between lines for proteins common to C11 and 12; (collagen 5-A2, complement factor-H, prostaglandin D2-syntahase, and moesin), common to C11 and C13; (heat shock protein 90-AA1 and super-oxide dismutase 2); and common to C12 and C13 (keratin 10).

Effect of TNFα

In isolation, TNFα exerted a potent inflammatory effect on intestinal myofibroblasts in terms of COX2 transcription and PGE2 secretion. Consequently secretomic LC/MS-MS analysis of TNFα-induced myofibroblast supernatants was performed, to identify proteins that might be increased in the niche in chronically inflamed mucosae; TNFα effected statistically significant differential secretion of 103, 45 and 44 proteins respectively, however none of these were common to all three MFB lines (figure 31c). 13 proteins were common to COX2 -high MFBs following rTNFα stimulation, including IL6, SERPINE1, PGD2, leukaemia inhibitory factor (LIF) and TNFα-stimulated gene 6 (TSG6). Differences in total spectra counts for these proteins, recognised for their role in bowel pathogenesis, were consistent across both MFB lines following TNFα stimulation (figure 31d-f). Qualitative total spectra counts for IL6 from COX2-high MFB lines were validated by Q-rt-PCR; both lines show significant induction of IL6 transcripts following stimulation with rTNFα (figure 30). Transcripts were recorded in case 13 MFBs at base line, but not identified by mass spec, suggesting that post-translational modifications activate secretion of IL6 in $COX2^{high}$ MFBs.

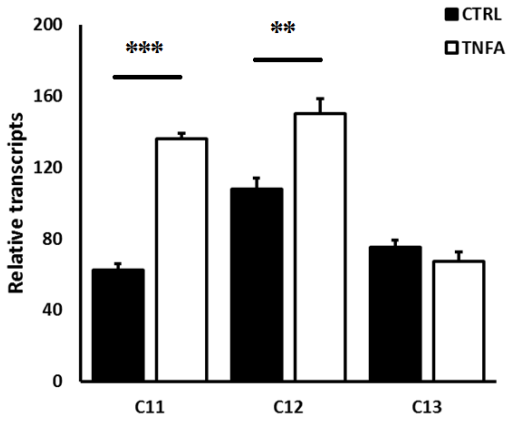

Figure 30 – Interleukin 6 transcription in MFBs. TNFα at 1ng/mL for 24 hours significantly induces IL6 transcripts in COX2/PGE2-high MFBs relative to COX2/PGE2-low (case 13) MFBs. This supports the observed increase in IL6 total spectra detected in case 11 and 12 supernatants. n=3, ** p<0.01, *** p<0.001. Data represent mean +/-SEM.

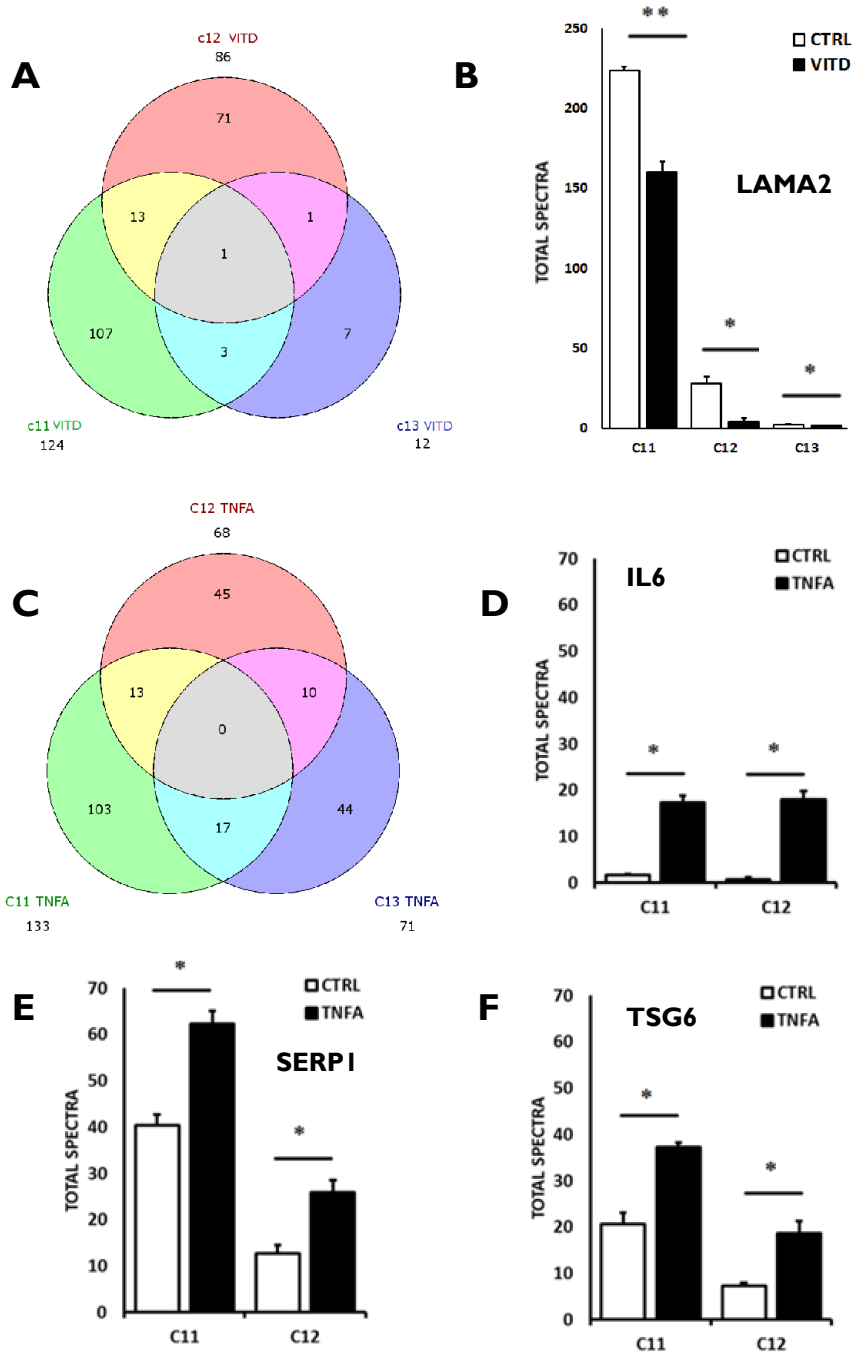

Figure 31 – The secretome of stimulated intestinal myofibroblasts lines n=3, *P<0.05, ** p< 0.01. Data represent the mean +/- the SEM. a) Venn diagram of secreted proteins differentially expressed following treatment with 1nmol VITAMIN D for 72 hours. Only 1 protein, lamanin2 (LAMA2) was common to all three lines b) LAMA2 total spectra are highest in case 11 at base line, and treatment with vitamin D ameliorates LAMA2 secretion in all three MFB lines c) No over-lap of any secreted protein was observed between lines treated with TNFα (1ng/mL) for 24 hours, however basally inflamed case 11 and 12 share 13 commonly secreted factors following TNFα induction. Three of these were identified to be both over expressed in IBD, and induced here by rTNFα. d) Interleukin 6 was weakly secreted at base line in both cases, treatment with TNFα (1ng/mL) for 24 hours significantly increases IL6 concentration in supernatants e) SERPINE1 (Plasminogen activator inhibitor-1) is over-expressed in inflammatory conditions, promoting fibrosis. Here, TNFα treatment induced significant increase in secreted SERPINE1 in both basally inflamed MFB lines, but was not detectable in case 13 supernatants. f) TNF-stimulated gene 6 protein (TSG6) is inducible in a variety of inflammatory conditions. In case 11 and 12 MFBs, TNFα stimulated TSG6 secretion from both basally inflamed MFB lines, but was not detected in case 13 MFBs.

Effects of myofibroblasts supernatants on the epithelia

MFB supernatants modulate DNAm profiles in case-matched colonic organoids and regulate DNMT transcription

The informing hypothesis is that mediators in the crypt niche, secreted by inflamed pericryptal myofibroblasts, accelerate age-dependent aberrant DNAm in cycling crypt stem cells. To investigate the consequence of a perturbed MFB secretome on uninvolved gut epithelia, the experimental protocol was repeated to condition media for use in routine organoid culture. Importantly, although TNFα peptides were not detected in any of the MFB supernatants, it must be noted that metabolites of rTNFα may still be present in supernatants at *t*=24 hours. Again, organoid methylomes were characterised *after* a wash out period to mitigate for transient effects on DNAm.

Case 11 and Case 12 matched organoids were cultured as described in biological triplicates for 30 days with the addition of 500ng/mL of concentrated MFB supernatants from either vehicle, vitamin D, or TNFα treated MFBs. Media were refreshed every 48 hours, and organoids were passaged every 10 days to increase yield, and encourage mitosis and propagation of DNAm patterns. Triplicate wells were pooled and recovered, DNA was bisulphite modified and interrogated by Infinium EPIC methylation bead chip. Infinium's updated chip determines DNAm status of 841,684 CpG sites (verses 486,428 in the previous iteration).

[A caveat must be observed to accompany the results; case 12 organoids treated with vehicle-induced MFB supernatants (CTRLs) failed to yield DNA suitable for the array. Analysis was focussed on results from case 11 organoids alone and, where trends identified, assessed in case 12 organoids using data substituted from control organoids *not* treated with MFB supernatants but after 30 days in culture (also included on the array). Loci-specific comparisons between the two cases are intended only to support observed trends, but should not imply validation of observations].

In case 11, average gene promoter DNAm status was significantly reduced by a small percentage in matched organoids treated with supernatants from vitamin

D-induced-MFBs. Surprisingly, TNFα-induced-MFB supernatants *also* precipitated a methylome-wide decrease in promoter DNAm status. Both changes were attenuated in combination (figure 32a). Whether this is useful in determining the validity of the hypothesis is questionable, however the trend is consistent with observations discussed subsequently detailing DNMT transcription.

A total of 14,182 single CpG sites (1.6%) that were hyperdynamic in response to vitamin D and TNFA supernatants consistent to the hypothesis were identified. The top 1% of these differentially methylated CpGs mapped to 11 assigned genes, of which two experience attenuation of TNFα-induced hypermethylation when treatments were combined; CCBE1, a tumour suppressor found to be silenced by hypermethylation in breast cancer(figure 32b)[353], and POU3F4, which was shown to be hypermethylated in lung cancer[354]. Furthermore, the variable DNAm at these sites was recapitulated in case 12 organoids, raising the possibility that the effects of vitamin D and TNFα on DNAm in these genes might be ubiquitous in inflamed mucosae.

With regards differentially methylated promoters, filtered according to previously defined criteria, 1918 (4.3% of the total interrogated) were hyper-methylated (+5% or more) by TNFα. Supernatants from the combined treatment attenuated TNFα-induced DNA hypermethylation of 1060 of these gene promoters (55.3%), suggestive that vitamin D may indirectly protect inflammation-mediated DNAm. Pathway analysis of vitamin D rescued genes revealed three regulating Wnt signalling (SFRP1, FRZB and FZD5), and two involved in vitamin D bioavailability (Klotho, frequently silenced in cancer by promoter hypermethylation, attenuated in combination here, and S100G), but variable DNAm of these genes observed in case 11 was not recapitulated in case 12 organoids.

The methylation status of the top 20 promoters hyper-methylated by TNFα in case 11, that were attenuated in combination, were mapped in case 12; six of these promoters also experience variable DNAm, but promoters represented un-assigned locations or pseudo-genes. The other 14 promoters were unaffected in case 12 organoids.

Finally, in both cases promoter methylation status was determined for the panel of genes identified by Tapp et al, whose methylation status in epithelial biopsies was associated with serum vitamin D. None of these promoters were significantly dynamic in either line with regards to MFB supernatant treatment, however four (SFRPs 1, 2, and 4, and MYOD1) exhibit non-significant trends supportive of the hypothesis that TNFα-stimulated MFB supernatants drive aberrant DNAm of Wnt antagonists (figure 32c and d).

To investigate a potential mechanism by which vitamin D/TNFα stimulated MFB supernatants might mediate aberrant DNAm patterns in organoids, matched organoids were treated for 24 hours with supernatants at a final concentration of 500ng/mL from all three validated MFB lines. RNA was interrogated to investigate transcription of DNA methyltransferases 1, 3a and 3b, and TET1. Transcripts for TET1 were not detectable in any of the three organoid lines, and DNMT1 transcription remained static in response to MFB supernatants. DNMT3a and 3b were both suppressed at 24 hours by vitamin D- and TNFα-stimulated MFB supernatants, consistent with the modest but significant effect each treatment had on over-all promoter DNAm status. The effect was significantly attenuated in all three organoid lines in response to the combined treatment supernatants (figure 32e and f). Lastly, to demonstrate that vitamin D was no longer present in MFB supernatants, CYP24a1 transcripts in the organoids were quantified. Cyp24a1 is the principal catabolic enzyme of vitamin D and is directly inducible as part of regulated feedback[355]. As well as treating case-matched organoids with MFB extracts, all three organoid lines were treated with an increasing dose of vitamin D. Cyp24a1 was induced in a dose-dependent fashion in all three organoid lines, as anticipated. In contrast, MFB supernatants from vitamin D-treated cells weakly suppress Cyp24a1 relative to vehicle controls. Theoretically this would increase epithelial sensitivity to vitamin D, and is consistent with the over-arching hypothesis that vitamin D promotes bowel health. It is of note that relative to untreated control organoids, vehicle-stimulated MFB supernatants significantly induce Cyp24a1 transcription in all three organoid lines, raising the possibility that the secretome of pericryptal MFBs may inform epithelial sensitivity to vitamin D (figure 33b).

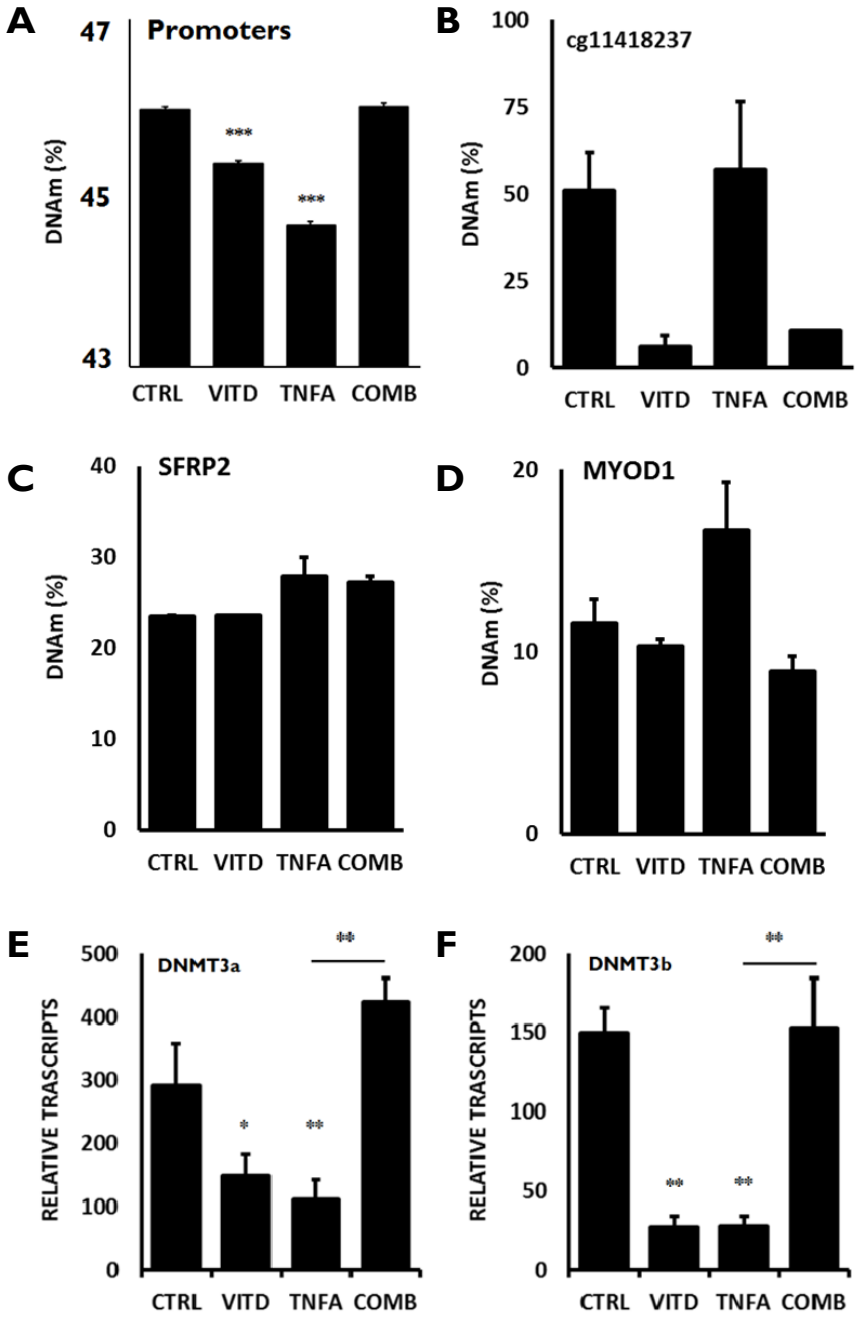

Figure 32 – <u>Myofibroblast supernatants effect partially differential DNAm patterns in case-matched colonic organoids.</u> Case 11 and 12 organoids were cultured in biological triplicate for 30 days +/- 500ng/mL of supernatants, from either ethanol vehicle, 1nM vitamin D, 1ng/mL TNFα, or combined treatment stimulated MFBs. A two day washout period was observed prior to DNA extraction. DNAm patterns were determined by Illumina EPIC array. A) Case 11 gene promoters in colonoids exhibit a modest but significant reduction in average DNAm status after incubation with both vitamin D and TNFα stimulated MFB supernatants, attenuated in combination B) A single CpG in the CCBE1 sequence exhibits a trend toward vitamin D-supernatant-mediated hypomethylation and TNFA-supernatant-mediated DNA hypermethylation (DNAm heterogeneity between C11 and C12 precludes statistical significance). C & D) Promoter DNAm in Wnt antagonists frequently hypermethylated in CRC - SFRP2 and MyoD1 shown - trends towards hypermethylation in both cases after incubation for 30 days with TNFα-stimulated MFB supernatants E&F) DNA methyltransferase transcription is suppressed in colonic organoids (average of three cases) after 24 hour stimulation with case matched MFB supernatants. vitamin D and TNFA-stimulated MFB supernatants both suppress DNMT3a and B transcription, attenuated in combination.

Finally, in respect of the observed increase in IL6 transcription and secretion from TNFα stimulated COX2-high myofibroblasts, the effect of exogenous recombinant IL6 on DNA methylation patterns in case 11 organoids was investigated, to determine if increased IL6 signalling in the crypt niche might affect aberrant DNAm in the epithelium. Organoids were seeded in Matrigel in biological triplicates, and treated for 6 days with the addition of either PBS vehicle, or increasing doses of rIL6 at 10, 100 and 1000pg/mL final concentration in the media. Triplicates were pooled, and harvested DNA bisulphite modified for interrogation by Infinium EPIC methylation array. Gene promoter methylation status was correlated to LOG transformed IL6 concentration. Statistical significance was determined by applying a students' 2-tailed T distribution to the correlation coefficient.

The average gene promoter methylation status in case 11 organoids was not affected by treatment with IL6 at any concentration, remaining static at 49.3% +/- 0.2%. However, recombinant IL6 significantly increased promoter DNAm in a dose-dependent fashion for 972 of the 44,848 genes interrogated (2.2%). Of these, 159 increased their promoter DNAm by more than 5% at the highest concentration, an ominous finding at a low concentration over a short period of time, relative to the *in vivo* paradigms commonplace in IBD. Pathway analysis suggests many of the genes differentially methylated by a short incubation with IL6 are regulated by Myc, a key transcription factor involved in proliferation and survival (figure 33a and c). It is of note that most of the genes susceptible to hypermethylation by IL6 under this protocol, were already partially methylated at base line; only 135 (13.8%) were *hypo*-methylated at base line. This raises the possibility that IL6 exacerbates an underlying CIMP-high phenotype affecting aberrant DNAm in these organoids recovered from diseased colons.

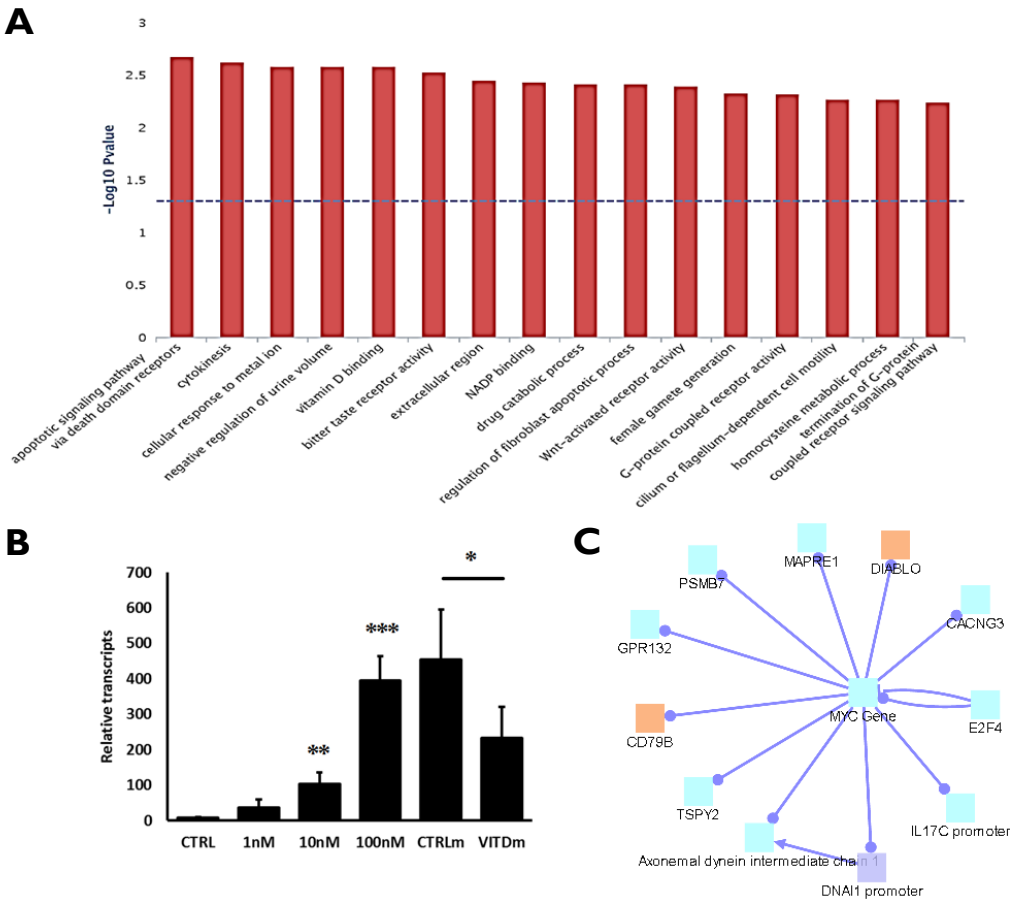

Figure 33 – <u>The effect of matched myofibroblasts conditioned media on epithelial organoids</u>. a) KEGG pathway analysis of the 1060 genes in case 11 identified as hypermethylated by TNFα-stimulated MFB supernatants, and attenuated in the combined treatment. Suggested upregulated pathways and implicated differentially methylated genes include; apoptotic signalling pathway (BMPR1B, SFRP1, ZSWIM2), vitamin D binding (KL, S100G), and Wnt activated receptor activity (FRZB FZD5 SFRP1). B) Vitamin D increases Cyp24a1 transcription in 3 human colonic organoid lines in a dose-dependent fashion (average across three lines +/- SEM). Myofibroblast supernatants (CTRLm) increased transcripts of Cyp24a1 in all cell lines, proposed to inhibit epithelial sensitivity to vitamin D, whereas vitamin D treated MFB supernatants (vitamin Dm) suppress Cyp24a1, confirming an absence of vitamin D in the conditioned media used to treat organoids, and suggested to potentiate epithelia to vitamin D's antiproliferative effects. C) Induced network analysis suggests a Myc as a master regulator of gene promoters hypermethylated in a dose-dependent fashion in response to treatment with rIL6 (seed nodes in black text, purple line denotes transcriptional control of protein product).

Vitamin D attenuates de novo DNA methylation and ameliorates hypermethylation in murine colonoids

In respect of vitamin D's ability to regulate PGE2 production by pericryptal myofibroblasts, the effect of PGE2 on DNA methylation patterns in both murine and human colonic organoids was investigated. As a proof of concept, organoids were generated from an 24 week old C57BL/6 mouse, and cultured in triplicate with either ethanol vehicle, vitamin D (1nM), PGE2 (100mM, 10x physiological dose), or in combination. Cultures were maintained for four weeks and passaged where appropriate to propagate material for interrogation. The methylation status of DKK1, SOX17, SFRP1 and WIF1 were determined by CoBRA.

SFRP1 and WIF1 remained hypomethylated in all samples at the end of the treatment regimen. Vitamin D treated organoids exhibit a reduction in DKK1 promoter methylation from 29.9% in vehicle controls to 14.7% in the D-treated wells. DKK1 methylation status was not determined at base line, so it isn't possible to speculate about the effect of IVA here; either vitamin D has attenuated an IVA-associated increase in DKK1 Methylation seen in the controls, or vitamin D has ameliorated methylation that was previously established. The PGE2-treated organoids show a trend towards DKK1 hypermethylation ($p = 0.0502$), and again in organoids cultured with both vitamin D and PGE2, DKK1methylation is reduced by a similar degree to that of the vitamin D treatment in isolation (figure 34a). The pattern for SOX17 did not reflect these observations; here, SOX17 is hypomethylated in both the controls and the D-treated organoids, with no meaningful difference between the two. However, PGE2 treated organoids show an increase of 12.2% ($p < 0.0001$) of the SOX17 promoter after four weeks, which is attenuated in in combination with vitamin D (figure 34b). These observations are encouraging in that they suggest a direct effect of both PGE2 and vitamin D on WA promoter DNAm, but questions are raised regarding the mechanism of the effect, which appears gene-specific in this instance. It is strongly recommended to attempt replication of these observations in other murine organoids.

Gene transcripts were quantified for several genes of interest, although at this time no validated Q-rt-PCR assay were available for murine SOX17 or DKK1. Curiously, DNMT1 and 3b are both suppressed by PGE2, an effect attenuated in combination with vitamin D, consistent with the observations regarding DNAm (figure 34c and d). Paradoxically, vitamin D induces LGR5 transcription, implying a promotion of the stem-like phenotype, but also induced MUC2, suggesting a move towards a more differentiated phenotype (figure 34 e and f). This may be explained as vitamin D simply exerting normal homeostatic mechanisms in these cells relative to the vitamin D-deprived controls, i.e. this is nothing more than media containing vitamin D allowing for routine cell metabolism. CyclinD1 was interrogated next as an indicator of TCF-LEF activity; vitamin D suppressed CYCD1 in isolation and in combination, supporting the observations regarding vitamin D's status as an anti-proliferative. PGE2 did not affect CYCD1 transcription (figure 34 g and h).

Finally, organoids were cultured from an 11 week old C57BL/6 mouse transfected via tail vein injection to conditionally over-express TNFα in liver hepatocytes. Elevated serum TNFα *in vivo* was confirmed via monoclonal TNFα ELISA (figure 34a). These organoids were cultured in triplicate for four weeks +/- vitamin D (1nM). D-treated cultures exhibited a decrease in the ratio of cystic spheroids to organoids with budding crypt like structures (figure 35b). This was attributable to increased organoid count (of any kind) in control wells, consistent both with vitamin D promoting differentiation and inhibiting proliferation. The ratio of cysts to differentiated organoids was estimated by light microscopy using image J. SOX17 methylation status was determined by CoBRA. Vehicle controls show a similar level of hypermethylation to the level effected by PGE2 previously (23.1% in vivo TNFα versus 18.1% in vitro PGE2). Encouragingly, treatment with vitamin D for four weeks shows a reduction in promoter methylation to 8.0% (figure 35c) $p = 0.0334$). Again a caveat must be observed that baseline methylation was not interrogated, making it impossible determine if the effect was to ameliorate, or attenuate in this instance.

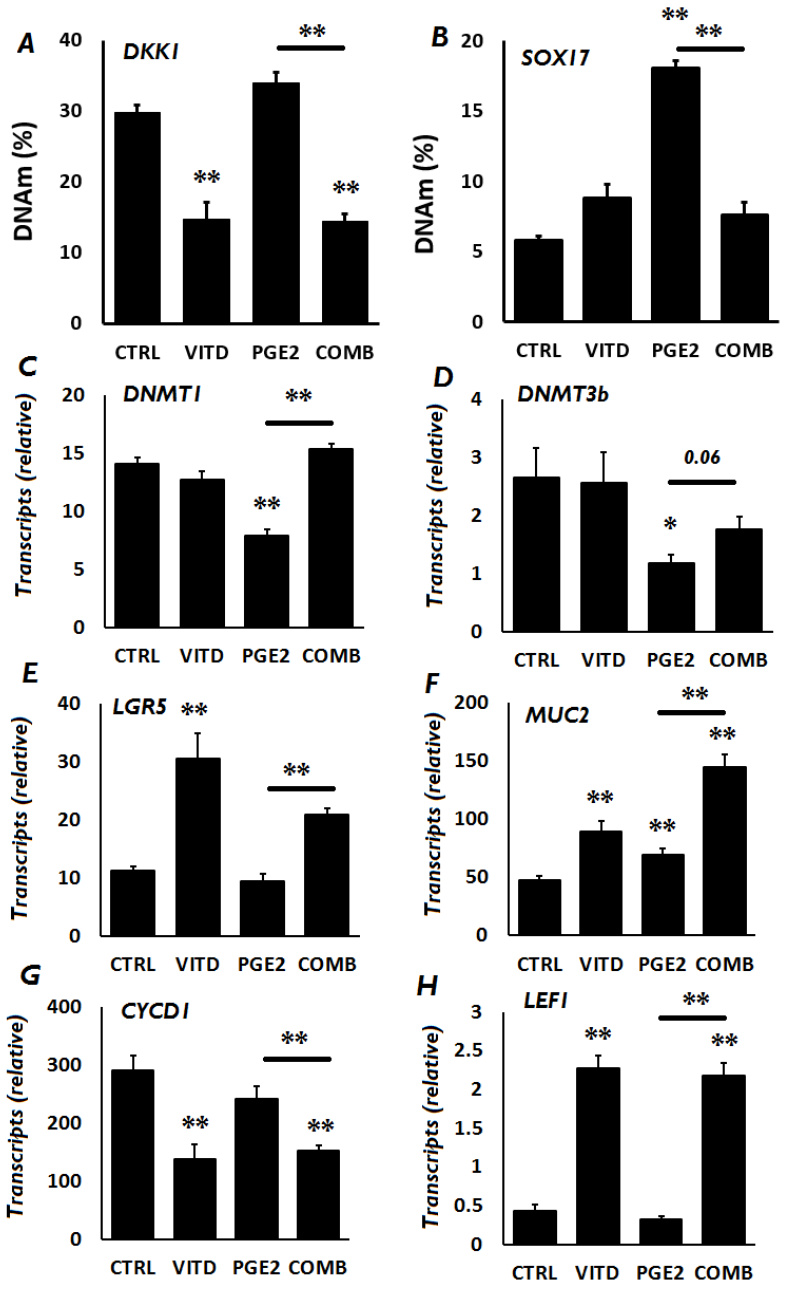

Figure 34 – <u>Healthy murine organoids cultured +/- vitamin D (1nM) and +/- PGE2 (x10 physiological).</u> A) Vitamin D reduces DKK1 promoter methylation. There was an insignificant increase in PGE treated organoids, which was attenuated in combination. B) Similarly, PGE2 promotes hypermethylation of SOX17, attenuated in combination. C and D) surprisingly, in light of PGE2 promoting de novo DNAm, PGE2 inhibits DNMTs 1 and 3b, which vitamin D attenuates in combination. DNMT3b transcripts are relatively low in these organoids. E and F) Paradoxically, both LGR5 and MUC2 are induced by vitamin D, speculated to exert opposing effects on cell phenotype, both towards and away from a differentiated phenotype. However, it is true that goblet cells populate the transit amplifying compartment, although LGR5 shouldn't be present here. G) Cyclin D1 transcripts are relatively high in these actively proliferating organoids. Vitamin D inhibits CYCD1 in isolation and in combination, supporting an antiproliferative effect. It is not possible to assign the effect to hypomethylation of DKK1 or SOX17 without further conditional experiments. H) Vitamin D induces LEF1, which seems counterintuitive, although there are reports that LEF1 targets promote differentiation of epidermal stem cells. n=3, * p<0.05, ** p< 0.01, data represent mean +/- SEM

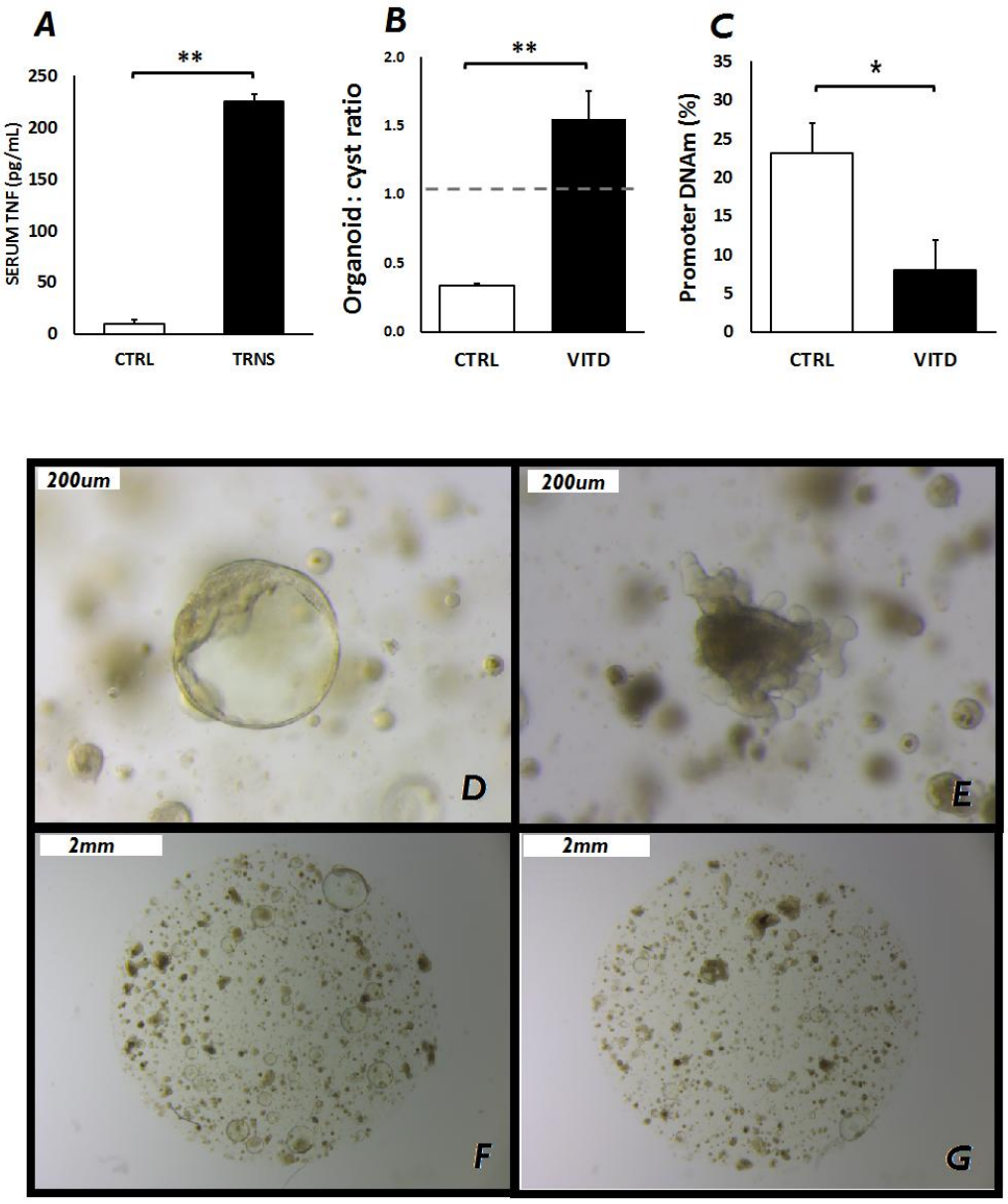

Figure 35 – Organoids from a systemically inflamed mouse transfected to over-express TNFα. A) Serum TNFα was determined by monoclonal ELISA for non-transfected mice from the same cohort. Serum TNFα is elevated in the transfected model prior to dissection. B) The ration of differentiated organoids is increased relative to spheroid cysts in D-treated samples. C) Culture for one month with 1nM vitamin D reduced DNAm in the SOX17 promoter, consistent with previous effects in un-inflamed models. D) Spheroid cyst in control wells E) differentiated organoids showing multiple branching crypt-like structures F) Control wells contained greater numbers of spheroid in comparison to G) D-treated wells where yield was depressed. Thick-walled differentiated organoids were more frequently observed in these wells.

Discussion

Vitamin D is a potent anti-inflammatory and promotes immune cell differentiation, mediating cytokine secretion and resolution of transient inflammation[356]. Pericryptal myofibroblasts contribute factors that inform crypt niche architecture and ECM, and have a modest role in secreted paracrine signalling that regulates Wnt-mediated stem cell turn-over and crypt homeostasis[107]. Chronic inflammation in the colonic mucosa is well described in IBD and associated with increased risk of transformation and aberrant age-related DNA methylation, silencing autocrine Wnt antagonists in crypt stem cells via promoter hypermethylation[170]. Furthermore, sub-epithelial myofibroblasts in the oesophagus were recently demonstrated to secrete pro-inflammatory cytokines, including IL6, in response to stressors via NFκB activation[357]. In this context it was sought to establish if TNFα, routinely found to be over-expressed in inflamed mucosal lesions[358], might precipitate a modified secretome in pericryptal myofibroblasts lines propagated from uninvolved mucosa of colorectal cancer bowel resections. Furthermore, it was set out to investigate if the secretory profile of TNFα-stimulated myofibroblasts impacted on DNA methylation patterns in case-matched colonoids, propagated from the same samples, and the ability of vitamin D to mediate any effects.

Tumour necrosis factor alpha is a key mediator of transient inflammation and repair in the colonic mucosae, with a well-documented role in IBD pathogenesis. So pivotal is TNFα signalling in instigating and maintaining IBD, that anti-TNFα chemotherapy that inhibits TNFα-mediated inflammation, is indicated in Crohn's disease and Ulcerative Colitis, inducing remission even in severe refractory disease states (TNFα-sequestering agent, Infliximab)[359]. At the paracrine level, TNFα-receptor signalling activates phosphorylation of IKKb complexes, nuclear translocation, and transcription of NFκB target genes via response element binding sites. COX2 possess one such site, and is demonstrated to be upregulated via NFκB activation in TNFα-stimulated gingival fibroblasts[349]. Furthermore, COX2 modulation via inflammatory stimuli is widely accepted to

promote PGE2 secretion, with pathological implications for homeostasis in the colonic mucosa[343].

An aetiological role for COX/prostaglandins in bowel disease is evidenced by a vast body of data that shows long-term inhibition of both COX1 (constituitive) and COX2 (inducible) by aspirin, that favourably influences incidence and mortality of CRC[360]. Vitamin D and analogues have been shown to inhibit COX2 in several macrophage models[346,347], although evidence of COX2 inhibition by vitamin D specifically in intestinal myofibroblasts is absent from the literature.

Our findings in four validated primary intestinal myofibroblast lines support the first observation; that TNFα promotes PGE2 secretion via induction of COX2, and this is consistent with reports that both TNFα and IL1β modulate secreted PGE2 in colonic fibroblasts[361]. PGE2 concentration in supernatants correlates well with TNFα-induced COX2 transcripts, raising the possibility that inhibition of TNFα-mediated COX2 transcription in intestinal myofibroblasts (by any means) might lower PGE2 concentrations in the crypt niche to promote bowel health

Regarding vitamin D's role, COX2 was only suppressed in embryonic InMyoFib. The trend was evident in case 13 MFBs, whose base line level of COX2 transcription was most similar to the embryonic line, but vitamin D did not suppress COX2 in the other two lines exhibiting relatively high levels of COX2 in the basal state. It may be that 1nM vitamin D for 72 hours in this instance wasn't powerful enough to redress the relatively high level of COX2 transcription, and proper dose/time dependency should be investigated in this respect – COX2 may in fact be suppressed by vitamin D at an earlier time point, as assessed in the test case. Importantly however, vitamin D did inhibit PGE2 secretion in all four lines, suggestive of a non-canonical or indirect mode of action, whereby vitamin D interferes with the secretory pathway downstream of COX2 regulation; this has in fact been previously documented in lung fibroblasts, where vitamin D reduces PGE2 secretion, but not COX2 transcription. Instead, vitamin D mediates degradation of PGE2 via induction of HPDG[362], and

verification of this alternative mechanism warrants investigation in our primary lines.

Myofibroblast lines were recovered from the uninvolved mucosa of colorectal cancer resection specimens. Given that these epithelia have already demonstrated a propensity to transformation (field cancerisation effects), and the role of CAFs in promoting tumourigenesis, it is rational to speculate that these pericryptal myofibroblasts may already have adopted a modified phenotype, relative to counterparts not associated with a cancer-prone epithelium (embryonic InMyoFib for example). InMyoFib supernatants were not characterised, however, relative to case 11 and 12, exhibit a COX2- and PGE2-low profile at base line, similar to case 13, and these respond as predicted to vitamin D treatment.

The base line levels of both COX2 transcripts and PGE2 secretion prompted a hypothesis that COX2-high MFBs represent a distinct phenotype to COX2-low MFBs with regards their inflammatory/secretory status. However a caveat must be observed regarding PGE quantitation; although supernatants were collected from 80%+ confluent wells following treatment, it is within the realms of possibility that the designation of PGE2-high secretion at base line - determined by ELISA - is an artefact of unspecified differences in monolayer density. Normalising the data to the control accounts for this discrepancy in the pooled data, but interpretation of individual levels of PGE2 secretion should take this into account. Thus, data are reported as pg/mL of conditioned media, and not pg/number of cells/24 hours. However, the synchronous COX2-high status in these two lines implies that this cautionary note may in fact be redundant, as transcription results are normalised twice during Q-rt-PCR protocols.

Prior to any stimulation, mass spec proteomics was employed to characterise the base line secretory profile of disease-associated myofibroblasts. Pathway analysis of the 124 commonly secreted factors showed top hits including ECM and collagen degradation. This is consistent with findings in tumour stromal CAFs in cervical, lung, and colorectal cancers[289,363,364], although in our case the MFBs are not true CAFs, and so may represent a transitory phenotype in the uninvolved

but predisposed stroma. On average 15.9% of all secreted proteins were associated with gene ontology for regulation of immune function, supportive of a role for MFBs in mediation of inflammation in the intestinal crypt niche[365].

Key to our informing hypothesis, vitamin D mediated a significant reduction of one secreted protein from all three MFB lines – Laminin 2 (LAMA2). Cytokine mediated dysregulation of laminin class protein transcription contributes to impaired barrier integrity in IBD[366], and specifically, LAMA2 is reported once in the literature to exhibit a 4.5-fold increase in expression in UC mucosae relative to healthy controls (although it's cellular origin was not identified)[367]. Further investigation is indicated to establish if this observation is both ubiquitous in inflamed mucosal myofibroblasts, and aetiological in loss of epithelial homeostasis; firstly, validation by Western blot and ELISA, secondly, recapitulation in other intestinal fibroblasts or CAF lines, and finally, elucidation of the effects of both recombinant LAMA2 and conditional LAMA2 knock-down on DNAm in intestinal epithelial models The immune response to LAMA2 in tissue-resident immune-cells should also be investigated.

The concept of dual phenotypes is supported by a greater diversity of proteins identified in COX2-high MFB supernatants that included pernicious soluble factors not detected in COX2-low MFB supernatant; IL6, SERPINE1, PGD2, LIF, and TSG6. Secreted IL6 is consistent with previous reports that aSMA+ve tumour stromal fibroblasts encourage inflammation and angiogenesis via IL6 secretion[299]. The role of IL6 in IBD driven carcinogenesis is reported to attenuate apoptotic pathways via induction of BCL-XL[368]. Our data suggest that the tumour promoting effects of IL6, secreted by MFBs in the niche, may be exacerbated by TNFα. The serine protease inhibitor SERPINE1 is over expressed in epithelium of UC patients, and associated with microsatellite instability in colorectal cancer[369,370], however ours is the first indication of a further non-epithelial source of SEPRINE1. Prostaglandin D2 synthase is another COX2-mediated protein involved in pathological prostaglandin metabolism, activated in Crohns disease[371]. Finally TNFα-stimulated gene six is recognised to mediate an anti-inflammatory effect[372], and it's presence here may contribute to negative

feedback in response to the underlying inflamed phenotype, evidenced by resolution of intestinal inflammation in mice injected with TSG6-secreting mesenchymal stem cells that localise to the peritoneum[373]. In both cases, SERPINE1 and PGD2 were inhibited by vitamin D, but the trend was not statistically significant. IL6 and TSG6 were not affected by vitamin D. All four proteins exhibit increased total spectra counts following TNFα stimulation of COX2-high MFBs.

The increase of secreted IL6 was validated by Q-rt-PCR, although the mass spec secretomic approach is considered qualitative only and so further validation of these findings should be performed by ELISA and/or Western blot. It would also be pertinent to explore the COX2-high hypothesis in MFBs in non-transformed, adenomatous, and carcinogenic mucosa alike, to determine if transition from healthy pericryptal myofibroblast to disease-associated myofibroblast is linear and/or associated with initiation and tumourigenesis.

It is of note that none of the previously discussed growth factors were identified in MFB supernatants, and less than 2% of identified proteins were associated with GO term 'growth'. This suggests either that the ability of MFBs to contribute those growth factors specifically used for organoids culture (RSPO1, JAG1, Wnt3a) has been over stated here and elsewhere[226], or that they fall beneath detectable levels in supernatants via the mass spec approach. This observation lends support to the alternative hypothesis that the regulation of GF transcription observed in MFBs (mediated by TGFβ1, TNFα and vitamin D) acts in an autocrine fashion to regulate MFB proliferation, not in a paracrine fashion to drive stem cell turn-over as previously hypothesised (paracrine effects being mediate by uncharacterised esoteric factors).

Data pertaining to DNAm profiles modified by inflamed MFB supernatants in case matched organoids must be considered with extreme caution; it was originally intended that the three propagated human colonic organoid lines would comprise three biological replicates for statistical comparison on the array – not only did two lines fail to yield sufficient DNA for analysis, stochastic variation between the lines in gene-specific DNAm (possibly established in the original

epithelia due to field effects) precluded significance – a finding not unanticipated given the difference between participants chronological age (45yo verses 65yo). This presents a fundamental flaw in the methodology for determining statistical significance; in retrospect, increasing the sample pool included on the array would better power analyses to reveal impacted genes.

However, it is encouraging that identified genes have been documented elsewhere in transformed epithelia; Collagen and calcium-binding EGF domains 1 (CCBE1) may poses a single CpG hypermethylated by inflamed supernatants that was attenuated by vitamin D-treated MFB supernatants in both case 11 and 12. In ovarian cancers, CCBE1 is poorly expressed compared to healthy cells. Knockdown of CCBE1 in ovarian cancer cells promotes migration and invasion, and the gene's promoter is frequently found to be hypermethylated in these cancers[353]. Similarly, the transcription factor POU3F4, required for Wnt-mediated proliferation of neural stem cells[374,375], experienced hypermethylation of a single CpG in organoids treated with inflamed MFB supernatants, an effect diminished with supernatants from the combined treatment. POU3F4 is hypermethylated in 55% of non-small cell lung cancers; if our results can be verified, chronic inflammation perpetuated by COX2-high MFBs may have implications for Wnt-mediated regulation of stem cell turnover in the colon.

With respect to findings of Tapp et al, that underpin this thesis hypothesis, it is encouraging that DNAm patterns in a number of genes identified in their paper appear to show a similar induction of hypermethylation here in response to inflamed MFB supernatants, although the trend was not significant for reasons outlined. MYOD1 is of particular interest because that was the gene with the most significant correlation with vitamin D status in their paper. Furthermore, suppression of DNMT3a and 3b by both TNFα-inflamed and vitamin d-quenched supernatants from all three MFB lines in matched organoids is in keeping with the modest but highly significant reduction in average gene promoter methylation status experience by case 11 organoids after one month in culture. Although DNMT3b typically mediates de novo DNAm, if control organoids are prone to hypermethylation (CIMP), the reduction observed relative to controls could be a

passive consequence of inhibited DNMT3b activity, that means controls advance their methylation over the 30 days, rather than stimulated supernatants ameliorating it. The case for a predisposition to DNA hypermethylation (CIMP-high) is supported by the observation that the average methylation status of the panel of Wnt antagonists outlined was 30.1% +/- 7.5% in both cases at base line, and only three were hypo-methylated according to our definition. Furthermore, CIMP-high typically presents in the proximal colon[376] - both samples were recovered 20cm proximal to recto-sigmoid tumours.

Finally, TET1 was silenced in all three organoid lines, consistent with reports elsewhere that TET1 down-regulation is an early finding in transformation. TET1 mediates its tumour suppressor effects by stereochemical association with gene promoters, inhibiting aberrant DNA hypermethylation at those sites[363]. Loss of TET1 in these organoids supports the CIMP-high hypothesis.

Lastly, a short note on vitamin D sensitivity; we demonstrate an anticipated dose dependent increase in Cyp24a1 in response to exogenous vitamin D in the three organoid lines. However, we also saw a significant induction of this vitamin D-deactivating enzyme in case matched organoids treated with vehicle-stimulated MFB supernatants – an effect attenuated by treatment with vitamin D; this suggests that disease-associated MFBs such as these might reduce epithelial sensitivity to vitamin D's antiproliferative effects by encouraging its catabolism – a novel finding not reported previously, but in keeping with observations that Cyp24a1 is routinely over-expressed in poorly differentiated CRC, and that conditional silencing potentiates vitamin D's anti-tumourigenic properties in CaCO2 cells[377,378]

Summary

Primary myofibroblasts from the uninvolved mucosa of colorectal cancer resections show an inflamed secretory profile at base line hypothesised to increase inflammatory signalling in the stem cell niche. Vitamin D partially attenuates, and TNFα promotes the secretory profile, and a COX2-high phenotype is proposed to explain differences between primary lines, at base line and in response to stimulation. It is not verified that an altered MFB secretome manifests aberrant DNA hypermethylation in epithelial Wnt antagonists, however observational data do not exclude the possibility. Enticingly, MFB supernatants are able to regulate methyltransferase transcription in matched epithelial cells, and the altered secretome may even pathologically promote vitamin D insensitivity of the epithelia via inactivation by Cyp24a1 – a finding that warrants further investigation. Vitamin D treated MFB supernatants resolved the induction of Cyp24a1, contributing another previously unrecognised role for vitamin D in promoting bowel health via indirectly increasing epithelial sensitivity to vitamin D's antiproliferative effects.

Experiments conducted in murine colonoids give an indication that PGE2 promotes hypermethylation of WAs in a phenotype or gene specific fashion. It is highly recommended that attempts are made to recapitulate these findings in other epithelial models.

Chapter 6

PHYSIOLOGICAL VITAMIN EXERTS ANTI-CANCER EFFECTS IN CACO2 CELLS VIA A MODIFIED METHYLOME

Preface to the work

The novel finding that vitamin D ameliorates SOX17 hypermethylation in previously inflamed tissues, raises the possibility that vitamin D might also possess the ability to resolve pathological patterns of acquired DNAm in transformed cells. It is well established that vitamin D status predicts the clinical course of CRC following diagnosis, and its actions as an anti-proliferative are comprehensively documented *in vitro* for a variety colorectal cancer cell lines. Specifically vitamin D inhibits proliferation via down regulation of Wnt signalling, and these effects are mediated in part by induction of tumour suppressors that antagonise Wnt[379]. We considered if these effects could be consequent to demethylation of promoter CGI mediated by vitamin D.

Preliminary experiments with four CRC cell lines (DLD1, HT29, HCT116, and CaCO2, selected for their genetic and epigenetic diversity, and differing degrees of differentiation), suggested that under optimised conditions vitamin D might be able to redress acquired DNAm (figure 36a-d).

The CaCO2 cell line became the focus of longer-term incubations due to anomalous results from a basic WST1 assay used to determine time/dose effects of treatment; cells cultured from high passage number stocks (passage 30 onwards) demonstrate phenotypic insensitivity to vitamin D in this respect. Surprisingly, subsequent Q-rt-PCR experiments, for which CaCO2 cells were incorporated as a negative control, showed that vitamin D also regulated transcription in these cells. The transcriptionally responsive cells were re-interrogated by WST1 assay, which suggested that, in cells with lower passage numbers (under 10), vitamin D's anti-proliferative effects remained intact. This raised the possibility that *in vitro* 'ageing' - specifically forced mitosis through repetitive passage (itself a stressful procedure for cells to endure) - might accelerate ongoing aberrant DNAm events across the methylome, driving progression and resistance to vitamin D.

As a proof of concept, we aged CaCO2 cells for ten weeks under routine conditions, and then stimulated them with supra-physiological vitamin D to investigate if extended culture effected C-MYC transcription (as a measure of

Wnt activity) and vitamin D sensitivity (figure 36 e and f). Encouragingly these experiments suggested that CaCO2 cells undergo transcriptional changes in the absence of vitamin D and establishes vitamin D insensitivity at higher passage number. We speculated that transcriptional variability could be due to ongoing aberrant methylation events typical in transformed epithelial cells, and set about characterising the effects of *in vitro* 'ageing' and vitamin D sufficiency on the methylome of colorectal cancer cell lines.

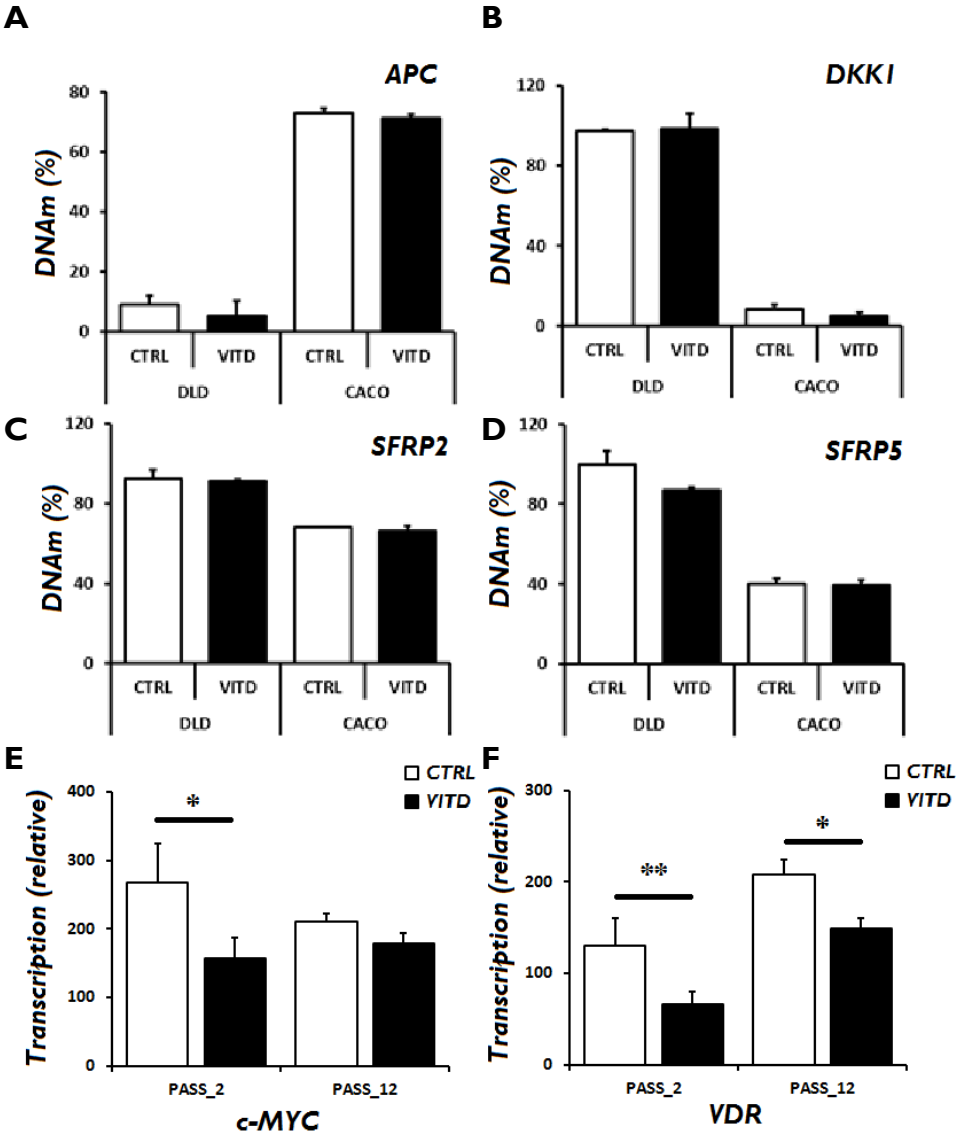

Figure 36 – Preliminary experiments with cancer cell lines. n=3, *p<0.05, **p<0.01. Data represent mean +/-SEM. A-D) DLD1 and CaCO2 cells were cultured for 6 days +/- 100nM vitamin D (supra-physiological). Bisulphite modified DNA was interrogated by CoBRA, and show modest, non-significant trends towards demethylation for APC, DKK1, SFRP2 and SFRP5, suggesting *hypomethylation* might be achieved under optimised conditions E) Vitamin D (100nM, 4 hours) suppresses C-MYC transcription in 'young' CaCO2 cells, but not in the same cells after ten passages, suggesting that *in vitro* ageing precipitates vitamin D insensitivity. F) This is supported by impaired suppression of VDR, a vitamin D responsive gene, in 'aged' cells. NB, aged cells in the un-primed state increase their sensitivity to vitamin D by increasing VDR transcription over time.

Abstract

Vitamin D status is associated with relative risk for bowel cancer. Furthermore, serum vitamin D at presentation is associated with survival and CRC-associated morbidity. *In vitro* vitamin D is shown to potentiate chemotherapies and independently inhibit constitutional activation of Wnt, via multi-level repression of autocrine signalling. Antagonists of the Wnt pathway are frequently inactivated in CRC via aberrant promoter methylation, and vitamin D status is inversely associated with rates of aberrant age-related DNAm. *De novo* expression of epigenetically inactivated tumour suppressors by vitamin D has been documented in other epithelial cancers. Furthermore demethylating agents such as azacytidine and decitabine are indicated in myelodysplastic disease, inhibiting DNMT1 activity that precipitates a loss of CGI methylation and reconstitution of epigenetically silenced genes. It was speculated that vitamin D sufficiency might ameliorate aberrant DNA methylation patterns in CRC cell lines, and set about characterising the effects of vitamin D sufficiency on the phenotype and methylome of CRC cell lines.

CaCO2 and DLD1 cells were cultured under routine conditions for ten weeks +/- 500pM vitamin D (~5x biological sufficiency). After treatment, a four day wash-out period was observed to mitigate for transcriptional effects of vitamin D. DNA was interrogated by Illumina 450K methylation bead chip array, and reveals genome-wide modifications to 5-methyl-cytosine patterns synchronous to induction of DNMT1 and 3b. In CaCO2 cells this was associated with inhibited proliferation, viability, RPS6Ka3 transcription, and ERK1 and 2 phosphorylation. Sufficiency did not ameliorate DNAm in the promoter regions of genes associated with aberrant DNAm in colorectal cancer (Wnt antagonists and CIMP+ genes), although supra-physiological vitamin D reduced SFRP5 methylation status in DLD1 cells, with trends in other Wnt antagonists. Aberrant DNAm was observed to increase in control cells from both lines, termed *in vitro* ageing.

Taken together, our data suggest that vitamin D improves CRC prognosis via epigenetic modifications that inhibit proliferation.

Introduction

Risk of neoplasia in any tissue typically increases with age, and the paradigm holds for colorectal cancer, with incidence peaking at 1 per 23, in the 7th decade of life onwards[380]. In Europe, this demographic is the fastest growing, with the disease representing the 3rd most prevalent cancer after prostate and lung cancer for men, and breast and lung cancer for women[381]. Treatment regimen, prognosis, and mortality depend largely upon factors that describe the tumour at clinical presentation. Tumours are staged according to the Duke's system which considers the size and extent of the tumour, the involvement of mesenteric lymph nodes or vasculature (which forebodes metastasis), and sites of distant metastasis (typically the liver, the ultimate destination for enteric blood and lymph). Duke's staging is a strong predictor of 5 year survival, being 93.2% and 6.6% for stage 1 tumours verses stage 4 tumours, respectively[382].

Several histological biomarkers are also used to predict the clinical course of the disease, pertaining to critical mutations or indicators of cancer phenotype (Ki67, EGFR, VEGF, and P53), with over-expression associated with an ~50% reduction in five year survival[383]. Other independent biological predictors of prognosis include lymphocytic infiltrate, microsatellite instability (MSI), chromosomal instability (CIN), and importantly, established aberrant DNA methylation patterns[384].

Pathogenic DNAm is reported in virtually every neoplastic tissue, and three forms are commonly reported in CRC; age-related gene specific *hypermethylation*, age-related global *hypomethylation* (both preceding transformation, but present throughout), and CG island methylator phenotype (subsequent to transformation), reported in up to 25% of sporadic CRCs[385]. The methylator phenotype describes tumours with wide-spread non-specific gene promoter hypermethylation in advancing tumours. Associations are noted with MSI, kRAS and bRAF mutations, maintained p53 functionality, proximal location, female sex, and older age[386]. The association of CIMP with MSI is an important one, as it is thought that hypermethylation of MLH1, a DNA mismatch repair protein

invariably silenced in CIMP tumours, is the driving aberration that precipitates MSI[387].

Importantly, MLH1 methylation is independent of the aforementioned age-related hypermethylation of tumour-suppressors, and as such defines the CIMP phenotype with a few other genes not affected in an age-dependent fashion (CDKN2A, RUNX3)[388]

Regardless, all three forms of aberrant DNAm are associated with rate of recurrence, 5 year survival, and for CIMP+ve tumours, their response to chemotherapy[198,389,390]. Presumably, resolution of aberrant DNAm patterns in cancer cells could potentiate a regain of control over constitutional pathway activation driving uncontrolled proliferation, preferable to chemotherapies that non-specifically block proliferation or induce apoptosis. After all, due to their dynamic nature, epigenetic modifications are potentially reversible, and unlike mutations, DNAm must be actively maintained during mitosis, making the process an attractive target. These observations have fuelled research into the use of DNA methyltransferase inhibitors, mainly cytidine analogues like 5-aza cytidine and 5-aza-2 deoxy-cytidine (decitabine), to induce passive *hypomethylation* at sites of aberrant CGI methylation over successive generations[391]. These are shown to be effective at promoting demethylation in colorectal cancer cell lines *in vitro,* potentiating the effects of chemotherapeutics[392], but are not currently indicated for solid gastrointestinal tumours due to toxicity at the effective dose, and non-specific effects that are as likely to reconstitute an aberrantly silenced Wnt tumour suppressor, as they are to re-activate a necessarily silenced oncogene[393,394].

It has also been observed that serum vitamin D sufficiency is not only associated with reduced rate of cancer incidence, but favourably predicts prognosis too[395]; higher pre-diagnosis serum vitamin D is associated with a significant improvement in overall survival[396], which is supported by observational studies demonstrating improved prognosis when CRC is diagnosed at the end of summer, when serum vitamin D levels peak, compared with winter presentation[397]. The relationship is maintained post-operatively, where serum D correlates with survival for stage 1 through 3 cancers. Here the authors also identify an interaction of recurrence with VDR polymorphisms, suggestive of a causative mechanism by which vitamin D influences the course of the disease[398].

Even in stage 4 metastatic CRC, serum vitamin D sufficiency still appears to enhance survival[399]. Conversely, impaired vitamin D metabolism in epithelial cancers is a negative prognostic indicator; over-expression of vitamin D-deactivating enzyme Cyp24a1 correlates with invasive depth, lymph node metastasis, reduced survival, and increased recurrence[400].

Vitamin D exerts a variety of anti-proliferative and pro-apoptotic effects on colorectal cancer cells *in vitro*, which are speculated to be in part due to vitamin D modulating aberrant DNA methylation patterns[60]. For example, vitamin D is documented to induce DKK1 and inhibit DKK4 transcription in SW480 CRC cells, simultaneously orchestrating nuclear export of BCAT via it's interaction with VDR, with consequent repression of TCF targets[379]. Vitamin D also down-regulates Wnt signalling via induction of ECAD in CRC in vitro, which effects BCAT stabilisation and differentiation[91]. There are isolated reports that vitamin D mechanistically reconstitutes expression of hyper-methylated ECAD in several VDR-competent breast cancer cell lines, promoting differentiation. The effect is recapitulated by treatment with demethylating agent 5AZA, and synergistic when the two treatments are combined. The authors report synchronous demethylation, induction, and differentiation, that is abrogated by conditional interference with VDR[94]. Similarly, vitamin D instigates demethylation and *de novo* transcription of epigenetically silenced PDLIM2, again in breast cancer cells. The protein functions in a similar way to ECAD, promoting cell-cell adhesion, and inhibiting migration[401]. Tapp et al report an apparent protective effect against *de novo* DNAm in macroscopically normal mucosa, but to date the ability of vitamin D to reverse established aberrant DNAm in transformed cells has yet to be investigated.

CaCO2 and DLD1 colorectal cancer cells were cultured for 10 weeks under routine conditions, with and without vitamin D at a physiologically relevant concentration. After a wash out period, bisulphite modified DNA was interrogated by Illumina 450K DNA methylation array, to identify differentially methylated regions governing gene transcription manifested by vitamin D.

Methods

Cell culture

For the main experiments, colorectal cancer cell lines CaCO2, DLD1, HCT116 and HT29 (form ATCC) were cultured under routine conditions detailed in General Methods. Passage number at the start of the extended culture period was 2 for CaCO2 cells and 9 for DLD1 cells. To establish a single lineage, cells were cultured to 80% confluence in a T75 flask, which was split by routine passage into six T25 flasks; three were treated with ethanol vehicle, and the other three received 500pM vitamin D (Tocris) final concentration (biological triplicates). Media was refreshed every 2-3 days.

Flasks were maintained for ten weeks, passaged once per week with a 1:10 split. Cell pellets at passage 2, 4, 6, 8, and 10 were rinsed, protease inhibitors added, and snap frozen on dry ice for subsequent RNA extraction and Q-rt-PCR (methods detailed previously). At the end of the treatment regimen, cells were seeded into new T25 flasks for a wash out period of 96 hours, which were washed with PBS every 24 hours and fresh media applied. Alternatively, cells were seeded at an appropriate density for WST1 assay on the fourth day to determine proliferation and viability (trypan blue). Washed-out cells from flasks were either collected for bisulphate modification/DNA interrogation, or whole-cell extract protein blots, probing for BCAT and ERK phosphorylation.

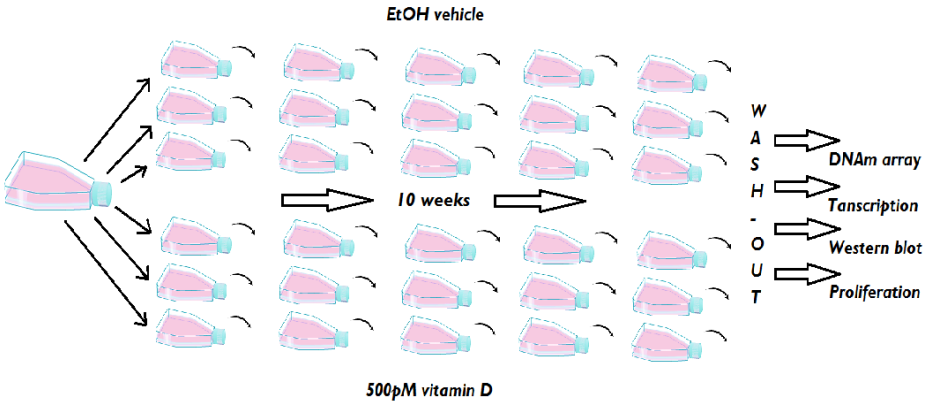

Figure 37 – Graphical methods for CRC cell line *in vitro* 'ageing' and vitamin D sufficiency. Cells were passaged once per week by routine methods and fresh treatment/media applied every 2-3 days for the duration of the experiment.

Infinium HumanMethylation450 bead chip array

DNA samples were prepared by phenol-chloroform extraction, rinsed with 70% ethanol, and resuspended in nuclease-free water. Concentration was determined from Nano-drop UV spectroscopy, and 500ng dispatched on dry ice for analysis using the RnBeads plugin for 'R' console as previously described. Data represent the mean of the three biological replicates for each line and treatment.

Western blot

Whole-cell protein extracts were prepared from one sample of each 'aged' washed-out CaCO2 treatment as previously described. Technical triplicates of 20ug protein were run by PAGE on a graduated density gel, and probed for total ERK1 and total ERK2 (NEB 9102, 1:2000 in 5% BSA), and phosphoERK1 and phosphoERK2 (NEB 4370 1:2000 in 5% BSA). Band intensity was calculated using ImageJ, and the normalised ratio of pERK : tERK reported as the mean of the 3 samples +/- the standard error.

Q-rt-PCR

RNA was extracted from washed-out samples and 500ng processed to cDNA as previously described. The primer sets used are detailed in appendix 6). Biological replicates were run in technical duplicate and CT values normalised to GAPDH. Data represent the mean +/- the standard error of the relative transcripts (determined by the delta CT method), and a non-parametric students T-test applied to the normalised CT values to determine significance.

CoBRA assays for Wnt antagonists

To reduce standard errors precluding significance for minor changes in WA promoter DNAm, 12 rather than 3 biological replicates of DLD1 cells were cultured for six days +/- 100nM vitamin D. The harvested DNA was bisulphite modified, amplified by bench-top PCR, and digested by 5mC-specfic restriction enzymes using the protocols for APC, DKK1, SFRP1, 2 and 5 in appendix 5. LINE1 was interrogated independently by QMSP as detailed in the general methods.

WST1 assay

The WST1 Assay (Roche) was performed in 96 well plates as outlined previously by the manufacturer's instructions. Cells were seeded at an appropriate density to ensure interrogation during the log-growth phase at either 2, 4, or 6 days post vitamin D treatment. Six technical replicates were used to determine statistical significance.

Pathways analysis

Lists of Ensembl codes for differentially methylated genes mapping to functional proteins, were uploaded to www.inateDB.com to determine which biological pathways and gene ontology terms that were significantly over-represented (represented more than expected by chance) in the lists. InnateDB incorporates pathway annotation from major public databases including KEGG, Reactome, NetPath, INOH, BioCarta and PID and is thus one of the most comprehensive sources of pathways available. A Gene Ontology (GO) over-representation analysis (ORA) examined the lists for the occurrence of GO annotation terms which are more prevalent in the dataset than expected by chance. For analysis and visualisation, the recommended hypergeometric algorithm with Benjamini Hochberg correction was selected.

Results

Effects of vitamin D in colorectal cancer cell lines

Vitamin D reduces proliferation of colorectal cancer cell lines in a dose-dependent fashion

Colorectal cancer cell lines CaCO2, DLD1, HCT116 and HT29 were selected for their diverse mutational and epigenetic profiles, to investigate if vitamin D's well established antiproliferative effects were recapitulated in these lines. Proliferation was interrogated by tetrazolium salt reduction assay (WST1) in replicates treated with either ethanol vehicle at the highest concentration, or increasing doses of vitamin D (10, 100 and 1000nM respectively) for 6 days. The concentrations used represent the supra-physiological range employed by others against these lines[99,402]. Data are reported as the mean +/- the standard error, normalised to the control.

After six days, all four cell lines exhibit dose-dependent inhibition of proliferation (figure 38). The DLD1 and HT29 lines show enhanced vitamin D sensitivity at the lowest concentration, not apparent in CaCO2 and HCT lines. Ultimately, the assay is a reflection of the ratio of actively proliferating cells, and while cells are seeded at identical densities, vitamin D is also reported to promote apoptosis, therefore it is not possible to determine whether impaired proliferation or impaired viability reduces cell numbers. In preliminary experiments, vitamin D was observed to induce transcription of FAS ligand and caspases 3 and 7 (cell line dependent), while sporadically suppressing FOS/MYC/JUN at various time points (data not shown), consistent with vitamin D acting via multiple phenotype-specific pathways to inhibit tumour cell growth *in vitro*[403].

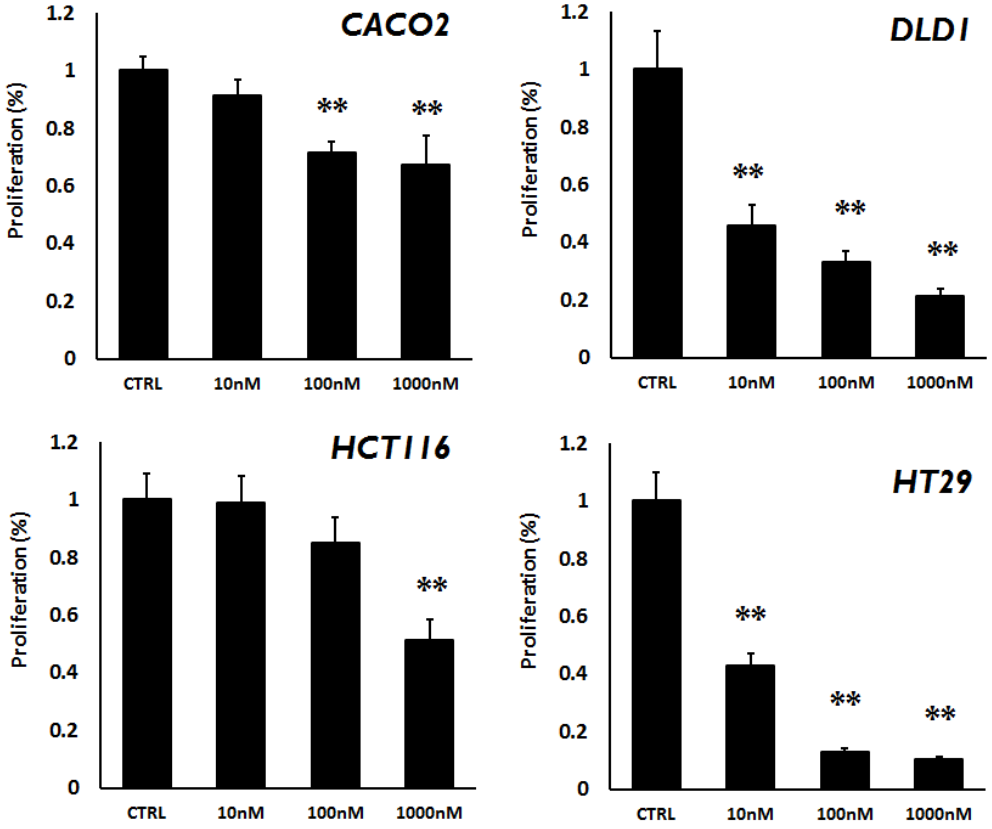

Figure 38 – <u>Anti-proliferative effect of vitamin D in CRC cell lines.</u> Vitamin D demonstrates a dose-dependent reduction in proliferation as determined by WST1 assay. Vitamin D sensitivity in DLD1 and HT29 cells appears to be greater than in CaCO2 and HCT116 cells. Cells were treated for six days, with media and treatments refreshed every 24 hours in respect of vitamin D's relatively short biological half-life. Data represent the mean of six technical replicates +/- the standard error, normalised to the control, for each line investigated.

Vitamin D effects SFRP5 promoter demethylation, increases LINE1 methylation, and is associated with sustained suppression of DNMT3b transcripts.

Previously, a modest, non-significant trend towards SFRP5 promoter *de*methylation was observed in DLD1 cells, treated for six days with 100nM vitamin D, and these cells show increased sensitivity to vitamin D over other lines. It was hypothesised that the methylation effect was true, but too weak to attain statistical significance due to error associated with insufficient replicates. Consequently the number of biological replicates was increased from 3 to 12, increasing the total number of data points for statistical comparison (non-parametric students T-test) from 9 to 36. Again, SFRP1 and 2 show an insignificant trend towards hypomethylation, but SFRP5, which showed the biggest response previously, experiences significant *de*methylation at this concentration over 6 days. The effect was concomitant to a modest but significant increase in global DNAm, as determined for LINE1 (figure 39a).

Synchronous to these experiments, DLD1 cells were also cultured with 100nM vitamin D and RNA harvested for Q-rt-PCR, to investigate DNMT3b transcription. Cells were harvested every 24 hours during the experimental protocol, and exhibit suppression of DNMT3b transcripts at every time point, except on the 3rd day when the suppression was not significant (figure 39b). Taken together, these data raise the possibility that vitamin D prevents the acquisition of *de novo* DNAm in the SFRP5 promoter, as opposed to ameliorating established DNAm, although it has been shown elsewhere that DNMT3b cooperates with DNMT1 in the maintenance of DNAm patterns, so the observed effect could be consequent to impaired replicative fidelity (DNMT1 transcription was not determined, and SFRP5 transcripts remain undetectable at 40 cycles). Interestingly, DNMT3b shows a linear decrease in control samples across the treatment period, also noted for D-treated cells. This raises the possibility that its transcription is enhanced in cells following passage insult, which diminishes as cells recover homeostasis and enter the log growth phase. If cellular stress really does elicit aberrant DNMT activity, there may be deleterious consequences for the methylomes of cell lines that are subject to frequent passage (termed *in vitro* 'ageing' - IVA).

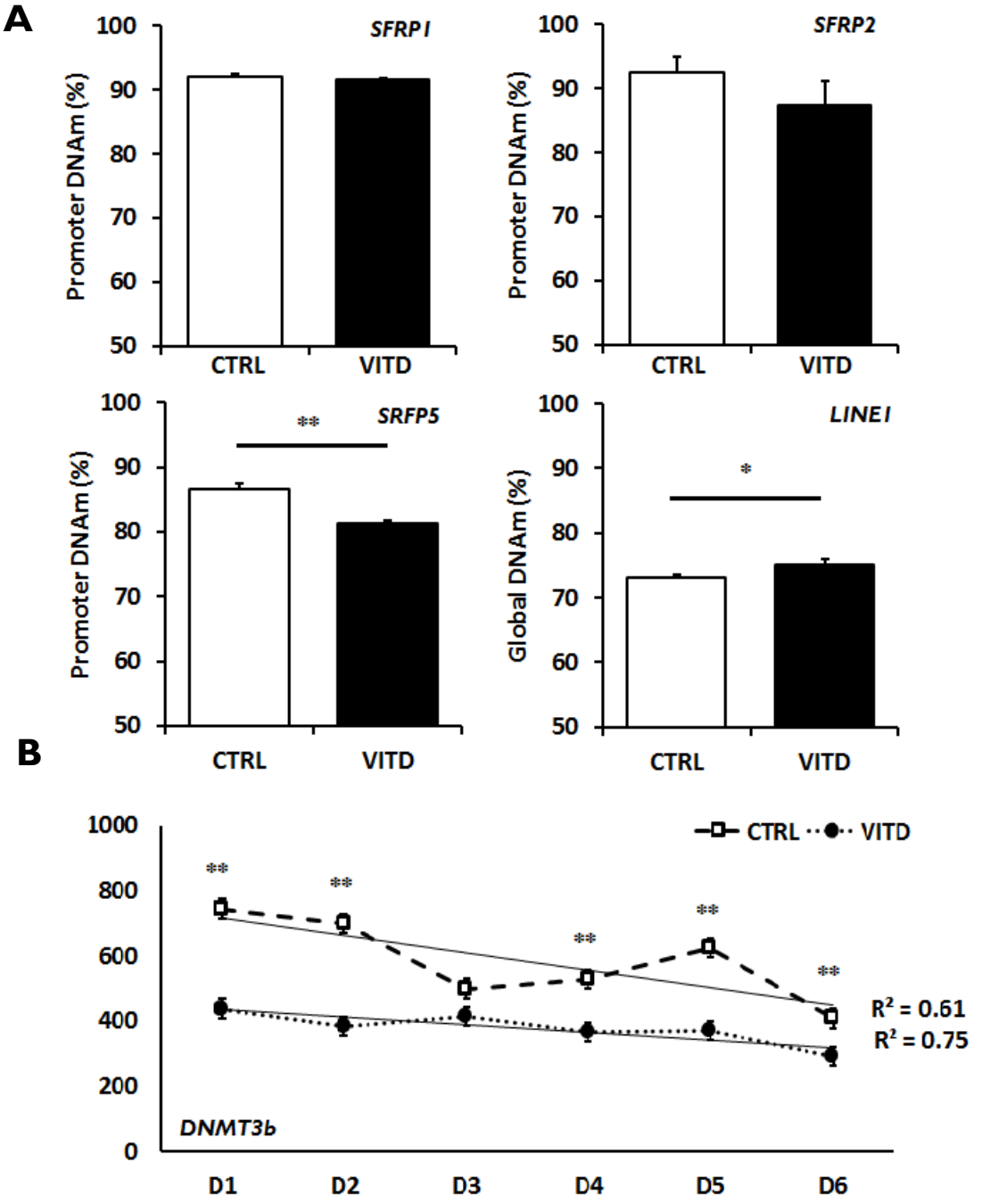

Figure 39 – Vitamin D effects differential methylation of SFRP5 and LINE1, synchronous to suppressed DNMT3b transcription. A) Bisulphite modified DNA was interrogated by CoBRA. Data represent the mean of 12 biological replicates, analysed in technical triplicate. SFRP1 and SFRP2 again exhibit a weak trend towards reduced promoter DNAm. SFRP5 promoter experiences significant suppression of DNAm, and vitamin D increases global 5mC as determined by LINE1 methylation, hypothesised to increase genomic stability B) DNMT3b transcription diminishes across the treatment period in both vehicle and D-treated cells, suggesting that transcription is increased in recently passaged cells prior to log growth phase. Regardless, vitamin D exerts suppressive effects on DNMT3b transcription relative to vehicle controls, postulated as a mechanism by which vitamin D modifies SFRP DNAm. Presumably, the mechanisms for decreasing gene-specific DNAm are independent of the mechanism by which vitamin D promotes LINE1 increased DNAm, as the effects oppose each other. *p<0.05, **p<0.01.

Effects of vitamin D on global DNA methylation patterns

Vitamin D modifies the cancer methylome, but does not affect methylation status of a panel of CRC-associated genes

To investigate *in vitro* ageing, and vitamin D's ability to modify the CRC methylome, CaCO2 and DLD1 cells were cultured under routine conditions for 10 weeks +/- 500pM vitamin D (at the top end of vitamin D's physiological reference range). Cells were passaged at 80% confluence and split 1:5 once per week. Media was replaced every 48 hours. Samples were collected for Q-rt-PCR at weeks 2, 4, 6, 8, and 10, prior to a wash-out period of four days, to mitigate for genomic effects of vitamin D. Samples were prepared in biological triplicate, and 500ng of washed-out bisulphite modified DNA interrogated on the Illumina 450K DNA methylation bead chip array. Data are reported as the mean +/- the standard error.

Exploratory analysis showed minimal variation between β-scores for treated and untreated samples. Predictably, given the provenance of the two cell lines, multi-dimensional scaling of the four sample groups suggests that CaCO2 and DLD 5mC patterns represent distinct methylomes with no overlap. However, both cells lines show weak clustering by treatment regimen with considerable overlap, suggesting modest effects of vitamin D on DNAm at the whole genome level. The effect is consistent in both lines (figure 40a). Scatter plots of the top 1000 differentially methylated single CG sites and top 1000 promoters, shows a trend toward *hypermethylation* as the dominant effect of sufficiency on both cell lines (figure 40b), recapitulated when results are filtered for statistically significant promoters experiencing differential DNAm of 5% or more; after wash out, CaCO2 cells exhibit 51 *hyper*-methylated promoters, but only 7 with reduced DNAm. Similarly DLD1 genome shows 41 promoters where DNAm increases, but only 10 that were ameliorated. Four *hypo*-methylated promoters from each line mapped to protein coding sequences, whose biological significance in CRC has not previously been reported elsewhere (figure 41 c and d).

Finally, these observations are supported by a 0.5% overall increase in the average methylation status of all 477,289 CGs interrogated across the genome ($p < 0.00001$), for both cell lines. No differences were noted for the average methylation status of either whole genes, gene promoters, or CG islands in non-coding sequences, which raises the possibility that the small increase in CG methylation translates to a larger increase in global (non-coding) methylation, masked by the null effect incorporated into the average figure from CGIs (figure 41 a and b). LINE1/surrogates for global methylation are not incorporated on the array for comparison.

To address the hypothesis that vitamin D ameliorates acquired gene-specific DNAm, data were extracted for a panel of genes frequently reported to be hypermethylated in CRC, representing those pertaining to age-related DNAm, and those associated with the CGI methylator phenotype[404]. No significant differences were noted for any of the genes selected after 10 weeks of vitamin D sufficiency, strongly suggesting that the null hypothesis should be accepted with regards these genes, and in contrast to the informing preliminary experiments (figure 42a). Control samples show severe *hypermethylation* of both WAs and CIMP-associated genes that are more frequently observed in the DLD1 cell line, in keeping with its mutational profile and poor degree of differentiation relative to the CaCO2 phenotype.

Regarding *in vitro* ageing (IVA); surprisingly, when samples are interrogated from t=0, several genes in this panel experience increases in promoter methylation in untreated controls over the ten passages, supportive of the concept of IVA. Certainly the methylome is not static, although it is not possible to elucidate if this is an effect of the cancer phenotype exerting persistent age-related aberrant DNAm, an effect of the ethanol vehicle, or if this is a consequence of passage stress/IVA. Notably, in DLD1 cells, CDKN2b experiences a 77% increase in promoter methylation over the ten passages (CDKN2a DNAm also increased in CaCO2 cells by 11.3%), and in general DLD1 cells experience greater increases in methylation (5/15, average increase of 23%) relative to CaCO2s (3/15, average increase of 3%). It was not possible to determine significance for these data as only one baseline sample was included on the array retrospectively for comparison. Having observed an epigenetic effect of IVA in both lines warrants further investigation in other lines, and may have important ramifications, particularly with regards replicative senescence in non-transformed cells. Perturbation of DNMT3b activity following passage, is posited as a potential mechanism for IVA.

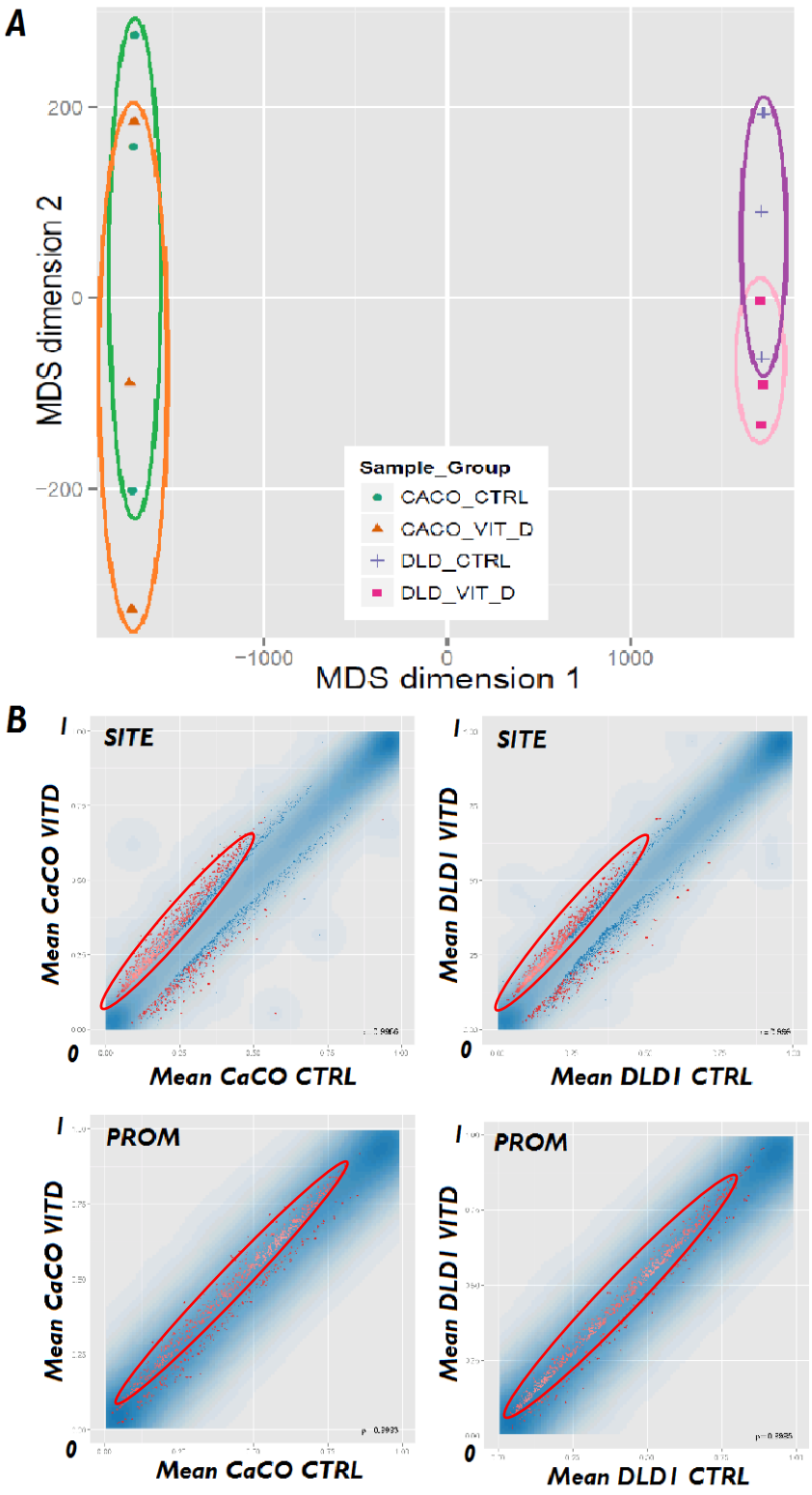

Figure 40 – Exploratory analysis of CRC methylomes in response to physiological vitamin D for 10 weeks after a wash out period of four days. Biological triplicates were probed in technical duplicate A) Multidimensional scaling – CaCO2 and DLD1 methylomes cluster separately (as anticipated). D-treated samples cluster separately to control samples, but demonstrate large overlap, suggestive of only weak effects mediated by vitamin D. B) The trend for both cell lines and single CG sites and promoter CGI was towards *hypermethylation*. Pink dots indicate the top 1000 ranking CGs and gene promoters, which cluster towards hypermethylation in all D-treated samples.

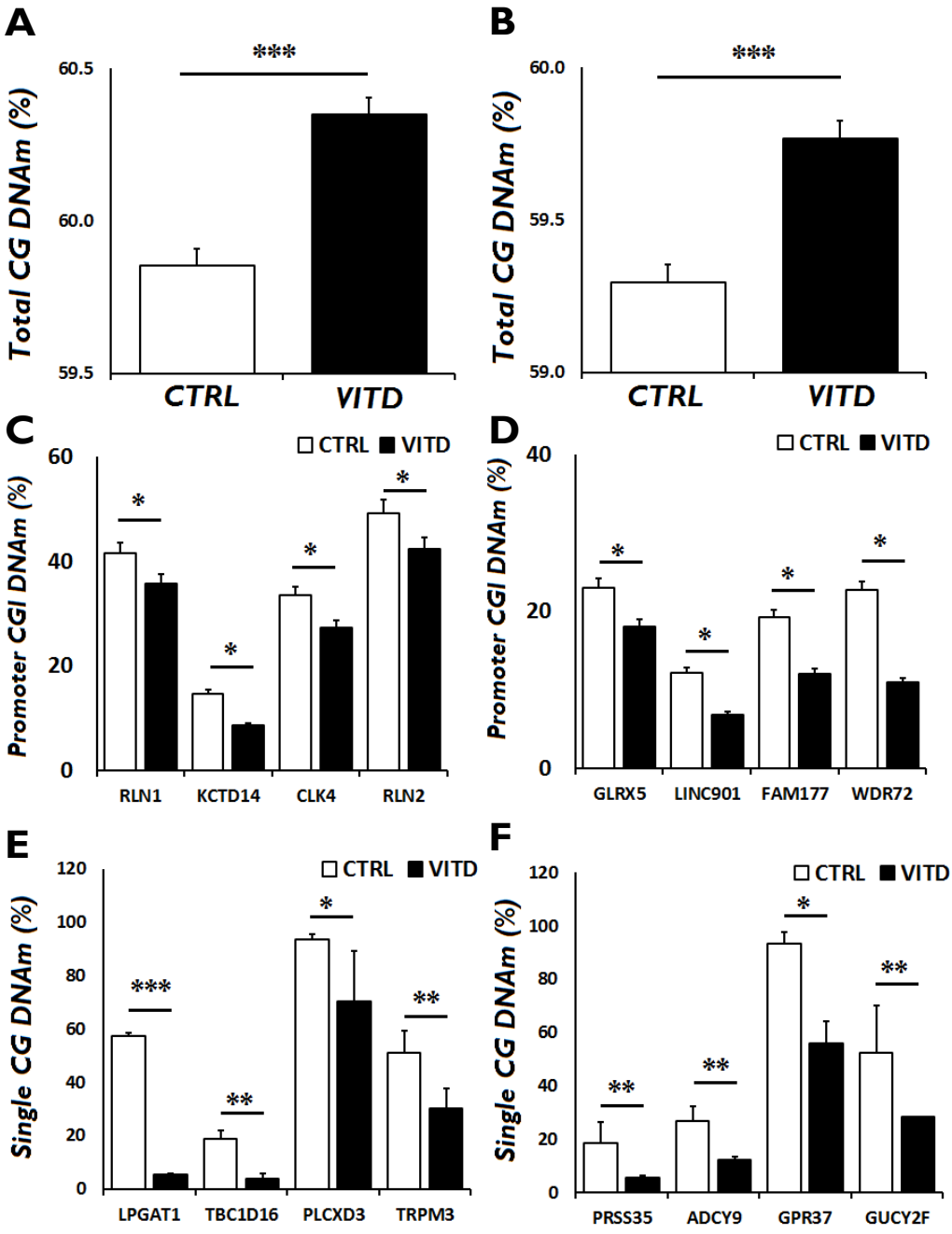

Figure 41 – Gene-specific effects of vitamin D sufficiency in DNAm after a 4 day wash out period a) VITAMIN D increases total 5mC by ~0.5% in CaCO2 cells, recapitulated in DLD1 cells (B). Although small, the change was highly significant (P<0.000001), and may actually represent a greater increase in global DNAm as this figure includes promoter island CGs in coding sequences, which, when determined separately show no over-all change in DNAm status. C) Four hypo-methylated gene promoters were identified in CaCO2 cells that mapped to functional proteins. D) Four hypo-methylated gene promoters were also identified in DLD1 cells that mapped to functional proteins. All of these genes meet the criteria for being partially methylated, and so may represent ongoing aberrant DNAm events. E) The four highest ranking single CG sites experiencing differential methylation in CaCO2 cells are represented F) The four highest ranking single CG sites experiencing differential methylation in DLD1 cells are represented. Biological significance of these is not well established for CRC, suggesting that these are anomalous or incidental findings which should be anticipated in any genomic array approach. n=3, *p<0.05, **p<0.01. Data represent mean +/-SEM.

Ignoring the criterion for a decrease of 5% or more (to allow more significant hits from database interrogation), and extracting promoters that were significantly differentially methylated (regardless of direction), 279 promoters are identified in CaCO2 cells, and 437 in DLD1 cells ($p<0.05$), of which 12 were common to both (figure 42b). Of these, only three mapped to RNA coding sequences and experienced a change in methylation in the same direction; vasoactive intestinal peptide (VIP), (↓1.0% in CaCO2, $p=0.03$, ↓3.2% in DLD, $p=0.02$); Schlafen-like1 (SLFNL1) (↑2.1% in CaCO2, $p=0.04$, ↑3.4% in DLD1, $p=0.02$); and MicroRNA 2355 (↑6.0% in CaCO2, $p=0.004$, ↑0.6% in DLD1, $p=0.007$). These small changes are assumed to be biologically negligible, but consistency between lines hints at a universal mechanism effected by vitamin D in CRC for these genes.

Over representation and gene ontology analysis was performed for the lists of differential methylated promoters, which reveals top hits in both cell lines specifically for olfactory (chemokine) sensing, and GPCR signal transduction, suggesting that vitamin D might affect these functions via methylome modification in CRC cells in general (figure 43a). Differentially methylated regions were not over represented on any particular chromosome when adjusted for size, suggesting that vitamin D effects are not chromosome-specific in this context. After excluding promoters not assigned to functional sequences, CaCO2 cells exhibit 86 significantly differentially methylated promoters, and DLD1, 142 – appended in 11. Several genes of biological relevance to colorectal cancer, DNAm, and/or vitamin D physiology were contained in these lists, detailed in figure 42b.

A

CACO

	CTRL t=0	CTRL (t=10)	VIT D (t=10)	ΔDNAm (IVA)	ΔDNAm (VIT D)
WIF1	92.5	96.7	96.5	4.2	-0.2
DKK1	5.1	3.9	4.5	-1.2	0.6
SFRP1	91.0	91.7	92.7	0.6	1.1
SFRP2	90.2	92.3	93.2	2.1	0.9
SFRP5	49.7	59.6	59.7	**9.9**	0.1
APC	24.1	31.2	31.4	**7.1**	0.2
MYOD	76.0	79.2	79.2	3.2	0.0
HPP1	73.0	70.5	70.9	-2.5	0.4
SOX17	92.5	96.8	96.9	4.4	0.1
MLH1	4.1	4.8	5.4	0.7	0.6
CDKN2	15.1	26.4	26.1	**11.3**	-0.3
MGMT	38.9	40.0	40.3	1.1	0.3
CDH1	16.0	13.1	13.0	-2.9	-0.1
RUNX3	88.3	88.1	89.6	-0.2	1.5
WNT5A	69.6	74.0	76.0	4.3	2.0

DLD1

	CTRL t=0	CTRL (t=10)	VIT D (t=10)	ΔDNAm (IVA)	ΔDNAm (VIT D)
WIF1	84.1	96.3	96.5	**12.2**	0.2
DKK1	86.2	90.4	91.0	4.2	0.6
SFRP1	81.1	85.1	85.7	4.0	0.6
SFRP2	91.5	93.8	94.2	2.3	0.5
SFRP5	90.6	92.1	92.3	1.4	0.3
APC	16.6	27.3	27.3	**10.7**	-0.1
MYOD	88.9	91.0	91.7	2.1	0.7
HPP1	89.1	84.5	85.5	-4.6	1.0
SOX17	92.5	96.0	96.2	3.5	0.2
MLH1	10.6	12.6	12.6	2.0	0.0
CDKN2	14.7	91.9	92.4	**77.2**	0.5
MGMT	54.1	60.4	60.6	**6.3**	0.2
CDH1	12.8	14.0	13.8	1.2	-0.2
RUNX3	89.8	91.9	92.4	2.1	0.5
WNT5A	32.6	41.7	44.6	**9.1**	2.9

B

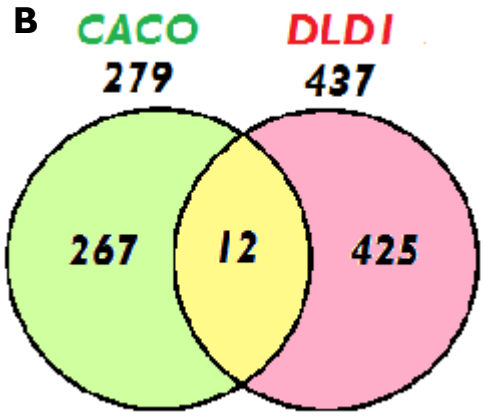

CACO	CTRL	VIT D	ΔDNAm	p.val
IL21	45.6	53.5	**7.9**	0.03
TLR2	82.1	86.2	4.2	0.03
TUSC7	83.7	87.8	4.1	0.05

DLD1	CTRL	VIT D	ΔDNAm	p.val
RHOA	11.2	14.5	3.4	0.04
CASP4	20.4	15.9	-4.5	0.01
CGA	70.1	76.1	**6.0**	0.01
LRP4	55.2	57.3	2.1	0.04

Figure 42 – Promoter methylation status (%) of epigenetically relevant genes in D-aged CRC cell lines. A) There was no significant reduction in either age-related hypermethylated genes or CIMP+ related hypermethylated genes, strongly suggesting that under experimental conditions, the null hypothesis should be accepted – Data do no support vitamin D sufficiency ameliorating gene-specific hypermethylation of epigenetically silenced genes in CRC as contributing to the association of sufficiency with prognosis. It is of note that most genes underwent increases in promoter methylation as a consequence of in vitro ageing alone, although this is only observational, as base line t0 samples were not analysed in replicate. Interestingly, CDKN2a appears to experience relatively spontaneous hypermethylation, also documented in CIMP+ tumours, raising the possibility that a transitional epigenetic event in DLD1 cells representing phenotype progression was observed. To a lesser extent, this was also observed in CaCO2 cells (+11.3%). B) Significantly differentially methylated promoters not achieving the 5% threshold or decreasing in value, reveal 12 CGI that were consistent between lines, that mapped to three functional sequences (VIP, SLFNL1 and MIR2355), not suggestive that a universal mechanism underpins vitamin D's methylome modifying effects in this context. Unique to CaCO2 and DLD1 separately, several genes of biological importance to CRC initiation are noted.

Filtering the array for single CG sites that were significantly hypomethylated, as per the informing hypothesis, revealed 70 unique sites in CaCO2 cells, which mapped to 58 functional gene products (appended in 12). Pathway analysis of these components identifies RPS6Ka3 as a key hub in the network (figure 43b). Ribosomal protein S6 kinase acts to phosphorylate members of the MAP kinase/ERK cascade, which is frequently up-regulated in CRC, driving proliferation[405]. While the RPS6Ka3 promoter itself only experienced a modest 2.5% reduction in methylation, the association with multiple differentially methylated genes suggested that its transcription might none-the-less be impacted by small cumulative changes across the network. Given that all nodes in this network experience *hypomethylation*, increased RPS6ka3 transcription was anticipated, however the converse was observed (figure 44d).

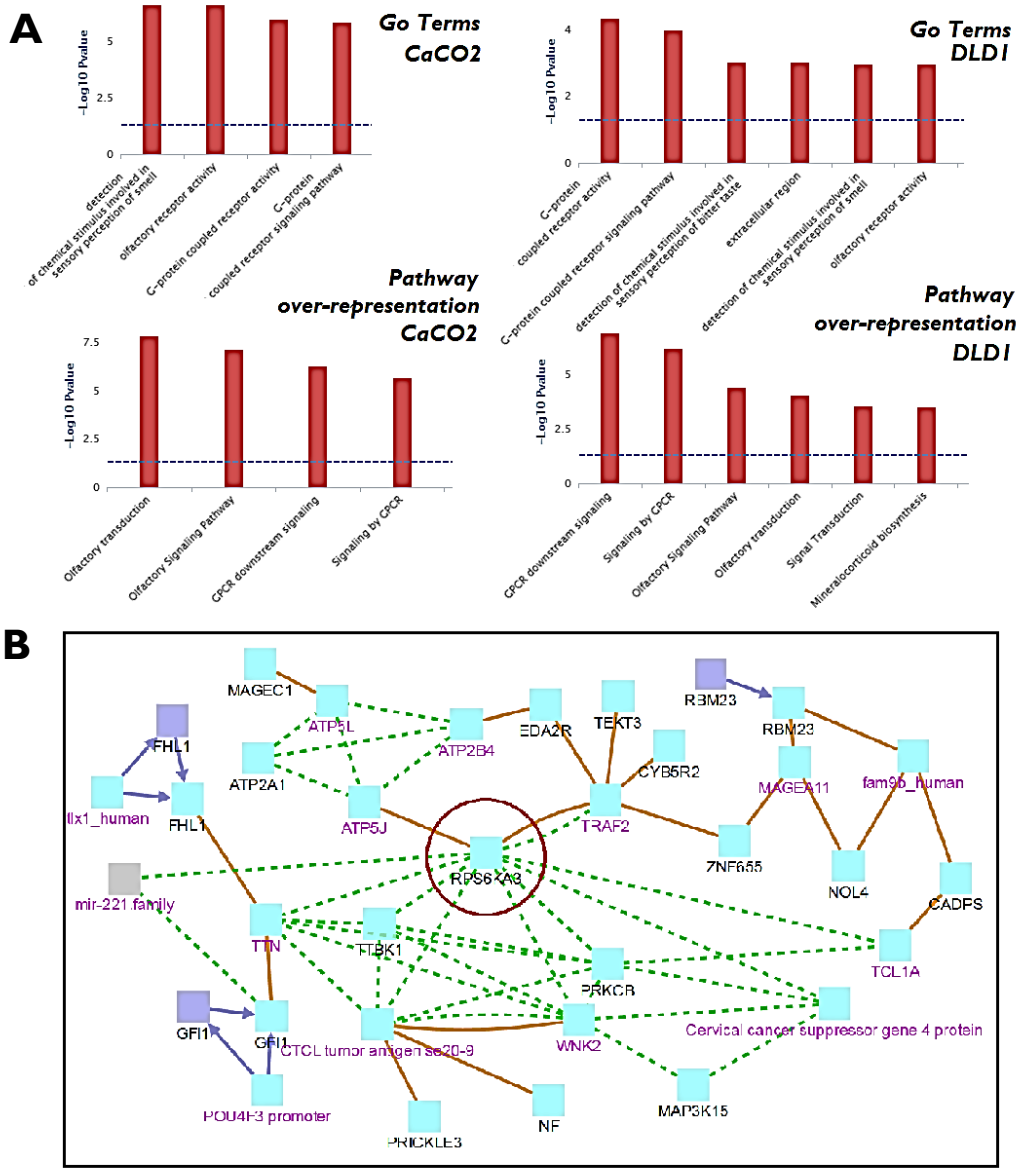

Figure 43 - Pathway analysis of vitamin D-aged CRC cell lines a) Gene ontology terms associated with 279 differentially methylated genes in CaCO2 cells show significant associations with olfactory receptor activity and G-protein coupled receptor activity. The GO association is recapitulated by the 437 differentially methylated genes identified in DLD1 cells. Over represented pathways support these association in both cell lines, suggesting that the vitamin D modified methylome of CRC cells affects olfactory receptor function and GPCR signal transduction. B) Single CGs differentially methylated in CaCO2 cells were present in 70 protein coding sequences. Pathway analysis of these 70 genes (black text) converge via intermediary proteins (pink text) on RPS6Ka3, recognised for it' role in ERK phosphorylation and thus MAPK signalling. Green dashes depict biochemical interactions, orange lines gene regulatory events, and purple lines indicate genetic interactions. Un-connected nodes not shown.

Vitamin D sufficiency effected tapering phenotypic changes in CaCO2 cells, but not DLD1.

To investigate any associated changes to the phenotype of the cells, proliferation was measured by WST1 assay at the end of the treatment regimen, prior to wash out (i.e. cells still under transcriptional regulation by vitamin D), and after a four day washout period, during which cells were rinsed with PBS and fresh media applied at 24 hour intervals (figure 44a). Proliferation was mildly inhibited in DLD1 cells before the washout regimen (8% reduction, not statistically significant), but this diminished after four days with repeated washes (data not shown). CaCO2 cells however, experienced a 35% reduction in proliferation at the end of the experiment, which was sustained at 29% inhibition after the washout period, suggesting that their modified methylome (also interrogated at this time point) could be suppressing proliferation here. Consistent with this observation, cultured cells exhibit reduced viability at day two during the washout period, and day four (again, not observed for the DLD1 line). Similarly, a tapering effect, with a regain of viability, is apparent at day four (figure 44b).

Supporting the observation of tapering inhibited proliferation, Ki67 transcription was suppressed following the washout period at t=48 but not at t=96 hours (figure 44c). Similarly, RSP6Ka3 transcription was inhibited, which persisted at t=96 hours, and suggests that MAP kinase signal transduction might be down regulated via reduced ERK phosphorylation, as a means to explain the reduced proliferation of CaCO2 cells (figure 44d). Whole cell extracts were prepared from washed out IVA cells and probed by Western blot for pERK1 and 2, normalised to total ERK1 and 2 (20ug from each sample run in technical triplicate). Consistent with the hypothesis that reduced RPS6ka3 activity prevents ERK phosphorylation, a significant reduction in the ratio of both pERK1 and pERK2 relative to total ERK1 and 2 is observed (figure 44e and f). Incidentally, transcription of ERK2 was also inhibited at t=48, but not at t=96. In preliminary experiments an insignificant trend towards increased BCAT phosphorylation was also noted in washed-out cells, hinting at inhibition of Wnt signalling associated with the D-induced methylome (data not shown).

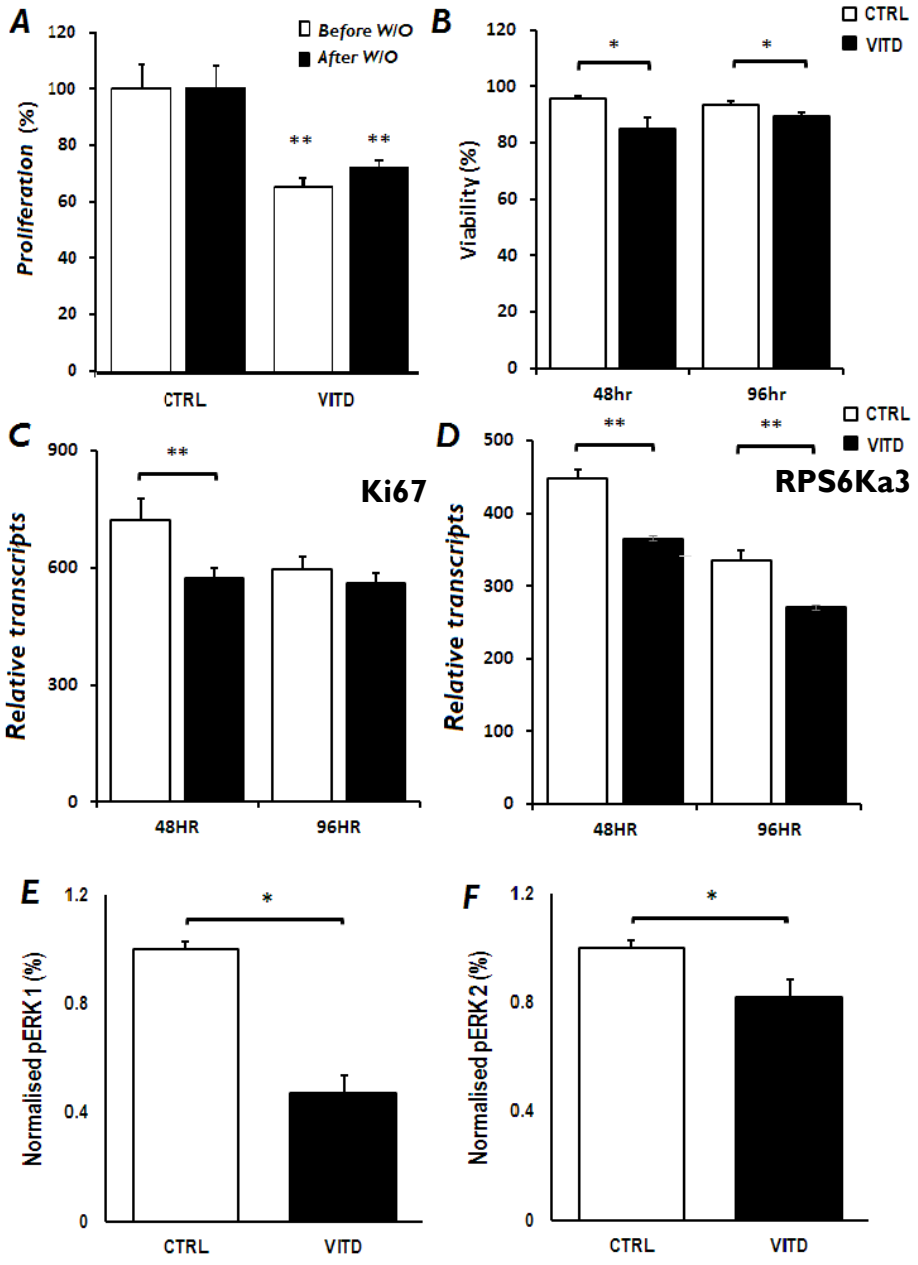

Figure 44 - *In vitro* ageing of CaCO2 cells shows a tapering phenotype is established by vitamin D sufficiency. n=3, *p<0.05, **p<0.01. Data represent mean +/-SEM. A) Cells under transcriptional regulation of vitamin D exhibit suppressed proliferation that is maintained, but trending toward reconstitution 96 hours after the withdrawal of treatment. B) This observation is supported by weakly decreased viability at 48 hours post-vitamin D, that persists, but is diminished, at 96 hours post treatment. C) Consistent with the above, Ki67 transcription is suppressed in D-aged cells, which is ameliorated after the full 96 hour washout period. Taken together, these data suggest that the antiproliferative effects of vitamin D sufficiency are genomic in action. D) In contrast, RSP6Ka3 – identified as a key node in the D-modified methylome, is consistently suppressed at 96 hours. The differences between relative Ki67 and RSP6kKa3 transcripts in un-primed cells may be an effect of cellular plasticity as cells re-establish 'routine' function following passage at t=0 i.e. t=48 represents lag growth phase, vs t=96 in log growth phase. E and F) Western blot of whole cell extracts (n=2, in triplicate with SEM) shows reduced phosphorylation of ERK1 and 2 normalised to total ERK, at 96 hours post-treatment in vitamin D aged-cells, consistent with sustained inhibition of MAPK signalling as a consequence of the modified methylome (RPS6Ka3 inhibition).

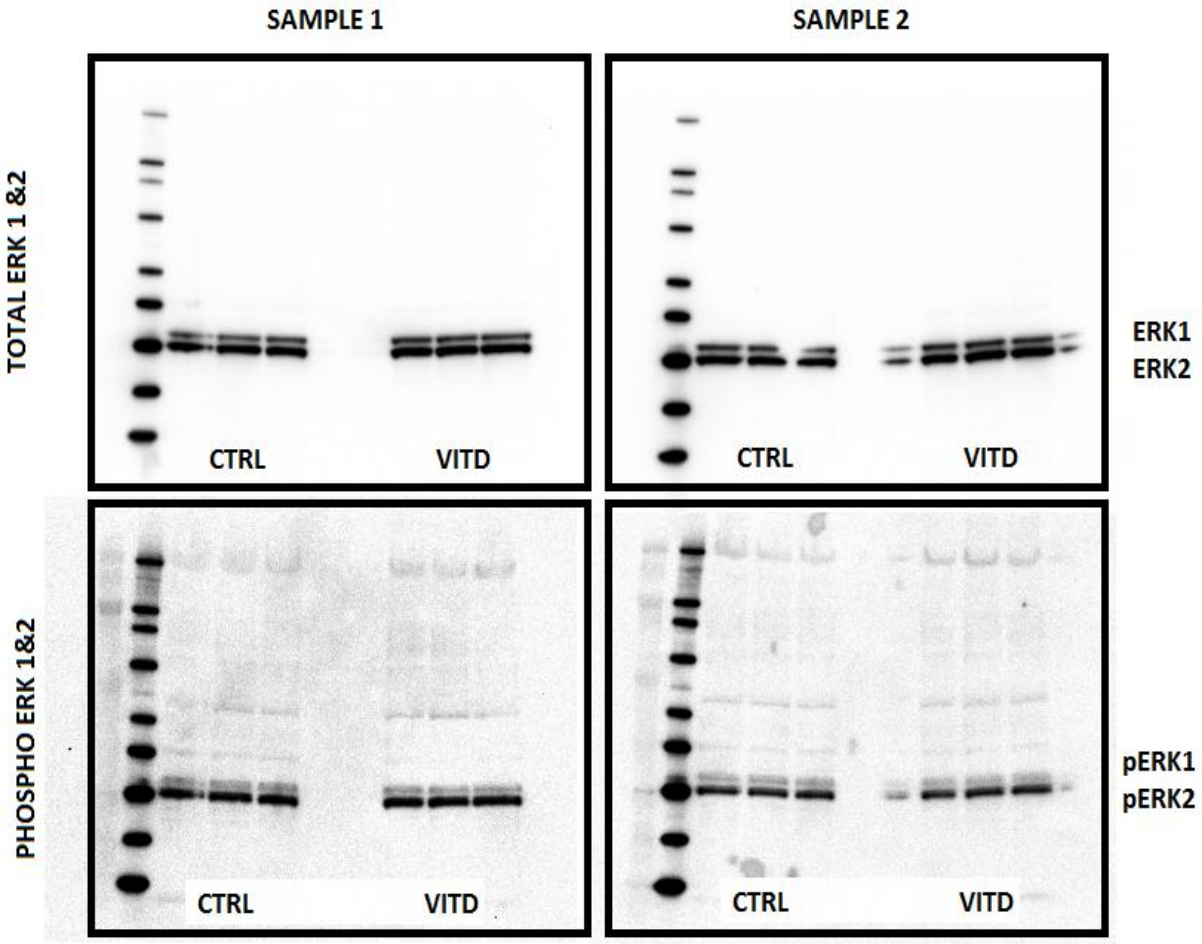

Figure 45 – <u>Phosphorylation of ERK1 and ERK2 in CaCO2 in response to vitamin D culture.</u> Band analysis revealed significantly reduced phosphorylation of both ERK1 and ERK2 in treated cells *as a ratio of the total ERK present* in whole cell extracts as detailed in 44E and F. n=2 (samples 1 and 2), technical triplicates. Validation of this result is strongly suggested to consolidate data with gene expression results to confirm a causal effect.

Finally, 5mC enzyme transcription was interrogated in CaCO2 cells at passages 2, 4, 6, 8, and 10 to investigate potential mechanisms; DNMTs 1 and 3b are initially suppressed in D-treated cells (similar to the effect in DLD1s over a short incubation), which rebounds half way through the experiment, both being significantly induced following passage 8 and 10 (figure 45). TET1 transcription was not altered, implying that any demethylation witnessed is passive in nature, or consequent to attenuation of further *de novo* DNAm. Vitamin D also promoted ECAD transcription in a similar fashion to the DNMTs, suppressed to begin with, but increasing over time, hypothesised to promote differentiation.

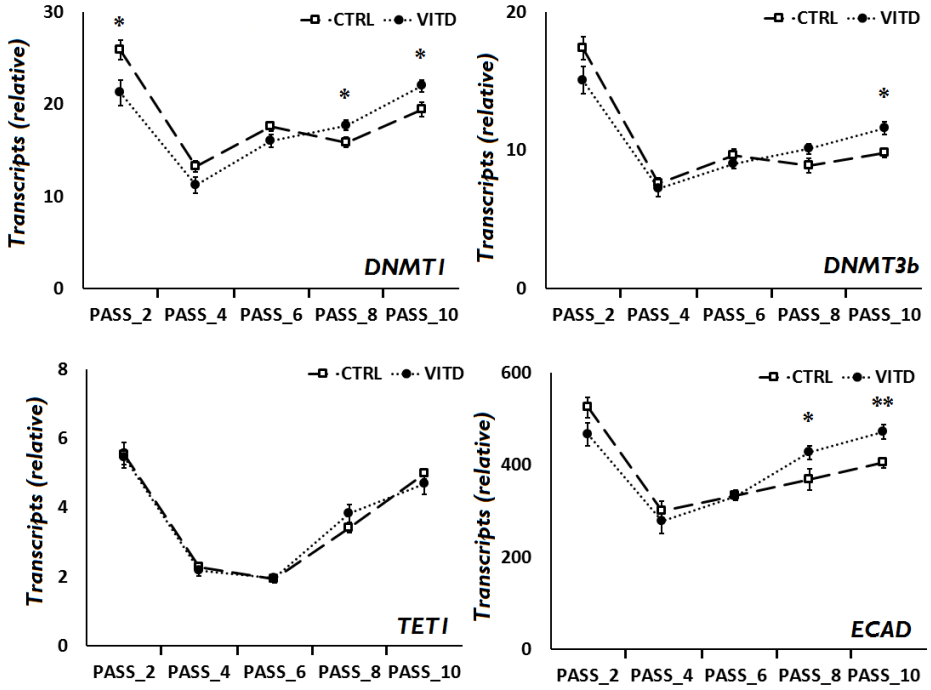

Figure 46 – <u>Methyltransferase transcription is modulated by vitamin D sufficiency</u> a) DNMT1 transcription after 2 weeks in culture is decreased in D-cultured CaCO2 cells. This is recovered over subsequent passages, and is significantly increased prior to wash out, hypothesised to improve maintenance fidelity during DNA replication b) a similar pattern is noted in DNMT3b transcripts, where the significant increase in expression at passage ten may contribute to the effect inferred from a small but highly significant increase in *de novo* global DNAm (0.5%). Weak promotion of DNMT3b activity may thus serve to reconstitute global genome stability. C) TET1 transcription remains static relative to EtOH vehicle, precluding a role for its dynamic transcription in weak demethylation of gene promoters documented. D) E-cadherin transcription is promoted by vitamin D towards the later stages of the 10 week experiment, proposed to promote differentiation by improving cell adhesion, and sequestering cytosolic BCAT, down-regulating TCF targets. The ECAD promoter was not observed to be hyper-methylated (13%) in untreated cells, suggesting that this transcriptional response to vitamin D sufficiency is via classical VDR /VDRE interaction. NB Patterns of transcription for all genes interrogated (and others not shown) appear to dip and recover between passages 4 through 8; this is suggestive of an artefact due to sampling discrepancies, perhaps lag vs log phase growth, or sampling technique/efficiency, and may not properly reflect the chronological relationship between the cells. This is inconsequential for comparisons between treatments at specific time points, which should be considered relevant.

Discussion

Although limited in their scope as a model for investigating the prevention of disease, validated CRC cells lines may be employed to identify chemo-therapeutics and mechanisms that mitigate for disease processes. Four CRC cell lines displaying mutational diversity were selected to investigate vitamin D's anticancer properties with regards established pathological DNAm. All four lines characterised during preliminary experiments are reported to demonstrate constitutional activation of Wnt signalling, uncontrolled proliferation, replicative immortality, and active paracrine secretion of Wnt ligands making them ideal candidates to investigate epigenetic regulation of Wnt by vitamin D in a neoplastic context (figure x). Importantly, Oksana et al recently reported that despite truncation of APC in CaCO2 and DLD1 cells, DC architecture and BCAT phosphorylation functionality is maintained, albeit somewhat impaired[406].

It is well established that vitamin D exerts antiproliferative effects in CRC cell lines in vitro[407]. Multiple pathways have been characterised as regulated by vitamin D in transformed cells[408]. In particular vitamin D is a potent modulator of Wnt signalling, even in cells with mutational incompetence of the BCAT destruction complex, suggesting that vitamin D also inhibits Wnt via non-canonical mechanisms. Indeed, vitamin D is reported to enhance ECAD transcription, which sequesters cytosolic BCAT at the plasma membrane, thus promoting differentiation and inhibiting TCF targets simultaneously. The VDR-RXR transcription complex also binds cytosolic BCAT, and classically, vitamin D is reported to induce DKK1 – frequently found to be hypermethylated in transformation prone epithelia and associated with vitamin D status[91,129,214,409]. Ultimately this results in a net decrease of c-MYC transcripts and blockade of transition to S-phase[410]. Our preliminary experiments confirmed inhibition of MYC by vitamin D in low-passage number CaCO2 cells, but the effect appeared diminished in older cells, which led us to investigate the effects of *in vitro* ageing in these cells. The DLD1 line was also selected in light of vitamin Ds antiproliferative effects at lower concentrations to HCT and HT29 cells, and furthermore SFRP promoters trended towards demethylation in preliminary experiments.

Serum vitamin D at presentation is established as a prognostic biomarker for CRC mortality[399,411]. Taken together with reports that sufficiency attenuates aberrant age-related DNA hypermethylation of WAs[212], and experimental data presented here suggesting amelioration of inflammation-induced *hypermethylation* and DNMT modulation in epithelial models, it was hypothesised that sufficiency might in part exert Wnt regulatory activities by effecting gradual reparation of the transformed CRC methylome, reconstituting WA transcriptional competence and/or genomic stability via improved global DNAm.

	CaCO2	**DLD1**	**HCT116**	**HT29**
APC	x	x	Wt	xx
β-CAT	Wt	Wt	x	x
B-RAF	Wt	Wt	Wt	x
K-RAS	Wt	x	x	Wt
TGβr2	Wt	x	x	Wt
p53	x	x	Wt	x

Figure 47 – Mutational profiles of colorectal cancer cell lines employed. X = heterozygous mutation, XX homozygous mutations, Wt = wild type. CaCO2 cells exhibit fewer late-stage mutations (with the exception of carcinogenic p53), suggesting that alternative pathways may be utilised to regulate proliferation. This is consistent with the slower-growing and better differentiated phenotype of these cells relative to DLD1 cells. Both lines are heterozygous for APC and are reported to have impaired but functional DC competence.

In respect of our informing hypothesis, for the cell lines interrogated the null hypothesis should probably be accepted; we saw no significant changes in promoter methylation status of CRC-associated genes relevant to this thesis, so it is unlikely their reconstitution contributed to the observed phenotypic effects suppressing proliferation. The implication is that, once established, these deleterious methyl marks become entrenched and may not be conditionally targeted by vitamin D via active or passive demethylation, despite vitamin D modulation of DNMTs.

Aguilera et al report DKK1 hypermethylation in 17% of CRC in their cohort analysis[129], and note that its induction by vitamin D is not via classical VDRE binding[409]. Rawson et al demonstrate an association with vitamin D status with DKK1 methylation in transformation-prone colonic epithelia; DKK1 was *hypo*-methylated in CaCO2 cells and *hyper*-methylated in DLD1, which was not corrected by vitamin D sufficiency, in support of the null hypothesis. Similarly ECAD is reported to be aberrantly methylated in breast cancer and expression is restored by vitamin D treatment[94]. Here, ECAD was hypomethylated in the basal state in both lines, which means comparisons cannot be made in this context. The ECAD promoter is also reported by others to be hyper-methylated in CRC, which suppresses its expression in ~50% of colitis-associated cancers[412], so validation of a primary line exhibiting ECAD *hypermethylation* to resolve its relationship with vitamin D is feasible and warranted - after all we observed induction of ECAD in D-aged cells, however ECAD is an established vitamin D target[413], raising the possibility that vitamin D induces ECAD transcription via dual genetic/epigenetic mechanisms.

This is not to say that vitamin D cannot favourably modify the cancer methylome; indeed we observed modest changes in a variety of genes that might impact on tumour progression given sufficient time. In preliminary experiments at a higher dose we also note reduced SFRP5 methylation, but this reduction was not sufficient to re-establish transcription as determined by Q-rt-PCR after 40 cycles (data not shown), nor determined after an appropriate wash-out. In this respect results are encouraging, given the relatively short intervention and use of a physiologically-relevant concentration; small epigenome-wide effects due to sufficiency might cumulatively contribute to cancer inhibition over longer periods if sustained. For example, interleukin 21 was noted to experience a 7.9% increase in promoter methylation ($p = 0.03$); IL21 is observed to be over-expressed in colitis-associated cancer, amplifying the inflammatory milieu in lesions[414] - should the change in methylation inhibit IL21 expression, an anticancer effect might be anticipated in time. This seems plausible in respect of reports that IL21 transcription inversely correlates with its expression in B-cell lymphoma[415], suggesting transcriptional regulation by promoter DNAm.

In both cell lines, gene ontology and pathway analysis identified GPCR signal transduction and olfactory receptor (OR) expression (themselves class A Rhodopsin-like GPCRs), as being over-represented in the lists of epigenetically modified genes. This raises the possibility that vitamin D sufficiency may exert anticancer effects via promotion of appropriate environmental sensing by CRC cells, particularly increasing sensitivity to growth-inhibiting hormones or anti-inflammatory cytokines, classical GPCR ligands. Very recently, ectopic olfactory receptor expression has been documented in colonic epithelial cells, and nutrient sensing by ORs is an emerging field[416], however, given that there are over 1000 functional OR genes[403], whose expression appears sporadic and is not determined to be tissue-specific[417], a functional interpretation here may be tenuous.

Our phenotypic data show that the vitamin D-associated methylome in CaCO2 cells was synchronous to antiproliferative effects, concomitant to a predicted inhibition of RPS6ka3 transcription and ERK phosphorylation, but the effect appeared to taper across the washout period. This could simply mean that observations are consequent to residual classical genomic effects (i.e. induction of ECAD/BCAT sequestration). Equally, sufficiency may need to be maintained to exert persistent modification of the methylome. Conversely, in the absence of vitamin D, pathological processes that effect aberrant DNAm in CRC may re-assert themselves to reconstitute methylation in those genes ameliorated by vitamin D – after all, we saw lower DNMT 1 and 3b transcription in D-deficient CaCO2 cells, and equally, an increase in methylation for genes of interest in control cells over the course of the experiment, supporting ongoing aberrant DNAm events (IVA). To establish if the phenotype effect was indeed caused by vitamin D's methylome modifying action and not by its regular transcriptional function, conditional knock-down of DNMTs in CRC lines might resolve this dichotomy, and further studies investigating the broader stability of the modified methylome are also indicated (we only probed the methylome once after 96 hours).

Regardless of stability, physiological vitamin D was able to effect demethylation of several genes that was sustained for at least 96hours post-treatment. In CaCO2 relaxins RLN1 and RLN2 were both significantly hypo-methylated. These proteins are over-expressed in a variety of neoplastic conditions[418]. Transcription of RLN1 was inhibited in CaCO2 cells after 48hours, and trended towards decreased expression at 96 hours, consistent with the tapering effect (data not shown). Its suppression here may contribute to the antiproliferative effect seen, and conditional interference should be investigated to reveal any contribution of relaxin expression to the CaCO2 phenotype.

Global DNA methylation in the colonic epithelia is associated with vitamin D status[212], and we saw a modest increase of LINE1 methylation in DLD1 cells at high dose over six days. In both CaCO2 cells and DLD1 cells, we also see a highly significant increase in total 5mC, so it is lamentable that no measure of non-CGI global methylation is included on the Illumina array, which means a genome-stabilising effect cannot fully be stated. Investigation of LINE1 methylation in response to vitamin D sufficiency in both cell lines is a key recommendation for further work.

Finally, an important observation regarding *in vitro* epigenetic ageing of cells must be addressed; both cell lines demonstrate advancing DNAm in the promoters of WAs and CIMP-associated genes, specifically CDKN2a, APC and WNT5a. DNA *de novo* hypermethylation of CDKN2b and RUNX3 is reported to effect replicative senescence *in vitro* in mesenchymal stem cells[419], and tumour suppressor silencing via DNAm is reported more frequently in cancer cell lines compared to *in vivo* counterparts[420], implying that these events are consequent to *in vitro* culture. This could be due to their redundancy in the *ex vivo* environment (use-it-or-lose it-hypothesis), or due to the fact that cells suited to lab culture are more likely to exhibit *hyper*-methylating tendencies. Enticingly, CDKN2a methylation is associated with Dukes CRC stage[421], supporting the idea that methylation of this gene advances relatively quickly *in vivo*. A new hypothesis is proffered, that passage number is associated with increasing hypermethylation,

which could be succinctly investigated in CRC cell lines and organoid models of healthy epithelia.

Incidentally, it was noted during the array analysis that the vitamin D receptor was *hyper*-methylated in both cell lines independent of treatment (92.1% in CaCO2 and 86.9% in DLD1). The two human epithelial cases included on the array demonstrate VDR promoter methylation at 53.9 +/- 0.04%, suggesting VDR might be aberrantly methylated in cancer-prone tissues. Insensitivity to vitamin D via VDR hypermethylation is noted in breast cancer, melanoma, hyperthyroidism and HIV infection[422-425], and oestrogen inhibits induced colorectal carcinogenesis via decreased VDR methylation and increased VDR transcription in a mouse model[426]. Miyamoto et al report three CGI proximal to the VDR transcription start site that also contain SP1 regulatory elements, posited to regulate DNMT activity at the site[427]. Conversely we note that *hypermethylation* of VDR in CaCO2 and DLD1 does not inhibit VDR transcription, which we observed by Q-rt-PCR in both lines on multiple occasions (average cycle threshold under 25), in clear contrast to the defunct paradigm that promoter hypermethylation silences genes. Our cells were responsive to vitamin D in terms of phenotype (proliferation), DNA methylome, and gene regulation. Thus, the mechanism by which vitamin D/VDR mediates its effects in CRC warrants further elucidation.

A linear increase in VDR transcripts in vitamin D deficient CaCO2 cells over the 10 passages (RSQ = 0.66), not associated with any meaningful change in DNAm, was also determined (data not shown), suggesting that cells increase VDR expression to enhance their vitamin D sensitivity in times of deficiency. This observation also warrants investigation in non-transformed models, as it suggests that low serum vitamin D might not impair cytosolic active vitamin D, if deficiency improves sensitivity. This might explain why correcting for low serum D fails to modify CRC disease risk, despite the overwhelming epidemiological association of serum sufficiency with disease risk. Thus low serum D may not equate to impaired vitamin D genomic functions (we also noted exponential suppression of Cyp24a1 in D-deficient cells over time (RSQ = 0.940), which would further increase D-sensitivity, and supports the idea that low serum D need not necessarily be aetiological in CRC initiation).

Summary

Physiological vitamin D effected modest remodelling of both the CaCO2 and DLD1 methylomes that was associated with a variety of postulated anticancer effects. In CaCO2 cells, proliferation and cell viability were inhibited, with an associated tapering effect on MAP kinase signalling. Supra-physiological vitamin D was able to ameliorate SFRP5 hypermethylation, but not sufficiently enough to reconstitute its expression in DLD1 cells. Vitamin D was able to modulate DNMT transcription in CaCO2 cells over time, and so DNMT activity assays should be deployed to investigate this further. Both cell lines underwent progressive *in vitro* aberrant DNA methylation in the un-primed state, raising questions about the effects of routine laboratory culture on primary cell methylomes, also noted in organoid models, warranting further investigation.

Taken together, results presented here support a mechanistic role for vitamin D sufficiency improving CRC prognosis via its modulation of 5mC patterns and DNMT activity.

Chapter 7

GENERAL DISCUSSION

Discussion

Vitamin D status is rigorously established to have an inverse association with colorectal cancer risk[428-430]. The NHNAES-III study in 2007 assessed a total cohort of 16,000 participants, and concluded that CRC mortality is reduced by up to 72% (95% CI 32-89%), when serum vitamin D exceeds 80 nmol/L relative to sub-50 nmol/L popualtions[431].

The relationship came to the attention of the scientific community through epidemiological studies in the late 70s and early 80s that suggested, once other factors were corrected for, that CRC risk increased with distance of the population from the equator, and by mean daily UVB exposure. While Garland and Garland's seminal paper of 1980 was the first to posit the association with sunlight hours and thus vitamin D status[432], the pair were undoubtedly influenced by earlier prophetic studies; these noted associations with over-all cancer risk by sunlight hours as early as 1941[433], that hypovitaminosis vitamin D-induced rickets occurred more frequently in urbanised areas versus arable communities in the tropics[434], and others postulated vitamin D deficiency as an aetiological factor in the racial disparity of CRC rates[435].

There are no studies that report either no association of CRC risk with serum vitamin D, or a positive correlation. Two opposing hypotheses are apparent, which remain unresolved even today; the first suggests that low vitamin D predisposes the colonic epithelia to transformation, either directly via vitamin D signalling in epithelial cells, or indirectly via other cell types and autocrine signalling factors that deregulate epithelial homeostasis. The alternative is that those mechanisms that bring about tumourigenesis (inflammation), simultaneously impair vitamin D metabolism. It is recognised that established disease, and to an extent age, compound chronic deficiency via impaired synthesis at key metabolic sites, and/or absorption in the gut[436], however these are independent of deficiency as a risk factor, which is observed to precede pathogenesis[430]. A great number of studies have endeavoured to resolve the dichotomy, investigating molecular mechanisms by which vitamin D might exert an anti-cancer effect.

The compounds direct genomic actions are well established to effect anti-proliferative, pro-apoptotic, and pro-differentiative effects *in vitro* and *ex vivo*[437], which are confirmed *in vivo* in the mouse[438]. Equally vitamin D is reported to enhance DNA mismatch repair mechanism in colonic crypts via induction of MLH1 and MSH2[439]. Similarly, vitamin D acts to reduce both systemic and local inflammation via prescribed pathways encapsulating TLRs, NFκB and cytokine production, as well as promoting immune function via proper leukocyte differentiation[440], all of which are shown to be associated with aberrant age-related DNAm too[441]. Vitamin D's genomic actions, via its cognate receptor VDR and hexameric response element, are discussed in detail previously, so it is not necessary to restate them here in their entirety. Suffice to say that vitamin D represses Wnt signalling in epithelia, and NFκB across the immune system, at multiple levels[91,356,442]. It seems reasonable that these whole-organism, multifactorial, pleiotropic modes of action, are likely to act cumulatively to contribute to epithelial and immune homeostasis, resulting in the consensus association of serum D with bowel health. Data presented here regarding vitamin D's effects on the methylome in a variety of cell types and models, are proposed *in addition* to the established genomic actions, to promote bowel health during aging.

However, these data have not (yet) been confirmed clinically. In 2015, Autier et al conducted a meta-analysis of vitamin D trials to date, and concluded that modulation of serum D via supplementation does not impact on CRC disease risk, and that further attempts to elicit causality would prove futile[66]. In respect of the background discussed, taken together with other data, this assertion should be considered with caution – Tapp et al report an inverse association with serum D and age-related DNAm in their cross-sectional study, and DNAm patterns are observed to vary longitudinally over the life time of organisms (from early childhood onwards)[258,443,444]; in light of these findings, it could be argued that the epigenetic component of vitamin D's action is modest at physiological concentrations in healthy epithelia, and thus status should be maintained over the lifetime of the organism to reap beneficial effects in older age; the longest intervention surmised by Autier was 8 years.

It is also premature to assume a null effect of supplementation as evidence for reverse causality; for example, deficiency at *any* point prior to intervention might impart irreversible homeostatic/metabolic deficits, regardless of future vitamin D status - a caveat overlooked by the authors. However, a more recent study by Skaaby et al report associations between vitamin D status and BMI, alcohol intake, physical activity, and diet, suggesting that lifestyle factors known to be associated with disease risk, also determine vitamin D status[445]. This is in support of Autier's reverse causality hypothesis. Thus, caution should be exercised in this respect until better trials, which do not conflate deficiency and insufficiency (where the effects are undoubtedly more pronounced and subtle respectively), are completed.

Tapp et al report that vitamin D status is associated with hypomethylation of WAs in the distal colon, and increased LINE1 methylation. In this context, it was set out to investigate if vitamin D exerted a protective effect against age-related DNA hypermethylation in the epithelia. Although the vast majority of mechanistic studies looking at vitamin D's anti-cancer effects in the bowel utilise transformed cell lines, there are also multiple reports that these are recapitulated in healthy epithelial models[99,403]. Aberrant DNAm across the epithelial sheet (field effects) are propagated by crypt fission[446,447], and the crypts themselves are populated by LGR5+ve stem cells in the crypt niche. It is established that the epigenetic defects detected in colonic biopsies are initially derived in these cells[186], which indicated that studies should ideally be performed exclusively in an epithelial model that maintains sufficient populations of LGR5+ve cells. In 2009 Sato published his revolutionary paper with detailed methods to procure and propagate colonic organoids from healthy mucosal biopsies[220,221], which have been utilised for this investigation. Although colonic organoids proved easy enough to establish, the number and quality of individual organoids rapidly diminished with subsequent passage. This study had set out to use a physiologically relevant dose of vitamin D over a longer period of time in order to allow for extrapolation to the *in vivo* environment, but in retrospect, in light of the propensity of cultures to fail over time, perhaps a larger dose for a shorter period would have been a better place to start as a proof-of-concept.

In support of these observations regarding longevity, since Sato, vast numbers of papers replicating his success have been published, however it should be noted that the majority utilise a) small intestine verses large intestine b) mouse organoids verses human, and c) interventions or transfections typically <7 days. Sato did not observe replicative senescence in their human colonic organoids, and this study endeavoured to replicate their culture and passage methods verbatim, but feel that for longer interventions with human colonic organoids, optimising the methods for procuring sufficient yields is a major barrier to overcome. The technique is still in its infancy, and it is likely that organoids will prove exceptionally useful for aging studies in the future. However, a concerning observation, is noted albeit in only one cell line; that DNAm patterns showed considerable variation between the crypts, organoids at passage 0 and at passage 4 in vehicle treated cells (ethanol <0.001% final dilution), implying an effect of *in vitro* culture on DNAm. Alcohol intake predisposes to CRC via acetaldehyde toxicity[448], and is noted to perturb folate/SAM metabolism[448], and be associated with age-related DNA methylation[449]. Perhaps the effect of ethanol, but certainly the effect of IVA, on colonic organoids in culture is worth exploring further, and may have implications for the validity of organoids as an *ex vivo* model of healthy gut epithelia. The effects of IVA are established in hyper-mutable transformed cell lines, recapitulated here – it seems plausible that the underpinning mechanisms may also be at play in organoids, so efforts should be made to determine if this is indeed the case, although their primary nature may afford greater plasticity, and it could be that the cancer phenotype drives IVA, not the *in vitro* environment.

Differential methylation was observed in primary human organoid models treated with inflamed myofibroblast supernatants, treated with vitamin D, treated with PGE2, and treated with IL6. Vitamin D attenuated the TNFα-induced production of both PGE2 and IL6, and also improved CRP status in a small intervention trial, and regulated TNFα in monocytes. Amelioration of SOX17 and DKK1 DNAm was also observed in healthy and inflamed mouse organoids. This suggests that Tapp's prospective findings are indeed due to a mechanistic deficit in D-deficient participants.

While data are in support of the primary hypotheses, firstly conditional interference with either DNMT activity or VDR competence in any of these models, is necessary to finally conclude a mechanistic effect. Secondly, an effect on phenotype should be established to demonstrate a functional effect of a D-modified methylome; this ideally would incorporate measures of proliferation (BRDU/WST1 assays, crypt length, and organoid morphology), and regulation of transcription and expression associated with differentially methylated genes. Furthermore, it is proposed that the effects of vitamin D are multifactorial, influencing systemic, niche, and autocrine inflammation and regulation of 5mC metabolism. It would be laborious to separate out the size of the anti-inflammatory effect versus the cell-intrinsic effects, which would require total repetition in models with impaired immune function (TLR knock down/ $MYD88^{-/-}$ mice). A key finding of Tapp et al was that vitamin D promoted maintenance of LINE1 hypermethylation; although the Illumina methylation arrays employed here do not include LINEs, it was possible to extrapolate an effect on global DNAm when no change in promoter or CGI DNAm was present, which together with preliminary data in CRC cell lines, suggested that vitamin D might improve LINE1 methylation. This is promising, and should be properly investigated in non-transformed epithelial models.

There are RNA samples available, collected during the treatment schedules of primary organoids, which would be useful to verify the impact of differential DNAm on the regulation of the genes affected. Furthermore, investigation of 5mC enzyme transcripts is warranted in these samples; perhaps the strongest indication of a pathway by which effects are manifest, is the non-tissue specific (monocytes, organoids, and CRC lines) regulation of the DNMTs and TET enzymes by vitamin D. Only about half of the genes reported to be regulated by vitamin D contain a catalogued response element. An eloquent and simple addition to these data would be the identification of vitamin D response elements in 5mC metabolic enzyme sequences, and work is under way to this end.

Two incidental observations also warrant separate elucidation in the future; the expression of the vitamin D-deactivating enzyme, Cyp24a1, is frequently dysregulated in CRC. Initially in early stage tumours, Cyp24a1 is down regulated, assumed to be a plastic response of the tumour as it struggles to moderate rampant proliferation, thereby increasing its sensitivity to vitamin Ds antiproliferative effects. In advanced tumours, the relationship is reversed – Cyp24a1 becomes aberrantly over-expressed, promoting vitamin D insensitivity[378,450,451]. It is noted that inflamed myofibroblast supernatants were able to regulate Cyp24a1 transcription. Despite their accepted role in informing stem cell metabolism[107,452], there are no reports in the literature detailing the effect of the pericryptal myofibroblasts regulating vitamin D metabolism in the epithelia. This would make for an exciting and novel project, particularly utilising protocols that optimised here for the recovery of myofibroblasts from the same biopsies used to propagate colonic organoids, allowing for case-matched investigation that truly emulate mucosal topography. These data suggest that the role of the pericryptal myofibroblast is incompletely characterised; classically myofibroblasts are considered architectural in nature, providing growth factor support, and protection for the stem cell niche. The proteomics data raises the possibility that pericryptal myofibroblasts also act in a sentinel fashion, re-interpreting and distributing the TNFα inflammatory message locally. The inflammatory role of pericryptal myofibroblasts in IBD has rarely been discussed – deregulated expression of TGFβ1, 2, and 3 has been reported in CD MFBs versus those recovered from the normal epithelium, even several weeks after their removal, suggesting a phenotype modification, not a transient response to local signals[453]. Pro-inflammatory TP12 expression is also deregulated in CD MFBs, leading to elevated COX2/PGE2, supporting the results presented here and the idea of functional diversity[454]. Their role as inflammatory mediators in the colonic epithelium may have been overlooked while more central players are investigated (*de novo* leukocyte infiltrates), and their ability to regulate CSC proliferation via Wnt ligand and WA secretion is still being catalogued[455].

It was also noted that the VDR promoter was hypermethylated (80 %+) in CaCO2 and DLD1 cancer cells, and partially methylated in the two organoid lines (50 %+), yet all four models demonstrate vitamin D sensitivity and VDR transcripts. Silencing via hypermethylation of VDR promotes vitamin D insensitivity in breast and adrenal tumours[422,456]. The discrepancy here warrants further investigation, and may reveal alternative non-canonical modes of action by which vitamin D may signal in intestinal epithelial cells.

With regards the suitability of the models used here; organoids were cultured from the uninvolved mucosa 20cm or more, proximal to recto-sigmoid adenocarcinomas. Vitamin D status was not determined for these patients. The ages were 45 and 65 years old respectively for cases 11 and 12 interrogated. We include organoid methylation values at base line for comparison with Tapp's data (figure 47). It is important to note that these patients had developed tumours, unlike Tapp's, who were determined to be disease-free during sampling. Consistent with this discrepancy, hypermethylation of ESR1 and N33, and partial methylation of WIF1 and SFRP2 is observed in the organoids relative to the means reported by Tapp. The two cases generally show increased DNAm in comparison, but the obvious caveat is that DNAm has only been determined in two instances. The small standard error reported suggests methylation was similar for all the genes between the two organoid lines. In retrospect, experiments utilising colonoids cultured from healthy, young patients (screened by colonoscopy) would presumably generate organoids with intact WA hypomethylation, which would allow an investigation of the ability to attenuate, as opposed to an investigation of the ability to ameliorate DNAm. In light of the mosaic nature of field effects, sampling throughout the length of the colon might also be considered pertinent in future. Furthermore, DNA methylation patterns are different in colonic stem cells to terminally differentiated counter parts at the luminal interface[457,458]; in these studies the genes that exhibit variable methylation were associated with phenotype, so it may be that whole-organoid DNAm correlates well with LGR5+ve DNAm patterns, but this could be resolved via FACS

One final adaption might be considered for any further *in vitro* work; the effect of vitamin D was investigated at 500pM, in comparison to a basal culture medium which is reported by the manufacturers to be vitamin D and metabolite free. This would be considered an extreme outlier in the normal physiological reference ranges, but is within the realms of possibility in light of confidence limits. It was just argued that deficiency drives aberrant DNAm; future experiments should include vitamin D-deficient organoids as a control (10pM), compared against vitamin D insufficient (30pM), and vitamin D sufficient (90pM), which would allow for better parallels to be drawn against the *in vivo* environment reported to be associated with aberrant DNAm. It seems likely in respect of the data presented here, that the complete absence of vitamin D in cell culture mediums is as likely to be associated with deleterious cell-intrinsic effects as would be experienced by an organism devoid of the compound.

An interesting phenotype was observed at base line in two of the three myofibroblast lines validated for experiments, termed $COX2^{high}$. Implicit with this discovery is that chronic inflammation in the mucosa, reported to accelerate age-related DNA hypermethylation, is in part mediated by the inflamed myofibroblast phenotype. Should this finding be recapitulated in further primary MFB cultures from uninvolved mucosa, new avenues for the treatment of inflammatory bowel disease and attenuation of colitis-associated tumourigenesis may reveal themselves. It is encouraging that the observed attenuation of PGE2 secretion by vitamin D in four separate primary lines, is consistent with the prevailing consensus by which aspirin modifies colorectal cancer morbidity and mortality via inhibition of COX2[459]. However, aspirin use is itself associated with an increased risk of haemorrhagic stroke (0.03% to 0.04% per year) and gastrointestinal bleeds 0.7% to 1.4% per year)[460]. It would be pertinent to investigate serum vitamin D with regards the myofibroblast phenotype *in vivo,* as outlined in Recommendations for further work. Vitamin D supplementation at the levels required to boost serum vitamin D into the sufficient range are not associated with toxicity or hypercalcaemia[461] and so might offer an alternative, or act synergistically with a lower dose of aspirin for the prevention of colorectal cancer.

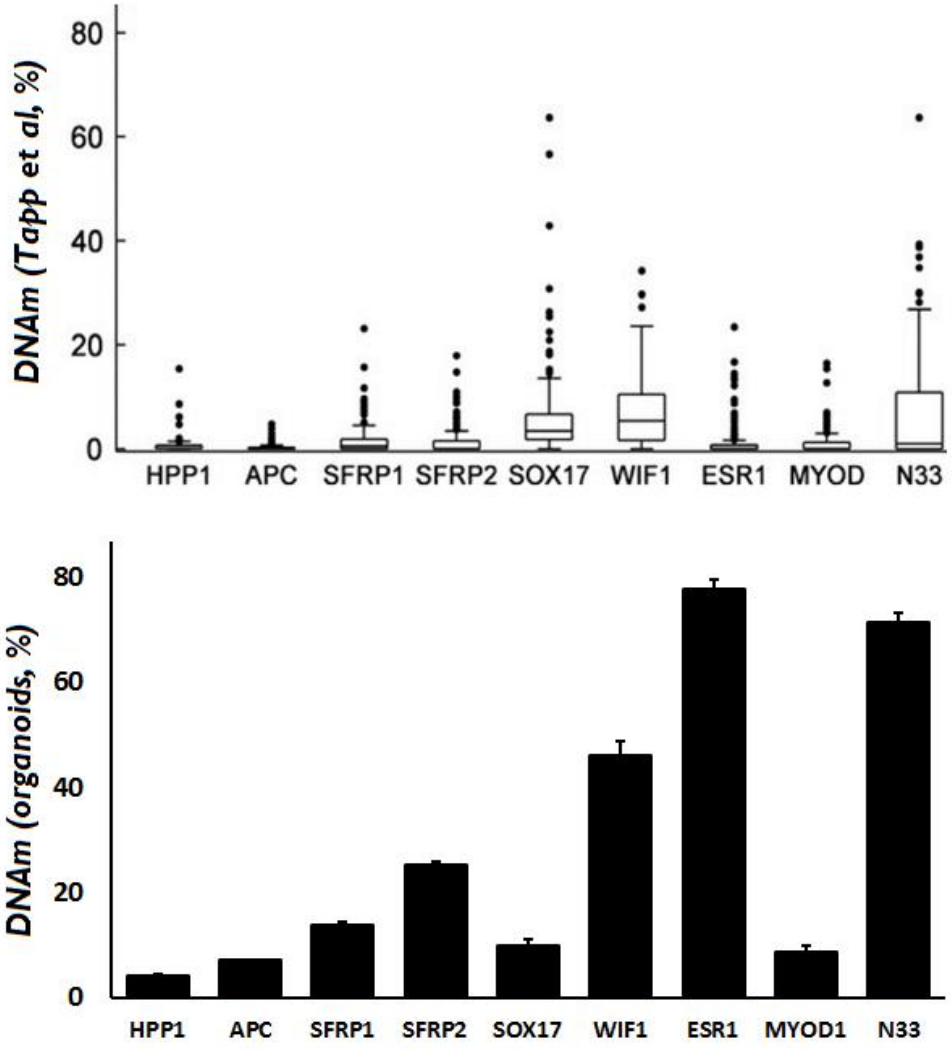

Figure 48 – <u>Comparison of DNAm status in WAs; healthy biopsies versus organoid models.</u> All genes in our two organoid lines show increased methylation relative to Tapp's modelling, specifically in the SFRPs, WIF1 ESR1 and N33. This implies that organoids cultured from uninvolved mucosa in CRC exhibit the field effects of age-related DNAm, and as such may not be the go-to option for investigating the attenuation of aberrant DNAm (conversely they are deemed suitable for investigating the amelioration of aberrant DNAm). Characterisation of the differences between crypts, and young and old organoids in terms of DNAm (IVA) is strongly advised.

Recommendations for further work

One of the key findings was that vitamin D appeared to ameliorate hypermethylation of DKK1 in an uninflamed mouse, and SOX17 in a TNFα-transfected mouse. The organoids were propagated from non-transformed colons. Although the results may be statistically significant within these individuals, ultimately n = 1. The prospect that improving vitamin D status could attenuate, or even ameliorate aberrant age-related or inflammation-associated DNAm (regardless of mechanistic route), is an enticing one, with broad translational implications for promotion of longevity. Such a study would have a significant sociological impact and contribute a good deal to community understanding of vitamin D status' relationship with health. Therefore, an intervention study in mice supplemented with vitamin D is proposed. Using a mouse model negates having to consider physiological relevance of the control group, as vitamin D is provided for in the whole organism, unlike cell culture. It would also be possible to recover other tissues and cell types (MFBs), for correlation of biomarkers with methylation status of an appropriate panel of genes identified here as likely to be differentially methylated. Array-based analysis of methylomes versus transcriptomes would yield all the necessary data to target genes for verification at the bench. These technologies are not presently available for murine models, but may soon be. Furthermore, in recent years epigenetic clocks that interrogate individual CG sites, whose methylation status strongly predicts biological age, have been developed[258]; these are a useful tool for researchers investigating the effects of any compound or intervention on the attenuation of DNAm ageing.

Perhaps a shorter experiment to complement these findings here, as opposed to recapitulating them in vivo, could investigate the necessity of aberrant DNAm for progression; typically, up to 80% of benign polyps present with an APC mutation[462], but aberrant DNAm is also known to be established in these tumours[463]. The CRISPR-Cas9 genome-editing system has recently been utilised to insert classic mutations (specifically APC, SMAD4, TP53, KRAS, and PIK3CA) into organoids propagated from healthy colonic epithelia. Here the authors investigated the ability of the organoids to proliferate in the absence of niche signalling and self-maintain when transplanted into common sites of metastasis[464]. By mutating APC in healthy organoids, it would be possible to investigate the transformative effects of DNA hypermethylation by means reported here (PGE2, IL6, MFB supernatants, IVA), or by conditional over-expression of DNMTs. Finally the ability of vitamin D (or other nutrients or anti-inflammatories) to attenuate the transformation could be characterised.

Concluding remarks

In this observational study the effects of vitamin D on DNA methylation patterns in multiple cell types have been characterised. The results presented suggest that the association between vitamin D status and aberrant DNAm in the transformation-prone colonic epithelial is causal, and that vitamin D exerts pleiotropic effects to promote bowel health that include the resolution of systemic and mucosal inflammation, and modulation of DNMT and TET enzyme transcription. These effects are postulated to contribute to the association of vitamin D status with colorectal cancer risk and prognosis. Further work is therefore indicated to validate these observations.

References

1 *McCollum, E. V., Simmonds, N., Becker, J. E. & Shipley, P. G. . Studies on experimental rickets. XXI. An experimental demonstration of the existence of a vitamin which promotes calcium deposition. J. Biol. Chem. 53, 293-312. (1922).*

2 *Hess, A. F. & Unger, L. J. Use of the carbon arc light in the prevention and cure of rickets. J. Am. Med. Assc.78, 1596-1598 (1922).*

3 *Steenbock, H. & Black, A. Fat soluable vitamins XXIII.The induction of growth promoting and calcifying properties in fats and their unsuponifiable constituents by exposure to light J. Biol. Chem. 64, 263-298 (1925).*

4 *Windaus, A. & Thiele, W. Über die Konstitution des Vitamins D2. Just. Lieb. Annal. Chem. 521, 160-175 (1936).*

5 *Vellus, L., Amiard, G. & Goffinet, B. Le précolciferol. Structure et photochimie. Son role dans le genése di calciferol, et des photoisoméres de l'ergostérol de l'ergostérol. Bull Soc Chim France 22, 1341-1348 (1955).*

6 *Holick, M. F. et al. Photosynthesis of previtamin D3 in human skin and the physiologic consequences. Sci.210, 203-205 (1980).*

7 *Ramagopalan, Sreeram V., et al. A ChIP-seq defined genome-wide map of vitamin D receptor binding: associations with disease and evolution. Gen. Res. 1352-1360. (2010).*

8 *Gröber, U., Spitz, J., Reichrath, J., Kisters, K. & Holick, M. F. Vitamin D: Update 2013: From rickets prophylaxis to general preventive healthcare. Dermato-Endocr.. 5, 331-347, (2013).*

9 *Holick, M. F. Vitamin D: A millenium perspective. J Cell Biochem 88, 296-307, (2003).*

10 *Bouillon, R. & Suda, T. Vitamin D: calcium and bone homeostasis during evolution. BoneKey Rep 3, (2014).*

11 *Yuen, A. W. & Jablonski, N. G. Vitamin D: in the evolution of human skin colour. Med. hypotheses 74, 39-44, (2010).*

12 *Goring, H. & Koshuchowa, S. Vitamin D - the sun hormone. Life in environmental mismatch. Biochem.. 80, 8-20, (2015).*

13 *Cross, H. S., Nittke, T. & Peterlik, M. Modulation of Vitamin D Synthesis and Catabolism in Colorectal Mucosa: A New Target for Cancer Prevention. Anticancer Res. 29, 3705-3712 (2009).*

14 *Haddad, J. G., Matsuoka, L. Y., Hollis, B., Hu, Y. Z. & Wortsman, J. Human plasma transport of vitamin D after its endogenous synthesis. J. Clin. Invest. 91, 2552 (1993).*

15 *Blunt, J., DeLuca, H. & Schnoes, H. 25-hydroxycholecalciferol. A biologically active metabolite of vitamin D3. Biochem. 7, 3317-3322 (1968).*

16 *Christakos, S., Ajibade, D. V., Dhawan, P., Fechner, A. J. & Mady, L. J. Vitamin D: Met.. Endocr. and Met. clinics of North Am. 39, 243 (2010).*

17 *Adegboyega, P. A., Mifflin, R. C., DiMari, J. F., Saada, J. I. & Powell, D. W. Immunohistochemical study of myofibroblasts in normal colonic mucosa, hyperplastic polyps, and adenomatous colorectal polyps. Arch Pathol Lab Med 126, 829-836 (2002).*

18 *Wootton, A. M. Improving the measurement of 25-hydroxyvitamin D. Clin. biochem. 26, 33-36 (2005).*

19 *Bischoff-Ferrari, H. A. Optimal serum 25-hydroxyvitamin D levels for multiple health outcomes. Adv Exp Med Biol 810, 500-525 (2014).*

20 *Heaney, R. P. Functional indices of vitamin D status and ramifications of vitamin D deficiency. Am. J. of Clin. Nut. 80, 1706S-1709S (2004).*

21 *Holick, M. F. Vitamin D Deficiency. New Engl. J. Med. 357, 266-281, (2007).*

22 *Bell, N. H., Shaw, S. & Turner, R. T. Evidence that 1,25-dihydroxyvitamin D3 inhibits the hepatic production of 25-hydroxyvitamin D in man. The J. Clin. inv.74, 1540-1544, (1984).*

23 *Mawer, E., Backhouse, J., Lumb, G. & Stanbury, S. Evidence for formation of 1, 25-dihydroxycholecalciferol during Met. of vitamin D in man. Nature 232, 188-189 (1971).*

24 *Zehnder, D. et al. Extrarenal Expression of 25-Hydroxyvitamin D3-1a-Hydroxylase. J. Clin. Endocr. & Met. 86, 888-894, (2001).*

25 *Norman, A. W. From vitamin D to hormone D: fundamentals of the vitamin D endocrine system essential for good health. The Am. J. of Clin. Nut. 88, 491S-499S (2008).*

26 *Gray, R. W., Omdahl, J. L., Ghazarian, J. G. & DeLuca, H. F. 25-Hydroxycholecalciferol-1-hydroxylase. Subcellular location and properties. The J. of Bio. Chem. 247, 7528-7532 (1972).*

27 *Cross, Heide S., and Enikoe Kallay. Regulation of the colonic vitamin D system for prevention of tumor progression: an update. 493-507. (2009).*

28 *Fraser, D. R. Regulation of the Met. of vitamin D. Physiol Rev 60, 551-613 (1980).*

29 *Zittermann, A. et al. Circulating Calcitriol Concentrations and Total Mortality. Clin. Chem. 55, 1163-1170, (2009).*

30 *Sigmundsdottir, H. et al. DCs metabolize sunlight-induced vitamin D3 to 'program' T cell attraction to the epidermal chemokine CCL27. Nat Immunol 8, 285-293, (2007).*

31 *Radermacher, J. et al. Expression Analysis of CYP27B1 in Tumor Biopsies and Cell Cultures. Anticancer Res. 26, 2683-2686 (2006).*

32 *Jacobs, E. T. et al. CYP24A1 and CYP27B1 Polymorphisms Modulate Vitamin D Met. in Colon Cancer Cells. Cancer Res., (2013).*

33 *Cross, H. S. et al. 25-Hydroxyvitamin D3-1a-hydroxylase and vitamin D receptor gene expression in human colonic mucosa is elevated during early cancerogenesis. Steroids 66, 287-292 (2001)*

34 *Cross, H. S., Bises, G., Lechner, D., Manhardt, T. & Kallay, E. The Vitamin D endocrine system of the gut–its possible role in colorectal cancer prevention. J Steroid Biochem Mol Biol 97, 121-128, (2005).*

35 *Sakaki, T., Kagawa, N., Yamamoto, K. & Inouye, K. Met. of vitamin D3 by cytochromes P450. Front Biosci 10, 119-134 (2005).*

36 *Albertson, D. G. et al. Quantitative mapping of amplicon structure by array CGH identifies CYP24 as a candidate oncogene. Nat. Genet. 25, 144-146 (2000).*

37 *Bises, G. et al. 25-hydroxyvitamin D3-1alpha-hydroxylase expression in normal and malignant human colon. J. Histochem. Soc. 52, 985-989, (2004).*

38 *Ladizesky, M. et al. Solar ultraviolet B radiation and photoproduction of vitamin D3 in central and southern areas of Argentina. J. of bone and mineral Res. : the official J. of the Am.n Society for Bone and Mineral Res. 10, 545-549, (1995).*

39 *Holick, M. F. McCollum Award Lecture, 1994: vitamin D - new horizons for the 21st century. Am J Clin Nutr 60, 619-630 (1994).*

40 *Wortsman, J., Matsuoka, L. Y., Chen, T. C., Lu, Z. & Holick, M. F. Decreased bioavailability of vitamin D in obesity. The Am. J. of Clin. Nut. 72, 690-693 (2000).*

41 *Tavakkoli, A., DiGiacomo, D., Green, P. H. & Lebwohl, B. Vitamin D Status and Concomitant Autoimmunity in Celiac Disease. J. Clin. gastroenterology 47, 515-519, (2013).*

42 *Gordon, C. Prevalence of vitamin d deficiency among healthy adolescents. Arch. Pediatr. Adolesc. Med. 158, 531-537, d (2004).*

43 *Public Health England. Press release - PHE publishes new advice on vitamin D, <https://www.gov.uk/government/news/phe-publishes-new-advice-on-vitamin-d> (2016).*

44 *Dobnig, H. et al. Independent association of low serum 25-hydroxyvitamin D and 1, 25-dihydroxyvitamin D levels with all-cause and cardiovascular mortality. Arch. of Int. Med.168, 1340 (2008).*

45 *Holick, M. F. Sunlight and vitamin D for bone health and prevention of autoimmune diseases, cancers, and cardiovascular disease. The Am. J. of Clin. Nut. 80, 1678S-1688S (2004).*

46 *Bertone-Johnson, E. R. et al. Plasma 25-hydroxyvitamin D and 1, 25-dihydroxyvitamin D and risk of breast cancer. Can. Epidem. Biom. & Prevention 14, 1991-1997 (2005).*

47 *Ahonen, M. H., Tenkanen, L., Teppo, L., Hakama, M. & Tuohimaa, P. Prostate cancer risk and prediagnostic serum 25-hydroxyvitamin D levels (Finland). Cancer Causes Control 11, 847-852 (2000).*

48 *Pludowski, P. et al. Vitamin D effects on musculoskeletal health, immunity, autoimmunity, cardiovascular disease, cancer, fertility, pregnancy, dementia and mortality- a review of recent evidence. Autoimmun. Rev. (2013).*

49 *Garland, C. F. & Garland, F. C. Do Sunlight and Vitamin D Reduce the Likelihood of Colon Cancer? Int. J. Epidemiol. 9, 227-231, (1980).*

50 *Lee, J. E. et al. Circulating levels of vitamin D and colon and rectal cancer: the Physicians' Health Study and a meta-analysis of prospective studies. Can. Prev. Res. (Philadelphia, Pa.) 4, 735-743, (2011).*

51 *Huhtakangas, J. A., OLiv.a, C. J., Bishop, J. E., Zanello, L. P. & Norman, A. W. The vitamin D receptor is present in caveolae-enriched plasma membranes and binds 1*

alpha,25(OH)2-vitamin D3 in vivo and in vitro. Mol. endocr. (Baltimore, Md.) 18, 2660-2671, (2004).

52 *Bouillon, R. et al. Vitamin D and human health: lessons from vitamin D receptor null mice. Endocr. Rev. 29, 726-776 (2008).*

53 *Carlberg, C., Seuter, S. & Heikkinen, S. The First Genome-wide View of Vitamin D Receptor Locations and Their Mechanistic Implications. Anticancer Res. 32, 271-282 (2012).*

54 *Hossein-nezhad, A., Spira, A. & Holick, M. F. Influence of Vitamin D Status and Vitamin D3 Supplementation on Genome Wide Expression of White Blood Cells: A Randomized Double-Blind Clinical Trial. PloS one 8, e58725, (2013).*

55 *Jurutka, P. W. et al. Mol. nature of the vitamin D receptor and its role in regulation of gene expression. Rev Endocr Metab Disord 2, 203-216 (2001).*

56 *Kröncke, K.-D. Zinc finger proteins as Mol. targets for nitric oxide-mediated gene regulation. Antioxid. Redox Signal. 3, 565-575 (2001).*

57 *Schräder, Magdalena, et al. Interaction between retinoic acid and vitamin D signaling pathways. J. of Bio. Chem. 268.24 (1993): 17830-17836..*

58 *Carlberg, C. & Dunlop, T. W. The impact of chromatin organization of vitamin D target genes. Anticancer Res. 26, 2637-2645 (2006).*

59 *Campbell, F. C., Xu, H., El-Tanani, M., Crowe, P. & Bingham, V. The yin and yang of vitamin D receptor (VDR) signaling in neoplastic progression: operational networks and tissue-specific growth control. Biochem Pharmacol 79, 1-9, (2010).*

60 *Deeb, K. K., Trump, D. L. & Johnson, C. S. Vitamin D signalling pathways in cancer: potential for anticancer therapeutics. Nat. Rev. Can. 7, 684-700, (2007).*

61 *Groman, R. P. Acute management of calcium disorders. Topics in companion animal medicine 27, 167-171 (2012).*

62 *Stroud, M. L., Stilgoe, S., Stott, V. E., Alhabian, O. & Salman, K. Vitamin D - a review. Australian family physician 37, 1002-1005 (2008).*

63 *Holick, M. F. Vitamin D Status: Measurement, Interpretation, and Clinical Application. Ann. Epidemiol. 19, 73-78, (2009).*

64 *Ma, Y. et al. Association Between Vitamin D and Risk of Colorectal Cancer: A Systematic Review of Prospective Studies. J. Clin. Onc. 29, 3775-3782, (2011).*

65 *Hyppönen, E. & Power, C. Hypovitaminosis D in British adults at age 45 y: nationwide cohort study of dietary and lifestyle predictors. The Am. J. of Clin. Nut. 85, 860-868 (2007).*

66 *Autier, P., Boniol, M., Pizot, C. & Mullie, P. Vitamin D status and ill health: a systematic review. The Lancet Diabetes & Endocr. 2, 76-89 (2014).*

67 *Lips, P. Vitamin D physiology. Prog. in Biophys. and Mol. Bio. 92, 4-8, (2006).*

68 *Balesaria, S., Sangha, S. & Walters, J. R. F. Human duodenum responses to vitamin D metabolites of TRPV6 and other genes involved in calcium absorption. Am. J. of Physiology - Gast. and Liv. Phys. 297, G1193-G1197, (2009).*

69 *Holick, M. F. Vitamin D and bone health. J. Nut. 126, 1159S (1996).*

70 *Howland, J. Biochem.: By D Voet and J G Voet. pp 1223. John Wiley and Sons, New York. 1990. $54.95 ISBN 0-471-61769-5. Biochem. Ed. 18, 212-212, (1990).*

71 *Suda, T. et al. Modulation of osteoclast differentiation and function by the new members of the tumor necrosis factor receptor and ligand families. Endocr. Rev. 20, 345 (1999).*

72 *Zittermann, A. & Gummert, J. F. Nonclassical vitamin D action. Nuts 2, 408-425, (2010).*

73 *Agmon-Levin, N., Theodor, E., Segal, R. M. & Shoenfeld, Y. Vitamin D in systemic and organ-specific autoimmune diseases. Clin Rev Allergy Immunol 45, 256-266, (2013).*

74 *Adams, J. S., Liu, P. T., Chun, R., Modlin, R. L. & Hewison, M. Vitamin D in Defense of the Human Immune Response. Ann. N. Y. Acad. Sci. 1117, 94-105, (2007).*

75 *Willis, K. S., Smith, D. T., Broughton, K. S. & Larson-Meyer, D. E. Vitamin D status and biomarkers of inflammation in runners. J. of Sports Med. 3, 35-42, (2012).*

76 *Schleithoff, S. S. et al. Vitamin D supplementation improves cytokine profiles in patients with congestive heart failure: a double-blind, randomized, placebo-controlled trial. The Am. J. of Clin. Nut. 83, 754-759 (2006).*

77 *Kelly, P., Suibhne, T. N., O'Morain, C. & O'Sullivan, M. Vitamin D status and cytokine levels in patients with Crohn's disease. Int. J. for vitamin and nutrition Res.. 81, 205-210, (2011).*

78 *Calton, E. K., Keane, K. N., Newsholme, P. & Soares, M. J. The Impact of Vitamin D Levels on Inflammatory Status: A Systematic Review of Immune Cell Studies. PLoS ONE 10, e0141770, (2015).*

79 *Chen, Y. et al. Vitamin D Receptor Inhibits NF-kB Activation by Interacting with IKKb Protein. J. Biol. Chem. (2013).*

80 *Khayyat, Y. & Attar, S. Vitamin D Deficiency in Patients with Irritable Bowel Syndrome: Does it Exist? Oman Medical J. 30, 115-118, (2015).*

81 *O'Sullivan, M. & O'Morain, C. Nutrition in inflammatory bowel disease. Best Practice & Res. Clin Gastro. 20, 561-573, (2006).*

82 *Kühl, A. A., Erben, U., Kredel, L. I. & Siegmund, B. Diversity of Intestinal Macrophages in Inflammatory Bowel Diseases. Front. in Immunol. 6, 613, (2015).*

83 *Murray, P. J. & Wynn, T. A. Protective and pathogenic functions of macrophage subsets. Nat Rev Immunol 11, 723-737 (2011).*

84 *Daigneault, M., Preston, J. A., Marriott, H. M., Whyte, M. K. B. & Dockrell, D. H. The Identification of Markers of Macrophage Differentiation in PMA-Stimulated THP-1 Cells and Monocyte-Derived Macrophages. PLoS ONE 5, e8668, (2010).*

85 *Hmama, Z. et al. 1a, 25-dihydroxyvitamin D3–induced myeloid cell differentiation is regulated by a vitamin D receptor–phosphatidylinositol 3-kinase signaling complex. The J. of exp.med. 190, 1583-1594 (1999).*

86 *Jacobs, E. T., Kohler, L. N., Kunihiro, A. G. & Jurutka, P. W. Vitamin D and colorectal, breast, and prostate cancers: A review of the epidemiological evidence. J. of Can. 7, 232 (2016).*

87 *Vieth, R. Vitamin D and Cancer Mini-Symposium: The Risk of Additional Vitamin D. Ann. Epidemiol. 19, 441-445, (2009).*

88 *Takai, Daiya and Peter A. Jones. The CpG Island Searcher: A new WWW resource. In silico bio. 3, 3, 235-40 (2003).*

89 *Salehi-Tabar, R. et al. Vitamin D receptor as a master regulator of the c-MYC/MXD1 network. Proc. Nat. Ac. Sci. USA 109, 18827-18832, (2012).*

90 *Irazoqui, A. P., Heim, N. B., Boland, R. L. & Buitrago, C. G. 1alpha,25 dihydroxi-vitamin D(3) modulates CDK4 and CDK6 expression and localization. Biochem Biophys Res Commun 459, 137-142, (2015).*

91 *Larriba, M. J. et al. Vitamin D Is a Multilevel Repressor of Wnt/b-Catenin Signaling in Cancer Cells. Cancers 5, 1242-1260, (2013).*

92 *Edwards, B. J. Anticancer effects of Vitamin D. Am. J. of Hem./Onc.11 (2015).*

93 *Ordonez-Moran, P. et al. RhoA-ROCK and p38MAPK-MSK1 mediate vitamin D effects on gene expression, phenotype, and Wnt pathway in colon cancer cells. J. Cell Biol. 183, 697-710, (2008).*

94 *Lopes, N. et al. 1Alpha,25-dihydroxyvitamin D-3 Induces de novo E-cadherin Expression in Triple-negative Breast Cancer Cells by CDH1-promoter Demethylation. Antican. Res. 32, 249-257 (2012).*

95 *Eelen, G. et al. Mechanism and potential of the growth-inhibitory actions of vitamin D and analogs. Curr. Med. Chem. 14, 1893-1910 (2007).*

96 *Colston, K. W. & Hansen, C. M. r. Mechanisms implicated in the growth regulatory effects of vitamin D in breast cancer. Endo.-Rel. Can. 9, 45-59, (2002).*

97 *Díaz, G. D., Paraskeva, C., Thomas, M. G., Binderup, L. & Hague, A. Apoptosis Is Induced by the Active Metabolite of Vitamin D3 and Its Analogue EB1089 in Colorectal Adenoma and Carcinoma Cells: Possible Implications for Prevention and Therapy. Can. Res. 60, 2304-2312 (2000).*

98 *Shabahang, M. et al. Growth Inhibition of HT-29 Human Colon Cancer Cells by Analogues of 1,25-Dihydroxyvitamin D3. Can. Res. 54, 4057-4064 (1994).*

99 *Thomas, M. G., Tebbutt, S. & Williamson, R. C. Vitamin D and its metabolites inhibit cell proliferation in human rectal mucosa and a colon cancer cell line. Gut 33, 1660-1663, (1992).*

100 *Shabahang, M. et al. 1, 25-Dihydroxyvitamin D3 receptor as a marker of human colon carcinoma cell line differentiation and growth inhibition. Can. Res. 53, 3712-3718 (1993).*

101 *Reinus, J. F. & Simon, D. Gastro. anat. phys. (John Wiley & Sons, 2014).*

102 *Barker, N. et al. Crypt stem cells as the cells-of-origin of intestinal cancer. Nature 457, 608-611, (2009).*

103 *Van der Wath, R. C., Gardiner, B. S., Burgess, A. W. & Smith, D. W. Cell Organisation in the Colonic Crypt: A Theoretical Comparison of the Pedigree and Niche Concepts. PLoS ONE 8, e73204, (2013).*

104 *Said, H. M. Physiology of the Gastro. Tract, Two Volume Set. (Academic Press (2012).*

105 *Barker, N. Adult intestinal stem cells: critical drivers of epithelial homeostasis and regeneration. Nat. rev.. Mol.cell bio.15, 19-33, (2014).*

106 *Bernstein, C. et al. Cancer and age related colonic crypt deficiencies in cytochrome c oxidase I. World J. of Gastro.Onc. 2, 429-442, (2010).*

107 *Kosinski, C. et al. Gene expression patterns of human colon tops and basal crypts and BMP antagonists as intestinal stem cell niche factors. Proc. Nat. Ac. Sci 104, 15418-15423, (2007).*

108 *Tetsu, O. & McCormick, F. b-Catenin regulates expression of cyclin D1 in colon carcinoma cells. Nature 398, 422-426 (1999).*

109 *Stamos, J. L. & Weis, W. I. The beta-catenin destruction complex. Cold Spring Harb Perspect Biol 5, a007898, (2013).*

110 *Mann, B. et al. Target genes of b-catenin–T cell-factor/lymphoid-enhancer-factor Sig.ing in human colorectal carcinomas. Proc. Nat. Ac. Sci 96, 1603-1608, (1999).*

111 *Boland, G. M., Perkins, G., Hall, D. J. & Tuan, R. S. Wnt 3a promotes proliferation and suppresses osteogenic differentiation of adult human mesenchymal stem cells. J Cell Biochem 93, 1210-1230 (2004).*

112 *Habib, S. J. et al. A Localized Wnt Sig. Orients Asymmetric Stem Cell Division in Vitro. Sci. 339, 1445-1448, (2013).*

113 *Hirokawa, Y., Yip, K. H., Tan, C. W. & Burgess, A. W. Colonic myofibroblast cell line stimulates colonoid formation. Am. J. of Phys.. Gastro. and Liv. Phys., (2014).*

114 *Kabiri, Z. et al. Stroma provides an intestinal stem cell niche in the absence of epithelial Wnts. Development 141, 2206-2215, (2014).*

115 *Powell, D. W., Pinchuk, I. V., Saada, J. I., Chen, X. & Mifflin, R. C. Mesenchymal Cells of the Intestinal Lamina Propria. Annu. Rev. Physiol. 73, 213-237, (2011).*

116 *Wissmann, C. et al. WIF1, a component of the Wnt pathway, is down-regulated in prostate, breast, lung, and bladder cancer. The J. of Path. 201, 204-212, (2003).*

117 *Krausova, M. & Korinek, V. Wnt Signaling in adult intestinal stem cells and cancer. Cell. Sig.. 26, 570-579, (2014).*

118 *Erben, U. et al. A guide to histomorphological evaluation of intestinal inflammation in mouse models. Int. J. Clin. and Exp. Path. 7, 4557-4576 (2014).*

119 *Park, H. S., Goodlad, R. A. & Wright, N. A. Crypt fission in the small intestine and colon. A mechanism for the emergence of G6PD locus-mutated crypts after treatment with mutagens. Am J Pathol 147, 1416-1427 (1995).*

120 *Nava, P. et al. Interferon-gamma regulates intestinal epithelial homeostasis through converging beta-catenin Signaling pathways. Immunity 32, 392-402, (2010).*

121 *Silva-Garc et al. The Wnt3/B2-Catenin Sig.ing Pathway Controls the Inflammatory Response in Infections Caused by Pathogenic Bacteria. Mediators of Inflammation 2014, 7, (2014).*

122 *Chai, H. & Brown, R. E. Field Effect in Cancer–An Update. Ann. Clin & Lab. Sci. 39, 331-337 (2009).*

123 *Cancer Genome Atlas Network. "Comprehensive molecular characterization of human colon and rectal cancer." Nature 487.7407 330.(2012).*

124 *Liu, W. et al. Mutations in AXIN2 cause colorectal cancer with defective mismatch repair by activating b-catenin/TCF Sig.ling. Nat. Genet. 26, 146-147 (2000).*

125 *Shakoori, A. et al. Deregulated GSK3b activity in colorectal cancer: its association with tumor cell survival and proliferation. Biochem. Biophys. Res. Commun. 334, 1365-1373 (2005).*

126 *White, B. D., Chien, A. J. & Dawson, D. W. Dysregulation of Wnt/b-catenin Sig.ing in Gastro. Cancers. Gastro. 142, 219-232, (2012).*

127 *Holcombe, R., Marsh, J., Waterman, M. & Lin, F. Expression of Wnt ligands and Frizzled receptors in colonic mucosa and in colon carcinoma. J. Clin. Pathol. 55, 220 (2002).*

128 *Caldwell, G. M. et al. The Wnt Antagonist sFRP1 in Colorectal Tumorigenesis. Cancer Res. 64, 883-888, (2004).*

129 *Aguilera, O. et al. Epigenetic inactivation of the Wnt antagonist DICKKOPF-1 (DKK-1) gene in human colorectal cancer. Oncogene 25, 4116-4121 (2006).*

130 *Fang, Y., Wang, L., Zhang, Y., Ge, C. & Xu, C. Wif-1 methylation and beta-catenin expression in colorectal serrated lesions. Chinese J. of Path. 43, 15-19 (2014).*

131 *Cheung, A. F. et al. Complete deletion of Apc results in severe polyposis in mice. Oncogene 29, 1857-1864 (2010).*

132 Dow, Lukas E. et al. Apc Restoration Promotes Cellular Differentiation and Reestablishes Crypt Homeostasis in Colorectal Cancer. Cell 161, 1539-1552, (2015).

133 Brenner, H. et al. Risk of progression of advanced adenomas to colorectal cancer by age and sex: estimates based on 840 149 screening colonoscopies. Gut 56, 1585-1589, (2007).

134 Holzheimer RG, Mannick JA, editors. Surgical Treatment: Evidence-Based and Problem-Oriented. Munich: Zuckschwerdt; 2001.

135 Baylin, S. B. & Ohm, J. E. Epigenetic gene silencing in cancer–a mechanism for early oncogenic pathway addiction? Nat. Rev. Can. 6, 107-116 (2006).

136 Labianca, R. et al. Early colon cancer: ESMO Clinical Practice Guidelines for diagnosis, treatment and follow-up. Ann. Oncol. 24, vi64-vi72, (2013).

137 Li, X.-L., Zhou, J., Chen, Z.-R. & Chng, W.-J. p53 mutations in colorectal cancer- Mol. pathogenesis and pharmacological reactivation. World J. of Gastro. : WJG 21, 84-93, (2015).

138 Abdel-Rahman, W. M. Genomic Instability and Carcinogenesis: An Update. Curr. Genomics 9, 535-541, (2008).

139 Sakai, E., Nakajima, A. & Kaneda, A. Accumulation of aberrant DNA methylation during colorectal cancer development. World J. of Gastro. : WJG 20, 978-987, (2014).

140 Lieberman, D. & Smith, F. Screening for colon malignancy with colonoscopy. The Am. J. of Gastro. 86, 946 (1991).

141 Jemal, A. et al. Cancer statistics, 2008. CA: a cancer J. for clinicians 58, 71-96 (2008).

142 Hubner, U. et al. Effect of 1 year B and D vitamin supplementation on LINE-1 repetitive element methylation in older subjects. Clinical Chem. and laboratory medicine : CCLM / FESCC 51, 649-655, (2013).

143 Trock, B., Lanza, E. & Greenwald, P. Dietary Fiber, Vegetables, and Colon Cancer: Critical Review and Meta-analyses of the Epidemiologic Evidence. J. Natl. Cancer Inst. 82, 650-661, (1990).

144 Cappellani, A. et al. Strong correlation between diet and development of colorectal cancer. Front Biosci 18, 190-198 (2013).

145 Bosman, F. T., Carneiro, F., Hruban, R. H. & Theise, N. WHO classification of tumours of the digestive system. (World Health Organization, 2010).

146 *Jemal, A. et al. Global cancer statistics. CA: a cancer J. for clinicians 61, 69-90, (2011).*

147 *Wilkes, G. & Hartshorn, K. Colon, rectal, and anal cancers. Seminars in Onc. nursing 25, 32-47, (2009).*

148 *Lieberman, D. Progress and Challenges in Colorectal Cancer Screening and Surveillance. Gastro. 138, 2115-2126, (2010).*

149 *Wiggers, T., Arends, J. W., Bosman, F. T., Schutte, B. & Volovics, L. A multivariate analysis of pathologic prognostic indicators in large bowel cancer. Cancer 61, 386-395 (1988).*

150 *Cunningham, D. et al. Colorectal cancer. The Lancet 375, 1030-1047, doi:*

151 *Botteri, E. et al. Smoking and colorectal cancer: a meta-analysis. JAMA : the J. of the Am.n Medical Association 300, 2765-2778, (2008).*

152 *Doubeni, C. A. et al. Contribution of behavioral risk factors and obesity to socioeconomic differences in colorectal cancer incidence. J Natl Cancer Inst 104, 1353-1362, (2012).*

153 *Chao A, T. M. J. C. C. J. & et al. MEat consumption and risk of colorectal cancer. JAMA: The J. of the Am.n Medical Association 293, 172-182, (2005).*

154 *Ferrari, P. et al. Lifetime and baseline alcohol intake and risk of colon and rectal cancers in the European prospective investigation into cancer and nutrition (EPIC). Int. J. of cancer. J. Int. du cancer 121, 2065-2072, (2007).*

155 *Terzić, J., Grivennikov, S., Karin, E. & Karin, M. Inflammation and Colon Cancer. Gastro. 138, 2101-2114.e2105, (2010).*

156 *Vazzana, N. et al. Obesity-driven inflammation and colorectal cancer. Curr Med Chem 19, 5837-5853 (2012).*

157 *Ostan, R. et al. Inflammaging and cancer: a challenge for the Mediterranean diet. Nuts 7, 2589-2621 (2015).*

158 *Lakatos, P. L. & Lakatos, L. Risk for colorectal cancer in ulcerative colitis: changes, causes and management strategies. World J. of Gastro.: WJG 14, 3937 (2008).*

159 *Jess, T. et al. Decreasing Risk of Colorectal Cancer in Patients With Inflammatory Bowel Disease Over 30 Years. Gastro. 143, 375-381.e371, (2012).*

160 *Grivennikov, S. I. Inflammation and colorectal cancer: colitis-associated neoplasia. Seminars in immunoPath. 35, 229-244, (2013).*

161 *Strober, W. & Fuss, I. J. Pro-Inflammatory Cytokines in the Pathogenesis of IBD. Gastro. 140, 1756-1767, (2011).*

162 *Drew, D. A., Cao, Y. & Chan, A. T. Aspirin and colorectal cancer: the promise of precision chemoprevention. Nat Rev Cancer 16, 173-186, (2016).*

163 *Liu, W. et al. Intestinal epithelial vitamin D receptor Sig.ing inhibits Exp. colitis. The J. Clin. investigation 123, 0-0, (2013).*

164 *Coussens, L. M. & Werb, Z. Inflammation and cancer. Nature 420, 860-867 (2002).*

165 *Leslie, A., Carey, F. A., Pratt, N. R. & Steele, R. J. The colorectal adenoma-carcinoma sequence. The British J. of surgery 89, 845-860 (2002).*

166 *Clark, J. C. et al. Prevalence of polyps in an autopsy series from areas with varying incidence of large-bowel cancer. Int. J. Cancer 36, 179-186 (1985).*

167 *Gillespie, P. et al. Colonic adenomas–a colonoscopy survey. Gut 20, 240-245 (1979).*

168 *Eide, T. J. Remnants of adenomas in colorectal carcinomas. Cancer 51, 1866-1872 (1983).*

169 *Worthley, D. L. et al. DNA methylation within the normal colorectal mucosa is associated with pathway-specific predisposition to cancer. Oncogene 29, 1653-1662, (2010).*

170 *Dhir, M. et al. Epigenetic Regulation of WNT Sig.ing Pathway Genes in Inflammatory Bowel Disease (IBD) Associated Neoplasia. J. of Gastro. Surgery 12, 1745-1753, (2008).*

171 *Biemont, C. From genotype to phenotype. What do epigenetics and epigenomics tell us?. Heredity 105, 1-3 (2010).*

172 *Nagamori, I. et al. Comprehensive DNA Methylation Analysis of Retrotransposons in Male Germ Cells. Cell Reports 12, 1541-1547 (2015).*

173 *Kelsey, G. & Feil, R. New insights into establishment and maintenance of DNA methylation imprints in mammals. Phil. Trans. R. Soc. B 368, 20110336 (2013).*

174 *Portela, A. & Esteller, M. Epigenetic modifications and human disease. Nat Biotech 28, 1057-1068, (2010).*

175 *Kulis, M. et al. Whole-genome fingerprint of the DNA methylome during human B cell differentiation. Nat Genet 47, 746-756, (2015).*

176 Hermann, A., Gowher, H. & Jeltsch, A. Biochem. and biology of mammalian DNA methyltransferases. Cellular and Mol. life Sci.s : CMLS 61, 2571-2587, (2004).

177 Lander, E. S. et al. Initial sequencing and analysis of the human genome. Nature 409, 860-921, (2001).

178 Larsen, F., Gundersen, G., Lopez, R. & Prydz, H. CpG islands as gene markers in the human genome. Genomics 13, 1095-1107 (1992).

179 Klose, R. J. & Bird, A. P. Genomic DNA methylation: the mark and its mediators. Trends Biochem. Sci. 31, 89-97 (2006).

180 Song, F. et al. Association of tissue-specific differentially methylated regions (TDMs) with differential gene expression. Proc. Nat. Ac. Sci of the United States of Am. 102, 3336-3341 (2005).

181 Wan, J. et al. Characterization of tissue-specific differential DNA methylation suggests distinct modes of positive and negative gene expression regulation. BMC Genomics 16, 1-11, (2015).

182 Irizarry, R. A. et al. The human colon cancer methylome shows similar hypo- and hypermethylation at conserved tissue-specific CpG island shores. Nat Genet 41, (2009).

183 Zhu, H., Wang, G. & Qian, J. Transcription factors as readers and effectors of DNA methylation. Nat. Rev.. Genetics 17, 551-565, (2016).

184 Cedar, H. & Bergman, Y. Programming of DNA Methylation Patterns. Annu. Rev. Biochem. 81, 97-117, (2012).

185 Belshaw, N. J. et al. Methylation of the ESR1 CpG island in the colorectal mucosa is an 'all or nothing' process in healthy human colon, and is accelerated by dietary folate supplementation in the mouse. Biochem. Soc. Trans. 33, 709-711 (2005).

186 Belshaw, N. J. et al. Patterns of DNA methylation in individual colonic crypts reveal aging and cancer-related field defects in the morphologically normal mucosa. Carcinogenesis 31, 1158-1163, (2010).

187 Ulrey, C. L., Liu, L., Andrews, L. G. & Tollefsbol, T. O. The impact of Met. on DNA methylation. Hum. Mol. Genet. 14, R139-R147, (2005).

188 *Charles, M. A., Johnson, I. T. & Belshaw, N. J. Supra-physiological folic acid concentrations induce aberrant DNA methylation in normal human cells in vitro. Epigenetics 7, 689-694, (2012).*

189 *Ren, J. et al. DNA hypermethylation as a chemotherapy target. Cell Sig. 23, 1082-1093, (2011).*

190 *He, Y. F. et al. Tet-mediated formation of 5-carboxylcytosine and its excision by TDG in mammalian DNA. Sci. 333, 1303-1307, (2011).*

191 *Chen, T., Ueda, Y., Dodge, J. E., Wang, Z. & Li, E. Establishment and Maintenance of Genomic Methylation Patterns in Mouse Embryonic Stem Cells by Dnmt3a and Dnmt3b. Mol. Cell. Biol. 23, 5594-5605, (2003).*

192 *Liao, J. et al. Targeted disruption of DNMT1, DNMT3A and DNMT3B in human embryonic stem cells. Nat Genet 47, 469-478, (2015).*

193 *Subramaniam, D., Thombre, R., Dhar, A. & Anant, S. DNA Methyltransferases: A Novel Target for Prevention and Therapy. Frontiers in Onc. 4, (2014).*

194 *Spada, F. et al. DNMT1 but not its interaction with the replication machinery is required for maintenance of DNA methylation in human cells. The J. of Cell Biology 176, 565-571, (2007).*

195 *Karpf, A. R. & Matsui, S.-i. Genetic Disruption of Cytosine DNA Methyltransferase Enzymes Induces Chromosomal Instability in Human Cancer Cells. Cancer Res. 65, 8635-8639, (2005).*

196 *Rhee, I. et al. DNMT1 and DNMT3b cooperate to silence genes in human cancer cells. Nature 416, 552-556 (2002).*

197 *Jones, P. A. & Baylin, S. B. The fundamental role of epigenetic events in cancer. Nat. Rev. Genetics 3, 415-428 (2002).*

198 *Ogino, S. et al. A Cohort Study of Tumoral LINE-1 Hypomethylation and Prognosis in Colon Cancer. J. Natl. Cancer Inst. 100, 1734-1738, (2008).*

199 *Feinberg, A. P., Ohlsson, R. & Henikoff, S. The epigenetic progenitor origin of human cancer. Nat. Rev. Genetics 7, 21-33 (2006).*

200 *Baba, Y. et al. Res. Epigenomic diversity of colorectal cancer indicated by LINE-1 methylation in a database of 869 tumors. (2010).*

201 Mima, K. et al. Tumor LINE-1 methylation level and colorectal cancer location in relation to patient survival. Oncotarget, (2016).

202 Lee, S., Cho, N. Y., Yoo, E. J., Kim, J. H. & Kang, G. H. CpG island methylator phenotype in colorectal cancers: comparison of the new and classic CpG island methylator phenotype marker panels. Arch Pathol Lab Med 132, 1657-1665, (2008).

203 Van Emburgh, B. O. & Robertson, K. D. Modulation of Dnmt3b function in vitro by interactions with Dnmt3L, Dnmt3a and Dnmt3b splice variants. Nucleic Acids Res. 39, 4984-5002 (2011).

204 Shen, L. et al. MGMT promoter methylation and field defect in sporadic colorectal cancer. J. Natl. Cancer Inst. 97, 1330-1338 (2005).

205 Linhart, H. G. et al. Dnmt3b promotes tumorigenesis in vivo by gene-specific de novo methylation and transcriptional silencing. Genes Dev 21, 3110-3122 (2007).

206 Nosho, K. et al. DNMT3B Expression Might Contribute to CpG Island Methylator Phenotype in Colorectal Cancer. Clinical cancer Res. : an official J. of the Am.n Association for Cancer Res. 15, 3663-3671, (2009).

207 Kanai, Y., Ushijima, S., Kondo, Y., Nakanishi, Y. & Hirohashi, S. DNA methyltransferase expression and DNA methylation of CPG islands and peri-centromeric satellite regions in human colorectal and stomach cancers. Int. J. of cancer. J. Int. du cancer 91, 205-212 (2001).

208 Niederwieser, C. et al. Prognostic and biologic significance of DNMT3B expression in older patients with cytogenetically normal primary acute myeloid leukemia. Leukemia 29, 567-575 (2015).

209 Worthley, D. et al. DNA methylation within the normal colorectal mucosa is associated with pathway-specific predisposition to cancer. Oncogene 29, 1653-1662 (2010).

210 Wallace, K. et al. Association between folate levels and CpG Island hypermethylation in normal colorectal mucosa. Cancer Prev Res 3, 1552-1564 (2010).

211 Davis, C. D. & Milner, J. A. Vitamin D and colon cancer. Expert Review of Gastro. & Hepatology 5, 67-81, (2011).

212 Tapp, H. S. et al. Nutritional factors and gender influence age-related DNA methylation in the human rectal mucosa. Aging cell 12, 148-155, (2013).

213 *Fu, B. et al. Epigenetic Regulation of BMP2 by 1,25-dihydroxyvitamin D3 through DNA Methylation and Histone Modification. PloS one 8 (2013).*

214 *Rawson, J. B. et al. Vitamin D Intake Is Negatively Associated with Promoter Methylation of the Wnt Antagonist Gene DKK1 in a Large Group of Colorectal Cancer Patients. Nutr Cancer 64, 919-928, (2012).*

215 *Stefanska, B., Karlic, H., Varga, F., Fabianowska-Majewska, K. & Haslberger, A. Epigenetic mechanisms in anti-cancer actions of bioactive food components–the implications in cancer prevention. Br. J. Pharmacol. 167, 279-297 (2012).*

216 *Reinisch, W. et al. Clinical relevance of serum interleukin-6 in Crohn's disease: single point measurements, therapy monitoring, and prediction of clinical relapse. Am J Gastroenterol 94, 2156-2164, (1999).*

217 *Sategna-Guidetti, C. et al. Tumor necrosis factor/cachectin in Crohn's disease. Relation of serum concentration to disease activity. Recenti progressi in medicina 84, 93-99 (1993).*

218 *Maeda, M. et al. Serum tumor necrosis factor activity in inflammatory bowel disease. Immunopharmacol Immunotoxicol 14, 451-461, (1992).*

219 *Sullivan, K. et al. Epigenetic regulation of tumor necrosis factor alpha. Mol. Cell. Biol. 27, 5147-5160 (2007).*

220 *Sato, T. et al. Long-term Expansion of Epithelial Organoids From Human Colon, Adenoma, Adenocarcinoma, and Barrett's Epithelium. Gastro. 141, 1762-1772, doi: (2011).*

221 *Sato, T. et al. Single Lgr5 stem cells build crypt-villus structures in vitro without a mesenchymal niche. Nature 459, 262-265, (2009).*

222 *Kuchler, R. J. Biochemical methods in cell culture and virology. (Dowden, Hutchinson & Ross Stroudsburg, 1977).*

223 *Ogino, S., Kawasaki, T., Kirkner, G. J., Loda, M. & Fuchs, C. S. CpG Island Methylator Phenotype-Low (CIMP-Low) in Colorectal Cancer: Possible Associations with Male Sex and KRAS Mutations. The J. of Mol. diagnostics : JMD 8, 582-588, (2006).*

224 *Lopez-Garcia, C., Klein, A. M., Simons, B. D. & Winton, D. J. Intestinal stem cell replacement follows a pattern of neutral drift. Sci. 330, 822-825, (2010).*

225 *Scoville, D. H., Sato, T., He, X. C. & Li, L. Current view: intestinal stem cells and Sig.ing. Gastro. 134, 849-864 (2008).*

226 *Lei, N. Y. et al. Intestinal Subepithelial Myofibroblasts Support the Growth of Intestinal Epithelial Stem Cells. PLoS ONE 9, e84651, (2014).*

227 *Lahar, N. et al. Intestinal Subepithelial Myofibroblasts Support in vitro and in vivo Growth of Human Small Intestinal Epithelium. PLoS ONE 6, e26898, (2011).*

228 *Assenov, Y. et al. Comprehensive analysis of DNA methylation data with RnBeads. Nat Meth 11, 1138-1140, (2014).*

229 *Xiong, Z. & Laird, P. COBRA: a sensitive and quantitative DNA methylation assay. Nucleic Acids Res 25, 2532 - 2534 (1997).*

230 *Wang, D. et al. A low-cost, high-throughput polyacrylamide gel electrophoresis system for genotyping with microsatellite DNA markers. Crop Sci. 43, 1828-1832 (2003).*

231 *Meissner, F., Scheltema, R. A., Mollenkopf, H.-J. & Mann, M. Direct Proteomic Quantification of the Secretome of Activated Immune Cells. Sci. 340, 475-478, (2013).*

232 *Nesvizhskii, A. I., Keller, A., Kolker, E. & Aebersold, R. A statistical model for identifying proteins by tandem mass spectrometry. Analytical Chem. 75, 4646-4658 (2003).*

233 *Ashburner, M. et al. Gene ontology: tool for the unification of biology: the Gene Ontology Consortium. Nat Genet 25, (2000).*

234 *Day, A., Lemberg, D. & Gearry, R. Inflammatory bowel disease in Australasian children and adolescents. Gastro. Res. and practice 2014 (2014).*

235 *Gearry, R. B. et al. High incidence of Crohn's disease in Canterbury, New Zealand: results of an epidemiologic study. Inflamm Bowel Dis 12, 936-943, (2006).*

236 *Cosnes, J., Gower–Rousseau, C., Seksik, P. & Cortot, A. Epidemiology and Natural History of Inflammatory Bowel Diseases. Gastro. 140, 1785-1794.e1784, (2011).*

237 *Lakatos, P. L. Recent trends in the epidemiology of inflammatory bowel diseases: up or down? World J. of Gastro. 12, 6102-6108 (2006).*

238 *Hendrickson, B. A., Gokhale, R. & Cho, J. H. Clinical Aspects and PathoPhys. of Inflammatory Bowel Disease. Clin. Microbiol. Rev. 15, 79-94, (2002).*

239 *Xavier, R. J. & Podolsky, D. K. Unravelling the pathogenesis of inflammatory bowel disease. Nature 448, 427-434, (2007).*

240 *Panes, J. Inflammatory bowel disease: pathogenesis and targets for therapeutic interventions. Acta Physiol Scand 173, 159-165, (2001).*

241 *Khor, B., Gardet, A. & Xavier, R. J. Genetics and pathogenesis of inflammatory bowel disease. Nature 474, 307-317 (2011).*

242 *Graham, D. B. & Xavier, R. J. From genetics of inflammatory bowel disease towards mechanistic insights. Trends Immunol. 34, 371-378, (2013).*

243 *Levin, A. & Shibolet, O. Infliximab in ulcerative colitis. Biologics : Targets & Therapy 2, 379-388 (2008).*

244 *Card, T., Hubbard, R. & Logan, R. F. A. Mortality in inflammatory bowel disease: a population-based cohort study. Gastro. 125, 1583-1590. (2003).*

245 *Ekbom, A., Helmick, C., Zack, M. & Adami, H. O. Increased risk of large-bowel cancer in Crohn's disease with colonic involvement. Lancet 336, 357-359 (1990).*

246 *Issa, J. P., Ahuja, N., Toyota, M., Bronner, M. P. & Brentnall, T. A. Accelerated age-related CpG island methylation in ulcerative colitis. Cancer Res 61 (2001).*

247 *Karatzas, P. S., Gazouli, M., Safioleas, M. & Mantzaris, G. J. DNA methylation changes in inflammatory bowel disease. Annals of Gastro. : Quarterly Publication of the Hellenic Society of Gastro. 27, 125-132 (2014).*

248 *Azarschab, P., Porschen, R., Gregor, M., Blin, N. & Holzmann, K. Epigenetic control of the E-cadherin gene (CDH1) by CpG methylation in colectomy samples of patients with ulcerative colitis. Genes Chromosomes Cancer 35, 121-126, (2002).*

249 *Brown, K. A. et al. Lamina propria and circulating interleukin-6 in newly diagnosed pediatric inflammatory bowel disease patients. Am J Gastroenterol 97, 2603-2608, (2002).*

250 *Kellermayer, R. et al. Colonic mucosal DNA methylation, immune response, and microbiome patterns in Toll-like receptor 2-knockout mice. The FASEB J. 25, 1449-1460, (2011).*

251 *Xia, D., Wang, D., Kim, S.-H., Katoh, H. & DuBois, R. N. Prostaglandin E2 promotes intestinal tumor growth via DNA methylation. Nat. Med. 18, 224-226 (2012).*

252 *Garcia-Albeniz, X. & Chan, A. T. Aspirin for the prevention of colorectal cancer. Best practice & Res.. Clinical Gastro. 25, 461-472, (2011).*

253 *Noreen, F. et al. Modulation of age- and cancer-associated DNA methylation change in the healthy colon by aspirin and lifestyle. J Natl Cancer Inst 106, (2014).*

254 *Triantafillidis, J. K., Nasioulas, G. & Kosmidis, P. A. Colorectal cancer and inflammatory bowel disease: epidemiology, risk factors, mechanisms of carcinogenesis and prevention strategies. Anticancer Res. 29, 2727-2737 (2009).*

255 *Lam, L. L. et al. Factors underlying variable DNA methylation in a human community cohort. Proc. Nat. Ac. Sci 109, 17253-17260, (2012).*

256 *Bjornsson, H. T. et al. Intra-individual change over time in DNA methylation with familial clustering. JAMA : the J. of the Am.n Medical Association 299, (2008).*

257 *Jung, M. & Pfeifer, G. P. Aging and DNA methylation. BMC Biol. 13, 1-8, (2015).*

258 *Horvath, S. DNA methylation age of human tissues and cell types. Genome Biology 14, R115 (2013).*

259 *Weidner, C. I. et al. Aging of blood can be tracked by DNA methylation changes at just three CpG sites. Genome Biol 15, (2014).*

260 *Amer, M. & Qayyum, R. Relation Between Serum 25-Hydroxyvitamin D and C-Reactive Protein in Asymptomatic Adults (From the Continuous National Health and Nutrition Examination Survey 2001 to 2006). The Am. J. of Cardiology 109, 226-230, (2012).*

261 *Ananthakrishnan, A. N. Environmental triggers for inflammatory bowel disease. Current Gastro. reports 15, 1-7 (2013).*

262 *Zhang, Y. et al. Vitamin D Inhibits Monocyte/Macrophage Proinflammatory Cytokine Production by Targeting MAPK Phosphatase-1. The J. of Immunol. 188, 2127-2135, (2012).*

263 *Neve, A., Corrado, A. & Cantatore, F. P. Immunomodulatory effects of vitamin D in peripheral blood monocyte-derived macrophages from patients with rheumatoid arthritis. Clinical and Exp. medicine 14, 275-283, (2014).*

264 *Simopoulos, A. P. Omega-3 fatty acids in inflammation and autoimmune diseases. J. of the Am.n College of Nutrition 21, 495-505 (2002).*

265 *Schmelzer, C. et al. Functions of coenzyme Q10 in inflammation and gene expression. BioFactors 32, 179-183 (2008).*

266 *Zhang, S. et al. Epigenetic regulation of TNFA expression in periodontal disease. J. of periodontology 84, 1606-1616, (2013).*

267 Tsuchiya, S. et al. Establishment and characterization of a human acute monocytic leukemia cell line (THP-1). Int. J. of cancer. J. Int. du cancer 26, 171-176 (1980).

268 Ananthakrishnan, A. N. et al. Higher Predicted Vitamin D Status Is Associated With Reduced Risk of Crohn's Disease. Gastro. 142, 482-489 (2012).

269 Grant, W. B. Relation between prediagnostic serum 25-hydroxyvitamin D level and incidence of breast, colorectal, and other cancers. J. Photochem. Photobiol. B: Biol. 101, 130-136 (2010).

270 Allin, K. H. & Nordestgaard, B. G. Elevated C-reactive protein in the diagnosis, prognosis, and cause of cancer. Critical reviews in clinical laboratory Sci.s 48, 155-170, (2011).

271 Erlinger, T. P., Platz, E. A., Rifai, N. & Helzlsouer, K. J. C-reactive protein and the risk of incident colorectal cancer. JAMA : the J. of the Am.n Medical Association 291, 585-590, (2004).

272 Konikoff, M. R. & Denson, L. A. Role of fecal calprotectin as a biomarker of intestinal inflammation in inflammatory bowel disease. Inflamm Bowel Dis 12, 524-534 (2006).

273 Raftery, T. et al. Vitamin D Status Is Associated with Intestinal Inflammation as Measured by Fecal Calprotectin in Crohn's Disease in Clinical Remission. Dig. Dis. Sci. 60, 2427-2435, (2015).

274 Komatsu, M. et al. Tumor Necrosis Factor-a in Serum of Patients with Inflammatory Bowel Disease as Measured by a Highly Sensitive Immuno-PCR. Clin. Chem. 47, 1297-1301 (2001).

275 Dionne, S., Hiscott, J., D'Agata, I., Duhaime, A. & Seidman, E. G. Quantitative PCR Analysis of TNF-a and IL-1b mRNA Levels in Pediatric IBD Mucosal Biopsies. Dig. Dis. Sci. 42, 1557-1566, (1997).

276 Mazlam, M. Z. & Hodgson, H. J. Peripheral blood monocyte cytokine production and acute phase response in inflammatory bowel disease. Gut 33, 773-778 (1992).

277 Campión, J., Milagro, F. I., Goyenechea, E. & Martínez, J. A. TNF-a Promoter Methylation as a Predictive Biomarker for Weight-loss Response. Obesity 17, 1293-1297 (2009).

278 *El Gazzar, M., Yoza, B. K., Hu, J. Y., Cousart, S. L. & McCall, C. E. Epigenetic silencing of tumor necrosis factor alpha during endotoxin tolerance. The J. of Bio. Chem. 282, 26857-26864, (2007).*

279 *Cao, Q. et al. Inhibiting DNA Methylation by 5-Aza-2'-deoxycytidine Ameliorates Atherosclerosis Through Suppressing Macrophage Inflammation. Endocr. 155, 4925-4938, (2014).*

280 *Wallner, S. et al. Epigenetic dynamics of monocyte-to-macrophage differentiation. Epigenetics & Chromatin 9, 1-17, (2016).*

281 *Takei, S., Fernandez, D., Redford, A. & Toyoda, H. Methylation status of 5'-regulatory region of tumor necrosis factor alpha gene correlates with differentiation stages of monocytes. Biochem. Biophys. Res. Commun. 220, 606-612 (1996).*

282 *Reinius, L. E. et al. Differential DNA Methylation in Purified Human Blood Cells: Implications for Cell Lineage and Studies on Disease Susceptibility. PLoS ONE 7, e41361, (2012).*

283 *Autier, P. & Gandini, S. Vitamin d supplementation and total mortality: A meta-analysis of randomized controlled trials. Archives of Internal Medicine 167, 1730-1737, (2007).*

284 *Valdivielso, J. M. & Fernandez, E. Vitamin D receptor polymorphisms and diseases. Clinica chimica acta; Int. J. Clin. Chem. 371, 1-12, (2006).*

285 *Muindi, J. R. et al. CYP24 splicing variants are associated with different patterns of constitutive and calcitriol-inducible CYP24 activity in human prostate cancer cell lines. J Steroid Biochem Mol Biol 103, 334-337, (2007).*

286 *Alkhouri, R. H., Hashmi, H., Baker, R. D., Gelfond, D. & Baker, S. S. Vitamin and Mineral Status in Patients With Inflammatory Bowel Disease. J. of Pediatric Gastro. and Nutrition 56, 89-92, (2013).*

287 *Hinz, B. et al. The Myofibroblast: One Function, Multiple Origins. The Am. J. of Path. 170, 1807-1816, (2007).*

288 *Desmouliere, A., Geinoz, A., Gabbiani, F. & Gabbiani, G. Transforming growth factor-beta 1 induces alpha-smooth muscle actin expression in granulation tissue myofibroblasts and in quiescent and growing cultured fibroblasts. J Cell Biol 122, 103-111 (1993).*

289 *De Boeck, A. et al. Differential secretome analysis of cancer-associated fibroblasts and bone marrow-derived precursors to identify microenvironmental regulators of colon cancer progression. Proteomics 13, 379-388 (2013).*

290 *Yen, T.-H. & Wright, N. A. The Gastro. tract stem cell niche. Stem Cell Reviews 2, 203-212, (2006).*

291 *Durand, A. et al. Functional intestinal stem cells after Paneth cell ablation induced by the loss of transcription factor Math1 (Atoh1). Proc. Nat. Ac. Sci of the United States of Am. 109, 8965-8970, (2012).*

292 *San Roman, Adrianna K., Jayewickreme, Chenura D., Murtaugh, L. C. & Shivdasani, Ramesh A. Wnt Secretion from Epithelial Cells and Subepithelial Myofibroblasts Is Not Required in the Mouse Intestinal Stem Cell Niche In Vivo. Stem Cell Reports 2, 127-134, doi: (2014).*

293 *Koch, S. et al. The Wnt Antagonist Dkk1 Regulates Intestinal Epithelial Homeostasis and Wound Repair. Gastro. 141, 259-268.e258 (2011).*

294 *Valcz, G. et al. Myofibroblast-Derived SFRP1 as Potential Inhibitor of Colorectal Carcinoma Field Effect. PLoS ONE 9, e106143 (2014).*

295 *Brittan, M. et al. Bone marrow derivation of pericryptal myofibroblasts in the mouse and human small intestine and colon. Gut 50, 752-757 (2002).*

296 *Hinz, B. Formation and function of the myofibroblast during tissue repair. The J. of investigative dermatology 127, 526-537, (2007).*

297 *Evans, R. A., Tian, Y. C., Steadman, R. & Phillips, A. O. TGF-beta1-mediated fibroblast-myofibroblast terminal differentiation-the role of Smad proteins. Exp Cell Res 282, 90-100 (2003).*

298 *Hinz, B. et al. Recent Developments in Myofibroblast Biology: Paradigms for Connective Tissue Remodeling. The Am. J. of Path. 180, 1340-1355, (2012).*

299 *Shiga, K. et al. Cancer-Associated Fibroblasts: Their Characteristics and Their Roles in Tumor Growth. Cancers 7, 2443-2458 (2015).*

300 *Hu, B., Gharaee-Kermani, M., Wu, Z. & Phan, S. H. Epigenetic regulation of myofibroblast differentiation by DNA methylation. The Am. J. of Path. 177, 21-28 (2010).*

301 *Bonnans, C., Chou, J. & Werb, Z. Remodelling the extracellular matrix in development and disease. Nat. Rev.. Mol. cell biology 15, 786-801(2014).*

302 *Babyatsky, M. W., Rossiter, G. & Podolsky, D. K. Expression of transforming growth factors alpha and beta in colonic mucosa in inflammatory bowel disease. Gastro. 110, 975-984 (1996).*

303 *Zerr, P. et al. Vitamin D receptor regulates TGF-beta Sig.ling in systemic sclerosis. Ann Rheum Dis 74, e20 (2015).*

304 *Livak, K. J. & Schmittgen, T. D. Analysis of relative gene expression data using real-time quantitative PCR and the 2(-Delta Delta C(T)) Method. Methods (San Diego, Calif.) 25, 402-408 (2001).*

305 *Evans, R. A., Tian, Y. a. C., Steadman, R. & Phillips, A. O. TGF-β1-mediated fibroblast–myofibroblast terminal differentiation—the role of smad proteins. Exp. Cell Res. 282, 90-100 (2003).*

306 *Calon, A. et al. Dependency of colorectal cancer on a TGF-beta-driven programme in stromal cells for metastasis initiation. Cancer Cell 22, 571-584 (2012).*

307 *Skeen, V. R. et al. BAG-1 suppresses expression of the key regulatory cytokine TGF-b1 in colorectal tumour cells. Oncogene 32, (2013).*

308 *Chen, A., Davis, B. H., Sitrin, M. D., Brasitus, T. A. & Bissonnette, M. Transforming growth factor-b1 Sig.ing contributes to Caco-2 cell growth inhibition induced by 1,25(OH)2D3. Am. J. of Phys. - Gastro. and Liv. Phys. 283, G864-G874, (2002).*

309 *Roessler, J. et al. Quantitative cross-validation and content analysis of the 450k DNA methylation array from Illumina, Inc. BMC Res. Notes 5, 1-7 (2012).*

310 *Li, Y., Spataro, B. C., Yang, J., Dai, C. & Liu, Y. 1,25-dihydroxyvitamin D inhibits renal interstitial myofibroblast activation by inducing hepatocyte growth factor expression. Kidney Int. 68, 1500-1510 (2005).*

311 *Ohchi, T. et al. Amphiregulin is a prognostic factor in colorectal cancer. Anticancer Res 32, 2315-2321 (2012).*

312 *Chen, H., Yang, W. W., Wen, Q. T., Xu, L. & Chen, M. TGF-beta induces fibroblast activation protein expression; fibroblast activation protein expression increases the proliferation, adhesion, and migration of HO-8910PM. Exp Mol Pathol 87, 189-194 (2009).*

313 *Ito, I. et al. A nonclassical vitamin D receptor pathway suppresses renal fibrosis. The J. Clin. investigation 123, 4579-4594 (2013).*

314 *R Skeen, V., Paterson, I., Paraskeva, C. & C Williams, A. TGF-β1 Sig.ling, connecting aberrant inflammation and colorectal tumorigenesis. Curr. Pharm. Des. 18, 3874-3888 (2012).*

315 *Beck, P. L. et al. Transforming Growth Factor-β Mediates Intestinal Healing and Susceptibility to Injury in Vitro and in Vivo Through Epithelial Cells. The Am. J. of Path. 162, 597-608 (2003).*

316 *Zi, Z., Chapnick, D. A. & Liu, X. Dynamics of TGF-b/Smad Sig.ing. FEBS Lett. 586, 1921-1928, (2012).*

317 *Massague, J. TGFβeta in Cancer. Cell 134, 215-230, (2008).*

318 *Seoane, J. Escaping from the TGFβeta anti-proliferative control. Carcinogenesis 27, 2148-2156, (2006).*

319 *Simmons, J. G., Pucilowska, J. B., Keku, T. O. & Lund, P. K. IGF-I and TGF-b1 have distinct effects on phenotype and proliferation of intestinal fibroblasts. Am. J. of Phys.-Gastro. and Liv. Phys. 283, G809-G818 (2002).*

320 *Vallance, B. A. et al. TGF-b1 gene transfer to the mouse colon leads to intestinal fibrosis. Am. J. of Phys.-Gastro. and Liv. Phys. 289, G116-G128 (2005).*

321 *Wynn, T. A. & Ramalingam, T. R. Mechanisms of fibrosis: therapeutic translation for fibrotic disease. Nat Med 18, 1028-1040 (2012).*

322 *Liu, J. et al. Wnt/b-catenin pathway forms a negative feedback loop during TGF-b1 induced human normal skin fibroblast-to-myofibroblast transition. J. of Dermatological Sci. 65, 38-49, (2012).*

323 *Akhmetshina, A. et al. Activation of canonical Wnt Sig.ling is required for TGF-b-mediated fibrosis. Nature Comm. 3, 735 (2012).*

324 *Gu, L. et al. Effect of TGF-beta/Smad Sig.ing pathway on lung myofibroblast differentiation. Acta pharmacologica Sinica 28, 382-391, (2007).*

325 *Hecker, L., Jagirdar, R., Jin, T. & Thannickal, V. J. Reversible Differentiation of Myofibroblasts by MyoD. Exp. Cell Res. 317, 1914-1921, (2011).*

326 *Messerschmidt, D. M., Knowles, B. B. & Solter, D. DNA methylation dynamics during epigenetic reprogramming in the germline and preimplantation embryos. Genes Dev. 28, 812-828, (2014).*

327 *Thillainadesan, G. et al. TGF-b-Dependent Active Demethylation and Expression of the p15ink4b Tumor Suppressor Are Impaired by the ZNF217/CoREST Complex. Mol. Cell 46, 636-649 (2012).*

328 *Cardenas, H. et al. TGF-b induces global changes in DNA methylation during the epithelial-to-mesenchymal transition in ovarian cancer cells. Epigenetics 9, 1461-1472 (2014).*

329 *Jorissen, R. N. et al. Metastasis-associated gene expression changes predict poor outcomes in patients with Dukes stage B and C colorectal cancer. Clin. Cancer. Res. 15, 7642-7651 (2009).*

330 *Saito, N., Nishimura, H. & Kameoka, S. Clinical significance of fibronectin expression in colorectal cancer. Mol. medicine reports 1, 77-81 (2008).*

331 *Hocevar, B. A., Brown, T. L. & Howe, P. H. TGF-beta induces fibronectin synthesis through a c-Jun N-terminal kinase-dependent, Smad4-independent pathway. The EMBO J. 18, 1345-1356 (1999).*

332 *Wikberg, M. L. et al. High intratumoral expression of fibroblast activation protein (FAP) in colon cancer is associated with poorer patient prognosis. Tumour Biology 34, 1013-1020 (2013).*

333 *Wu, M. Y. & Hill, C. S. TGF-b Superfamily Sig.ing in Embryonic Development and Homeostasis. Dev. Cell 16, 329-343 (2009).*

334 *Powell, D. W. et al. Myofibroblasts. II. Intestinal subepithelial myofibroblasts. Am. J. of Phys. - Cell Phys. 277, C183-C201 (1999).*

335 *Quail, D. F. & Joyce, J. A. Microenvironmental regulation of tumor progression and metastasis. Nat. Med. 19, 1423-1437 (2013).*

336 *Chassaing, B. & Darfeuille–Michaud, A. The Commensal Microbiota and Enteropathogens in the Pathogenesis of Inflammatory Bowel Diseases. Gastro. 140, 1720-1728.e1723 (2011).*

337 *Ghosh, S. & Ashcraft, K. An IL-6 link between obesity and cancer. Frontiers in bioSci. (Elite edition) 5, 461-478 (2012).*

338 Ramos-Nino, M. E. The Role of Chronic Inflammation in Obesity-Associated Cancers. ISRN Onc. 2013, 25 (2013).

339 Shivappa, N. et al. Inflammatory potential of diet and risk of colorectal cancer: a case-control study from Italy. The British J. of nutrition 114, 152-158 (2015).

340 Cader, M. Z. & Kaser, A. Recent advances in inflammatory bowel disease: mucosal immune cells in intestinal inflammation. Gut 62, 1653-1664 (2013).

341 Singer, II et al. Cyclooxygenase 2 is induced in colonic epithelial cells in inflammatory bowel disease. Gastro. 115, 297-306 (1998).

342 Kuroda, E. & Yamashita, U. Regulation of immune responses by prostaglandin. J. of UOEH 24, 289-299 (2002).

343 Greenhough, A. et al. The COX-2/PGE2 pathway: key roles in the hallmarks of cancer and adaptation to the tumour microenvironment. Carcinogenesis 30, 377-386 (2009).

344 Xia, D., Wang, D., Kim, S.-H., Katoh, H. & DuBois, R. N. Prostaglandin E2 promotes intestinal tumor growth via DNA methylation. Nat Med 18, 224-226 (2012).

345 Ogino, S. et al. Cyclooxygenase-2 expression is an independent predictor of poor prognosis in colon cancer. Clinical cancer Res. : an official J. of the Am.n Association for Cancer Res. 14, 8221-8227 (2008).

346 Aparna, R. et al. Selective inhibition of cyclooxygenase-2 (COX-2) by 1a, 25-dihydroxy-16-ene-23-yne-vitamin D3, a less calcemic vitamin D analog. J. Cell. Biochem. 104, 1832-1842 (2008).

347 Wang, Q. et al. Vitamin D inhibits COX-2 expression and inflammatory response by targeting thioesterase superfamily member 4. The J. of Bio. Chem. 289, 11681-11694 (2014).

348 Powell, D. W. et al. Myofibroblasts. I. Paracrine cells important in health and disease. The Am. J. of Phys. 277, C1-9 (1999).

349 Nakao, S. et al. TNF-a-induced prostaglanding E2 release is mediated by the activation of COX-2 transcription via NFkB in human gingival fibroblasts. Mol. Cell. Biochem. 238, 11-18 (2002).

350 Lin, C. C. et al. Tumor necrosis factor-alpha-induced cyclooxygenase-2 expression in human tracheal smooth muscle cells: involvement of p42/p44 and p38 mitogen-activated protein kinases and nuclear factor-kappaB. Cell Sig. 16, 597-607 (2004).

351 *Ke, J. et al. Role of NF-kappaB in TNF-alpha-induced COX-2 expression in synovial fibroblasts from human TMJ. J Dent Res 86, 363-367 (2007).*

352 *Dieckgraefe, B., Stenson, W., Korzenik, J., Swanson, P. & Harrington, C. Analysis of mucosal gene expression in inflammatory bowel disease by parallel oligonucleotide arrays. Physiol. Genomics 4, 1-11 (2000).*

353 *Barton, C. A. et al. Collagen and calcium-binding EGF domains 1 is frequently inactivated in ovarian cancer by aberrant promoter hypermethylation and modulates cell migration and survival. Br. J. Cancer 102, 87-96 (2010).*

354 *Heller, G. et al. Genome-wide CpG island methylation analyses in non-small cell lung cancer patients. Carcinogenesis 34, 513-521 (2013).*

355 *Prosser, D. E. & Jones, G. Enzymes involved in the activation and inactivation of vitamin D. Trends Biochem Sci 29, 664-673 (2004).*

356 *Aranow, C. Vitamin D and the Immune System. J. of investigative medicine : the official publication of the Am.n Federation for Clinical Res. 59, 881-886 (2011).*

357 *Gargus, M. et al. Human esophageal myofibroblasts secrete proinflammatory cytokines in response to acid and Toll-like receptor 4 ligands. Am. J. of Phys.. Gastro. and Liv. Phys. 308, G904-923 (2015).*

358 *Neurath, M. F. Cytokines in inflammatory bowel disease. Nat Rev Immunol 14, 329-342 (2014).*

359 *Zenlea, T. & Peppercorn, M. A. Immunosuppressive therapies for inflammatory bowel disease. World J. of Gastro. : WJG 20, 3146-3152 (2014).*

360 *Rothwell, P. M. et al. Long-term effect of aspirin on colorectal cancer incidence and mortality: 20-year follow-up of five randomised trials. The Lancet 376, 1741-1750 (2010)*

361 *Kim, E. C. et al. PGE expression in human colonic fibroblasts. Am. J. of Phys. - Cell Phys. 275, C988-C994 (1998).*

362 *Liu, X. et al. Vitamin D Modulates Prostaglandin E2 Synthesis and Degradation in Human Lung Fibroblasts. Am. J. of Respiratory Cell and Mol. Biology 50, 40-50 (2013).*

363 *Neri, S. et al. Cancer cell invasion driven by extracellular matrix remodeling is dependent on the properties of cancer-associated fibroblasts. J Cancer Res Clin Oncol 142, 437-446 (2016).*

364 Fullár, A. et al. Remodeling of extracellular matrix by normal and tumor-associated fibroblasts promotes cervical cancer progression. BMC Cancer 15, 1-16 (2015).

365 Owens, B. M. J. Inflammation, Innate Immunity, and the Intestinal Stromal Cell Niche: Opportunities and Challenges. Frontiers in Immunol. 6, 319 (2015).

366 Spenlé, C. et al. Dysregulation of laminins in intestinal inflammation. Pathol. Biol. 60, 41-47, doi: (2012).

367 Dieckgraefe, B. K., Stenson, W. F., Korzenik, J. R., Swanson, P. E. & Harrington, C. A. Analysis of mucosal gene expression in inflammatory bowel disease by parallel oligonucleotide arrays. Physiol. Genomics 4, 1-11 (2000).

368 Atreya, R. & Neurath, M. F. Involvement of IL-6 in the pathogenesis of inflammatory bowel disease and colon cancer. Clin. Rev. Allergy Immunol. 28, 187-195 (2005).

369 Mazzoccoli, G. et al. ARNTL2 and SERPINE1: potential biomarkers for tumor aggressiveness in colorectal cancer. J. Cancer Res. Clin. Oncol. 138, 501-511 (2012).

370 Gillespie, E. et al. Plasminogen activator inhibitor-1 is increased in colonic epithelial cells from patients with colitis-associated cancer. J. of Crohn's and Colitis 7, 403-411 (2013).

371 Le Loupp, A.-G. et al. Activation of the prostaglandin D2 metabolic pathway in Crohn's disease: involvement of the enteric nervous system. BMC Gastro. 15, 112 (2015).

372 Milner, C. M. & Day, A. J. TSG-6: a multifunctional protein associated with inflammation. J. Cell Sci. 116, 1863-1873 (2003).

373 Sala, E. et al. Mesenchymal Stem Cells Reduce Colitis in Mice via Release of TSG6, Independently of Their Localization to the Intestine. Gastro. 149, 163-176.e120 (2015).

374 Pei, Y. et al. WNT Sig.ing increases proliferation and impairs differentiation of stem cells in the developing cerebellum. Development 139, 1724-1733 (2012).

375 Zou, L. et al. Proliferation, migration, and neuronal differentiation of the endogenous neural progenitors in hippocampus after fimbria fornix transection. The Int. J. of neuroSci. 120, 192-200 (2010).

376 Ang, P. W. et al. Comprehensive profiling of DNA methylation in colorectal cancer reveals subgroups with distinct clinicopathological and Mol. features. BMC Cancer 10, 227 (2010).

377 Hobaus, J. et al. Increased copy-number and not DNA hypomethylation causes overexpression of the candidate proto-oncogene CYP24A1 in colorectal cancer. Int. J. of cancer. J. Int. du cancer (2013).

378 Kósa, J. P. et al. CYP24A1 inhibition facilitates the anti-tumor effect of vitamin D3 on colorectal cancer cells. World J. of Gastro.: WJG 19, 2621 (2013).

379 Pendas-Franco, N., Aguilera, O., Pereira, F., Gonzalez-Sancho, J. M. & Munoz, A. Vitamin D and Wnt/beta-catenin pathway in colon cancer: role and regulation of DICKKOPF genes. Anticancer Res 28, 2613-2623 (2008).

380 Siegel, R., Naishadham, D. & Jemal, A. Cancer statistics, 2012. CA: a cancer J. for clinicians 62, 10-29 (2012).

381 Ouakrim, D. A. et al. Trends in colorectal cancer mortality in Europe: retrospective analysis of the WHO mortality database. (2015).

382 Haggar, F. A. & Boushey, R. P. Colorectal cancer epidemiology: incidence, mortality, survival, and risk factors. Clinics in colon and rectal surgery 22, 191-197 (2009).

383 Meteoglu, I. et al. Nuclear Factor Kappa B, Matrix Metalloproteinase-1, p53, and Ki-67 Expressions in the Primary Tumors and the Lymph Node Metastases of Colorectal Cancer Cases. Gastro. Res. and practice 2015 (2015).

384 Ogino, S. & Goel, A. Mol. Classification and Correlates in Colorectal Cancer. The J. of Mol. Diagnostics : JMD 10, 13-27 (2008).

385 Toyota, M. et al. CpG island methylator phenotype in colorectal cancer. Proc. Nat. Ac. Sci 96, 8681-8686 (1999).

386 Ogino, S. et al. Evaluation of Markers for CpG Island Methylator Phenotype (CIMP) in Colorectal Cancer by a Large Population-Based Sample. The J. of Mol. diagnostics : JMD 9, 305-314 (2007).

387 Mojarad, E. N., Kuppen, P. J. K., Aghdaei, H. A. & Zali, M. R. The CpG island methylator phenotype (CIMP) in colorectal cancer. Gastro. and Hepatology From Bed to Bench 6, 120-128 (2013).

388 Issa, J.-P. CpG island methylator phenotype in cancer. Nat. Rev. Can. 4, 988-993 (2004).

389 *de Sousa E Melo, F. et al. Methylation of Cancer-Stem-Cell-Associated Wnt Target Genes Predicts Poor Prognosis in Colorectal Cancer Patients. Cell Stem Cell 9, 476-485 (2011).*

390 *Juo, Y. Y. et al. Prognostic value of CpG island methylator phenotype among colorectal cancer patients: a systematic review and meta-analysis. Annals of Onc. : official J. of the European Society for Medical Onc. / ESMO 25, 2314-2327 (2014).*

391 *Gnyszka, A., Jastrzebski, Z. & Flis, S. DNA methyltransferase inhibitors and their emerging role in epigenetic therapy of cancer. Anticancer Res. 33, 2989-2996 (2013).*

392 *Flis, S., Gnyszka, A. & Flis, K. DNA Methyltransferase Inhibitors Improve the Effect of Chemotherapeutic Agents in SW48 and HT-29 Colorectal Cancer Cells. PLoS ONE 9, e92305 (2014).*

393 *Lyko, F. & Brown, R. DNA Methyltransferase Inhibitors and the Development of Epigenetic Cancer Therapies. J. Natl. Cancer Inst. 97, 1498-1506 (2005).*

394 *Cheray, M., Pacaud, R., Nadaradjane, A., Vallette, F. M. & Cartron, P.-F. Specific inhibition of one DNMT1-including complex influences tumor initiation and progression. Clinical Epigenetics 5, 9-9 (2013).*

395 *Robsahm, T. E., Tretli, S., Dahlback, A. & Moan, J. Vitamin D3 from sunlight may improve the prognosis of breast-, colon- and prostate cancer (Norway). Cancer Causes Control 15, 149-158 (2004).*

396 *Ng, K. et al. Circulating 25-Hydroxyvitamin D Levels and Survival in Patients With Colorectal Cancer. J. Clin. Onc. 26, 2984-2991 (2008).*

397 *Moan, J. et al. Solar radiation, vitamin D and survival rate of colon cancer in Norway. J. of photoChem. and photobiology. B, Biology 78, 189-193 (2005).*

398 *Zgaga, L. et al. Plasma Vitamin D Concentration Influences Survival Outcome After a Diagnosis of Colorectal Cancer. J. Clin. Onc. (2014).*

399 *Wesa, K. M. et al. Serum 25-hydroxy vitamin D and survival in advanced colorectal cancer: a retrospective analysis. Nutr. Cancer 67, 424-430 (2015).*

400 *Sun, H. et al. CYP24A1 is a potential biomarker for the progression and prognosis of human colorectal cancer. Human Path. 50, 101-108 (2016).*

401 *Vanoirbeek, E. et al. PDLIM2 expression is driven by vitamin D and is involved in the pro-adhesion, and anti-migration and -invasion activity of vitamin D. Oncogene 33, 1904-1911 (2014).*

402 *Giuliano, A. R. & Wood, R. J. Vitamin D-regulated calcium transport in Caco-2 cells: unique in vitro model. The Am. J. of Phys. 260, G207-212 (1991).*

403 *Samuel, S. and Sitrin, M. D., Vitamin D's role in cell proliferation and differentiation. Nutrition Reviews, 66: S116–S124 (2008)*

404 *Kim, M. S., Lee, J. & Sidransky, D. DNA methylation markers in colorectal cancer. Cancer Metastasis Rev 29, 181-206 (2010).*

405 *Fang, J. Y. & Richardson, B. C. The MAPK Sig.ling pathways and colorectal cancer. The Lancet. Onc. 6, 322-327 (2005).*

406 *Voloshanenko, O. et al. Wnt secretion is required to maintain high levels of Wnt activity in colon cancer cells. Nature Comm. 4 (2013).*

407 *Gonzalez-Sancho, J. M., Larriba, M. J., Ordonez-Moran, P., Palmer, H. G. & Munoz, A. Effects of 1 alpha,25-dihydroxyvitamin D-3 in human colon cancer cells. Anticancer Res. 26, 2669-2681 (2006).*

408 *Byers, S. W., Rowlands, T., Beildeck, M. & Bong, Y.-S. Mechanism of action of vitamin D and the vitamin D receptor in colorectal cancer prevention and treatment. Rev. Endocr. Metab. Disord. 13, 31-38 (2012).*

409 *Aguilera, O. et al. The Wnt antagonist DICKKOPF-1 gene is induced by 1 alpha,25-dihydroxyvitamin D-3 associated to the differentiation of human colon cancer cells. Carcinogenesis 28 (2007).*

410 *Rohan, J. N. P. & Weigel, N. L. 1a,25-Dihydroxyvitamin D(3) Reduces c-Myc Expression, Inhibiting Proliferation and Causing G(1) Accumulation in C4-2 Prostate Cancer Cells. Endocr. 150, 2046-2054 (2009).*

411 *Mezawa, H. et al. Serum vitamin D levels and survival of patients with colorectal cancer: Post-hoc analysis of a prospective cohort study. BMC Cancer 10, 1-8, (2010).*

412 *Wheeler, J. M. et al. Hypermethylation of the promoter region of the E-cadherin gene (CDH1) in sporadic and ulcerative colitis associated colorectal cancer. Gut 48, 367-371 (2001).*

413 Pálmer, H. G. et al. Vitamin D3 promotes the differentiation of colon carcinoma cells by the induction of E-cadherin and the inhibition of ß-catenin Sig.ing. The J. of Cell Biology 154, 369-387 (2001).

414 Stolfi, C. et al. Involvement of interleukin-21 in the regulation of colitis-associated colon cancer. J Exp Med 208, 2279-2290 (2011).

415 Shaknovich, R. et al. DNA methylation signatures define Mol. subtypes of diffuse large B cell lymphoma. Blood (2010).

416 Kaji, I., Karaki, S. & Kuwahara, A. Taste sensing in the colon. Curr Pharm Des 20, 2766-2774 (2014).

417 Feldmesser, E. et al. Widespread ectopic expression of olfactory receptor genes. BMC Genomics 7, 1-18 (2006).

418 Nair, V. B., Samuel, C. S., Separovic, F., Hossain, M. A. & Wade, J. D. Human relaxin-2: historical perspectives and role in cancer biology. Amino Acids 43, 1131-1140 (2012).

419 Bork, S. et al. DNA methylation pattern changes upon long-term culture and aging of human mesenchymal stromal cells. Aging cell 9, 54-63 (2010).

420 Ueki, T. et al. Aberrant CpG island methylation in cancer cell lines arises in the primary cancers from which they were derived. Oncogene 21, 2114-2117 (2002).

421 Yi, J. et al. P16 gene methylation in colorectal cancers is associated with Duke s staging. World J. of Gastro. 7, 722-725 (2001).

422 Marik, R. et al. DNA methylation-related vitamin D receptor insensitivity in breast cancer. Cancer Biology & Therapy 10, 44-53 (2010).

423 Essa, S. et al. Signature of VDR miRNAs and epigenetic modulation of vitamin D Sig.ing in melanoma cell lines. Anticancer Res. 32, 383-389 (2012).

424 Hofman-Bang, J., Gravesen, E., Olgaard, K. & Lewin, E. Epigenetic methylation of parathyroid CaR and VDR promoters in Exp. secondary hyperparathyroidism. Int. J. of nephrology 2012 (2012).

425 Chandel, N. et al. VDR hypermethylation and HIV-induced T cell loss. J. Leukocyte Biol. 93, 623-631 (2013).

426 Smirnoff, P., Liel, Y., Gnainsky, J., Shany, S. & Schwartz, B. The protective effect of estrogen against chemically induced murine colon carcinogenesis is associated with

decreased CpG island methylation and increased mRNA and protein expression of the colonic vitamin D receptor. Oncol. Res. 11, 255-264 (1999).

427 Miyamoto, K. et al. Structural organization of the human vitamin D receptor chromosomal gene and its promoter. Mol. Endocr. (Baltimore, Md.) 11, 1165-1179 (1997).

428 Pilz, S., Tomaschitz, A., Obermayer-Pietsch, B., Dobnig, H. & Pieber, T. R. Epidemiology of Vitamin D Insufficiency and Cancer Mortality. Anticancer Res. 29, 3699-3704 (2009).

429 Grant, W. B. & Mohr, S. B. Ecological studies of ultraviolet B, vitamin D and cancer since 2000. Ann. Epidemiol. 19, 446-454 (2009).

430 Giovannucci, E. et al. Prospective study of predictors of vitamin D status and cancer incidence and mortality in men. J Natl Cancer Inst 98 (2006).

431 Freedman, D. M., Looker, A. C., Chang, S. C. & Graubard, B. I. Prospective study of serum vitamin D and cancer mortality in the United States. J Natl Cancer Inst 99 (2007).

432 Garland, C. F. & Garland, F. C. Do sunlight and vitamin D reduce the likelihood of colon cancer? Int J Epidemiol 9 (1980).

433 Apperly, F. L. The relation of solar radiation to cancer mortality in North Am.. Cancer Res. 1, 191-195 (1941).

434 Hendrickse, R. Diseases of Children in the Subtropics and Tropics. Arch. Dis. Child. 53, 524 (1978).

435 Fiscella, K., Winters, P., Tancredi, D., Hendren, S. & Franks, P. Racial Disparity in Death from Colorectal Cancer: Does Vitamin D Deficiency Contribute? Medical laboratory Sci.s 33, 13 (1976).

436 Nair, R. & Maseeh, A. Vitamin D: The "sunshine" vitamin. J. of Pharmacology & Pharmacotherapeutics 3, 118-126 (2012).

437 Krishnan, A. V. & Feldman, D. Mol. pathways mediating the anti-inflammatory effects of calcitriol: implications for prostate cancer chemoprevention and treatment. Endocrine-Related Cancer 17, R19-R38 (2010).

438 *Kallay, E. et al. Characterization of a vitamin D receptor knockout mouse as a model of colorectal hyperproliferation and DNA damage. Carcinogenesis 22, 1429-1435 (2001).*

439 *Sidelnikov, E. et al. Effects of calcium and vitamin D on MLH1 and MSH2 expression in rectal mucosa of sporadic colorectal adenoma patients. Cancer epidemiology, biomarkers & prevention : a publication of the Am.n Association for Cancer Res., cosponsored by the Am.n Society of Preventive Onc. 19, 1022-1032 (2010).*

440 *Krishnan, A. V. & Feldman, D. Mechanisms of the anti-cancer and anti-inflammatory actions of vitamin D. Annu Rev Pharmacol Toxicol 51, 311-336 (2011).*

441 *Hartnett, L. & Egan, L. J. Inflammation, DNA methylation and colitis-associated cancer. Carcinogenesis, bgs006 (2012).*

442 *Fleet, J. C., DeSmet, M., Johnson, R. & Li, Y. Vitamin D and Cancer: A review of Mol. mechanisms. The Biochemical J. 441, 61-76 (2012).*

443 *Heijmans, B. T. et al. Persistent epigenetic differences associated with prenatal exposure to famine in humans. Proc. Nat. Ac. Sci 105, 17046-17049 (2008).*

444 *Jones, M. J., Goodman, S. J. & Kobor, M. S. DNA methylation and healthy human aging. Aging cell 14, 924-932 (2015).*

445 *Skaaby, T. et al. Longitudinal associations between lifestyle and vitamin D: A general population study with repeated vitamin D measurements. Endocrine 51, 342-350 (2016).*

446 *Mandir, N., FitzGerald, A. J. & Goodlad, R. A. Differences in the effects of age on intestinal proliferation, crypt fission and apoptosis on the small intestine and the colon of the rat. Int. J. of Exp. Path. 86, 125-130 (2005).*

447 *Giovannucci, E. & Ogino, S. DNA Methylation, Field Effects, and Colorectal Cancer. J. Natl. Cancer Inst. 97, 1317-1319 (2005).*

448 *Seitz, H. K. & Becker, P. Alcohol Met. and cancer risk. Alcohol Res. and Health 30, 38 (2007).*

449 *Sauer, J. et al. Ageing, chronic alcohol consumption and folate are determinants of genomic DNA methylation, p16 promoter methylation and the expression of p16 in the mouse colon. The British J. of nutrition 104, 24-30 (2010).*

450 Horváth, H. C. et al. The Candidate Oncogene CYP24A1: A Potential Biomarker for Colorectal Tumorigenesis. J. of HistoChem. & CytoChem. 58, 277-285 (2010).

451 Anderson, M. G., Nakane, M., Ruan, X., Kroeger, P. E. & Wu-Wong, J. R. Expression of VDR and CYP24A1 mRNA in human tumors. Cancer Chemotherapy and Pharmacology 57, 234-240 (2006).

452 Mahida, Y. R. et al. Adult human colonic subepithelial myofibroblasts express extracellular matrix proteins and cyclooxygenase-1 and -2. Am. J. of Phys. - Gastro. and Liv. Phys. 273, G1341-G1348 (1997).

453 McKaig, B. C., Hughes, K., Tighe, P. J. & Mahida, Y. R. Differential expression of TGF-beta isoforms by normal and inflammatory bowel disease intestinal myofibroblasts. Am. J. of Phys.. Cell Phys. 282, C172-182 (2002).

454 Roulis, M. et al. Intestinal myofibroblast-specific Tpl2-Cox-2-PGE(2) pathway links innate sensing to epithelial homeostasis. Proc. Nat. Ac. Sci of the United States of Am. 111, E4658-E4667 (2014).

455 Hughes, K. R., Sablitzky, F. & Mahida, Y. R. Expression profiling of Wnt family of genes in normal and inflammatory bowel disease primary human intestinal myofibroblasts and normal human colonic crypt epithelial cells. Inflamm Bowel Dis 17, 213-220 (2011).

456 Pilon, C. et al. Methylation Status of Vitamin D Receptor Gene Promoter in Benign and Malignant Adrenal Tumors. Int. J. of Endocr. 2015, 7 (2015).

457 Vincent, A. et al. Cryosectioning the intestinal crypt-villus axis: An ex vivo method to study the dynamics of epigenetic modifications from stem cells to differentiated cells. Stem Cell Res. 14, 105-113 (2015).

458 Sheaffer, K. L. et al. DNA methylation is required for the control of stem cell differentiation in the small intestine. Genes Dev. 28, 652-664, (2014).

459 Flower, R. What are all the things that aspirin does?: This fascinating but simple and cheap drug has an assured future. BMJ : British Medical J. 327, 572-573 (2003).

460 Cohen, B. A., Mitra, R. D., Hughes, J. D. & Church, G. M. A computational analysis of whole-genome expression data reveals chromosomal domains of gene expression. Nat Genet 26 (2000).

461 *Hathcock, J. N., Shao, A., Vieth, R. & Heaney, R. Risk assessment for vitamin D. Am J Clin Nutr 85, 6-18 (2007).*

462 *Fearnhead, N. S., Britton, M. P. & Bodmer, W. F. The ABC of APC. Hum. Mol. Genet. 10, 721-733 (2001).*

463 *Petko, Z. et al. Aberrantly methylated CDKN2A, MGMT, and MLH1 in colon polyps and in fecal DNA from patients with colorectal polyps. Clin. Cancer. Res. 11, 1203-1209 (2005).*

464 *Matano, M. et al. Modeling colorectal cancer using CRISPR-Cas9-mediated engineering of human intestinal organoids. Nat Med 21, 256-262 (2015).*

465 *Takashiba, S., Van Dyke, T. E., Amar, S., Murayama, Y., Soskolne, A. W., & Shapira, L.. Differentiation of Monocytes to Macrophages Primes Cells for Lipopolysaccharide Stimulation via Accumulation of Cytoplasmic Nuclear Factor κB. Infection and Immunity, 67(11), 5573–5578 (1999).*

466 *Tahan, Gulgun, et al. "Vitamin E has a dual effect of anti-inflammatory and antioxidant activities in acetic acid-induced ulcerative colitis in rats." Canadian J. of surgery 54.5: 333. (2011).*

467 *Yasui, Yumiko, et al. "Dietary astaxanthin inhibits colitis and colitis-associated colon carcinogenesis in mice via modulation of the inflammatory cytokines." Chemico-biological interactions 193.1: 79-87. (2011).*

468 *Saboori, S., et al. "Effect of vitamin E supplementation on serum C-reactive protein level: a meta-analysis of randomized controlled trials." European J. Clin. nutrition 69.8 : 867-873. (2015).*

469 *Stoker, M. G. P., and H. Rubin. "Density dependent inhibition of cell growth in culture." Nature 215.5097: 171-172. (1967).*

470 *Blagosklonny, Mikhail V., and Arthur B. Pardee. "The restriction point of the cell cycle." Cell cycle 1.2: 102-109. (2002).*

471 *Buchkovich, Karen, Linda A. Duffy, and Ed Harlow. "The retinoblastoma protein is phosphorylated during specific phases of the cell cycle." Cell 58.6: 1097-1105. (1989).*

472 *Surget, S., Khoury, M. P., & Bourdon, J.-C.. Uncovering the role of p53 splice variants in human malignancy: a clinical perspective. OncoTargets and Therapy, 7, 57–68. (2014).*

473 *Abbas T, Dutta A. p21 in cancer: intricate networks and multiple activities. Nat. Rev. Can..;9(6):400-414 (2009)*

474 *Martin Schuler, Ella Bossy-Wetzel, Joshua C. Goldstein, Patrick Fitzgerald,and Douglas R. Green. p53 Induces Apoptosis by Caspase Activation through Mitochondrial Cytochrome c ReleaseJ. Biol. Chem. 275: 7337 (2000)*

475 *Fridman, Jordan S., and Scott W. Lowe. "Control of apoptosis by p53." Oncogene 22.56: 9030-9040. (2003).*

476 *Goodrich, David W., et al. "The retinoblastoma gene product regulates progression through the G1 phase of the cell cycle." Cell 67.2: 293-302. (1991).*

477 *Bast Jr, Robert C., Carlo M. Croce, William N. Hait, Waun Ki Hong, Donald W. Kufe, Martine Piccart-Gebhart, Raphael E. Pollock, Ralph R. Weichselbaum, Hongyang Wang, and James F. Holland, eds. Holland-frei cancer medicine. John Wiley & Sons, (2017).*

478 *Hanahan, Douglas, and Robert A. Weinberg. "The hallmarks of cancer." cell 100.1: 57-70. (2000).*

479 *Moses, Harold L., Edmund Y. Yang, and Jennifer A. Pietenpol. "TGF-β stimulation and inhibition of cell proliferation: new mechanistic insights." Cell 63.2: 245-247. (1990).*

480 *Witsch, Esther, Michael Sela, and Yosef Yarden. "Roles for growth factors in cancer progression." Phys. 25.2: 85-101. (2010).*

481 *Fulda, Simone. "Tumor resistance to apoptosis." Int. J. of Cancer 124.3: 511-515. (2009).*

482 *Hornsby, Peter J. "Replicative senescence and cancer." Biological Basis of Geriatric Onc.. Springer US, 2005. 53-73.*

483 *Nishida, Naoyo, et al. "Angiogenesis in cancer." Vascular health and risk management 2.3: 213. (2006).*

484 *Hanahan, Douglas, and Robert A. Weinberg. "Hallmarks of cancer: the next generation." cell 144.5: 646-674. (2011).*

Appendices

1- Reagents and compounds

Supplier	*Description*
CALTAG-MEDSYSTEMS LIMITED	CoEpiCM (Colonic Epithelial Cell Medium)
VWR INTERNATIONAL GMBH	100 RXN Q SCRIPT CDNA SUPERMIX
R & D SYSTEMS EUROPE LTD	10mg Wnt 3a
CALTAG-MEDSYSTEMS LIMITED	1L21
R & D SYSTEMS EUROPE LTD	25MG R-SPONDIN1
SIGMA-ALDRICH CO LTD	5-AZA-2'-DEOXYCYTIDINE
BIOLINE REAGENTS LTD	50 PREPS ISOLATE II RNA MINI KIT
BIOLINE REAGENTS LTD	500RXNS IMMOMIX
CAMBRIDGE BIOSCIENCE LIMITED	96 WELL PROSTAGLANDIN E2 EIA KIT
SIGMA-ALDRICH CO LTD	ACRYLAMIDE/BIS-ACRYLAMIDE, 40% SOLUTION
THERMO FISHER SCIENTIFIC (HEMEL)	Advanced DMEM/F-12
MERCK CHEMICALS LTD	Amicon Ultra-4 Centrifugal Filter Unit with Ultracel-3 membrane
ABCAM LTD	Anti-GPCR GPR49 antibody [EPR3065Y]
ABCAM LTD	Anti-TATA binding protein TBP [1TBP18] antibody
CALTAG-MEDSYSTEMS LIMITED	APP
THERMO FISHER SCIENTIFIC (HEMEL)	B-27® Supplement (50X), serum free
CALTAG-MEDSYSTEMS LIMITED	B-ACT
THERMO FISHER SCIENTIFIC (HEMEL)	BCA Protein Assay Kit
NEW ENGLAND BIOLABS (UK) LTD	beta-Catenin 6B3 Rabbit mAb
R & D SYSTEMS EUROPE LTD	CALCITRIOL 1.25 DIHYDROXYVITAMIN D3
NEXCELOM BIOSCIENCE LTD	Cell count slides with protective film
SIGMA-ALDRICH CO LTD	CORNING COSTAR CELL CULTURE PLATES,
VWR INTERNATIONAL GMBH	Corning® Matrigel® Basement Membrane Matrix, growth factor reduced (GFR)
CALTAG-MEDSYSTEMS LIMITED	DCLK1
LIFE TECHNOLOGIES LTD INVITROGEN DIV	DMEM F12 + Glutamax
NEW ENGLAND BIOLABS (UK) LTD	DNase I Reaction Buffer
CAMBRIDGE BIOSCIENCE LIMITED	EZ DNA Methylation Kit Gold for 200 DNA modifications. Supplied with capped columns
NEW ENGLAND BIOLABS (UK) LTD	Gel Loading Dye Blue 6X
SIGMA-ALDRICH CO LTD	GenElute MAMMALIAN GENOMIC DNA MINIPREP
NEW ENGLAND BIOLABS (UK) LTD	HinfI
NEW ENGLAND BIOLABS (UK) LTD	HpyCH4IV
PEPROTECH EC LIMITED	HS RECOMBINANT NOGGIN
PEPROTECH EC LIMITED	Human recombinant TGFβ1
THERMO FISHER SCIENTIFIC (HEMEL)	iBlot® 2 Transfer Stacks, PVDF, regular size
BIOLINE REAGENTS LTD	IMMOMIX 500RXNS
LONZA VERVIERS SPRL	InMyoFib-Intestinal Myofibroblasts
BIOLINE REAGENTS LTD	Isolate II mini kit 50 preps
PROMEGA UK LTD	Luciferase Assay System with Reporter Lysis Buffer
CALTAG-MEDSYSTEMS LIMITED	mettl7b
THERMO FISHER SCIENTIFIC (HEMEL)	N2 supp. x100
NEW ENGLAND BIOLABS (UK) LTD	NF-kappaB1 p105p50 D7H5M Rabbit mAb
NEW ENGLAND BIOLABS (UK) LTD	Non-phospho Active beta-Catenin Ser3337Thr41 D13A1 Rabbit mAb
SIGMA-ALDRICH CO LTD	PHOSPHATE BUFFERED SALINE TABLET,*TRU-ME
THERMO FISHER SCIENTIFIC (HEMEL)	Pierce beta-Galactosidase Assay Reagent
GILSON SCIENTIFIC LTD	Pipette Tip Holder for PIPETMAN P10
CAMBRIDGE BIOSCIENCE LIMITED	Prostaglandin E2 EIA Kit - Monoclonal
4TITUDE LIMITED	qPCR seals
VWR INTERNATIONAL GMBH	qScript™ cDNA SuperMix, 25 reactions
R & D SYSTEMS EUROPE LTD	r-spondin1
ABCAM LTD	Rabbit monoclonal [EPR3776] to Vimentin - Cytoskeleton Marker - 10uL
PEPROTECH EC LIMITED	Recombinant Human DKK-1
PEPROTECH EC LIMITED	Recombinant Human TGF-β1 (HEK293 derived)
CALTAG-MEDSYSTEMS LIMITED	RSPO1 Antibody
SIGMA-ALDRICH CO LTD	S-ADENOSYL-L-METHIONINEP-TOLUENESULFONAT
SIGMA-ALDRICH CO LTD	SB 202190
CALTAG-MEDSYSTEMS LIMITED	SCUBE3
LONZA VERVIERS SPRL	SmGM-2 BulletKit (CC-3181 & CC-4149)
LONZA VERVIERS SPRL	SmGM-2 BULLETKIT (CC-3181 & CC-4149) AS PER
FISHER SCIENTIFIC LIMITED	TC Flask EasyFlask angled neck
CALTAG-MEDSYSTEMS LIMITED	TSLP Antibody
CAMBRIDGE BIOSCIENCE LIMITED	Universal Methylated Mouse DNA Standard and Control Primers
R & D SYSTEMS EUROPE LTD	Valporic acid
R & D SYSTEMS EUROPE LTD	WNT-3A 10MG
ROCHE DIAGNOSTICS LTD	WST-1 assay reagent
MERCK CHEMICALS LTD	y27632

2- Links to relevant online materials

Cell Proliferation Reagent WST-1 (Roche, product number **11644807001**)

https://pim-eservices.roche.com/LifeScience/Document/c4c412ae-96ed-e311-98a1-00215a9b0ba8

EZ DNA Methylation-Gold™ Kit (Zymo, product number **D5006**)

https://www.zymoresearch.com/epigenetics/dna-methylation/bisulfite-conversion/ez-dna-methylation-gold-kit

Prostaglandin E2 ELISA Kit – Monoclonal (Cayman, product number **514010**)

https://www.caymanchem.com/pdfs/514010.pdf

ISOLATE II RNA Mini Kit (Bioline, product number **BIO-52072**)

http://www.bioline.com/us/downloads/dl/file/id/885/isolate_ii_rna_mini_kit_product_manual.pdf

GenElute™ Mammalian Genomic DNA Miniprep Kit Protocol (Sigma Aldrich, prosuct number **G1N70**)

http://www.sigmaaldrich.com/content/dam/sigmaaldrich/docs/Sigma/Datasheet/7/g1n70dat.pdf

Pierce™ BCA Protein Assay Kit (Thermo Fischer Scientific, product number **23225**)

https://tools.thermofisher.com/content/sfs/manuals/MAN0011430_Pierce_BCA_Protein_Asy_UG.pdf

M-PER™ Mammalian Protein Extraction Reagent (Thermo Fischer Scientific, product number **78510**)

https://tools.thermofisher.com/content/sfs/manuals/MAN0011378_MPER_Mammal_Protein_Extract_Reag_UG.pdf

NE-PER™ Nuclear and Cytoplasmic Extraction Reagents (Thermo Fischer Scientific, product number **78833**)

https://tools.thermofisher.com/content/sfs/manuals/MAN0011398_NEPER_Nuc_Cytoplasmic_Extract_Reag_UG.pdf

Infinium MethylationEPIC BeadChip Kit (32 samples) (Illumina, product number **WG-317-1002**)

3- Participant information for organoid cultures

	DATE	*AGE*	*SEX*	*DIAGNOSIS*	*LOCATION*	*SAMPLE*	*MFB*	*ORGS*	*POLYPS*	*BX*
CASE1	15.1.14	77	m	acrc	hep flex	10cm prox	y	n	n	n
CASE2	24.1.14	46	f	acrc	rec sig	15cm prox	y	n	n	n
CASE3	29.1.14	57	f	acrc	sig col	20cm prox	y	y	n	n
CASE4	26.2.14	59	m	acrc	sig col	15cm prox	n	n	n	NNUH TB (MW)
CASE5	17.3.14	81	f	acrc	sig col	20cm prox	n	y	n	NNUH TB (MW)
CASE6	1.5.14	54	f	acrc	rec sig	10cm prox	n	n	n	NNUH TB (MW)
CASE7	20.5.14	72	f	acrc	rec sig	10cm prox	Processed	n	n	NNUH TB (MW)
CASE8	2.6.14	53	m	acrc	rectal	25cm prox	Processed	n	n	NNUH TB (MW)
CASE9	8.9.14	74	m	acrc	rectal	10cm prox	n	y	y	NNUH TB (MW)
CASE10	2.2.15	70	m	acrc	sig col	20 cm prox	n	n	n	NNUH TB (MW)
CASE11	22.6.15	45	m	acrc	rec sig	20cm prox	y	y	n	NNUH TB (MW)
CASE12	29.6.15	65	m	acrc	rectal	20cm prox	y	y	n	NNUH TB (MW)
CASE13	2.7.15	61	m	acrc	rectal	20cm prox	y	y	n	NNUH TB (MW)

Supplier Cat. No.	Item Description	Supplier
12587-010	10ML B27 SUPPLEMENT	LIFE TECHNOLOGIES LTD INVITROGEN DIV
17502-048	N2 SUPPLEMENT	LIFE TECHNOLOGIES LTD INVITROGEN DIV
688000	1MG Y - 27632	MERCK CHEMICALS LTD
P0409	1MG PROSTAGLANDIN E2	SIGMA-ALDRICH CO LTD
120-10C	20UG RECOMBINANT HUMAN NOGGIN	PEPROTECH EC LIMITED
F9665	500ML FETAL BOVINE SERUM	SIGMA-ALDRICH CO LTD
734-1100	10ML BD MATRIGEL BASEMENT MEMBRANE MATRIX	VWR INTERNATIONAL GmbH
734-1312	100ML BD DISPASE 5000 CASEINOLYTIC UNITS	VWR INTERNATIONAL GmbH
734-0107	100ML BE CELL RECOVERY SOLUTION	VWR INTERNATIONAL GmbH
PHG0311	EGF RECOMBINANT HUMAN	LIFE TECHNOLOGIES LTD INVITROGEN DIV
GIN70-KIT	GENELUTE MAMMALIN GENOMIC DNA MINIPREP	SIGMA-ALDRICH CO LTD
CLS3516-50EA	COSTAR CELL CULTURE PLATES 6 WELL	SIGMA-ALDRICH CO LTD
CLS3524-100EA	CORNING COSTAR CELL CULTURE PLATES	SIGMA-ALDRICH CO LTD
S7067-5MG	SB 202190	SIGMA-ALDRICH CO LTD
2815	VALPROIC ACID SODIUM SALT	R & D SYSTEMS EUROPE LTD

HUMAN

GENE	FWD	REV	ANNEAL	ENZYME	TEMP
TNFA	GGAAGTTAGAAGGAAATAGATTATAGATT	ACAAACATCAAAAATACCCCT	58	HINFI	37DEG
IL8	TGTGGAGTTTTAGTATTTTAAATGTA	TGTATAAGTTTTTTAGTAGGGTGAT	60	XMNI	37DEG
APC	GGAGTAAAGATTAGAAGAGAGGAA	AAACCACTCCTCACTCCA	58	FAUI	55DEG
DKK1	AGAGGGAGGTTGTAGAGAGTTATTATTGT	CTAATAACCCACACTCTAAAATAAACTAAACA	59	MAEII	37DEG
SFRP5	GTTTAGGTGGGTGGTAGTTTG	AAAAAACAAAAAACCCTAAAAAAAA	55DEG	BSIEI	60DEG
SFRP1	AGGTTAAGAAAATTTTGGTTGTGTTT	CCTACTCCAACACCTCCTTCATA	60	HINFI	37DEG
SFRP2	GTTTTTTAAGGGGTGTTGAGT	CAAACTTCCAAAAACCTCC	59DEG	FAUI	55DEG

MOUSE

GENE	FWD	REV	ANNEAL	ENZYME	TEMP
SOX17	AGATTGTAGGGTTTGGTTTGA	CCTCAAAATCTACCTCTAAAAACA	58	BSIEI	60DEG
DKK1	AGAGGGAGGTTGTAGAGAGTTATTATTGT	CTAATAACCCACACTCTAAAATAAACTAAACA	59	MAEII	37DEG
WIF1	TGGGGGGAAAGGGATTATATCTAAATCATCACTCAAACCTCCT	TCTAAATCATCACTCAAACCTCCT	60	HINFI	37DEG
SFRP5	GGAGGTGAGGGGGATTA	TCCAAACCACCCACATA	58	MAEII	37DEG

6 - Q-rt-PCR assays

Human

GENE	DIR	SEQUENCE	ANNEAL
CYP24A1	FWD	ATGAGCACGTTTGGGAGGAT	60
CYP24A2	REV	TGCCAGACCTTGGTGTTGAG	
VDR	FWD	CTGACCCTGGAGACTTTGAC	60
VDR	REV	TTCCTCTGCACTTCCTCATC	
MYC	FWD	GCCACGTCTCCACACATCAG	60
MYC	REV	TGGTGCATTTTCGGTTGTTG	
Ecad	FWD	TGAAGGTGACAGAGCCTCTGGAT	60
Ecad	REV	TGGGTGAATTCGGGCTTGTT	
LGR5	FWD	accagactatgcctttggaaac	60
LGR5	REV	ttcccagggagtggattctat	
VIM	FWD	Tggtctaacggtttccccta	60
VIM	REV	Gacctcggagcgagagtg	
aSMA	FWD	ctgttccagccatccttcat	60
aSMA	REV	tcatgatgctgttgtaggtggt	
RSPO1	FWD	CCCTTAAAGGACGGGAGAAA	60
RSPO1	REV	AAAGTCCTCCTTTATAGCTGACCA	
IL6	FWD	GATGAGTACAAAAGTCCTCGATCCA	60
IL6	REV	CTGCAGCCACTGGTTCTGT	
actb	FWD	CTGGAACGGTGAAGGTGACA	60
actb	REV	AAGGGACTTCCTGTAACAATGCA	
gapd	FWD	TGCACCACCAACTGCTTAGC	60
gapd	REV	GGCATGGACTGTGGTCATGAG	
TGFβ**1r-1**	FWD	gcagacttaggactggcagtaag	60
TGFβ**1r-2**	REV	agaacttcaggggccatgt	
cd14	FWD	gttcggaagacttatcgacca	60
cd14	REV	atcgtccagctcacaaggtt	
cd68	FWD	gtccacctcgacctgctct	60
cd68	REV	cactggggcaggagaaact	
f4/80	FWD	tgcagctgtcaagttggatt	60
f4/80	REV	tgcacattcatccacgtctt	
tet1	FWD	tctgttgttgtgcctctgga	60
tet1	REV	gcctttaaaactttgggcttc	
cd16a	FWD	gggggctttttgggagta	60
cd16a	REV	ggttgacactgccaaacctt	
cd11b	FWD	ggcatccgcaaagtggta	60
cd11b	REV	ggatcttaaaggcattctttcg	
jag 1	FWD	ggcaacaccttcaacctca	60
jag 1	REV	gcctccacaagcaacgtatag	
fn1	FWD	gaactatgatgccgaccagaa	60
fn1	REV	ggttgtgcagatttcctcgt	

FAP	FWD	TGGCGATGAACAATATCCTAGA	60
FAP	REV	ATCCGAACAACGGGATTCTT	
Mettl7b	FWD	cgcaagatggagagcaaga	60
Mettl7b	REV	ggctcctgtaagccccttta	
RPSKA3	FWD	gacagcgctgagaatggac	60
RPSKA3	REV	tgtgtgattgcaatttctttgat	
TNFα	FWD	gacaagcctgtagcccatgt	60
TNFα	REV	tctcagctccacgccatt	
dnmt1	FWD	cagccaacagaggacaacaa	60
dnmt1	REV	ccggctatccaggtcctc	
dnmt3b	FWD	ggaaattagaatcaaggaaatacga	60
dnmt3b	REV	aatttgtcttgaggcgcttg	
TET1	FWD	tctgttgttgtgcctctgga	60
TET1	REV	gcctttaaaactttgggcttc	
TET2	FWD	acgcttggaagcaggagat	60
TET2	REV	aaggctgccctctagttgaa	
TET3	FWD	cgcctctatccgggaact	60
TET3	REV	tccccgtgtagatgaccttc	
EGF	FWD	tggttgtggttcatccattg	60
EGF	REV	tcacagcctccgttttgata	
HGF	FWD	cagcatgtcctcctgcatc	60
HGF	REV	tcttttcctttgtccctctgc	
BMP-1	FWD	accctgggcagctacaagt	60
BMP-1	REV	tgaggaatccgccacaag	
kI67	FWD	AAGTTCACACGGACGTCAG	60
kI67	REV	GATGCTCTTGCCATCTCC	
MUC2	FWD	TGGGTGTCCTCGTCTCCTACA	60
MUC2	REV	TGTTGCCAAACCGGTGGTA	
VEGF	FWD	cctccgaaaccatgaacttt	60
VEGF	REV	atgattctgccctcctcctt	
ICAM1	FWD	ccttcctcaccgtgtactgg	60
ICAM1	REV	agcgtagggtaaggttcttgc	
TGFB**1**	FWD	actactacgccaaggaggtcac	60
TGFB**1**	REV	tgcttgaacttgtcatagatttcg	
COX2	FWD	cttcacgcatcagtttttcaag	60
COX2	REV	tcaccgtaaatatgatttaagtccac	
ERK1	FWD	ccctagcccagacagacatc	60
ERK1	REV	gcacagtgtccattttctaacagt	
ERK2	FWD	caaagaactaatttttgaagagactgc	60
ERK2	REV	tcctctgagcccttgtcct	

Mouse

Gene	DIR	SEQUENCE	ANNEAL
Mouse Muc2	FWD	GCTGACGAGTGGTTGGTGAATG	60
Mouse Muc2	REV	GATGAGGTGGCAGACAGGAGAC	
Mouse Mki67	FWD	ACGTATACATATGCCAGGGGA	60
Mouse Mki67	REV	AAAGCTTTGATATCCTCACACTCA	
Mouse Lgr5	FWD	GCCTGAACTAAGAACACTGA	60
Mouse Lgr5	REV	CTGGGGAAGAGATGAGAT	
Mouse Lgr5_2	FWD	GACGACGGCAACAGTGTGGAC	60
Mouse Lgr5_2	REV	AGGCGAGCACTGCACCGA	
Mouse dnmt1	FWD	TGGTGCTGAAGCTCACACTG	60
Mouse dnmt1	REV	CCATACTGTCCAGCCTGGAG	
Mouse dnmt3a	FWD	CGGCAGAATAGCCAAGTTCA	60
Mouse dnmt3a	REV	CTGGTCTTTGCCCTGCTTTA	
Mouse dnmt3b	FWD	CCAGTCTTGGAGGCAATCTG	60
Mouse dnmt3b	REV	CTG GAG ACC TCC CTC TTA GAC AG	
GAPDH	FWD	TGTGTCCGTCGTGGATCTGA	60
GAPDH	REV	TTGCTGTTGAAGTCGCAGGAG	
ACTB	FWD	CCACTGCCGCATCCTCTTCC	60
ACTB	REV	CTCGTTGCCAATAGTGATGACCTG	
RNA Pol II	FWD	GACAAAACTGGCTCCTCTGC	60
RNA Pol II	REV	GCTTGCCCTCTACATTCTGC	
LEF1	FWD	ACAGCTGCCTACATCTGAAACA	60
LEF1	REV	CTGGGGTTTCAACAAGCTTC	
CCND1	FWD	ATTTGCTCTGAGTCTCCGGT	60
CCND1	REV	AGCACTGCAGCTGGCTT	

Myofibroblast secretory profiles (BIOLOGICAL PROCESS)

Case 11

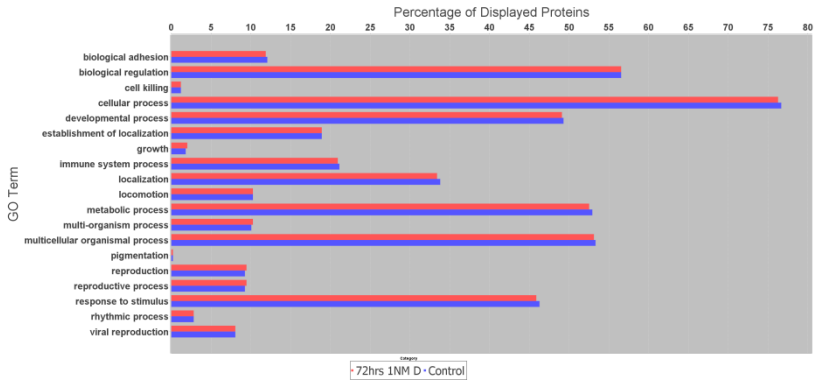

Case 12

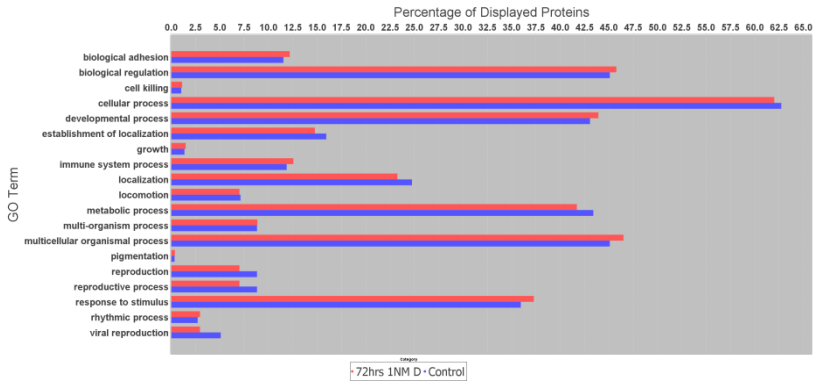

Case 13

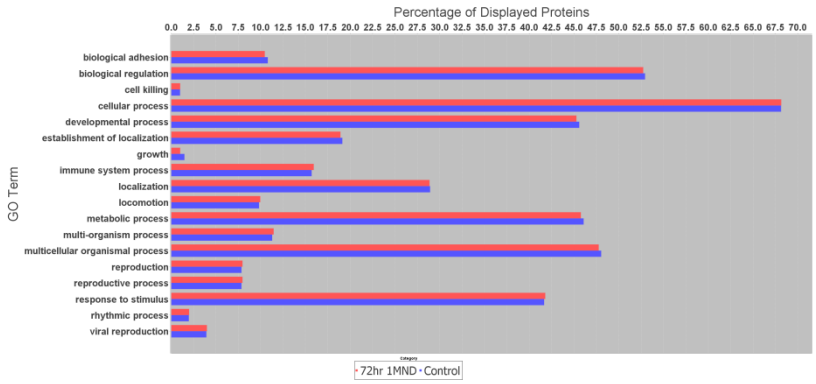

Myofibroblast secretory profiles (CELLULAR COMPONENT)

Case 11

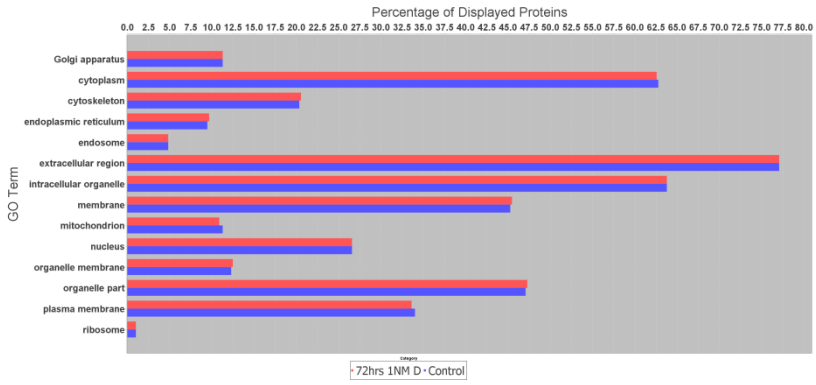

Case 12

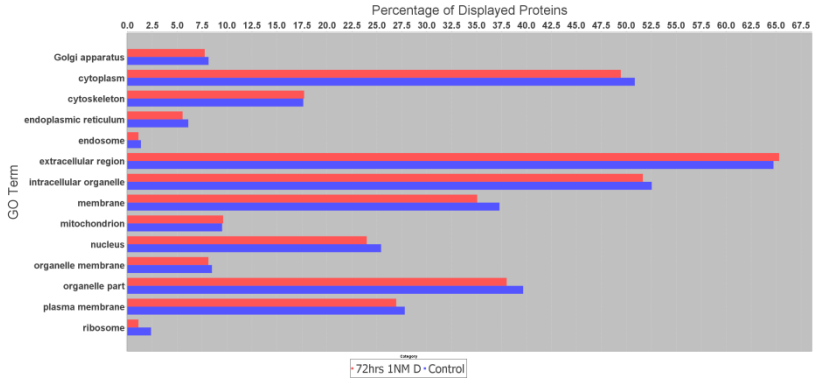

Case 13

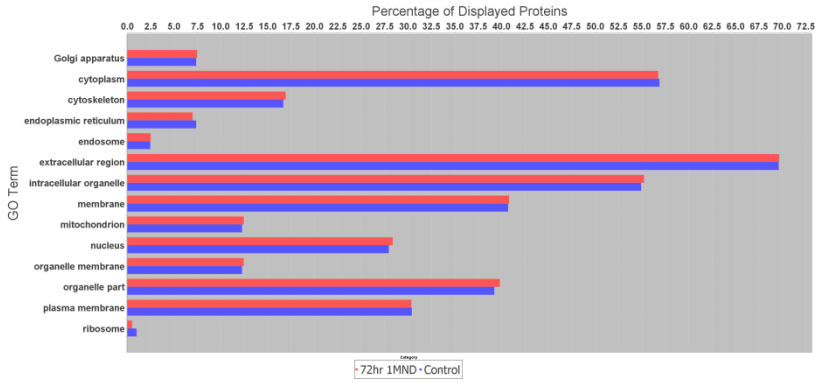

Myofibroblast secretory profiles (MOLECULAR FUNCTION)

Case 11

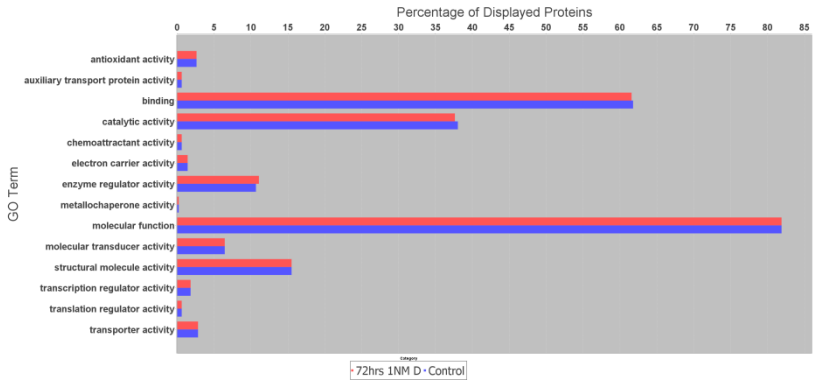

Case 12

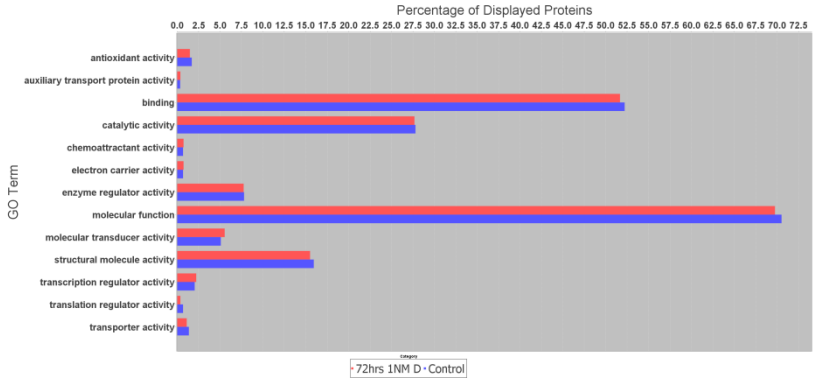

Case 13

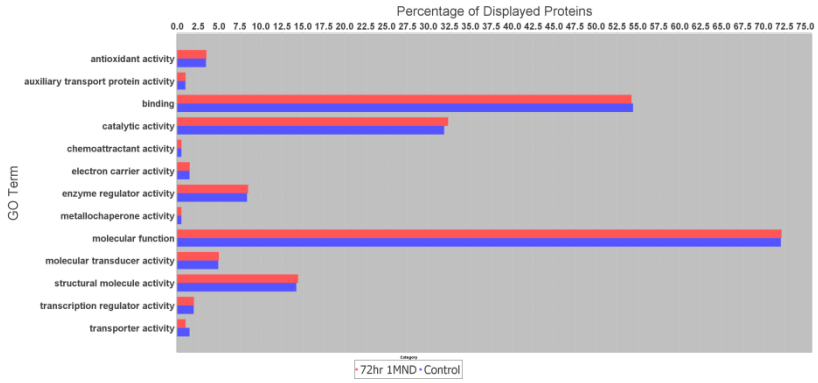

8 – Case 11 MFB, proteins induced by vitamin D (n=124 p<0.05)

6-phosphogluconate dehydrogenase, decarboxylating OS=Homo sapiens GN=PGD PE=1 SV=3
Amyloid beta A4 protein OS=Homo sapiens GN=APP PE=1 SV=3
Aspartate aminotransferase, cytoplasmic OS=Homo sapiens GN=GOT1 PE=1 SV=3
Aspartate aminotransferase, mitochondrial OS=Homo sapiens GN=GOT2 PE=1 SV=3
ATP-citrate synthase OS=Homo sapiens GN=ACLY PE=1 SV=3
Actin, cytoplasmic 2 OS=Homo sapiens GN=ACTG1 PE=1 SV=1
Actin, alpha skeletal muscle OS=Homo sapiens GN=ACTA1 PE=1 SV=1
Agrin OS=Homo sapiens GN=AGRN PE=1 SV=5
Serum albumin OS=Homo sapiens GN=ALB PE=1 SV=2
Fructose-bisphosphate aldolase A OS=Homo sapiens GN=ALDOA PE=1 SV=2
Fructose-bisphosphate aldolase C OS=Homo sapiens GN=ALDOC PE=1 SV=2
Attractin OS=Homo sapiens GN=ATRN PE=1 SV=2
Serine/threonine-protein phosphatase 2A 65 kDa regulatory subunit A alpha isoform OS=Homo sapiens GN=PPP2R1A PE=1 SV=1
Complement factor B OS=Homo sapiens GN=CFB PE=2 SV=1
Cytochrome c (Fragment) OS=Homo sapiens GN=CYCS PE=1 SV=1
Dipeptidyl peptidase 1 OS=Homo sapiens GN=CTSC PE=1 SV=2
Cathepsin L1 OS=Homo sapiens GN=CTSL PE=1 SV=2
Cathepsin Z OS=Homo sapiens GN=CTSZ PE=1 SV=1
Carbonyl reductase [NADPH] 1 OS=Homo sapiens GN=CBR1 PE=1 SV=3
CD109 antigen OS=Homo sapiens GN=CD109 PE=1 SV=2
Complement factor H OS=Homo sapiens GN=CFH PE=1 SV=4
Chitinase-3-like protein 1 OS=Homo sapiens GN=CHI3L1 PE=1 SV=2
60 kDa heat shock protein, mitochondrial OS=Homo sapiens GN=HSPD1 PE=1 SV=2
Chloride intracellular channel protein 1 OS=Homo sapiens GN=CLIC1 PE=1 SV=4
Collagen alpha-1(IV) chain OS=Homo sapiens GN=COL4A1 PE=1 SV=3
Collagen alpha-1(V) chain OS=Homo sapiens GN=COL5A1 PE=1 SV=3
Collagen alpha-2(V) chain OS=Homo sapiens GN=COL5A2 PE=1 SV=3
Collagen alpha-3(VI) chain OS=Homo sapiens GN=COL6A3 PE=1 SV=5
Complement component C7 OS=Homo sapiens GN=C7 PE=1 SV=2
Coactosin-like protein OS=Homo sapiens GN=COTL1 PE=1 SV=3
UPF0556 protein C19orf10 OS=Homo sapiens GN=C19orf10 PE=1 SV=1
Hepatocyte growth factor activator OS=Homo sapiens GN=HGFAC PE=3 SV=1
N(G),N(G)-dimethylarginine dimethylaminohydrolase 1 OS=Homo sapiens GN=DDAH1 PE=1 SV=3
Glutamate dehydrogenase 1, mitochondrial OS=Homo sapiens GN=GLUD1 PE=1 SV=2
Dickkopf-related protein 3 OS=Homo sapiens GN=DKK3 PE=1 SV=2
Dipeptidyl peptidase 3 OS=Homo sapiens GN=DPP3 PE=1 SV=2
Dipeptidyl peptidase 4 OS=Homo sapiens GN=DPP4 PE=1 SV=2
Epididymal secretory protein E1 OS=Homo sapiens GN=NPC2 PE=1 SV=1
Kaliocin-1 OS=Homo sapiens GN=LTF PE=1 SV=1
Thrombospondin-4 OS=Homo sapiens GN=THBS4 PE=4 SV=1
Puromycin-sensitive aminopeptidase OS=Homo sapiens GN=NPEPPS PE=1 SV=1
Elongation factor 1-alpha 1 OS=Homo sapiens GN=EEF1A1 PE=1 SV=1
Elongation factor 2 OS=Homo sapiens GN=EEF2 PE=1 SV=4
EMILIN-1 OS=Homo sapiens GN=EMILIN1 PE=1 SV=2
Endoplasmic reticulum aminopeptidase 1 OS=Homo sapiens GN=ERAP1 PE=1 SV=3
Alpha-2-HS-glycoprotein OS=Homo sapiens GN=AHSG PE=1 SV=1
Farnesyl pyrophosphate synthase OS=Homo sapiens GN=FDPS PE=1 SV=4
Ferritin heavy chain OS=Homo sapiens GN=FTH1 PE=1 SV=2
Ferritin light chain OS=Homo sapiens GN=FTL PE=1 SV=2
Cartilage oligomeric matrix protein OS=Homo sapiens GN=COMP PE=4 SV=1
Glucose-6-phosphate 1-dehydrogenase OS=Homo sapiens GN=G6PD PE=1 SV=4
Glucose-6-phosphate isomerase OS=Homo sapiens GN=GPI PE=1 SV=4
Neutral alpha-glucosidase AB OS=Homo sapiens GN=GANAB PE=1 SV=3
Guanine nucleotide-binding protein subunit beta-2-like 1 OS=Homo sapiens GN=GNB2L1 PE=1 SV=3
Rho GDP-dissociation inhibitor 1 OS=Homo sapiens GN=ARHGDIA PE=1 SV=3
Glia-derived nexin OS=Homo sapiens GN=SERPINE2 PE=1 SV=1
1,4-alpha-glucan-branching enzyme OS=Homo sapiens GN=GBE1 PE=1 SV=3
Glucosamine-6-phosphate isomerase 1 OS=Homo sapiens GN=GNPDA1 PE=1 SV=1
N-acetylglucosamine-6-sulfatase OS=Homo sapiens GN=GNS PE=1 SV=3
Glypican-1 OS=Homo sapiens GN=GPC1 PE=1 SV=2
Glutathione S-transferase P OS=Homo sapiens GN=GSTP1 PE=1 SV=2
Hemoglobin subunit alpha OS=Homo sapiens GN=HBA1 PE=1 SV=2
Hypoxanthine-guanine phosphoribosyltransferase OS=Homo sapiens GN=HPRT1 PE=1 SV=2
Heat shock protein HSP 90-alpha OS=Homo sapiens GN=HSP90AA1 PE=1 SV=5
Heat shock protein HSP 90-beta OS=Homo sapiens GN=HSP90AB1 PE=1 SV=4
Heat shock 70 kDa protein 13 OS=Homo sapiens GN=HSPA13 PE=1 SV=1

Heat shock 70 kDa protein 1A/1B OS=Homo sapiens GN=HSPA1A PE=1 SV=5
Heat shock cognate 71 kDa protein OS=Homo sapiens GN=HSPA8 PE=1 SV=1
Isocitrate dehydrogenase [NADP] cytoplasmic OS=Homo sapiens GN=IDH1 PE=1 SV=2
Inter-alpha-trypsin inhibitor heavy chain H1 OS=Homo sapiens GN=ITIH1 PE=1 SV=3
Inter-alpha-trypsin inhibitor heavy chain H3 OS=Homo sapiens GN=ITIH3 PE=1 SV=2
Low-density lipoprotein receptor (Fragment) OS=Homo sapiens GN=LDLR PE=1 SV=1
Pyruvate kinase PKM OS=Homo sapiens GN=PKM PE=1 SV=4
Laminin subunit alpha-2 OS=Homo sapiens GN=LAMA2 PE=1 SV=4
Laminin subunit beta-2 OS=Homo sapiens GN=LAMB2 PE=1 SV=2
L-lactate dehydrogenase A chain OS=Homo sapiens GN=LDHA PE=1 SV=2
Galectin-1 OS=Homo sapiens GN=LGALS1 PE=1 SV=2
Leukemia inhibitory factor OS=Homo sapiens GN=LIF PE=1 SV=1
Lumican OS=Homo sapiens GN=LUM PE=1 SV=2
Malate dehydrogenase, mitochondrial OS=Homo sapiens GN=MDH2 PE=1 SV=3
Lactadherin OS=Homo sapiens GN=MFGE8 PE=1 SV=2
Moesin OS=Homo sapiens GN=MSN PE=1 SV=3
Alpha-N-acetylgalactosaminidase OS=Homo sapiens GN=NAGA PE=1 SV=2
Protein NOV homolog OS=Homo sapiens GN=NOV PE=1 SV=1
Group XV phospholipase A2 OS=Homo sapiens GN=PLA2G15 PE=1 SV=2
Protein DJ-1 OS=Homo sapiens GN=PARK7 PE=1 SV=2
Programmed cell death 6-interacting protein OS=Homo sapiens GN=PDCD6IP PE=1 SV=1
Protein disulfide-isomerase OS=Homo sapiens GN=P4HB PE=1 SV=3
Phosphatidylethanolamine-binding protein 1 OS=Homo sapiens GN=PEBP1 PE=1 SV=3
Phosphoglycerate mutase 1 OS=Homo sapiens GN=PGAM1 PE=1 SV=2
Plasminogen OS=Homo sapiens GN=PLG PE=1 SV=2
Procollagen-lysine,2-oxoglutarate 5-dioxygenase 3 OS=Homo sapiens GN=PLOD3 PE=1 SV=1
Purine nucleoside phosphorylase OS=Homo sapiens GN=PNP PE=1 SV=2
Peptidyl-prolyl cis-trans isomerase A OS=Homo sapiens GN=PPIA PE=1 SV=2
Peptidyl-prolyl cis-trans isomerase B OS=Homo sapiens GN=PPIB PE=1 SV=2
Peptidyl-prolyl cis-trans isomerase C OS=Homo sapiens GN=PPIC PE=1 SV=1
Peroxiredoxin-1 OS=Homo sapiens GN=PRDX1 PE=1 SV=1
Peroxiredoxin-2 OS=Homo sapiens GN=PRDX2 PE=1 SV=5
Profilin-1 OS=Homo sapiens GN=PFN1 PE=1 SV=2
Vitamin K-dependent protein S OS=Homo sapiens GN=PROS1 PE=1 SV=1
Proteasome subunit beta type-4 OS=Homo sapiens GN=PSMB4 PE=1 SV=4
Prostaglandin-H2 D-isomerase OS=Homo sapiens GN=PTGDS PE=1 SV=1
Nucleoside diphosphate kinase OS=Homo sapiens GN=NME1-NME2 PE=1 SV=1
Spliceosome RNA helicase DDX39B OS=Homo sapiens GN=DDX39B PE=1 SV=2
Translationally-controlled tumor protein OS=Homo sapiens GN=TPT1 PE=1 SV=1
Selenium-binding protein 1 OS=Homo sapiens GN=SELENBP1 PE=1 SV=2
Serpin H1 OS=Homo sapiens GN=SERPINH1 PE=1 SV=2
Superoxide dismutase [Mn], mitochondrial OS=Homo sapiens GN=SOD2 PE=1 SV=2
Cornifin-A OS=Homo sapiens GN=SPRR1A PE=1 SV=2
Erythrocyte band 7 integral membrane protein OS=Homo sapiens GN=STOM PE=1 SV=3
Transaldolase OS=Homo sapiens GN=TALDO1 PE=1 SV=2
Tubulin alpha-1A chain OS=Homo sapiens GN=TUBA1A PE=1 SV=1
Tubulin alpha-1B chain OS=Homo sapiens GN=TUBA1B PE=1 SV=1
Thyroxine-binding globulin OS=Homo sapiens GN=SERPINA7 PE=1 SV=2
Thioredoxin OS=Homo sapiens GN=TXN PE=1 SV=3
Triosephosphate isomerase OS=Homo sapiens GN=TPI1 PE=1 SV=3
Serotransferrin OS=Homo sapiens GN=TF PE=1 SV=3
Thioredoxin reductase 1, cytoplasmic OS=Homo sapiens GN=TXNRD1 PE=1 SV=3
Thrombospondin-1 OS=Homo sapiens GN=THBS1 PE=1 SV=2
Thrombospondin-2 OS=Homo sapiens GN=THBS2 PE=1 SV=2
Protein tweety homolog 3 OS=Homo sapiens GN=TTYH3 PE=1 SV=3
Thioredoxin domain-containing protein 17 OS=Homo sapiens GN=TXNDC17 PE=1 SV=1
Ubiquitin-like modifier-activating enzyme 1 OS=Homo sapiens GN=UBA1 PE=1 SV=3
WD repeat-containing protein 1 OS=Homo sapiens GN=WDR1 PE=1 SV=4

9 – Case 12 MFB, proteins induced by vitamin D (n=86 p<0.05)

Nidogen-1 OS=Homo sapiens GN=NID1 PE=1 SV=3
Laminin subunit gamma-1 OS=Homo sapiens GN=LAMC1 PE=1 SV=3
Proteasome subunit alpha type OS=Homo sapiens GN=PSMA6 PE=1 SV=1
Chondroitin sulfate proteoglycan 4 OS=Homo sapiens GN=CSPG4 PE=1 SV=2
Phosphoglycerate kinase 1 OS=Homo sapiens GN=PGK1 PE=1 SV=3
Moesin OS=Homo sapiens GN=MSN PE=1 SV=3
78 kDa glucose-regulated protein OS=Homo sapiens GN=HSPA5 PE=1 SV=2
Procollagen C-endopeptidase enhancer 1 OS=Homo sapiens GN=PCOLCE PE=1 SV=2
Heparan sulfate proteoglycan 2 (Perlecan), isoform CRA_b OS=Homo sapiens GN=HSPG2 PE=4 SV=1
Xaa-Pro dipeptidase OS=Homo sapiens GN=PEPD PE=1 SV=3
Proteasome subunit beta type-6 OS=Homo sapiens GN=PSMB6 PE=1 SV=4
Glutamate dehydrogenase 1, mitochondrial OS=Homo sapiens GN=GLUD1 PE=1 SV=2
Fructose-bisphosphate aldolase A OS=Homo sapiens GN=ALDOA PE=1 SV=2
Protein disulfide-isomerase OS=Homo sapiens GN=P4HB PE=1 SV=3
Tyrosine-protein kinase receptor OS=Homo sapiens GN=SDC4-ROS1_S4;R32 PE=2 SV=1
Keratin, type II cytoskeletal 2 epidermal OS=Homo sapiens GN=KRT2 PE=1 SV=2
Complement factor H OS=Homo sapiens GN=CFH PE=1 SV=4
Transforming growth factor-beta-induced protein ig-h3 OS=Homo sapiens GN=TGFBI PE=1 SV=1
Keratin, type II cytoskeletal 75 OS=Homo sapiens GN=KRT75 PE=1 SV=2
cDNA FLJ55694, highly similar to Dipeptidyl-peptidase 1 (EC 3.4.14.1) OS=Homo sapiens PE=2 SV=1
Collagen alpha-2(I) chain OS=Homo sapiens GN=COL1A2 PE=1 SV=1
Glypican-1 OS=Homo sapiens GN=GPC1 PE=1 SV=2
Laminin subunit beta-1 OS=Homo sapiens GN=LAMB1 PE=1 SV=1
Lysosomal Pro-X carboxypeptidase OS=Homo sapiens GN=PRCP PE=1 SV=1
Aspartate aminotransferase, cytoplasmic OS=Homo sapiens GN=GOT1 PE=1 SV=3
Collagen alpha-2(V) chain OS=Homo sapiens GN=COL5A2 PE=1 SV=3
L-lactate dehydrogenase A chain OS=Homo sapiens GN=LDHA PE=1 SV=2
Sulfhydryl oxidase 1 OS=Homo sapiens GN=QSOX1 PE=1 SV=3
Decorin OS=Homo sapiens GN=DCN PE=1 SV=1
Pentraxin-related protein PTX3 OS=Homo sapiens GN=PTX3 PE=1 SV=3
Calreticulin OS=Homo sapiens GN=CALR PE=1 SV=1
EGF-containing fibulin-like extracellular matrix protein 1 OS=Homo sapiens GN=EFEMP1 PE=1 SV=2
Insulin-like growth factor-binding protein 4 OS=Homo sapiens GN=IGFBP4 PE=1 SV=2
Keratin, type I cytoskeletal 14 OS=Homo sapiens GN=KRT14 PE=1 SV=4
Keratin, type I cytoskeletal 17 OS=Homo sapiens GN=KRT17 PE=1 SV=2
Aldose reductase OS=Homo sapiens GN=AKR1B1 PE=1 SV=3
Prolow-density lipoprotein receptor-related protein 1 OS=Homo sapiens GN=LRP1 PE=1 SV=2
Keratin, type II cytoskeletal 6B OS=Homo sapiens GN=KRT6B PE=1 SV=5
Lumican OS=Homo sapiens GN=LUM PE=1 SV=2
Prosaposin (Variant Gaucher disease and variant metachromatic leukodystrophy) variant (Fragment) OS=Homo sapiens PE=2 SV=1
Dihydrolipoyl dehydrogenase, mitochondrial OS=Homo sapiens GN=DLD PE=1 SV=2
Serine/threonine-protein phosphatase CPPED1 OS=Homo sapiens GN=CPPED1 PE=1 SV=3
Keratin, type I cytoskeletal 10 OS=Homo sapiens GN=KRT10 PE=1 SV=6
Alpha-enolase OS=Homo sapiens GN=ENO1 PE=1 SV=2
Laminin subunit alpha-2 OS=Homo sapiens GN=LAMA2 PE=1 SV=4
Complement C1s subcomponent OS=Homo sapiens GN=C1S PE=1 SV=1
Vinculin OS=Homo sapiens GN=VCL PE=1 SV=4
Glucose-6-phosphate isomerase (Fragment) OS=Homo sapiens GN=GPI PE=1 SV=1
Lactoferrin OS=Homo sapiens PE=2 SV=1
Putative uncharacterized protein DKFZp686M0562 (Fragment) OS=Homo sapiens GN=DKFZp686M0562 PE=2 SV=1
Keratin, type II cytoskeletal 6A OS=Homo sapiens GN=KRT6A PE=1 SV=3
Collagen alpha-1(VI) chain OS=Homo sapiens GN=COL6A1 PE=1 SV=3
Keratin, type II cytoskeletal 5 OS=Homo sapiens GN=KRT5 PE=1 SV=3
Transketolase (Fragment) OS=Homo sapiens PE=2 SV=1
Neuropilin-1 OS=Homo sapiens GN=NRP1 PE=4 SV=1
Alpha-actinin-4 OS=Homo sapiens GN=ACTN4 PE=1 SV=2
Lysosomal protective protein OS=Homo sapiens GN=CTSA PE=4 SV=1
Alpha-actinin-1 OS=Homo sapiens GN=ACTN1 PE=1 SV=2
Keratin 1 OS=Homo sapiens GN=KRT1 PE=3 SV=1
L-lactate dehydrogenase B chain OS=Homo sapiens GN=LDHB PE=1 SV=2
Cathepsin L1 OS=Homo sapiens GN=CTSL1 PE=2 SV=1
Laminin, alpha 4, isoform CRA_b OS=Homo sapiens GN=LAMA4 PE=4 SV=1
Collagen alpha-1(XII) chain OS=Homo sapiens GN=COL12A1 PE=1 SV=2
YWHAE/FAM22A fusion protein (Fragment) OS=Homo sapiens GN=YWHAE/FAM22A fusion PE=2 SV=1
Collagen alpha-1(XIV) chain OS=Homo sapiens GN=COL14A1 PE=1 SV=3
Macrophage colony-stimulating factor 1 OS=Homo sapiens GN=CSF1 PE=1 SV=2

Tripeptidyl-peptidase I OS=Homo sapiens GN=TPP1 PE=1 SV=2
Glutathione reductase, mitochondrial OS=Homo sapiens GN=GSR PE=1 SV=2
Tryptophan--tRNA ligase, cytoplasmic OS=Homo sapiens GN=WARS PE=1 SV=2
Filamin-A OS=Homo sapiens GN=FLNA PE=1 SV=4
Phosphoserine aminotransferase OS=Homo sapiens GN=PSAT1 PE=1 SV=2
Keratin, type II cytoskeletal 1b OS=Homo sapiens GN=KRT77 PE=2 SV=3
Fumarylacetoacetase OS=Homo sapiens GN=FAH PE=1 SV=2
Metalloproteinase inhibitor 2 OS=Homo sapiens GN=TIMP2 PE=1 SV=2
72 kDa type IV collagenase OS=Homo sapiens GN=MMP2 PE=1 SV=2
Selenium-binding protein 1 OS=Homo sapiens GN=SELENBP1 PE=1 SV=2
Endothelial protein C receptor OS=Homo sapiens GN=PROCR PE=1 SV=1
Suprabasin OS=Homo sapiens GN=SBSN PE=2 SV=2
Complement component 1, r subcomponent variant (Fragment) OS=Homo sapiens PE=2 SV=1
Protein-glutamine gamma-glutamyltransferase E OS=Homo sapiens GN=TGM3 PE=1 SV=4
Transitional endoplasmic reticulum ATPase OS=Homo sapiens GN=VCP PE=1 SV=4
Triosephosphate isomerase OS=Homo sapiens GN=TPI1 PE=1 SV=3
Beta-hexosaminidase subunit beta OS=Homo sapiens GN=HEXB PE=1 SV=3
Collagen alpha-1(V) chain OS=Homo sapiens GN=COL5A1 PE=1 SV=1
Neogenin OS=Homo sapiens GN=NEO1 PE=1 SV=2
Phosphatidylethanolamine-binding protein 1 OS=Homo sapiens GN=PEBP1 PE=1 SV=3

10 – Case 13 MFB, proteins induced by vitamin D (n=12 p<0.05)

Fibrillin-1 OS=Homo sapiens GN=FBN1 PE=1 SV=3
Superoxide dismutase [Mn], mitochondrial OS=Homo sapiens GN=SOD2 PE=1 SV=2
Endoplasmin OS=Homo sapiens GN=HSP90B1 PE=1 SV=1
Alpha-actinin-1 OS=Homo sapiens GN=ACTN1 PE=1 SV=1
Laminin subunit alpha-2 OS=Homo sapiens GN=LAMA2 PE=1 SV=4
Keratin, type I cytoskeletal 10 OS=Homo sapiens GN=KRT10 PE=1 SV=6
Spondin-2 OS=Homo sapiens GN=SPON2 PE=1 SV=3
Heat shock protein HSP 90-alpha OS=Homo sapiens GN=HSP90AA1 PE=1 SV=5
Keratin, type II cytoskeletal 78 OS=Homo sapiens GN=KRT78 PE=2 SV=2
Keratin, type I cytoskeletal 9 OS=Homo sapiens GN=KRT9 PE=1 SV=3
Profilin-1 OS=Homo sapiens GN=PFN1 PE=1 SV=2
Stromelysin-1 OS=Homo sapiens GN=MMP3 PE=1 SV=2

11 – Vitamin D differentially methylated promoters CaCO2 and DLD1 (array 1, experiment 2)

86 coding promoters differentially methylated by vitamin D in CACO2

id	*Chromosome*	*symbol*	*CACO_CTRL*	*CACO_VIT_D*	*mean.diff*	*comb.p.val*
ENSG00000184227	chr14	ACOT1	0.47	0.48	0.00	0.04
ENSG00000196344	chr4	ADH7	0.88	0.92	-0.04	0.02
ENSG00000187546	chr7	AGMO	0.64	0.76	-0.12	0.02
ENSG00000225556	chr1	C2CD4D	0.53	0.53	0.00	0.04
ENSG00000243715	chr3	CACNA2D3-AS1	0.67	0.75	-0.07	0.04
ENSG00000205021	chr17	CCL3L1	0.81	0.85	-0.04	0.04
ENSG00000113240	chr5	CLK4	0.34	0.27	0.06	0.05
ENSG00000188603	chr16	CLN3	0.95	0.96	-0.01	0.04
ENSG00000182372	chr8	CLN8	0.60	0.67	-0.07	0.02
ENSG00000186115	chr19	CYP4F2	0.79	0.84	-0.05	0.03
ENSG00000077279	chrX	DCX	0.61	0.74	-0.13	0.02
ENSG00000088367	chr20	EPB41L1	0.33	0.39	-0.05	0.05
ENSG00000182473	chr17	EXOC7	0.93	0.94	-0.01	0.05
ENSG00000155875	chr9	FAM154A	0.82	0.87	-0.04	0.04
ENSG00000162746	chr1	FCRLB	0.18	0.25	-0.07	0.04
ENSG00000171049	chr19	FPR2	0.20	0.23	-0.03	0.04
ENSG00000164946	chr9	FREM1	0.94	0.92	0.02	0.04
ENSG00000144820	chr3	GPR128	0.91	0.92	-0.01	0.05
ENSG00000182793	chr6	GSTA5	0.67	0.69	-0.02	0.05
ENSG00000181211	chr7	HECW1-IT1	0.03	0.05	-0.02	0.05
ENSG00000138684	chr4	IL21	0.46	0.54	-0.08	0.03
ENSG00000151364	chr11	KCTD14	0.15	0.09	0.06	0.05
ENSG00000197084	chr1	LCE1C	0.12	0.17	-0.05	0.00
ENSG00000179676	chr18	LINC00305	0.58	0.67	-0.09	0.03
ENSG00000248307	chr4	LINC00616	0.86	0.90	-0.04	0.03
ENSG00000224382	chr10	LINC00703	0.62	0.71	-0.08	0.04
ENSG00000246898	chr16	LINC00920	0.45	0.47	-0.02	0.04
ENSG00000130368	chr6	MAS1	0.81	0.80	0.01	0.05
ENSG00000211520	chr2	MIR216B	0.88	0.90	-0.02	0.03
ENSG00000253008	chr2	MIR2355	0.86	0.92	-0.06	0.00
ENSG00000199127	chr8	MIR383	0.38	0.48	-0.10	0.03
ENSG00000266705	chr2	MIR4437	0.74	0.81	-0.07	0.02
ENSG00000264319	chr4	MIR4801	0.14	0.21	-0.06	0.02
ENSG00000207629	chr19	MIR526A1	0.59	0.64	-0.05	0.05
ENSG00000199165	chr9	MIRLET7A1	0.83	0.86	-0.04	0.05
ENSG00000172680	chr8	MOS	0.75	0.80	-0.05	0.04
ENSG00000102891	chr16	MT4	0.60	0.66	-0.06	0.05
ENSG00000138386	chr2	NAB1	0.97	0.98	-0.01	0.03
ENSG00000162599	chr1	NFIA	0.27	0.42	-0.15	0.01
ENSG00000260305	chr15	NTRK3-AS1	0.52	0.61	-0.09	0.00
ENSG00000255582	chr14	OR10G2	0.74	0.80	-0.06	0.05
ENSG00000196248	chr11	OR10S1	0.21	0.28	-0.07	0.01
ENSG00000186306	chr1	OR10T2	0.06	0.05	0.01	0.02
ENSG00000196944	chr1	OR2T4	0.06	0.08	-0.02	0.02
ENSG00000176895	chr11	OR51A7	0.22	0.29	-0.06	0.04
ENSG00000180785	chr11	OR51E1	0.78	0.83	-0.05	0.04
ENSG00000232268	chr11	OR52I1	0.21	0.27	-0.06	0.01

ENSG00000179626	chr12	OR6C4	0.91	0.93	-0.03	0.02
ENSG00000172381	chr11	OR6Q1	0.05	0.10	-0.05	0.00
ENSG00000172487	chr11	OR8J1	0.14	0.22	-0.08	0.01
ENSG00000172199	chr11	OR8U1	0.15	0.23	-0.08	0.01
ENSG00000149090	chr11	PAMR1	0.82	0.88	-0.06	0.02
ENSG00000172840	chr16	PDP2	0.96	0.98	-0.01	0.03
ENSG00000230082	chr3	PRRT3-AS1	0.28	0.23	0.05	0.05
ENSG00000172780	chr3	RAB43	0.94	0.96	-0.02	0.04
ENSG00000130701	chr20	RBBP8NL	0.17	0.18	-0.02	0.04
ENSG00000134533	chr12	RERG	0.35	0.43	-0.08	0.02
ENSG00000111445	chr12	RFC5	0.18	0.30	-0.12	0.01
ENSG00000107018	chr9	RLN1	0.42	0.36	0.06	0.04
ENSG00000107014	chr9	RLN2	0.49	0.42	0.07	0.03
ENSG00000207200	chr11	RNU6-45P	0.89	0.91	-0.03	0.04
ENSG00000104237	chr8	RP1	0.79	0.86	-0.07	0.03
ENSG00000163993	chr4	S100P	0.96	0.95	0.01	0.04
ENSG00000174326	chr17	SLC16A11	0.88	0.84	0.05	0.05
ENSG00000171790	chr1	SLFNL1	0.93	0.95	-0.02	0.04
ENSG00000109208	chr4	SMR3A	0.48	0.64	-0.16	0.00
ENSG00000209582	chr17	SNORA48	0.70	0.72	-0.01	0.05
ENSG00000238317	chr2	SNORD11	0.93	0.95	-0.02	0.04
ENSG00000214929	chr9	SPATA31D1	0.48	0.58	-0.11	0.00
ENSG00000166211	chr12	SPIC	0.43	0.57	-0.14	0.01
ENSG00000159516	chr1	SPRR2G	0.24	0.29	-0.05	0.04
ENSG00000241186	chr3	TDGF1	0.94	0.95	-0.01	0.05
ENSG00000137462	chr4	TLR2	0.82	0.86	-0.04	0.03
ENSG00000165091	chr9	TMC1	0.88	0.91	-0.03	0.02
ENSG00000181634	chr9	TNFSF15	0.72	0.77	-0.05	0.04
ENSG00000211701	chr7	TRGV1	0.92	0.88	0.04	0.03
ENSG00000233306	chr7	TRGV2	0.18	0.24	-0.06	0.02
ENSG00000166007	chr11	TRIM51HP	0.23	0.30	-0.07	0.02
ENSG00000243197	chr3	TUSC7	0.84	0.88	-0.04	0.05
ENSG00000220205	chr17	VAMP2	0.55	0.52	0.03	0.04
ENSG00000146469	chr6	VIP	0.24	0.23	0.01	0.03
ENSG00000146007	chr5	ZMAT2	0.92	0.94	-0.02	0.05
ENSG00000147117	chrX	ZNF157	0.88	0.93	-0.04	0.02
ENSG00000158805	chr16	ZNF276	0.09	0.10	-0.01	0.05
ENSG00000197857	chr19	ZNF44	0.32	0.38	-0.06	0.05
ENSG00000176083	chr1	ZNF683	0.80	0.85	-0.06	0.01

142 coding promoters differentially methylated by vitamin D in DLD1

id	*Chromosome*	*symbol*	*DLD_CTRL*	*DLD_VIT_D*	*diff*	*comb.p.val*
ENSG00000123165	chrX	ACTRT1	0.268119	0.412335	-0.14422	0.015769
ENSG00000159322	chr15	ADPGK	0.566053	0.66238	-0.09633	0.024263
ENSG00000186471	chrX	AKAP14	0.789977	0.825109	-0.03513	0.027671
ENSG00000125363	chrX	AMELX	0.960124	0.970782	-0.01066	0.043623
ENSG00000163297	chr4	ANTXR2	0.944883	0.963396	-0.01851	0.013948
ENSG00000243478	chr2	AOX2P	0.831792	0.867926	-0.03613	0.017628
ENSG00000134817	chr11	APLNR	0.303875	0.331675	-0.0278	0.045655
ENSG00000103375	chr16	AQP8	0.608477	0.660297	-0.05182	0.034385
ENSG00000067842	chrX	ATP2B3	0.627358	0.674478	-0.04712	0.049484
ENSG00000126895	chrX	AVPR2	0.431314	0.468286	-0.03697	0.048653
ENSG00000160862	chr7	AZGP1	0.623527	0.681335	-0.05781	0.018188
ENSG00000172530	chr16	BANP	0.973481	0.97887	-0.00539	0.037396
ENSG00000215277	chr14	C14orf164	0.735496	0.783247	-0.04775	0.026107
ENSG00000198854	chr1	C1orf68	0.123195	0.167465	-0.04427	0.030614
ENSG00000172247	chr11	C1QTNF4	0.367616	0.40647	-0.03885	0.035893
ENSG00000181215	chr4	C4orf50	0.072308	0.101396	-0.02909	0.045844
ENSG00000164898	chr7	C7orf55	0.978067	0.985144	-0.00708	0.028063
ENSG00000021852	chr1	C8B	0.549816	0.519557	0.030259	0.033205
ENSG00000164972	chr9	C9orf24	0.915525	0.915877	-0.00035	0.044452
ENSG00000196954	chr11	CASP4	0.20436	0.158919	0.045441	0.013583
ENSG00000163492	chr2	CCDC141	0.894329	0.921638	-0.02731	0.022452
ENSG00000108700	chr17	CCL8	0.046012	0.059461	-0.01345	0.03329
ENSG00000074276	chr5	CDHR2	0.330226	0.385556	-0.05533	0.027157
ENSG00000147883	chr9	CDKN2B	0.035039	0.036181	-0.00114	0.048728
ENSG00000135346	chr6	CGA	0.700712	0.761037	-0.06032	0.010915
ENSG00000141076	chr16	CIRH1A	0.84252	0.79634	0.04618	0.021222
ENSG00000166509	chr16	CLEC3A	0.376825	0.378551	-0.00173	0.04046
ENSG00000005243	chr17	COPZ2	0.214389	0.223038	-0.00865	0.027487
ENSG00000135047	chr9	CTSL	0.888645	0.908279	-0.01963	0.021891
ENSG00000265766	chr18	CXADRP3	0.071327	0.117699	-0.04637	0.011852
ENSG00000088782	chr20	DEFB127	0.812053	0.843311	-0.03126	0.04188
ENSG00000147570	chr8	DNAJC5B	0.647765	0.682541	-0.03478	0.017367
ENSG00000116675	chr1	DNAJC6	0.92351	0.889422	0.034087	0.004101
ENSG00000128886	chr15	ELL3	0.123064	0.158223	-0.03516	0.036676
ENSG00000188833	chr9	ENTPD8	0.214838	0.237948	-0.02311	0.045144
ENSG00000138018	chr2	EPT1	0.978474	0.973838	0.004636	0.049655
ENSG00000164283	chr5	ESM1	0.097093	0.093093	0.004	0.027124
ENSG00000151327	chr14	FAM177A1	0.192457	0.120102	0.072355	0.015011
ENSG00000122378	chr10	FAM213A	0.123501	0.145752	-0.02225	0.042932
ENSG00000151474	chr10	FRMD4A	0.534981	0.527373	0.007608	0.032248
ENSG00000158089	chr2	GALNT14	0.560335	0.522311	0.038024	0.007729

ENSG00000182512	chr14	GLRX5	0.230337	0.180164	0.050174	0.00315
ENSG00000205336	chr16	GPR56	0.961592	0.972036	-0.01044	0.010327
ENSG00000113088	chr5	GZMK	0.097093	0.093093	0.004	0.027124
ENSG00000213934	chr11	HBG1	0.765661	0.807311	-0.04165	0.017351
ENSG00000029993	chrX	HMGB3	0.736788	0.782406	-0.04562	0.019695
ENSG00000179362	chr15	HMGN2P46	0.725235	0.798017	-0.07278	0.012664
ENSG00000203859	chr1	HSD3B2	0.901618	0.897865	0.003753	0.048058
ENSG00000137142	chr9	IGFBPL1	0.898942	0.918342	-0.0194	0.030544
ENSG00000168685	chr5	IL7R	0.968973	0.975379	-0.00641	0.026621
ENSG00000177301	chr1	KCNA2	0.112966	0.081357	0.031609	0.022879
ENSG00000170871	chr4	KIAA0232	0.955217	0.970662	-0.01545	0.016532
ENSG00000186965	chr21	KRTAP19-2	0.06671	0.097344	-0.03063	0.01748
ENSG00000204571	chr11	KRTAP5-11	0.143076	0.194623	-0.05155	0.004144
ENSG00000235106	chr9	LINC00094	0.288663	0.301341	-0.01268	0.041821
ENSG00000196553	chr14	LINC00238	0.897722	0.919781	-0.02206	0.046946
ENSG00000231674	chr13	LINC00410	0.919336	0.936639	-0.0173	0.049423
ENSG00000241469	chr3	LINC00635	0.776074	0.796176	-0.0201	0.027645
ENSG00000243629	chr3	LINC00880	0.942882	0.960811	-0.01793	0.028091
ENSG00000242385	chr3	LINC00901	0.121934	0.068443	0.053491	0.043745
ENSG00000261742	chr16	LINC00922	0.374622	0.381563	-0.00694	0.039737
ENSG00000259361	chr15	LINC00927	0.112917	0.1302	-0.01728	0.046628
ENSG00000259150	chr15	LINC00929	0.2759	0.320122	-0.04422	0.019221
ENSG00000253138	chr8	LINC00967	0.033288	0.045818	-0.01253	0.038215
ENSG00000134569	chr11	LRP4	0.551964	0.572881	-0.02092	0.04095
ENSG00000161572	chr17	LYZL6	0.502666	0.533645	-0.03098	0.042634
ENSG00000166986	chr12	MARS	0.855032	0.866679	-0.01165	0.036424
ENSG00000185231	chr18	MC2R	0.533305	0.562099	-0.02879	0.040556
ENSG00000207939	chrX	MIR223	0.104488	0.132764	-0.02828	0.041636
ENSG00000207621	chrX	MIR224	0.217749	0.296859	-0.07911	0.013031
ENSG00000253008	chr2	MIR2355	0.978667	0.984314	-0.00565	0.007131
ENSG00000264139	chr22	MIR3667	0.315901	0.36543	-0.04953	0.044154
ENSG00000265432	chr14	MIR4308	0.969646	0.976111	-0.00647	0.046815
ENSG00000264302	chr17	MIR4723	0.960193	0.970451	-0.01026	0.047725
ENSG00000266459	chr17	MIR4724	0.534389	0.557531	-0.02314	0.049925
ENSG00000265438	chr19	MIR4751	0.940463	0.963243	-0.02278	0.002835
ENSG00000265329	chr20	MIR4758	0.937303	0.957732	-0.02043	0.022978
ENSG00000207738	chr19	MIR520C	0.503432	0.526322	-0.02289	0.026045
ENSG00000207815	chr3	MIR563	0.628087	0.680134	-0.05205	0.047943
ENSG00000266099	chr12	MIR5700	0.032037	0.043344	-0.01131	0.006025
ENSG00000144029	chr2	MRPS5	0.951075	0.957776	-0.0067	0.048597
ENSG00000105835	chr7	NAMPT	0.071108	0.040707	0.030401	0.002679
ENSG00000160703	chr11	NLRX1	0.170003	0.2147	-0.0447	0.037491
ENSG00000105954	chr7	NPVF	0.759824	0.782873	-0.02305	0.034067
ENSG00000124657	chr6	OR2B6	0.782589	0.853815	-0.07123	0.023023

ENSG00000177489	chr1	OR2G2	0.505475	0.501366	0.004109	0.016502
ENSG00000177233	chr1	OR2M1P	0.202822	0.170352	0.03247	0.029729
ENSG00000176253	chr14	OR4K13	0.46141	0.527169	-0.06576	0.016651
ENSG00000181963	chr11	OR52K2	0.310231	0.335517	-0.02529	0.048551
ENSG00000181023	chr11	OR56B1	0.035284	0.046282	-0.011	0.019716
ENSG00000183303	chr11	OR5P2	0.268317	0.28487	-0.01655	0.022626
ENSG00000188324	chr12	OR6C6	0.096432	0.147209	-0.05078	0.019371
ENSG00000181689	chr11	OR8K3	0.100092	0.145729	-0.04564	0.048779
ENSG00000172199	chr11	OR8U1	0.09099	0.067832	0.023158	0.034863
ENSG00000181631	chr3	P2RY13	0.945726	0.949485	-0.00376	0.042059
ENSG00000072682	chr5	P4HA2	0.030954	0.021289	0.009664	0.048931
ENSG00000249504	chr5	PCDHA14	0.725271	0.728933	-0.00366	0.032048
ENSG00000159763	chr7	PIP	0.526587	0.563795	-0.03721	0.033992
ENSG00000105171	chr19	POP4	0.937016	0.921895	0.015121	0.027256
ENSG00000137709	chr11	POU2F3	0.050516	0.067457	-0.01694	0.016511
ENSG00000146250	chr6	PRSS35	0.080082	0.051166	0.028916	0.034691
ENSG00000258223	chr7	PRSS58	0.047446	0.070099	-0.02265	0.023822
ENSG00000188921	chr9	PTPLAD2	0.979361	0.984447	-0.00509	0.02913
ENSG00000124839	chr2	RAB17	0.79142	0.832721	-0.0413	0.023383
ENSG00000011454	chr9	RABGAP1	0.093705	0.071937	0.021768	0.030827
ENSG00000160439	chr19	RDH13	0.496431	0.503315	-0.00688	0.021404
ENSG00000172023	chr2	REG1B	0.180739	0.253316	-0.07258	0.030453
ENSG00000143954	chr2	REG3G	0.100432	0.116551	-0.01612	0.040039
ENSG00000067560	chr3	RHOA	0.111628	0.145472	-0.03384	0.044758
ENSG00000267128	chr17	RNF157-AS1	0.680614	0.691131	-0.01052	0.019211
ENSG00000184719	chr10	RNLS	0.853768	0.871178	-0.01741	0.03977
ENSG00000120341	chr1	SEC16B	0.52214	0.543815	-0.02167	0.024303
ENSG00000100095	chr22	SEZ6L	0.485717	0.514707	-0.02899	0.016525
ENSG00000089060	chr12	SLC24A6	0.560444	0.589673	-0.02923	0.002054
ENSG00000183780	chr1	SLC35F3	0.911124	0.915399	-0.00428	0.047524
ENSG00000151812	chr14	SLC35F4	0.505161	0.561587	-0.05643	0.028139
ENSG00000211584	chr12	SLC48A1	0.955994	0.968726	-0.01273	0.016732
ENSG00000171790	chr1	SLFNL1	0.928723	0.963179	-0.03446	0.019056
ENSG00000163206	chr1	SMCP	0.396033	0.432362	-0.03633	0.020646
ENSG00000201700	chr14	SNORD113-3	0.023757	0.035532	-0.01178	0.048891
ENSG00000202142	chr14	SNORD114-18	0.036346	0.059959	-0.02361	0.045662
ENSG00000199942	chr14	SNORD114-19	0.036346	0.059959	-0.02361	0.045662
ENSG00000199390	chr14	SNORD114-7	0.721162	0.747362	-0.0262	0.021287
ENSG00000199970	chr15	SNORD115-3	0.439074	0.493546	-0.05447	0.045339
ENSG00000202188	chr15	SNORD115-31	0.258897	0.281237	-0.02234	0.013137
ENSG00000173898	chr11	SPTBN2	0.93745	0.970733	-0.03328	0.01164
ENSG00000113387	chr5	SUB1	0.123035	0.184695	-0.06166	0.008114
ENSG00000132872	chr18	SYT4	0.118384	0.145328	-0.02694	0.032213
ENSG00000121314	chr12	TAS2R8	0.578823	0.666617	-0.08779	0.047418

ENSG00000122145	chrX	TBX22	0.097592	0.10431	-0.00672	0.018616
ENSG00000145850	chr5	TIMD4	0.230878	0.289551	-0.05867	0.036731
ENSG00000065717	chr19	TLE2	0.355402	0.377419	-0.02202	0.041378
ENSG00000163762	chr3	TM4SF18	0.211306	0.32227	-0.11096	0.000475
ENSG00000123610	chr2	TNFAIP6	0.850479	0.87758	-0.0271	0.030854
ENSG00000120337	chr1	TNFSF18	0.809958	0.851456	-0.0415	0.028445
ENSG00000167460	chr19	TPM4	0.067351	0.089832	-0.02248	0.010034
ENSG00000108448	chr17	TRIM16L	0.066939	0.094141	-0.0272	0.018539
ENSG00000167118	chr9	URM1	0.031323	0.043951	-0.01263	0.01835
ENSG00000146469	chr6	VIP	0.239673	0.207967	0.031706	0.018681
ENSG00000166415	chr15	WDR72	0.227076	0.109069	0.118008	0.042173
ENSG00000010539	chr16	ZNF200	0.034947	0.048366	-0.01342	0.036302
ENSG00000261221	chr19	ZNF865	0.233945	0.297343	-0.0634	0.017926

12 – Vitamin D differentially methylated single sites CaCO2 (array 1, experiment 2). Used for pathway analysis

gene	*cgid*	*CACO_CTRL*	*CACO_VIT_D*	*mean.diff*	*diffmeth.p.val*
NF	cg24928333	0.94	0.84	0.10	0.02
PLCXD3	cg09499856	0.94	0.70	0.23	0.02
NF	cg17526103	0.93	0.83	0.10	0.04
TTBK1	cg27363327	0.88	0.78	0.10	0.00
DIP2C	cg15551781	0.87	0.77	0.10	0.00
ALOXE3	cg18700133	0.85	0.73	0.12	0.01
IDUA	cg05327835	0.85	0.74	0.11	0.02
NF	cg27179866	0.84	0.68	0.16	0.00
NF	cg03543893	0.82	0.72	0.10	0.00
NF	cg21503053	0.81	0.70	0.11	0.05
KCNIP4	cg07204550	0.81	0.71	0.10	0.02
BCL2L10	cg14540387	0.81	0.69	0.12	0.00
ZNF655	cg05165378	0.79	0.68	0.11	0.00
TMEM140	cg21363348	0.79	0.68	0.11	0.02
NF	cg10883069	0.79	0.69	0.10	0.01
RPS6KA3	cg12456011	0.78	0.64	0.14	0.00
NF	cg12322450	0.77	0.66	0.11	0.01
NF	cg18266853	0.76	0.65	0.11	0.03
TTC23L	cg11183001	0.74	0.63	0.11	0.01
FBXO47	cg10600889	0.74	0.62	0.12	0.01
TEKT3	cg02016419	0.73	0.63	0.11	0.04
ELOVL4	cg04107099	0.73	0.62	0.10	0.03
NF	cg26331343	0.72	0.60	0.12	0.03
C8orf84	cg04367680	0.71	0.59	0.12	0.04
HPCA	cg05660436	0.71	0.51	0.19	0.01
SPINK1	cg14452346	0.71	0.61	0.10	0.03
NF	cg03730474	0.71	0.60	0.10	0.01
KLHL4	cg07897414	0.70	0.56	0.14	0.02
ZNF350	cg18649745	0.70	0.59	0.11	0.01
NF	cg16005540	0.69	0.57	0.13	0.02
NF	cg23601397	0.69	0.57	0.12	0.01
ATP2A1	cg16606674	0.68	0.57	0.11	0.01
HPCA	cg02631838	0.67	0.57	0.11	0.00
CECR2	cg13762691	0.66	0.55	0.12	0.01
GFI1	cg25320328	0.65	0.54	0.11	0.03
NF	cg00241427	0.64	0.54	0.10	0.01
NF	cg26645509	0.64	0.52	0.12	0.01
MGC2889	cg08376864	0.64	0.51	0.13	0.01
NF	cg10098888	0.63	0.52	0.11	0.03

PCDH19	cg26401825	0.63	0.52	0.11	0.01
MAP3K15	cg00072587	0.63	0.49	0.14	0.00
RAB9B	cg02547323	0.63	0.49	0.14	0.01
MAGEC1	cg24761827	0.62	0.49	0.14	0.01
HLA-DQB1	cg18902440	0.62	0.51	0.11	0.02
SLMO1	cg07207726	0.61	0.50	0.10	0.01
SLMO1	cg20984502	0.61	0.45	0.16	0.00
NF	cg16324725	0.60	0.41	0.19	0.03
FRMD7	cg06647694	0.59	0.46	0.13	0.00
NF	cg07916101	0.59	0.48	0.11	0.01
NF	cg00188409	0.58	0.47	0.11	0.02
NF	cg02603022	0.58	0.45	0.13	0.02
LPGAT1	cg13064658	0.57	0.05	0.52	0.00
BCL11B	cg12961080	0.57	0.44	0.13	0.03
FHL1	cg12623328	0.56	0.45	0.12	0.03
CACNA2D	cg15603311	0.56	0.46	0.10	0.02
TTC23L	cg07895169	0.55	0.45	0.10	0.03
GGN	cg25922163	0.54	0.38	0.16	0.01
CYB5R2	cg18791121	0.54	0.40	0.14	0.00
NOL4	cg22287067	0.54	0.40	0.14	0.01
PRKCB	cg05632631	0.54	0.40	0.13	0.00
CNPY1	cg26388509	0.53	0.42	0.11	0.04
BCL2L10	cg19114050	0.52	0.41	0.10	0.04
RBM23	cg01529538	0.51	0.40	0.12	0.05
UNC5D	cg08701686	0.51	0.39	0.12	0.00
TRPM3	cg21171320	0.51	0.30	0.21	0.00
EDA2R	cg10153260	0.51	0.40	0.11	0.04
PRICKLE3	cg04675919	0.51	0.39	0.12	0.00
BIN3	cg07164659	0.50	0.40	0.11	0.01
CADPS	cg21534264	0.50	0.39	0.12	0.01
RNLS	cg06079710	0.50	0.37	0.13	0.00

The End